

Bioadhesive Microparticles and Liposomes of Anti-Parkinson Drugs for Nasal Delivery

By

Nozad Rashid Hussein

**A thesis submitted in partial fulfilment for the requirements for the degree
of Doctor of Philosophy at the University of Central Lancashire**

June/2014

STUDENT DECLARATION FORM

Concurrent registration for two or more academic awards:

I declare that while registered as a candidate for the research degree, I have not been a registered candidate or enrolled student for another award of the University or other academic or professional institution.

Material submitted for another award:

I declare that no material contained in the thesis has been used in any other submission for an academic award and is solely my own work.

Signature of Candidate: _____



Type of Award:

PhD (Doctor of philosophy)

School:

Pharmacy and Biomedical Science

ABSTRACT

The nasal route is highly promising for the delivery of drugs exerting local effects in the nose or for therapeutic molecules having systemic or CNS effect. This is attributed to the fact that the nasal epithelium is highly vascularized and permeable, which ensures rapid absorption of the drug. The limitation of short residence time of the formulations in the nose and poor bioavailability of hydrophilic drugs could be overcome by the inclusion of bioadhesive agents into formulation.

The main objective of this study was to develop novel bioadhesive microspheres and liposomes entrapping the anti-Parkinson drugs ropinirole hydrochloride (RH). The microspheres were prepared via spray drying in combination with chitosan or sodium alginate and the liposomes were prepared using the ethanol-based proliposome method. This study has investigated the potential of powdered mucoadhesive microparticles and liquid liposomes for nasal delivery via Miat[®] nasal insufflator and nasal spray devices respectively.

Optimum mucoadhesive chitosan microparticles were prepared by co-spray drying of chitosan glutamate and ropinirole hydrochloride (90:10 w/w). Characterization studies have revealed that the drug following spray drying was amorphous and the microparticles were spherical and offered drug entrapment efficiency values in the range of 93 - 99%. The optimum formulation provided maximum swelling capacity and slowest drug release. *Ex vivo* toxicity study using isolated sheep nasal mucosa proved the safety of the optimized formulations for intranasal delivery. Investigation of powder delivery demonstrated that the Miat[®] nasal insufflator could deliver 90% of the dose with the first puff regardless of the loading weight used to fill the capsule fitted into the nasal device. The spray cloud had elongated shape and was homogenous; this is expected to enhance the impaction of the formulation in the nose following delivery from the nasal device.

The properties of sodium alginate microparticles prepared via spray drying were highly dependent on inlet temperature of the spray drier, affecting particle morphology and product yield percent. The best performing particles were obtained when the inlet temperature was 140°C. Alginate to RH ratio had marked effect on particle size (2.60 - 4.37µm), entrapment efficiency (101 - 109%), physical state of the encapsulated RH, and morphology and surface smoothness of the particles as shown by scanning electron microscopy (SEM). *In vitro* drug release profile showed the amount of sodium alginate in formulations has controlled the rate of drug release. Results revealed that RH-alginate microparticles in 90:10 w/w polymer to drug ratio was the best performing spray dried formulation. Toxicity study proved safety of RH loaded sodium alginate for intranasal delivery. In contrast to RH-chitosan microparticles, particle trajectories was found from the cloud generated from emitted powder and laser diffraction demonstrated that powder was less likely to deposit in the lower respiratory tract owing to particle agglomeration.

Ethanol-based proliposome technology produced oligolamellar liposomes from lipid ethanolic solutions as revealed by transmission electron microscopy (TEM). The resultant liposomes entrapped approximately 23.30% of the drug. Using five different bioadhesive agents, inclusion of any of these agents (0.2% w/v) caused a decrease in drug entrapment except for carboxymethyl chitosan which had no effect on the drug entrapment (25.97%). Investigation of aerosolized liposome dispersion using a range of nasal spray devices demonstrated integrity of liposomes were not changed (i.e particle size, Span, and drug entrapment efficiency were unaffected) and RH-loaded liposomes were efficiently delivered from the devices.

In conclusion, the finding of this study explored mucoadhesive microspheres entrapped the anti-Parkinson drug, RH, and can potentially be applicable for nasal delivery to enhance nose to brain transport using nasal insufflator for improvement of the symptoms of Parkinson disease and Restless legs syndrome. Similar findings using nasal sprays were found for liposomes. *In vivo* studies are required in the future to determine the amount of the drug that may reach the blood circulation and brain.

TABLE OF CONTENTS

DECLARATION.....	I
ABSTRACT	II
TABLE OF CONTENTS.....	III
LIST OF FIGURES	X
LIST OF TABLES	XVI
AKNOWLEDGEMENTS.....	XVIII
DEDICATIONS	XIX
LIST OF ABBREVIATIONS AND ACRONYMS	XX
CHAPTER 1: INTRODUCTION.....	1
1.1 Nasal drug delivery	2
1.1.1 Historical background	2
1.1.2 Why the nasal route?	3
1.1.3 Anatomy of the nose	6
1.1.4 Applications of nasal delivery.....	9
1.2 Mechanisms of drug transport following intranasal administration.....	14
1.3 Factors affecting nasal drugs delivery.....	16
1.4 Barrier interfering nasal drug delivery	17
1.4.1 Low drug bioavailability	17
1.4.2 Mucociliary clearance	17
1.4.3 Enzymatic degradation.....	19
1.5 Dosage forms for intranasal administration	20
1.5.1 Liquid formulations.....	20
1.5.2 Nasal Powders	21
1.5.3 Nasal Gels	22
1.6 Factors affecting particle deposition in nasal cavity	22

1.7	Mucoadhesive drug delivery systems.....	24
1.7.1	Chitosan.....	25
1.7.2	Sodium alginate.....	26
1.8	Microspheres as a drug delivery system.....	28
1.8.1	Preparation of microspheres.....	28
1.9	Liposomes	30
1.9.1	Classification of liposomes	32
1.9.2	Liposomes in nasal drug delivery.....	34
1.10	Parkinson’s disease and restless legs syndrome (RLS).....	35
1.11	Ropinirole hydrochloride (RH)	36
1.12	Devices used for nasal delivery.....	38
1.12.1	Nasal drops.....	38
	i) Drops delivered with a pipette.....	38
	ii) Squeeze bottles	38
1.12.2	Nasal Sprays.....	39
	i) Metered- dose spray pumps.....	39
	ii) Nasal pressurized metered-dose inhalers (pMDIs).....	41
1.12.3	Delivery devices of powdered nasal formulations	41
	i) Nasal insufflators for experimental purposes	42
	ii) Bi-Directional TM nasal insufflators.....	42
	Bi-Directional TM nasal insufflators	42
	iii) Miat [®] monodose nasal insufflator	43
	iv) Monopowder P [®] insufflator.....	43
1.13	Hypothesis and objectives.....	44
	CHAPTER 2: GENERAL METHODOLOGY.....	46
2.1	Materials.....	47

2.2	Compatibility studies.....	48
2.3	Standard calibration curve of RH.....	48
2.4	Preparation of phosphate buffers (pH 6 and 6.5)	49
2.5	Preparation of microspheres	50
2.5.1	Viscosity measurements of feeding solution.....	51
2.6	Characterizations of mucoadhesive microspheres	53
2.6.1	Production yield	53
2.6.2	Particle size measurement	53
2.6.3	Zeta potential analysis	55
2.6.4	Powder tapped and bulk density measurement	55
2.6.5	Encapsulation efficiency and drug loading	56
2.6.6	Swelling index.....	57
2.6.7	Scanning electron microscopy	57
2.6.8	X-Ray Diffraction	57
2.6.9	Differential scanning calorimetry.....	58
2.6.10	Thermogravimetric analysis.....	59
2.6.11	In vitro drug release.....	60
2.6.12	Histopathological study.....	60
2.7	Characterization of microspheres emitted from a nasal device.....	61
2.7.1	Quantative determination of dose uniformity	61
2.7.2	Qualitative analysis of spray pattern of microsphere formulations	61
2.8	Liposome formulations	63
2.8.1	Ethanol-based proliposomes	63
2.8.2	Polymer-coated liposomes	63
2.8.3	Drug entrapment studies.....	63
2.8.4	Liposome morphology study using transmission electronic microscopy	64

2.8.5	Size analysis of droplets emitted from nasal devices using laser diffraction	64
2.8.6	Determination of shot weight and spray content uniformity.....	65
2.9	Nasal spray characteristics	66
2.10	Statistical analysis	69
CHAPTER 3: PREPARATION OF ROPINIROLE HYDROCHLORIDE LOADED CHITOSAN MICROPARTICLES VIA SPRAY DRYING		70
3.1	Introduction	71
3.2	Methodology	73
3.2.1	Compatibility studies.....	73
3.2.2	Preparation of chitosan microspheres	73
3.2.3	Characterization of microspheres.....	74
3.3	Results and discussion.....	74
3.3.1	Compatability studies.....	74
3.3.2	Percentage yield	76
3.3.3	Particle size and distribution	77
3.3.4	Zeta potential.....	80
3.3.5	Entrapment efficiency and drug loading	81
3.3.6	Tapped and bulk density	82
3.3.7	Swelling index.....	83
3.3.8	Mucoadhesion	85
3.3.9	Surface morphology of microparticles.....	87
3.3.10	X-Ray diffraction	91
3.3.11	Thermo Gravimetric analysis	93
3.3.12	Differential scanning calorimetry.....	94
3.3.13	Drug release from microspheres	96
3.3.14	Toxicity of RH-loaded chitosan microspheres.....	97

3.3.15	Characterization of RH loaded chitosan microspheres delivered using Miat [®] nasal device	102
3.3.15.1	Determination of shot weight (Fraction of delivered formulation)	102
3.3.15.2	Physical particle size analysis using laser diffraction	103
3.3.15.3	Determination of plume geometry and spray pattern	104
3.4	Conclusions	107
CHAPTER 4: ROPINIROLE HYDROCHLORIDE LOADED SODIUM ALGINATE MICROPARTICLES PREPARED BY SPRAY DRYING		108
4.1	Introduction	109
4.2	Methodology	111
4.2.1	Compatibility Study	111
4.2.2	Optimization of sodium alginate microsphere formulation	111
4.2.3	Preparation of RH loaded alginate	112
4.2.4	Characterization of RH loaded alginate microparticles	112
4.3	Results and discussion.....	113
4.3.1	Compatability study	113
4.3.2	Optimization of sodium alginate microparticles	115
4.3.3	Characterization of RH loaded sodium alginate	120
4.3.3.1	Product yield.....	120
4.3.3.2	Size and size distribution of microparticles.....	120
4.3.3.3	Drug loading and entrapment efficiency	123
4.3.3.4	Zeta potential of microparticles.....	124
4.3.3.5	Surface morphology of microparticles	125
4.3.3.6	X-Ray diffraction	129
4.3.4	Thermo gravimetric analysis (TGA).....	131
4.3.4.1	Differential Scanning Calorimetry (DSC).....	132
4.3.4.2	Dissolution test	134
4.3.4.3	Histopathological study of RH-loaded sodium alginate.....	135

4.3.5	Characterization of delivered RH loaded sodium alginate microspheres using Miat [®] nasal device.....	138
4.3.5.1	Determination of shot weight	138
4.3.5.2	Particle size analysis using laser diffraction.....	139
4.3.5.3	Determination of plume geometry and spray pattern	140
4.4	Conclusions	143
CHAPTER 5: FORMULATION OF ROPINIROLE HYDROCHLORIDE LOADED LIPOSOMES USING ETHANOL-BASED PROLIPOSOME METHOD		145
5.1	Introduction	146
5.2	Methodology	147
5.2.1	Manufacture of RH liposomes	147
5.2.2	Characterization of liposomes	148
5.2.3	Formulation of mucoadhesive liposome	148
5.2.4	Liposome morphology study using Transmission Electronic Microscopy	148
5.2.5	Characterisation of liposomes after delivery using nasal spray devices	148
5.3	Results and Discussion.....	149
5.3.1	Characterization of RH loaded in liposomes.....	149
5.3.1.1	Size and size distribution of liposomes	149
5.3.1.2	Zeta potential measurement of liposomes	151
5.3.1.3	Entrapment efficiency of RH	152
5.3.2	Effect of inclusion of mucoadhesive agents in liposome formulations	153
5.3.2.1	Size and size distribution of liposomes	154
5.3.2.2	Zeta potential	156
5.3.2.3	Drug entrapment efficiency	157
5.3.3	Transmission electron microscopy study	158
5.3.4	Influence of nasal spray device on the spray cloud characteristics.....	160
5.3.4.1	Determination of priming, tail off and shot weight.....	160

5.3.4.2	Droplet size distribution (DSD)	164
5.3.4.3	Spray pattern and plume geometry studies.....	165
5.4	Conclusions	172
6	CHAPTER 6: GENERAL CONCLUSIONS	173
6.1	Nasal insufflator system using bioadhesive polymers	174
6.2	Nasal spray devices using proliposome technology.....	175
6.3	Final conclusion of the thesis	176
6.4	Future work	176
7	CHAPTER 7: REFERENCES	178

LIST OF FIGURES

CHAPTER 1: INTRODUCTION

Figure 1. 1: Consuming snuff with large V-shaped straws called ‘Tipi’, by a partner.	2
Figure 1. 2: Serum level of propranolol after administration using nasal, i.v and oral routes.....	4
Figure 1. 3: Anatomy of the human nasal cavity.	6
Figure 1. 4: (a) Nose to brain pathway (Adapted from Olson, 2008), (b) a schematic illustration of the possible drug molecule transfer delivered nasally. (---) indicates limited substrate delivery via this route, and (?) indicates the exact pathway is unclear.....	13
Figure 1. 5: Mechanisms of drug transport across epithelial cells: [A1] Intercellular spaces, [A2] Tight junctions, [B1] Passive diffusion, [B2] Active transport, and [C] Transcytosis	15
Figure 1. 6: Barriers interfering with drug delivery via the nasal route.....	16
Figure 1. 7: Nasal mucociliary clearance.....	18
Figure 1. 8: Chemical structure of chitin and chitosan	26
Figure 1. 9: Chemical structure of alginic acid unites "M" (is mannuronic acid and "G" is guluronic acid)	27
Figure 1. 10: General methods used for microspheres preparation	29
Figure 1. 11: Mini spray dryer B-290 (Büchi -290 Mini Spray-Drying, Büchi Laboratories, Switzerland).....	30
Figure 1. 12: Structure of liposomes and the entrapment of lipophilic and hydrophilic drug molecules.....	31
Figure 1. 13: Liposome classification based on residue size and morphology (Adapted from Laouini et al., 2012).....	34
Figure 1. 14: Chemical structure of ropinirole hydrochloride.	37
Figure 1. 15: (a) Nasal drops with pipette, and (b) nasal squeeze bottles.....	39
Figure 1. 16: (a) Airless nasal device with collapsible bag (Bag on valve system), and (b) airless nasal device with sliding piston	40
Figure 1. 17: (a) Preservative free pump with air filter, and (b) nasal unit-dose system with glass container	41

Figure 1. 18: (a) Penn-Century Dry Powder Insufflator™ - Model DP-4 connected with commercial syringe, (b) Dry Powder Insufflator™ Air Pump Assembly	42
Figure 1. 19: (a) Optinose Bi-Directional™ nasal insufflator, and (b) Miat® monodose nasal insufflator.	43

CHAPTER 2: GENERAL METHODOLOGY

Figure 2. 1: Nasal spray devices used in this study.....	47
Figure 2. 2: Calibration curve of ropinirole hydrochloride.	49
Figure 2. 3: A schematic presentation of spray drying (Adapted from Büchi -290 Mini Spray-Drying, Büchi Laboratories, Switzerland).	51
Figure 2. 4: (a) Automated Microviscometer, (b) cylindrical tube (Adapted from AMVn Automated Microviscometer, Anton-Paar)	52
Figure 2. 5: The Malvern Mastersizer instrument used in the present study (upper picture) and a schematic illustration of light scattering from small and large particles (lower picture) (Malvern-Instruments Ltd, 2012).	54
Figure 2. 6: Malvern Zetasizer Nanoseries 2000 used in the present study.....	55
Figure 2. 7: Schematic presentation showing the principal components of a DSC equipment.	59
Figure 2. 8: Schematic diagram of a TGA equipment.	60
Figure 2. 9: An illustration of (A) technique used to determine spray pattern of powder, and (B) an example of spray pattern.....	62
Figure 2. 10: The Malvern Spraytec system used to characterize particles since delivered from nasal sprays or insufflators.....	65
Figure 2. 11: Schematic illustration of (a) the technique used to determine spray pattern, and (b) an example of spray pattern.....	67
Figure 2. 12: Schematic illustration of the technique used to monitor the plume geometry.	68

CHAPTER 3: PREPARATION OF ROPINIROLE HYDROCHLORIDE LOADED CHITOSAN MICROPARTICLES VIA SPRAY DRYING

Figure 3. 1: FTIR spectrum of (A) RH, (B) chitosan glutamate, (C) physical mixture of chitosan 50% w/w and RH 50% w/w, and (D) RH loaded microspheres. The lower graph magnifies the wave numbers area between 900 and 1850 cm ⁻¹	75
---	----

Figure 3. 2: Percentage yield of chitosan microsphere formulations (F1 – F5) for formulation composition refer to table 3.1...	77
Figure 3. 3: Particle size and size distribution of RH-chitosan microparticles.....	78
Figure 3. 4: Relationship between chitosan concentration and viscosity of the solution.	79
Figure 3. 5: Relationship between viscosity of the solution and particle size and size distribution (Span).	79
Figure 3. 6: Zeta potential of chitosan microparticles.....	80
Figure 3. 7: Drug loading (DL) and entrapment efficiency (EE) in spray-dried microspheres at various drug/polymer ratios.....	81
Figure 3. 8: Bulk density (BD), tapped density (TD) and Hausner's ratio of RH free and RH-loaded chitosan formulations.	83
Figure 3. 9: Swelling index of RH free microspheres and RH-loaded chitosan microspheres.	84
Figure 3. 10: Relationship between swelling index and zeta potential of spray dried particles.....	85
Figure 3. 11: Zeta potential of the mucin and the mixture of mucin from porcine stomach (Type II) with the microsphere formulations.....	87
Figure 3. 12: SEM images of RH (a) before spray drying and (b) RH after spray drying. Magnification: 750x (a) and 1200x (b).....	88
Figure 3. 13: SEM images of (a) the blank microspheres F1, (b) F2, and (c) F3. Magnification: 2500x.....	89
Figure 3. 14: SEM images of (a) is F4 and (b) is F5. Magnification: 2500x.....	90
Figure 3. 15: X-Ray spectra of (a) pure RH and mucoadhesive formulations of (b) drug free microspheres (F1), (c) F5, (d) F4, (e) physical mixture (co-ground) of chitosan and RH, 70:30 ratio, (f) F3, (g) physical mixture (co-ground) of chitosan and RH, 90:10 ratio, and (h) F2.	92
Figure 3. 16: X-Ray spectra of (a) fresh F2 formulation, (b) F2 formulation stored at fridge and (c) F2 formulation stored at room temperature for two months.....	92
Figure 3. 17: Weight loss of chitosan microparticle formulations.....	93
Figure 3. 18: DSC thermograms of (a) drug free microsphere, (A) physical mixture of chitosan-RH; (b) 90:10, (c) 70:30, (d) 50:50, (e) 30:70 and (B) RH loaded chitosan microspheres; (b) F2, (c) F3, (d) F4, (e) F5 and (f) pure drug.....	95
Figure 3. 19: <i>In-vitro</i> dissolution profiles of spray dried RH loaded chitosan microsphere formulations carried out in phosphate buffer solution (pH 6.5).	97

Figure 3. 20: Microscopic (Olympus) images of sheep nasal mucosa treated by; (a) negative control (phosphate buffer pH 6.5) (10 x 10 magnification, n=3) and (b) positive control (Sodium deoxycollate) (10x 10 magnification, n=3). "S" means sloughed, "N" means necrosis, "I" means inflammation.	100
Figure 3. 21: Microscopic (Olympus) images of sheep nasal mucosa treated by (a) formulation F2, (b) drug-free microspheres and (c) RH solutions (10 x 10 magnification, n=3). "S" means sloughed, "N" means necrosis, "I" means inflammation.....	101
Figure 3. 22: Spray pattern of RH-chitosan microparticles (90:10 w/w, chitosan glutamate to RH) at 3cm distance from the nasal device tip.	105
Figure 3. 23: RH-chitosan microspheres delivery sequences from Miat® monodose insufflator monitored by videography.	106

CHAPTER 4: ROPINIROLE HYDROCHLORIDE LOADED SODIUM ALGINATE MICROPARTICLES PREPARED BY SPRAY DRYING

Figure 4. 1: FTIR spectrum of (A)RH, (B) sodium alginate, (C) physical mixture of sodium alginate and RH (1:1) ratio, and (D) spray dried RH loaded sodium alginate microparticles. The lower graph magnifies the wave numbers area between 900 and 1900 cm^{-1}	114
Figure 4. 2: Relationship between inlet air temperature and the production yield (%).	116
Figure 4. 3: Relationship between inlet air temperature ($^{\circ}\text{C}$) and particle size (VMD) of sodium alginate microparticles.	117
Figure 4. 4: Relationship between inlet air temperature ($^{\circ}\text{C}$) and Span of sodium alginate microparticles.	117
Figure 4. 5: SEM images of sodium alginate microparticles where inlet air temperatures were: (a) 160°C , (b) 140°C , and (c) 120°C . Magnification: 2500x	119
Figure 4. 6: Production yield (%) of sodium alginate microsphere formulations.....	120
Figure 4. 7: Relationship between viscosity of formulations and particle size of spray-dried RH loaded sodium alginate microspheres.	122
Figure 4. 8: Relationship between viscosity of formulations and size distribution of spray-dried RH loaded sodium alginate microspheres.	122
Figure 4. 9: Drug loading and entrapment efficiency of spray-dried microspheres at various drug to sodium alginate ratios.....	123
Figure 4. 10: Zeta potential of sodium alginate microparticle formulations.....	125

Figure 4. 11: EM images of RH (a) before spray drying (magnification: 750x) and (b) after spray drying (magnification: 1200x).....	126
Figure 4. 12: SEM images of (a) drug-free microspheres, (b) A2 and (c) A3. Magnification: 3000x.....	127
Figure 4. 13: SEM images of (a) A4 and (b) A5 (magnification: 3000x).....	128
Figure 4. 14: X-Ray diffractogram of (a) drug free microparticles, (b) A2, (c) A2 physical mixture, (d) A3, (e) A4, (f) A5, and (g) RH raw material. For composition of formulations refer to table 4.2	130
Figure 4. 15: X-Ray diffractogram of (a) fresh A2 formulation, (b) A2 formulations stored at fridge (5±1) and (c) A2 formulations stored at room temperature (20±2) for two months.....	130
Figure 4. 16: Moisture content (%) of sodium alginate microparticle formulations. r.	131
Figure 4. 17: DSC thermograms of (a) drug-free microsphere, physical mixture of alginate-RH; (b) 90:10, (c) 70:30, (d) 50:50, (e) 30:70, RH loaded alginate microspheres; (b) A2, (c) A3, (d) A4, (e) A5 and (f) pure drug.	133
Figure 4. 18: Dissolution profile of various spray dried RH-loaded sodium alginate microsphere formulations carried out in phosphate buffer solution (pH 6.5).	135
Figure 4. 19: Microscopic (Olympus) images of sheep nasal mucosa treated with (a) A2 formulations, (b) drug free microparticles, and (c) positive control (10 x 10 magnification, n=3). "S" means sloughed, "N" means necrosis, "I" means inflammation.....	137
Figure 4. 20: Spray pattern of formulation A2 at 3cm distance from the insufflator device tip (n= 4).....	141
Figure 4. 21: RH-sodium alginate microspheres delivery from Miat® monodose insufflator as monitored using videography (n= 4).	142

CHAPTER 5: FORMULATION OF ROPINIROLE HYDROCHLORIDE LOADED LIPOSOMES USING ETHANOL-BASED PROLIPOSOME METHOD

Figure 5. 1: Size (VMD) of liposomes generated from ethanol-based proliposomes using a range of RH concentrations (0 – 8 mg/ml).....	150
Figure 5. 2: Size distribution (Span) of liposomes generated from ethanol-based proliposomes using a range of RH concentrations (0 – 8 mg/ml).	150
Figure 5. 3: Zeta potential of liposomes generated from ethanol-based proliposomes using a range of RH concentrations (0-8 mg/ml).	152

Figure 5. 4: Entrapment efficiency (%) of RH loaded into liposomes generated from ethanol-based proliposome formulations in relation to drug concentration. represent	153
Figure 5. 5: Size of liposomes containing drug (2mg/ml) in relation to the inclusion of different mucoadhesive agents in concentration of 0.2%	155
Figure 5. 6: Size distribution (Span) of liposomes containing drug (2mg/ml) in relation to the inclusion of different mucoadhesive agents in concentration of 0.2%	155
Figure 5. 7: Zeta potential of liposomes containing drug (2mg/ml) in relation to the inclusion of different mucoadhesive agents in concentration of 0.2%	157
Figure 5. 8: Drug entrapment (%) by liposomes in relation to the inclusion of different mucoadhesive agents in concentration of 0.2%	158
Figure 5. 9: TEM images of (a) drug free liposomes, (b) drug loaded liposome, and (c) carboxymethyl chitosan-coated drug free liposomes. Magnification: 93000x	159
Figure 5. 10: Number of actuations required for priming the devices, full actuations delivered and the number of actuations in the tail off phase.	161
Figure 5. 11: Mean delivered volume (μ l) by nasal spray devices at fully actuation state.	162
Figure 5. 12: Effect of spraying on the retained EE (%) of RH loaded liposomes coated by carboxymethyl chitosan compared to non-sprayed liposome (NSL) using nasal spray devices A, B and C	163
Figure 5. 13: Generation of plume from nasal spray device A showing the different phases of spray cloud development as monitored by videography.	168
Figure 5. 14: Generation of plume from nasal spray device B showing the different phases of spray cloud development as monitored by videography.	168
Figure 5. 15: Generation of plume from nasal spray device C showing the different phases of spray cloud development as monitored by videography.	169
Figure 5. 16: Spray pattern images for water and liposome dispersion using nasal device A (a and d respectively), nasal device B (b and e respectively) and nasal device C (c and f respectively) using Canon EOS 550D digital camera.	170

LIST OF TABLES

CHAPTER 1: INTRODUCTION

Table 1. 1: Advantage and limitations of nasal route.....	5
Table 1. 2: Human nasal epithelium characteristics.....	8
Table 1. 3: Nasal Proteins, Peptides and non-peptide formulations for systemic effect available in the market.	10
Table 1. 4: Recent studies carried out to deliver drug molecules to the brain via nasal route.	12
Table 1. 5: Pathological conditions that may affect nasal mucociliary clearance.	19

CHAPTER 2: GENERAL METHODOLOGY

Table 2. 1: Formulation composition of mucoadhesive microparticles.	50
--	----

CHAPTER 3: PREPARATION OF ROPINIROLE HYDROCHLORIDE LOADED CHITOSAN MICROPARTICLES VIA SPRAY DRYING

Table 3. 1: Microsphere formulations using various ratios of chitosan to drug.	73
Table 3. 2: Frequency of functional groups of pure RH physically mixed with polymer and drug-loaded microspheres.	76
Table 3. 3: The comparative histopathological evaluation of nasal mucosa treated with a range of formulation.	99
Table 3. 4: Percent of RH loaded chitosan microspheres delivered using Miat [®] nasal insufflator.....	103

CHAPTER 4: ROPINIROLE HYDROCHLORIDE LOADED SODIUM ALGINATE MICROPARTICLES PREPARED BY SPRAY DRYING

Table 4. 1: Conditions for the preparation of sodium alginate microspheres.	111
Table 4. 2: Composition of sodium alginate microparticle formulations.	112
Table 4. 3: Particle size, size distribution and viscosity of alginate microparticle formulations.	121
Table 4. 4: The comparative histopathological evaluation of nasal mucosa treated with a range of formulations and RH-loaded sodium alginate microparticles.	136

Table 4. 5: Fraction delivered of RH-loaded chitosan microspheres using Miat® nasal insufflator.....	139
--	-----

CHAPTER 5: FORMULATION OF ROPINIROLE HYDROCHLORIDE LOADED LIPOSOMES USING ETHANOL-BASED PROLIPOSOME METHOD

Table 5. 1: Particle size (VMD), size distribution (Span) and zeta potential of carboxymethyl chitosan coated RH liposomes compared to non-sprayed liposomes using nasal spray devices A, B and C.....	163
--	-----

Table 5. 2: Droplet size, size distribution and percentage of droplets below 10µm for RH loaded into liposome formulation coated by carboxymethyl chitosan.	165
--	-----

Table 5. 3: Plume angle, width and height for sprays generated from nasal devices A, B and C.....	167
---	-----

Table 5. 4: Spray patterns (D_{max} , D_{min} and ovality ratio) generated from nasal spray devices A, B and C.	171
---	-----

AKNOWLEDGEMENTS

I would like to thank Allah for giving me a golden opportunity to do a PhD and for my good health, patience and grace to finish this work.

I am immensely thankful and indebted to my director of study Professor Waqar Ahmed and second supervisor Dr. Abdelbary Elhissi for their guidance, encouragement and constant support during my study.

I wish to acknowledge the kind financial support from the Ministry of Higher Education and Scientific Affairs-Kurdistan Regional Government/ Iraq for funding my PhD at UCLAN.

My sincere thanks go to my colleagues and friends especially, Huner Omer, Dana Ameen, Adnan Qadir, Azad Azabani, Ava Ismael, Rawand Mustafa, Bahjat Saeed, Mohamad Alhnan, Ka-Wai Wan, Basel Arafat, Iftikhar Khan, Sakib Yousaf, Tanem Garanti, Sneha Subramanian, Oshadie Korale for a friendly support and valuable advice. I also in the bottom of my heart thank Professor Jaipaul Singh for his kind advice and continuous support as Research Degree Tutor.

I appreciate the support of UCLAN technical and academic staff for their help and encouragement.

I forward my deep gratitude to my beloved family; my brothers (Niaz, Nabaz, Rebaz and Azad), my sisters (Benaz, Mahabad and Nazahat). Many thanks are due to my uncles, aunts and relatives for their appreciation and love.

Lastly my very special and lovely thank go to my wife Choppy Ahmed and my Parents Rashid and Neamah for their patience, trust and sacrifice during my PhD.

DEDICATIONS

This work and thesis is dedicated to my parents, Rashid and Neamah, my wife Chopy and her parents Star and Qumry and my brothers Niaz, Nazab, Rebaz and Azad and sisters Banaz, Mahabad and Nazahat. This work would not have been possible without their love, support and sacrifice.

LIST OF ABBREVIATIONS AND ACRONYMS

%	Percentage
°C	Degree centigrade
µg	Microgram
µl	Microlitre
µm	Micrometre
ACN	Acetonitrile
AUC	Area under curve
BBB	Blood brain barrier
BD	Bulk density (gm/ml)
CDER	Center for drug evaluation and research
Chg	Chitosan glutamate
cm	Centimetre
CNS	Central nervous system
DSC	Differential scanning microscopy
DSD	Droplet size distribution
EE	Entrapment efficiency
FDA	Food and drug Administration
FT-IR	Fourier transformed-infrared spectroscopy
g	gram
h	Hour
HPLC	High performance liquid chromatography
LD	Loading drug
LUVs	Large unilamellar vesicles
MCC	Mucociliary clearance
mg	Milligram
min	Minute
ml	Millilitre
MLVs	Mltlamellar vesicles
mm	Millimetre
mPa·s	Millipascal-second
OLVs	Oligolamellar vesicles
PBS	Phosphate buffer solution
PC	phosphatidylcholines
PE	Phosphatidylethanolamines
pMDI	Pressurized metered dose inhaler
PS	Particle size
PS	Phosphatidylserines
RH	Ropinirole hydrochloride
rpm	Rotation per minute
SD	Standard deviation
sec	Second
SEM	Scanning electron microscopy
Span	It is unit less term use to express range of

SPC	particle size distribution
SUVs	Soya phosphatidylcholine
TD	Small unilamellar vesicles
TGA	Tapped density (gm/ml)
TLC	Thermogravimetric analysis
VMD	Thin layer chromatography
	Volume median diameter (μm)

CHAPTER 1

INTRODUCTION

1.1 Nasal drug delivery

1.1.1 Historical background

Since last century intranasal delivery has been used for various purposes such as for relieving nasal decongestion, rhinitis and migraine. Crushed leaves of *Ranunculus acris* have been used via nasal inhalation by the Red Indian of North America to relieve headache. In China, extracts of aloe wood and sandalwood were used for treating emesis by inhalation through the nasal route. The nasal route has also been used to administer tobacco by nasal snuffing (Quraishi et al., 1997). American Indians used it as early as the 1400s (Christen et al., 1982). Indian tribes in Brazil used V-shape instrument known as ‘*Tipi*’ to blow powdered tobacco to one another for enjoyment and relaxation, and refresh their memory (www.snuffhouse.org) (Figure 1.1). The American Indian used an instrument known as ‘*tobaca*’ or ‘*tobago*’, which is a hollow Y-shape pipe to inhale powdered tobacco. For snuffing, they placed two ends of the Y-shape pipe into each nostril and the lower end near the powdered tobacco (Christen et al., 1982). The nose is still the favoured route for drug abuse, for instance when using opium drugs (Davis, 1999).



Figure 1. 1: Consuming snuff with large V-shaped straws called ‘*Tipi*’, by a partner (www.snuffhouse.org).

1.1.2 Why the nasal route?

The oral route is the most convenient and popular route for drug delivery. Despite the popularity of oral route alternative routes such as transmucosal delivery have been extensively investigated for drugs lacking effective systemic absorption via the gastrointestinal tract (GIT), therapeutic agents having chemical instability in the GIT fluids, drugs that undergo first-pass hepatic deactivation and therapeutic molecules which cause GIT adverse effects. Alternative routes have been investigated such as intra-nasal and parenteral in order to achieve faster and higher drug absorption and hence offering improved drug bioavailability, enhanced therapeutic effect and promoted patient compliance (Mathias and Hussain, 2010). Significant enhancement in the drug absorption following nasal administration compared to oral delivery has been demonstrated (Dhakar et al., 2011). However, for improvement of intranasal drug absorption with molecules larger than 1000 Daltons, permeation enhancers are needed in the formulation (Ozsoy et al., 2009).

Nasal delivery is appropriate for administration of drugs to treat local nasal diseases such as sinusitis and allergic rhinitis since low doses are sufficient to provide therapeutic effects with low systemic side effects. In addition, nasal delivery might be suitable for drugs which are effective in low doses and have low oral bioavailability (Dhakar et al., 2011). The rate of absorption, and the pharmacokinetic properties of small drug molecules used for systemic therapeutic effects, administration via the nose are comparable to the parenteral route due to the nature of the nasal pathway which provide a large surface area, rich vascularity and drug high permeability (Illum, 2003; Dhakar et al., 2011) (Figure 1.2). Nasal delivery is also applicable in emergency cases (Bitter et al., 2011).

Despite the nose has lower surface area compared to the lung, it provides an efficient site for systemic absorption particularly for drugs with low water solubility (Davis, 1999). Many drugs do not reach the brain following oral or parenteral administration due to the blood-brain barrier (BBB). The olfactory region of the nose is not covered by the blood brain barrier, hence evasion the BBB following nasal administration might be possible. This approach is effective for drug targeting to the brain (Wen, 2011). Furthermore, the nose is attractive for vaccine delivery since provoking mucosal secretory antibodies at the site of entry of pyrogens may provide additional

immunoprotection for immunization (Burt et al., 2011). Nasal drug delivery offers many advantages, but has some limitations (Table 1.1).

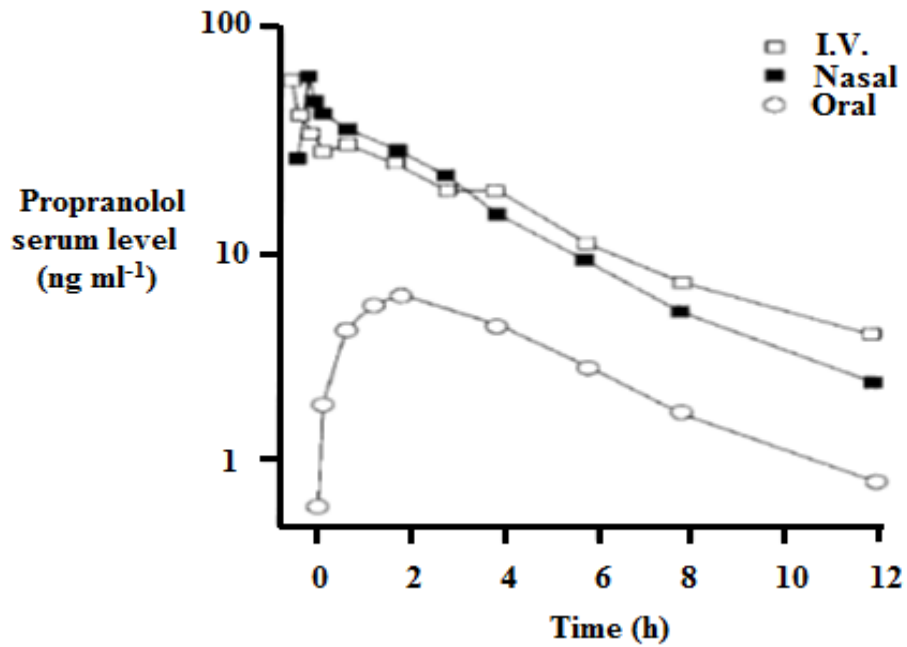


Figure 1. 2: Serum level of propranolol after administration using nasal, i.v and oral routes (Adapted from Washington et al., 2001).

Table 1. 1: Advantage and limitations of nasal route (Behl et al., 1998; Singh et al., 2012).

Advantages	Limitations
Suitable for drugs that are acid labile in the stomach	Volume that can be delivered into nasal cavity is restricted to 25–200 μ l
Applicable for drugs that undergo extensive hepatic first-pass effect	High molecular weight compounds cannot be delivered through this route (mass cut off \approx 1 kDa)
Rapid drug absorption and onset of action	Adversely affected by pathological conditions of the nose
Offers higher drug bioavailability, thus lower doses of drug are needed	Large interspecies and patient to patient variabilities are observed when using this route
Offers large surface area for drug absorption (approximately about 150 cm^2)	Normal defense mechanisms like mucociliary clearance can affect the absorption of drug
No particular skills or expertise are required for nasal drug administration	Local enzymes in the nasal cavity might degrade some drugs
Direct transportation of drug to the systemic circulation or CNS is possible	Local side effects like irritation might be happen
Offers lower risk of overdosing	Small surface area compared to the GIT
Needle-free and patient friendly	Nasal congestion from colds and flues may interfere with efficient drug delivery via this route
Offers induction of immune response when used for vaccine delivery	Frequent delivery of drugs may cause mucosal damage, hence patient becomes liable to microbial invasion through the nasal epithelium

1.1.3 Anatomy of the nose

The nasal passage is 12-14 cm deep and runs from the nasal vestibule to the nasopharynx. It has three main regions; vestibular, respiratory and olfactory regions. The nose has a volume of 16-19 cm³ and a surface area of approximately 180 cm² with two cavities (i.e. nostrils) separated by the nasal septum (Figure 1.3).

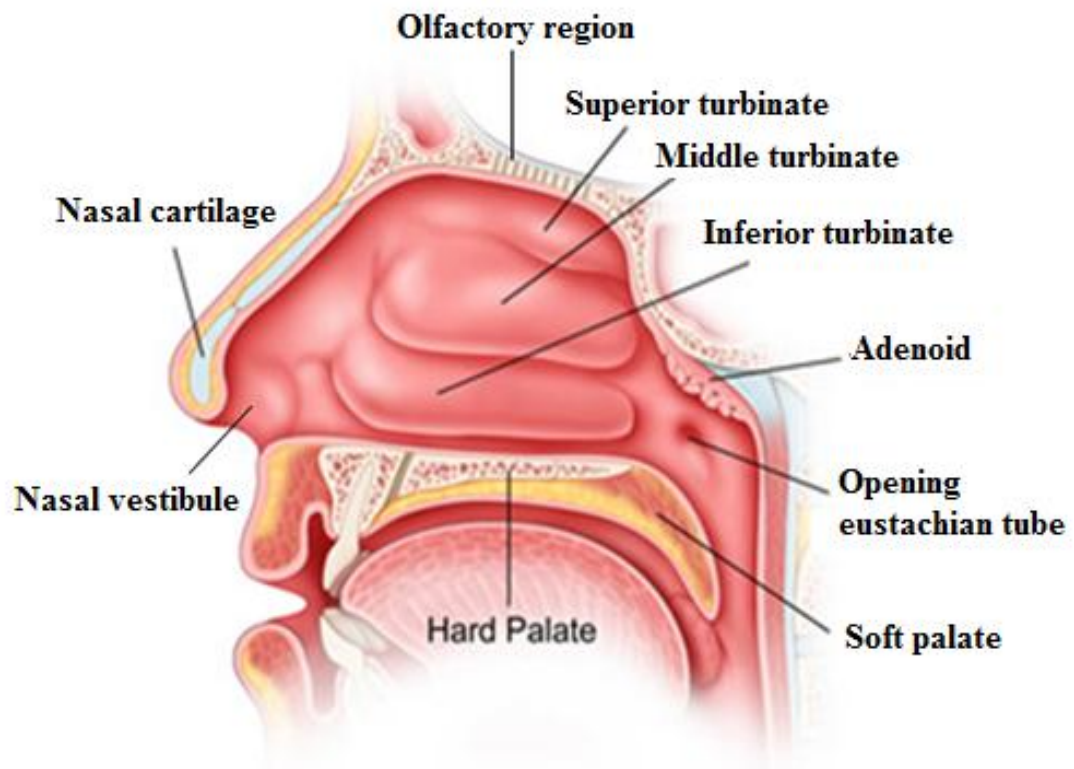


Figure 1. 3: Anatomy of the human nasal cavity (Adapted from www.lasinus.com).

The vestibular region is located at the front opening of the nasal passages which filters out particles from the inhaled air. However, drug delivery and absorption in this region is least important. This area is covered with hairs which filter the air to prevent airborne particles entering the respiratory system. The respiratory area is large with a high degree of vascularity and a surface area of about 130 cm². In this region the majority of drug absorption occurs. It is lined with pseudostratified columnar epithelium and covered with a dense layer of mucus which moves towards the posterior apertures of the nasal cavity because of the ciliary rhythmic movements (Chien et al., 1989). The olfactory region is important for transporting the drug to brain and cerebro-spinal fluid and has a surface area of about 15 cm². It is made of thick connective tissue and lamina

propria, into which the olfactory epithelium rests. The thickness of nasal mucosa ranges between 2 and 4 mm. The epithelium cells line the nasal passage and are covered by a mucus layer 5µm in thickness which traps unwanted particles. The mucous secretion consists of water (95%), mucin (2%), salts (1%), proteins (1%) such as albumin, immunoglobulin, lysozyme, and lactoferrin, and lipids (1%). IgA, IgE and IgG are also present in the mucous secretion (Ozsoy et al., 2009). The pH of the nasal secretion is ranged from 5 to 6.5 (Ugwoke et al., 2005). Ciliary action is responsible for clearing the mucus layer from the nasal cavity and mucus is renewed 4 - 6 times per hour. The mucus moves through the nose at a rate of 5-6 mm/min (Graf, 1986). The characteristics of human nasal epithelium are summarised in Table 1.2.

Table 1. 2: Human nasal epithelium characteristics (Adapted from Pires et al. 2009).

Nasal regions	Histology of nasal epithelium	Functions	Surface area	Blood supply (i.e. vascularity)	Permeability
Vestibule	Stratified squamous and keratinized epithelial cells with nasal vibrissae	Support and protection	$\approx 0.6 \text{ cm}^2$	Low	Poor
Atrium	Stratified squamous cells and pseudostratified cells	Support	---	Low	Reduced
Respiratory region	Columnar non-ciliated cells, Columnar ciliated cells Globo cells Basal cells	Support to nasal function Clearance of particles Secretes mucus Progenitors of other cell types	$\approx 130 \text{ cm}^2$	Very high	Good
Olfactory region	Sustentacular cells, Receptor cells Basal cells	Support and bears synthetic olfactory Olfaction sensation Progenitors of other cell type	$\approx 15 \text{ cm}^2$	High	Direct path to CNS

1.1.4 Applications of nasal delivery

i) Local effects

The nose is exploited to treat regional disorders at relatively low effective doses with less systemic effects. Low molecular weight water-soluble or hydrophobic drugs are used to treat local pathological conditions in the nose. For example, Azelastine (Horak, 2008) is a rapid acting antihistamine, mainly acts as an antagonist on H₁- receptors, and as a mast cell stabilizer available as a nasal spray. Beclometasone (Ghimire et al., 2007) is an anti-inflammatory corticosteroid used to reduce inflammation and local allergy. It is a well-established drug for the treatment of allergic rhinitis. Nasal decongestants such as oxymetazoline are also administered via the nose for treating common colds (Pires et al., 2009; Sharma et al., 2006).

ii) Systemic effects

Nasal delivery is convenient for acid labile drugs, proteins and peptides when rapid action is required such as in migraine relief (Swamy and Abbasb, 2012). Nasal delivery offers a rapid action and efficient drug absorption compared to oral and intravenous delivery (Furubayashi et al., 2007). Most protein and peptide drugs have low bioavailability (1–2%) due to their high molecular weight and polarity, causing poor absorption through the nasal mucosal membranes. In contrast, the bioavailability of progesterone and propranolol via nasal epithelium is comparable to parenteral administration (O'Hagan and Illum, 1990). Lower bioavailability can be improved by using absorption enhancers in the formulations, thus prolonging the contact time of the drug with the mucous membranes using bioadhesive agents. A significant change in the relative bioavailability of isosorbide dinitrate was observed using 0.1% N-succinyl chitosan as absorption enhancer (69.85%) compared to the 0.5% chitosan (55.36%) and control groups (43.32%) in rats (Na et al., 2013). Steyn and co-workers have reported that the bioavailability of recombinant human growth hormone was increased significantly after nasal delivery in combination with N-trimethyl chitosan chloride as an absorption enhancer used in pheroid technology (Steyn et al., 2010). Examples of marketed intranasal drug delivery products of proteins, peptides and small molecules are summarized in Table 1.3.

Table 1. 3: Nasal Proteins, Peptides and non-peptide formulations for systemic effect available in the market (Adapted from Singh et al., 2012).

Name of the product	Indication (s)	Manufacturer
Miacalcin [®] (Calcitonin nasal spray)	Postmenopausal osteoporosis	Novartis Pharma
Lazanda [®] (fentanyl nasal spray)	Management breakthrough cancer pain	Archimedes Pharma
Suprecur [®] (Buserelin acetate)	Prostate cancer, endometriosis, infertility	Sanofi-Aventis
Oxytocin [™] factor	Stress relief	ABC Nutraceuticals
Zolmist [®] (Zolmitriptan)	Migraine	Cipla
Migranal [®] (Dihydroergotamin)	Migraine	Novartis Pharma
Aerodiol [®] (Estradiol)	Postmenopausal hormone replacement	Servier
MSH2-Pro [™] (Melanocyte-stimulating hormone)	Reduce appetite and increases libido	International Antiaging Systems
DDAVP [®] (Desmopressin acetate)	Antidiuretic hormone	Sanofi-Aventis
Nascobal [®] (Cyanocobalamin)	Vitamin B12 deficiency	Strativa Pharmaceuticals

iii) Vaccines delivery

Vaccines and their applications via nose to treat respiratory infections have been investigated. The localization of immune system components in the mucosal membrane means that the respiratory epithelium is the first defence line in the body against infections (Bitter et al., 2011). Nasal mucosa is further enriched by lymphoid tissue. It enhances the systemic levels of specific immunoglobulin G and nasal secretory immunoglobulin A and the local immune responses which provide additional protection against invading microbes (Mestecky et al., 1997). Nasal mucosa is advantageous for immunization due to its permeability, low enzymatic activity and accommodation of the nose-associated lymphoid tissue (NALT) (Bitter et al., 2011). The delivery of vaccine via the nose represents a convenient needle-free procedure for vaccination. Furthermore, the nose-associated lymphoid tissue (NALT) is an effective immune system (Brandtzaeg, 2011). Nasal vaccines that have been investigated include influenza A and B (Huang et al. 2004), proteasome-influenza (Langley et al., 2006), adenovirus-vectored influenza (Van Kampen et al., 2005), attenuated respiratory syncytial virus and parainfluenza 3 virus (Belshe et al., 2004). Commercially available nasal vaccines include nasal spray of Human influenza vaccine (FluMist[®]) and nasal drop of Equine influenza vaccine (Flu Avert[®]) manufactured by MedImmune Inc. and Heska respectively.

iv) CNS delivery

The intranasal route is promising for the delivery of drugs to the brain via the exploitation of the olfactory neuroepithelium in the nose (Figure 1.4a), possible pathways to transfer drugs from nose to the brain have been explained by Illum, (2000) (Figure 1.4b). This strategy has been considered for the treatment of Alzheimer's disease, brain tumours, epilepsy, pain and sleep disorders (Pires et al., 2009). Delivery of nerve growth factor to the brain in rodents has been reported (Frey et al., 1997; Chen et al., 1998) and in humans studies insulin (Hinchcliffe and Illum, 1999) and proteins (Pietrowsky et al., 1996) have been directly transferred through olfactory path to the CNS via nasal cavity. Successfully transnasal delivery 0.5mg/kg of siRNA to the CNS with highly brain concentration compared to the other tissue has been reported by Malhotra co-workers to treat neurological disorders using peptide-tagged PEGylated chitosan nanoparticles formulations to deliver siRNA via nose (Malhotra et al., 2013). Recent publications that investigated brain targeting via the nose are summarized in Table 1.4.

Table 1. 4: Recent studies carried out to deliver drug molecules to the brain via nasal route.

Drug molecule	Purpose	Reference
siRNA	Treatment of neurological disorder	(Malhotra et al., 2013)
Levodopa	Treatment of Parkinson's disease	(Sharma et al., 2013)
Clonazepam	Prevent and control seizures	(Abdel-Bar et al., 2013)
Folic Acid	Treatment or prevention of Alzheimer's disease	(Nagaraju et al., 2013)
duloxetine	Treatment of depression	(Alam et al., 2013)

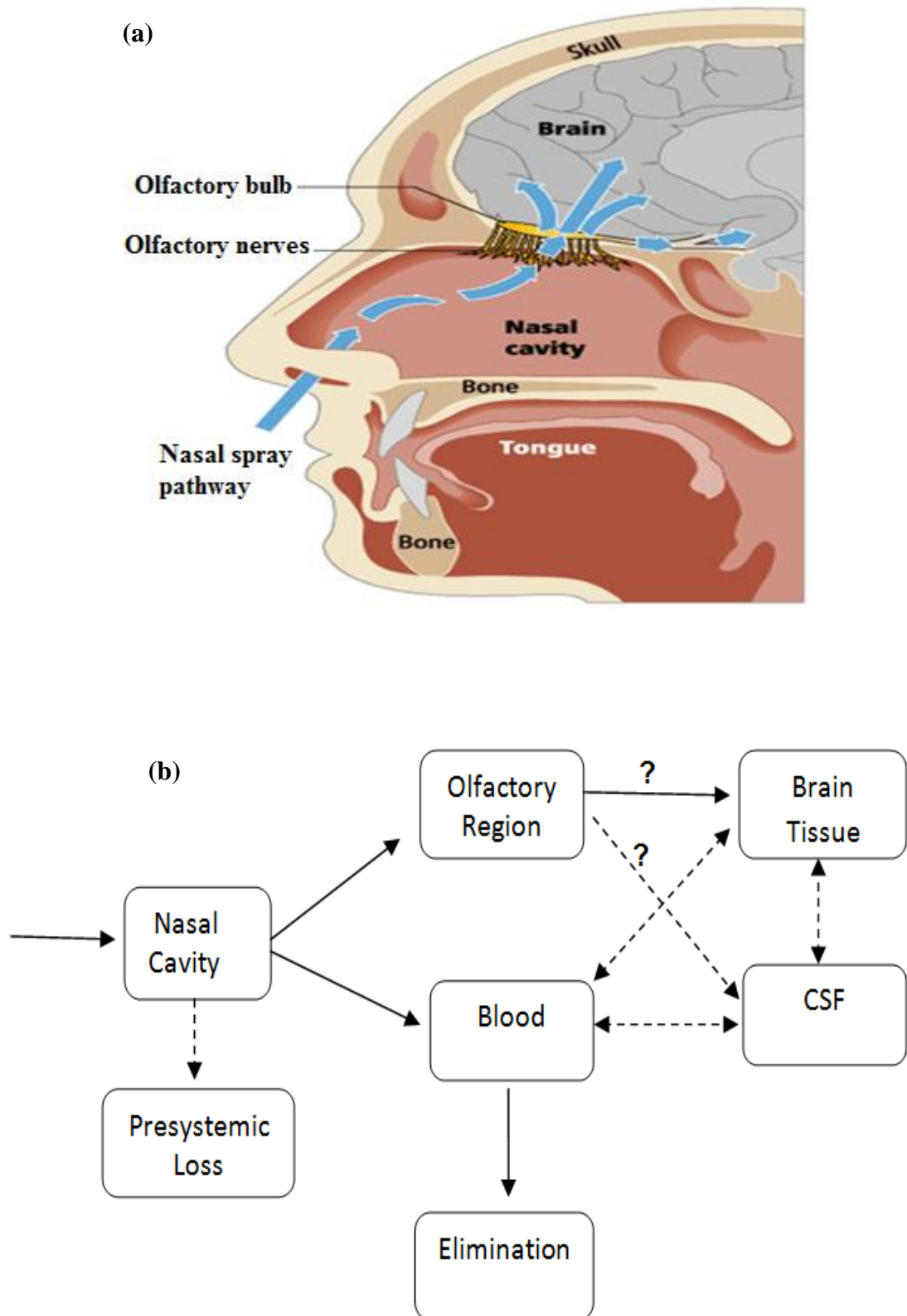


Figure 1. 4: (a) Nose to brain pathway (Adapted from Olson, 2008), (b) a schematic illustration of the possible drug molecule transfer delivered nasally. (---) indicates limited substrate delivery via this route, and (?) indicates the exact pathway is unclear (Adapted from Illum, 2000).

1.2 Mechanisms of drug transport following intranasal administration

The drug must pass through the mucus layer of the nasal cavity for absorption to take place. Uncharged molecules pass through the mucus much more readily than charged molecules. Two main mechanisms of drug absorption through nasal mucosa have been proposed: paracellular absorption and transcellular absorption (Figure 1.5).

Firstly, the paracellular route is energy independent and occurs by drug passing through the aqueous spaces between the cells via a slow passive diffusion. In general, as the molecular size of the drug increases the intranasal absorption via this route decreases. For example, a drug with a molecular weight greater than 1 kDa has poor systemic bioavailability following nasal administration (McMartin et al., 1987), and bioavailability of these molecules can be enhanced using absorption enhancers (Ozsoy et al., 2009). Zhang et al. (2005) demonstrated that the systemic absorption of large molecular weight of recombinant hirudin-2 (rHV2) (6900 Daltons) improved intranasally by including absorption enhancer (e.g. chitosan 0.5%, hydroxypropyl- β -cyclodextrin 5%, or ammonium glycyrrhizinate 1%) into the formulation.

Secondly, transcellular absorption mechanism is applicable to lipophilic drugs, which are readily absorbed by diffusion through the epithelial cellular membranes of the nose. Transcellular transport of drugs might be carrier mediated or may involve opening of tight junctions for drug absorption. Excipients used in nasal formulations such as chitosan opens the tight junctions between cells and thus the drug transportation from nasal cavity to the systemic circulation is facilitated (Dodane et al., 1999; Mathiowitz et al., 1999).

Thirdly, substances in the nasal mucosa particularly in the olfactory mucosa include: P-glycoprotein, organic cation transporter, dopamine transporter, and amino acid transporters. These transporters transfer amino acids, amines and cations (Agu et al., 2003; Kandimalla and Donovan, 2005a, 2005b). This mechanism is known as carrier mediated processes (Kimura et al., 1989).

Fourthly, the mechanism for drug transportation is endocytosis. In this mechanism materials are engulfed into the cell. The uptake of particles by nasal epithelial cells is mediated by the M cells. Endocytosis is the predominant mechanism for transporting

compounds that have molecular weights higher than 1000 Da such as proteins, peptides (Costantino et al., 2007), polypeptides and polypeptide-coated nanospheres in the range of 500 nm (Porta et al., 2000). It has been reported that the absorption of polar molecules (Illum, 2000) and larger peptides (Hinchcliffe and Illum, 1999) are greatly improved by the incorporation of absorbing enhancers into the formulation such as surfactants (e.g. sodium laurylsulfate), enzyme inhibitors (e.g. bestatin), bile salts (e.g. sodium deoxycholate), chitosan, and cyclodextrins (Davis and Illum, 2003; Jadhav et al., 2007).

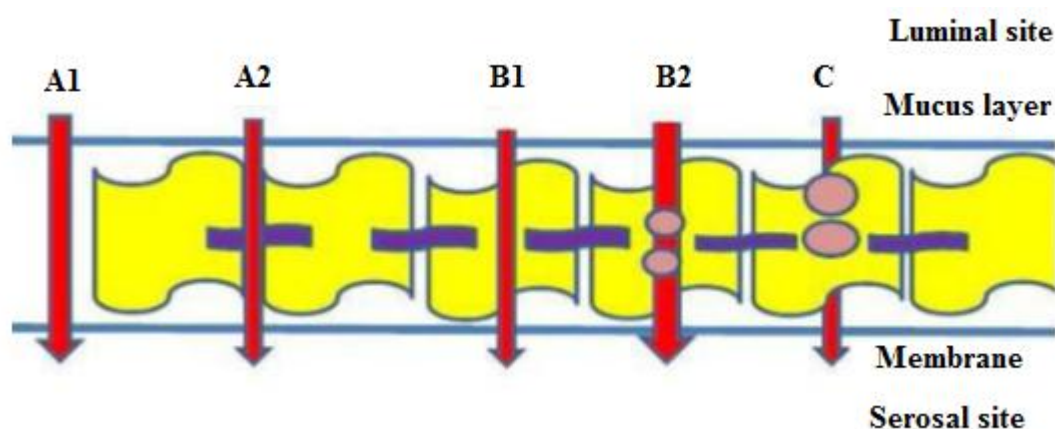


Figure 1. 5: Mechanisms of drug transport across epithelial cells: [A1] Intercellular spaces, [A2] Tight junctions, [B1] Passive diffusion, [B2] Active transport, and [C] Transcytosis (Adapted from Kushwaha et al., 2011).

Permeation enhancers accelerate the rate of transportation of hydrophilic and larger protein and peptide molecules through mucosal membranes. A number of parameters control the safety and efficacy of nasal permeation enhancer, such as enzymatic activities of Cytochrome P450 isoenzymes in the nose, mucociliary clearance, duration of contact between formulation and nasal mucosa (Merkus et al., 1998). Absorption enhancers reversibly change the nasal mucosa, effectively increasing the drug absorption and do not cause local or systemic irritation or toxicity and their action is reversible (Aurora, 2008).

1.3 Factors affecting nasal drugs delivery

For applications in brain targeting, local delivery and systemic delivery of drugs several factors should be considered prior to designing intranasal formulations. These are the physicochemical properties of drug, excipients to be included in formulation and the physiological condition of the nasal cavity (Figure 1.6) (Behl et al., 1998; Dhakar et al., 2011) .

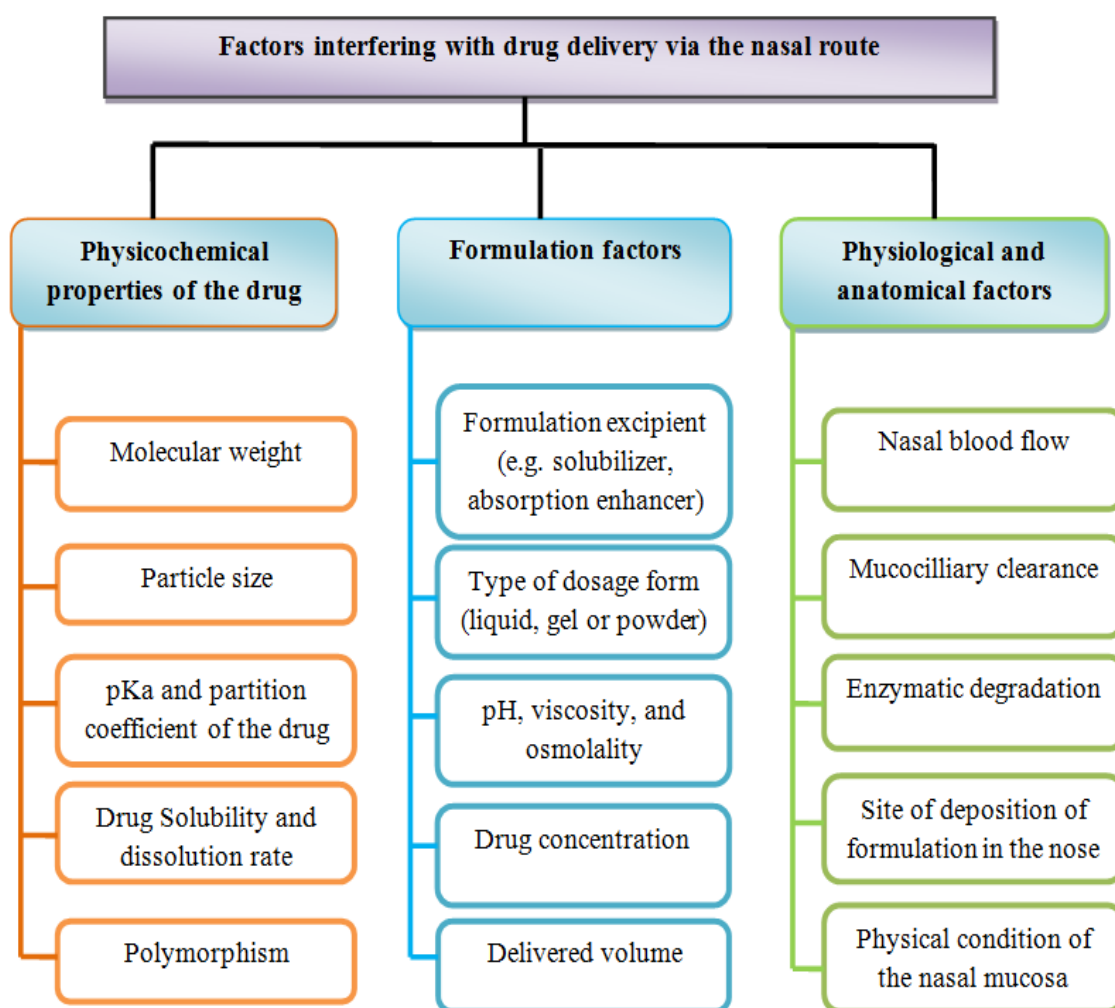


Figure 1. 6: Barriers interfering with drug delivery via the nasal route (Adapted Behl et al., 1998; Dhakar et al., 2011).

1.4 Barrier interfering nasal drug delivery

1.4.1 Low drug bioavailability

Low bioavailability of some drugs might be ascribed to the high polarity or large molecular size (e.g. peptides and proteins). It has been reported that bioavailability of low molecular weight of hydrophilic drugs is around 10%, whereas less than 1% of larger molecules such as proteins (calcitonin) and peptides (insulin) are bioavailable (Illum, 2002). Nasal route is efficient, rapid and suitable for delivery of drug molecules having molecular weight less than 1000 Da. For particulate materials, particle size has an effect on absorption through the nasal epithelium. It has been reported that particles smaller than 1 μm may rapidly be absorbed following intranasal delivery (Donovan & Huang 1998).

Proteins and peptides are transported across nasal epithelium in low proportions via endocytosis (Jadhav et al., 2007). The low bioavailability of polar drugs, peptides and small proteins could be improved by using permeation enhancers (Dhakar et al., 2011; Illum, 2000). Chitosan is a natural mucoadhesive permeation enhancer for water soluble drugs (e.g. Atenolol) by opening the tight junctions between cells (Schipper et al., 1999). Tengamnuay et al. (2000) have shown that chitosan can enhance the nasal absorption of peptides. The absorption of relatively impermeable small drug molecules also improved since it was prepared as an amino acid prodrug. For example, the absorption of acyclovir increased to 8% within 90 min when acyclovir was formulated as amino acid prodrug with L-Aspartate beta-ester, suggesting that prodrug might be transferred across mucosal membrane by active transportation rather than passing through pores (Yang et al., 2001).

1.4.2 Mucociliary clearance

Mucociliary clearance (MCC) is an essential defense mechanism for the elimination of foreign materials, pathogens and particles from the nose. Materials are trapped in the mucus layer and are subsequently transported by ciliary beating to the nasopharynx and eventually to the gastrointestinal tract (Merkus et al., 1998) (Figure 1.7). This process reduces the nasal absorption of drugs (Jadhav et al., 2007). Overcoming the MCC and increasing the residence time of drug in the nasal cavity are obtained by incorporation of

mucoadhesive agents into formulation, which may enhance nasal absorption. Soane et al. (1999) have shown that the clearance half-life of radiolabeled material in liquid was 15 minutes from the nasal cavity using conscious sheep. By contrast, using bioadhesive chitosan solutions the half-life was 43 min and when employing bioadhesive chitosan microspheres the half-life exceeded 110 min. Chitosan may decrease MCC, hence increasing contact time of the delivery system with nasal mucosa, which enhances the drug bioavailability (Soane et al., 1999).

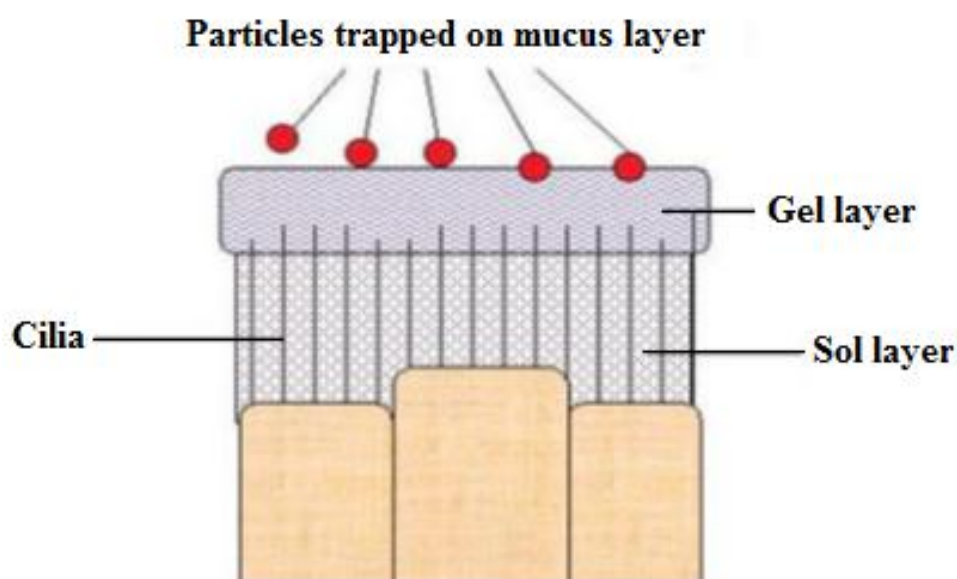


Figure 1. 7: Nasal mucociliary clearance (Adapted from Aurora, 2008).

MCC can also be influenced by targeting the region of drug deposition in the nose. Posterior part of the nose is more ciliated than its anterior part, therefore the clearance of the drug deposited posteriorly might be faster than the drug deposited in the anterior part of the nose (Ugwoke et al., 2000). For example, nasal sprays deposit drugs mainly in the anterior sections of the nasal cavity, leading to slower clearance than nasal drops which are directly instilled into the deeper regions of the nose (Illum, 2003).

Hydrophilic molecules are highly soluble in the mucous and are highly cleared by MCC and their passage across the nasal membrane is very slow. Hence, factors that influence the MCC may modify the drug absorption profile. Environmental factors such as cold air (Diesel et al., 1991) and air pollution (e.g. presence of sulfur dioxide) (Wolff, 1986) caused reduction in the MCC. Cigarettes may increase the viscosity of the mucus and

decrease the MCC (Houtmeyers et al., 1999). Pathological factors also affect the MCC, for instance, in asthmatic and chronic obstructive pulmonary disease (COPD) patients (Merkus et al., 1998) (Table 1.5).

Table 1. 5: Pathological conditions that may affect nasal mucociliary clearance (Adapted from Merkus et al., 1998).

Pathological conditions	MCC activity	Proposed mechanism
Asthma	Increased Decreased	Irritation and inflammatory process Epithelium damage
Diabetes mellitus	Impaired	dehydration and damaging of microvascular
Cystic fibrosis	Impaired	Epithelium damage
Bacterial and viral infections	Impaired	Loss of cilia and change of mucus properties
Primary ciliary dyskinesia	Impaired	Absence or dysfunction of cilia

1.4.3 Enzymatic degradation

Bogdanffy (1990) showed that some drugs, proteins and peptides may degrade by the enzymatic activity in the nose. Carboxyl esterases, aldehyde dehydrogenases, epoxide hydrolases, glutathione S-transferases and cytochrome P450 isoenzymes are present in the nasal epithelial cells and play a role in the degradation of drugs in the nasal mucosa (Bogdanffy, 1990). The enzymatic barrier may be overcome by using either enzyme inhibitors or enzyme saturators (Morimoto et al., 1991a). Morimoto, (1991a) used camostat mesilate as a proteolytic enzyme inhibitors. This strategy enhances the permeation of vasopressin and desmopressin across the nasal mucosa. It has also been reported that protection of salmon calcitonin by poly(ethylene glycol) from enzymatic degradation may enhance the absorption of salmon calcitonin across the epithelium (Na et al., 2004; Shin et al., 2004).

1.5 Dosage forms for intranasal administration

Delivery of drugs via the nose has some challenges. Physicochemical properties of the drug and nasal formulations must be considered to achieve appropriate delivery. Effectiveness of the drug in low dose, aqueous solubility, minimal nasal irritation, absence of toxicity on the nasal mucosa and chemical stability of the drug administration via nose should all be considered (Behl et al., 1998).

Nasal formulation design depends on the therapeutic requirements of the particular drug molecule, the time needed for the drug to elicit its therapeutic effect, the duration of therapy, patient population, proposed indication and marketing preferences. The nasal route provides potential for both controlled and conventional drug release. The mode of drug delivery whether it is local or systemic determines the type of excipients to be used (Jadhav et al., 2007). Three major types of dosage form are available for nasal administration: liquids, powders, and gels. Ointments and emulsion are also available but less common (Behl et al., 1998).

1.5.1 Liquid formulations

Liquid dosage forms are usually aqueous solutions, suspensions or emulsions, however, formulations made with oily or alcoholic vehicles are also available. Humidifying effect is important for nasal mucosa as allergy and irritation are mainly related to dryness of the mucus membrane. The main drawbacks of liquid dosage forms are:

- (i) The microbial growth is possible, necessitating the use of preservatives.
- (ii) Long-term use of liquid dosage forms may interfere with nasal mucociliary function and cause irritation due to the presence of preservatives in the nasal formulations.
- (iii) Short half-life of the drug because of its liability for degradation (Kublik and Vidgren, 1998).
- (iv) Probability of dripping out of the liquid dose from the nostril following administration (Keldmann, 2005). Liquid dosage forms are easily removed to the posterior part of the respiratory tract by mucociliary clearance (Jiménez-castellanos et al., 1993).

1.5.2 Nasal Powders

Preparation of chemically unstable drugs as powders enhance their stability profile compared to their solutions or dispersions. Powder dosage form is suitable for non-peptide and peptide drugs with no preservatives or freeze storage being required (Huang et al., 2004; Jadhav et al., 2007). Residence of the powdered drug in the nose can be improved compared to liquid formulations and patient compliance might also be enhanced, especially with drugs having unpleasant odour or taste. However, when preparing nasal powders several factors need to be considered. These are solubility of the drug, particle size of the powdered formulation, aerodynamic properties of the particles and the possible irritation of the drug or excipients on the nasal epithelium (Kublik and Vidgren, 1998). Ideally, particles larger than 10 μ m are likely to deposit in the nasal passages (Behl et al., 1998), whilst particles larger than 0.5 μ m filtered out in the nose (Burgess et al., 2004). Depending on the bulk density of the powder, it is possible to administer up to 50 mg of the formulation, whilst the maximum volume of liquid administration for each nostril in one time is 150 μ l (Davis, 1999).

The polymer in powder formulations enhances the interaction between the drug and mucosa by converting into a viscous gel following contact with the fluids in the nasal cavity, resulting in decreased mucociliary clearance and prolonged residence of the drug in the nasal cavity. This can improve drug permeation, increase drug bioavailability and sustain drug release from its viscous matrix (Illum et al., 1987; Soane et al., 2001). Using sheep as an animal model and gamma scintigraphy for imaging, Soane et al. (2001) have found the rate of clearance of chitosan microparticles from nasal cavity to be slower than chitosan solution.

Powder formulations consisting of water insoluble and non-swellable drug carriers improve the bioavailability of hydrophilic drug molecules. Ishikawa et al., (2001) showed systemic bioavailability of the elcatonin based on calcium carbonate in rabbits and rats increased after nasal administration compared to the liquid form. Optimization of particle size and morphology for nasal formulations may reduce the risk of mucosal irritation and enhance the deposition (Gad, 2008). The mucosal irritation, difficulty and cost of the formulation due to optimization of particle size and morphology are major limitations for development of powdered nasal formulations (Behl et al., 1998). Insufflators are convenient and simple devices for nasal administration of powders (Kublik and Vidgren, 1998).

1.5.3 Nasal Gels

Pharmaceutical gels are semisolid preparations in which the drug is dispersed in a polymeric matrix. Gels have several advantages including:

- (i) Reduced mucociliary clearance owing to the high viscosity of gels.
- (ii) Masked unpleasant taste of the formulation due to reduced accessibility of the formulation to the nasopharynx.
- (iii) Reduced loss of the formulation from nostril while breathing or sneezing.
- (iv) Minimized irritation due to the soothing effect of excipients used in nasal gel.
- (v) Enhanced contact between the drug and nasal mucosa, which may enhance the absorption profile of the drug (Behl et al., 1998). Vitamin B12 was the first nasal gel introduced to the market. TBS-3 is an intranasal gel formulation of dopamine used for the treatment of Parkinson's disease (www.trimelpharmaceuticals.com).

1.6 Factors affecting particle deposition in nasal cavity

The nasal system is responsible for filtering air during inhalation of harmful materials, which may deposit in the respiratory airways. Five mechanisms have been proposed for deposition of nasally inhaled particles, which are impaction, sedimentation, diffusion, interception and electrostatic precipitation. However, only diffusion, impaction and sedimentation have major roles in nasal deposition of particles (Lippmann et al., 1980).

Interception mechanism is important for deposition of fibrous molecules when the trajectory of particle is close to the epithelium. Straight fibres such as amphibole asbestos may have higher probability to travel to the alveolar region than chrysotile asbestos (non-needle shape) of similar size, because the fibres may orientate themselves parallel to the air flow streamline (Lippmann et al., 1980).

Brownian diffusion mechanism is important for particles smaller than 0.5 μm , resulting in possible deposition in the alveolar region, small airways and airway bifurcations. In the small conducting airways, bronchioles, and the alveolar region when the air velocity is low the deposition of particles mainly occurs by gravitational sedimentation which is

influenced by changes of particle size (Lippmann et al., 1980; Kublik and Vidgren, 1998). Stoke's equation (Eq. 1.1) describes the rate of particle settling being proportional to the square of the particle diameter (Kublik and Vidgren, 1998).

$$(\rho - \sigma)gd^2/\gamma \quad (\text{Eq. 1.1})$$

Where: ρ is density of the particle; σ is density of the air; d is diameter of the particle; g is gravitational acceleration, and γ is viscosity of the air.

The diffusion mechanism is prominent for deposition than sedimentation mechanism when the settling velocity of the particles falls below 0.5cm/s (Lippmann et al., 1980). Impaction mechanism is significant for deposition in the nose and oropharynx when the particles are larger than 1 μ m and occurs when the particle changes its direction during inhalation (Kublik and Vidgren, 1998). The probability of deposition by impaction mechanism in bend airway can be described by equation 1.2:

$$(Ud^2 \sin\theta)/R \quad (\text{Eq. 1.2})$$

Where: θ is angle of the bend; U is airstream velocity; d is particle aerodynamic diameter and R is airway radius.

It has been concluded from Eq.1.2 that the anatomy of the airways and inhaled particle size and the velocity of airstream all have effects on particle deposition by impaction (Kublik and Vidgren, 1998).

1.7 Mucoadhesive drug delivery systems

The concept of mucoadhesion, also called bioadhesion, has been applied since 1980s, in order to increase the residence time of formulations at the site of absorption for local or systemic therapeutic effects (Patil and Sawant, 2008). Mucoadhesive agents are synthetic or natural polymers which adhere to biological or mucosal surfaces (Carvalho et al., 2010). Mucoadhesion results from strong interactions between polymer and the mucus (Lee et al. 2000).

Mucoadhesive systems are formulations used to slow down the mucociliary movement, decrease mucosal enzymatic activity and open the tight junctions to enhance permeation of drug through the epithelial tissue (Smith et al., 2004; Chaturvedi et al., 2011). Mucoadhesive systems thus improve therapeutic outcomes by keeping the drug at the site of action for extended time, target the drug to the specific tissue and control the drug release, resulting in decreased frequency of drug administration and improve patient compliance (Carvalho et al., 2010; Shaikh et al., 2011).

Mucoadhesive systems may also improve the dissolution of poorly water-soluble drugs (Gavini et al., 2011). Gavini et al. (2011) observed improvements in the solubility of rokitamycin loaded into chitosan microspheres compared to the free drug when the intranasal drug absorption was assessed *in vivo* using rat as animal model. Mucoadhesion is suitable for tissues covered with mucus such as those in the buccal, sublingual, vaginal, rectal, ocular, gastrointestinal and nasal regions, resulting in improved drug absorption (Smart et al. 1984; Tsuneji et al. 1984; Morimoto et al. 1991). A number of theories explain the mechanisms involved in the interactions between polymers and mucus. An optimal degree of polarity is required for the polymer to wet and swell sufficiently when contacting the mucus layer, and interpenetration between mucus and polymer chains should take place to achieve bioadhesion (Patil and Sawant, 2008).

Various biocompatible and biodegradable polymers have been used to formulate mucoadhesive system for examples, poly-vinyl alcohol (Swamy and Abbas, 2012), PLGA (Guerrero et al., 2008), chitosan (Alhalaweh et al., 2009) and hydroxypropylmethylcellulose, hydroxypropyl- cellulose and sodium alginate (Rathananand et al., 2007).

1.7.1 Chitosan

In recent years chitosan has been used in drug delivery formulations and widely in the pharmaceutical industry due to safety and availability (He et al., 1999, 1998). Chitosan polymer is a useful drug delivery matrix due to its polycationic nature, ability to improve dissolution of poorly water soluble drugs, biodegradability, biocompatibility non-toxicity, mucoadhesive properties and convenience in manipulating the physical characteristics and chemical structure (Sinha et al., 2004). Chitosan is a linear polysaccharide derived by the deacetylation of chitin obtained from crustacean shells (Figure 1.8). It is a weak base, poorly soluble in water and practically insoluble in all common organic solvents, however it dissolves in acidic aqueous solutions (dos Santos et al., 2005).

Chitosan is used in tablet formulations as a disintegrant, binder or vehicle for controlling the drug release and improving the dissolution and bioavailability of poorly soluble drugs (Sinha et al., 2004). Chitosan has been formulated as microspheres for controlled drug delivery, for example, many drugs such as zolmitriptan (Alhalaweh et al., 2009), 5-fluorouracil (Sun et al., 2010), aceclofenac (Nagda et al., 2010), ketorolac (Nagda et al., 2012), cisplatin (Singh et al., 2012), albendazole (García et al., 2013), and ofloxacin (Park et al., 2013) have been formulated as chitosan microspheres. The mucoadhesiveness of chitosan arises from the electrostatic interactions between the cationic amino groups on the chitosan and the anionic moieties on the mucus layer such as sialic and sulphonic acid groups (Lachman et al. 1986). *In vitro* studies of mucoadhesion on sheep nasal mucosa conducted by Patil and Murthy (2006) demonstrated that when the concentration of chitosan was increased the level of mucoadhesion also increased due to the increase of the number of cationic amino groups available for interaction with sialic acid residues of the mucin. Chitosan can also enhance the epithelial permeability of the drug through the epithelial cells (Fernandez-Urrusuno et al., 1999; Smith et al., 2004) and can decrease the nasal mucociliary clearance, resulting in prolonged drug contact with nasal epithelium and enhanced drug absorption (Soane et al. 1999).

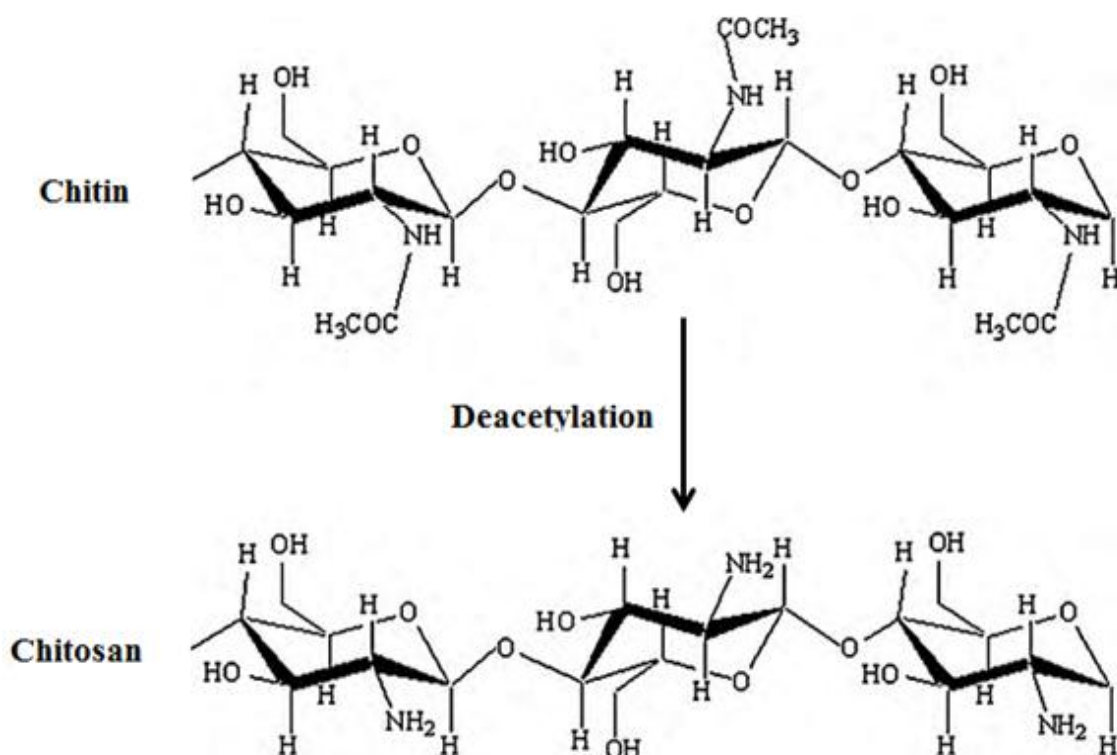


Figure 1. 8: Chemical structure of chitin and chitosan (Adapted from Jayakumar et al., 2010).

1.7.2 Sodium alginate

Alginic acid also called algin or alginate is a hydrophilic colloidal natural polysaccharide, consisting of a linear copolymer of (1,4)-linked β-Dmannuronic acid (block M) and α-L-guluronic acid residues (block G) (Figure 1.9) (Gombotz and Wee, 1998), and a sodium ion attached to carboxylate groups to balance its charges. It is available in filamentous, granular or powdered forms usually having a white to yellowish-brown colour. It is an anionic polysaccharide extracted from cell walls of brown algae (seaweed). When it contacts with water alginate forms a viscous gum due to its aqueous solubility and can absorb more than 100 times its weight of water (Rowe et al., 2009). Different methods have been used for manufacturing alginate microparticles, including spray drying (Coppi et al., 2002), ionotropic pregelation (Sarmiento et al., 2006), and nanoemulsion dispersion (Reis et al., 2006).

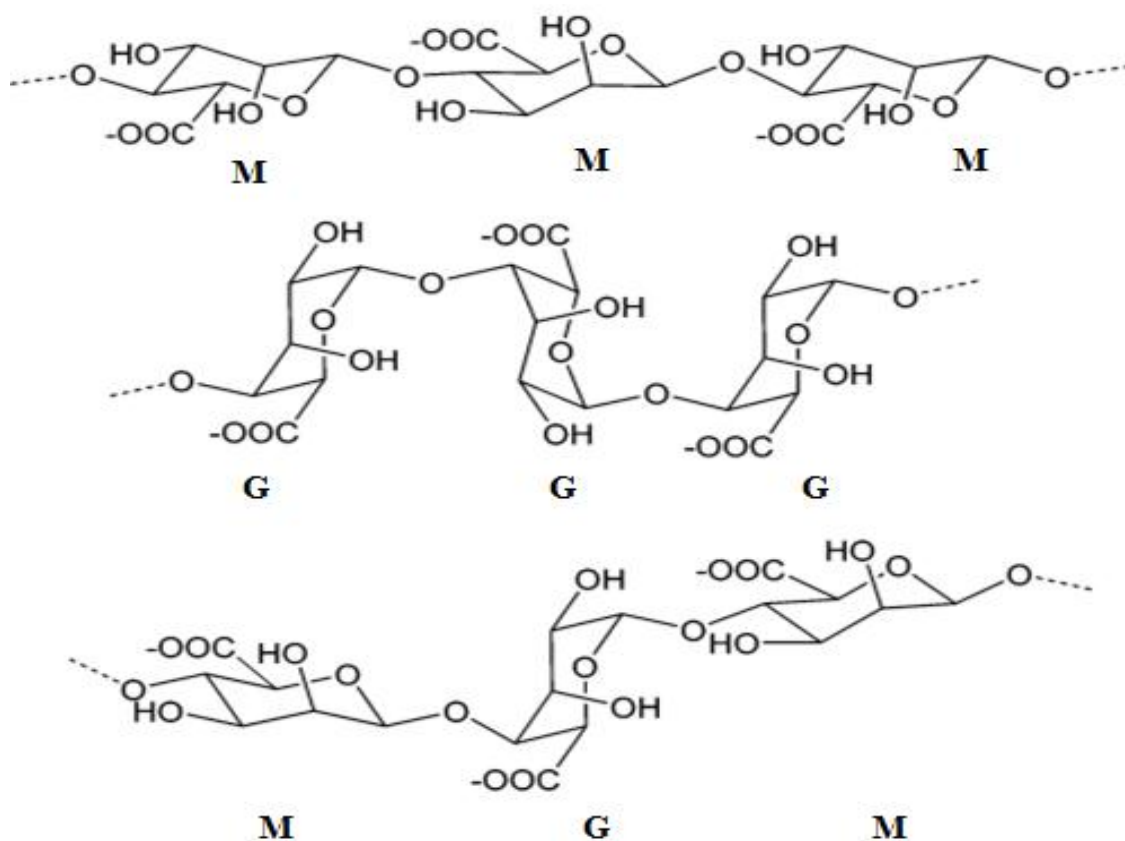


Figure 1. 9: Chemical structure of alginic acid unites "M" is mannuronic acid and "G" is guluronic acid) (Adapted from Bu et al., 2005).

Alginic acid has attractive physicochemical properties such as non-toxicity, biodegradability, non-immunogenicity and abundance for commercial use for micro and nano encapsulation (Soares et al., 2004). It can be used as a coating polymer, resulting in prolonged diffusion rate of the drug through the porous gel of the polymer. Furthermore, alginate is gelled in aqueous media by the presence of divalent cation such as calcium (Gombotz and Wee, 1998). The mucoadhesive properties can be attributed to the anionic carboxyl groups, facilitating the adherence to the mucous membranes by forming hydrogen bonds (Raj & Sharma 2003). Tafaghodi et al. (2004) showed that alginate has potential mucoadhesion properties and it can be used to formulate mucoadhesive delivery systems for intranasal administration.

Alginate has been used to formulate microparticles for controlling drug release. For examples, metformin (Balasubramaniam et al., 2007), theophylline (Soni et al., 2010), norfloxacin (Chakraverty, 2011), diclofenac sodium (Amin et al., 2013), and furosemide (Sunilbhai et al., 2014) have been formulated as alginate based microspheres.

1.8 Microspheres as a drug delivery system

Microspheres are polymeric spheres in the size range of 1 - 1000 μm . Due to their high surface area, microspheres can interact with mucin and increase residence time of the formulation with epithelial cells (Vasir et al., 2003). Microparticle carriers protect drug from the enzymatic or chemical degradation *in vivo* (Morimoto et al., 2001). Particulate bioadhesive systems may accommodate the drug and release it over a long period of time, resulting in reduced dosing frequency (Vasir et al., 2003).

Mucoadhesive microspheres have the ability to swell and form viscous gels upon contact with mucous layer retaining the drug for extended time at the site of absorption. Mucoadhesive particles may also open the tight junctions between the cells further promoting drug absorption (Pereswetoff-Morath, 1998). Gungor co-workers (2010) have reported ondansetron loaded chitosan microparticles may give significant plasma drug concentration with maintaining plasma drug level for longer periods compared to the intranasal ondansetron solution using rat as animal model (Gungor et al., 2010).

1.8.1 Preparation of microspheres

There are many methods use for preparation of microspheres (Figure 1.10). Among these methods, spray drying is a common technology for manufacturing dry powders, granules and agglomerates from drug-excipient solutions or suspensions (Figure 1.11). It involves atomization followed by drying and deposition of powders in collecting vessel (Maa et al., 1998). The first stage involves supplying a liquid feed dispersed through an atomizer into fine droplets in inert gas in the drying chamber. The large surface area promotes rapid solvent evaporation. Dried particles are passed over to a cyclone compartment for separation and a narrow particle size distribution (1 - 5 μm) is yielded depending on the spray drying parameters. Various methods have been used to prepare microspheres by spray drying. Microspheres made of water-insoluble polymer polylactic acid (PLA) or poly(lactide coglycolide) (PLGA) were used to prepare paclitaxel loaded microspheres (Mu and Feng, 2001), ketotifen loaded microspheres (Guerrero et al., 2008) and for the encapsulation of water-soluble materials such 5-Fluorouracil (Blanco et al., 2005). However, water-soluble polymers such as chitosan glutamate and sodium alginate were used to prepare zolmitriptan loaded microspheres (Alhalaweh et al., 2009) and levocetirizine dihydrochloride loaded microspheres (Rathananand et al., 2007). Spray drying involves dissolving the polymer in a suitable

solvent with the drug dispersed in the polymeric solution. The solvent is then evaporated in the drying chamber to form the dried microspheres.

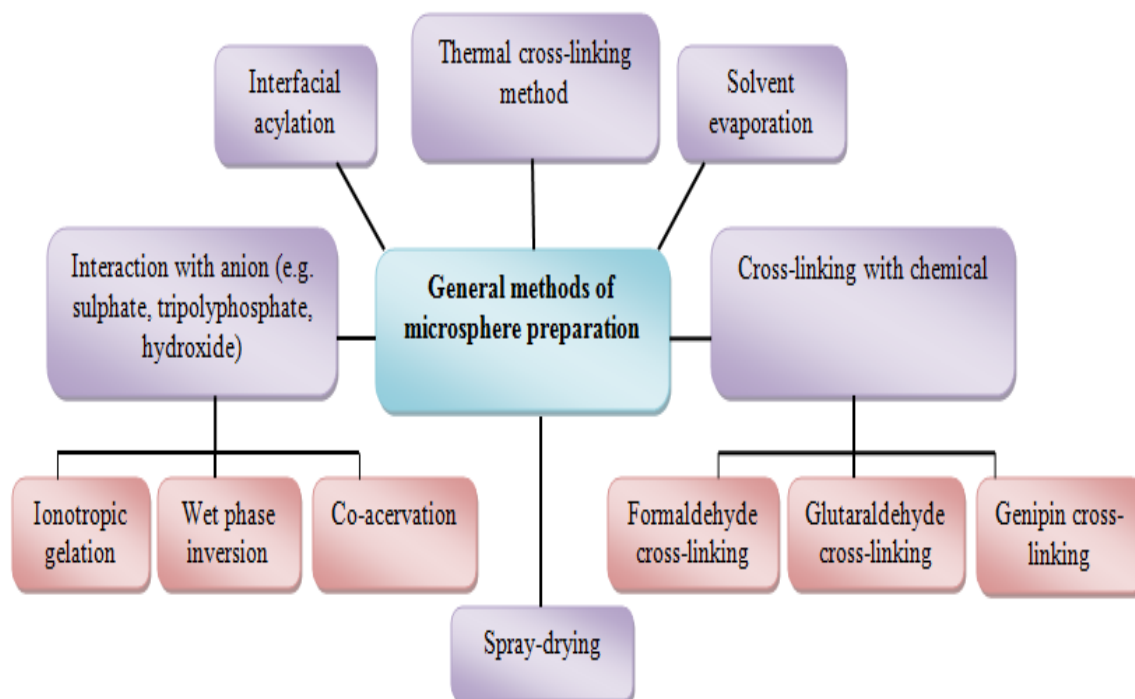


Figure 1. 10: General methods used for microspheres preparation (adapted from Sinha et al., 2004).

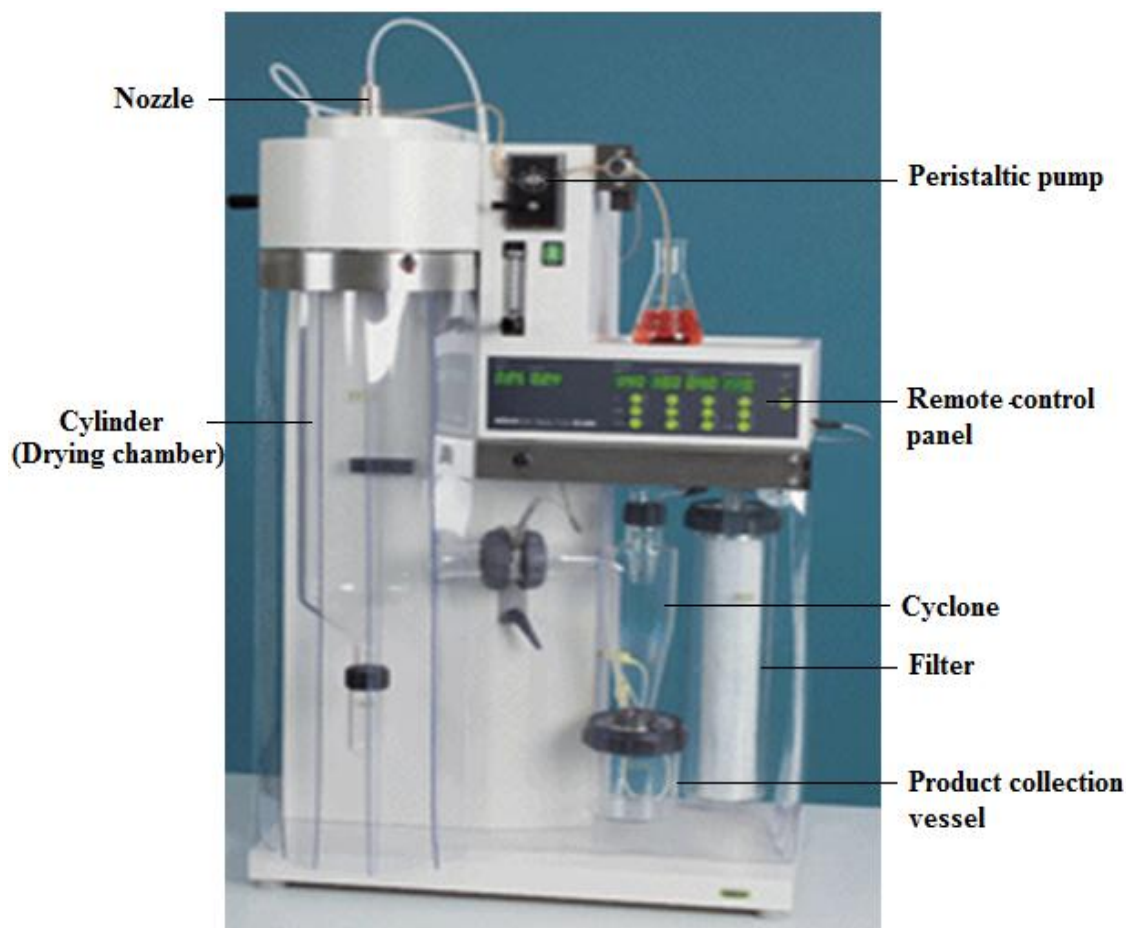


Figure 1. 11: Mini spray dryer B-290 (Büchi -290 Mini Spray-Drying, Büchi Laboratories, Switzerland) (www.mybuchi.com).

1.9 Liposomes

Liposomes are microscopic phospholipid bilayer vesicles that can entrap a wide range of therapeutic molecules (Laouini et al., 2012) (Figure 1.12). Liposomes are composed of biodegradable and biocompatible materials, such as phospholipids including phosphatidylcholines (PC), phosphatidylserines (PS) and phosphatidylethanolamines (PE) (Fukunaga et al., 1991).

Liposomes consist of one or several bilayers each has a thickness of around 4 nm, and the final size ranges falls between 20 nm and to 20 μm . Liposomes were first developed by Alec Bangham (Bangham et al., 1965). Upon hydration of phospholipid phase, polar head groups expand and vesicles are formed (Lasic, 1988) .

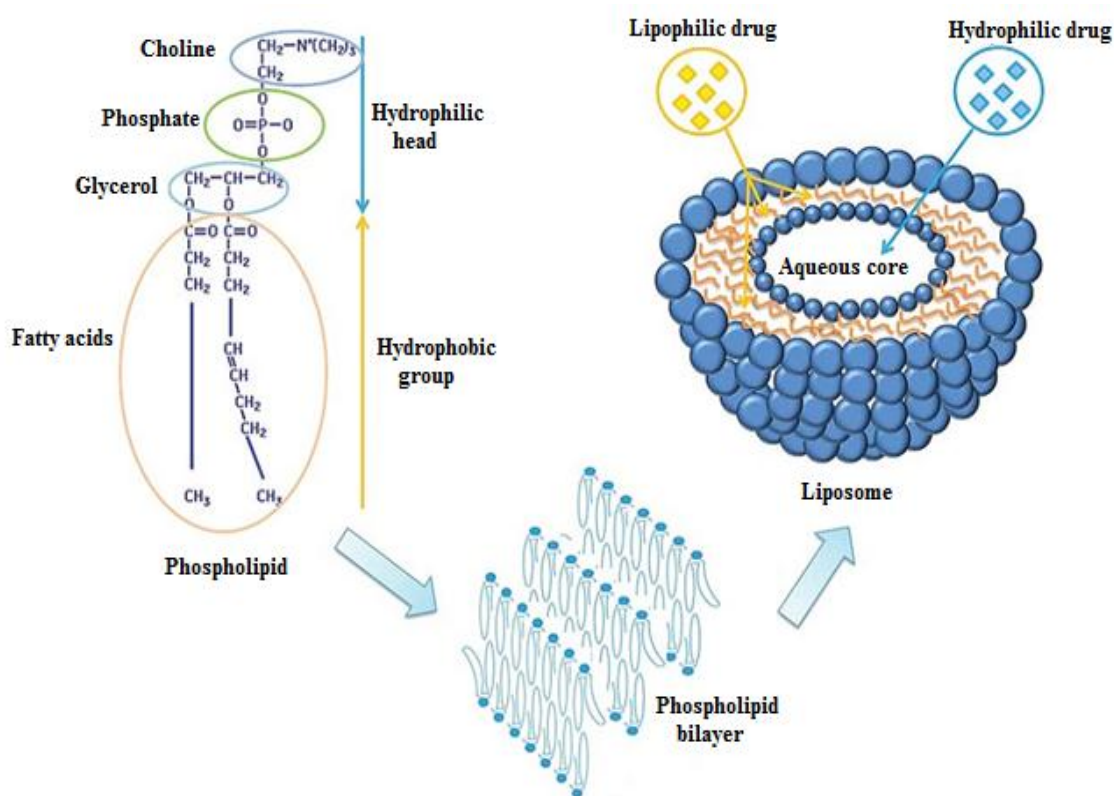


Figure 1. 12: Structure of liposomes and the entrapment of lipophilic and hydrophilic drug molecules (Adapted from Laouini et al., 2012).

Liposomes improve the therapeutic efficiency by targeting the drug to its site of action, enhancing absorption and provide protection from enzymatic degradation and immune recognition (Kisel et al., 2001) by facilitating the drug uptake by cells via endocytosis. Liposomes sustain the release of the drug, resulting in maintained drug level within the therapeutic window for a prolonged time (Gregoriadis and Florence, 1993).

Liposomes are prone to fusion, aggregation and hydrolysis, hence poor stability does not allow storage for long periods. Incorporating cholesterol into liposome formulations improves liposome stability (Kirby et al., 1980). Proliposomes are dry products consisting of encapsulated drug into phospholipid; upon addition of water proliposome may generate liposomes (Shaji and Bhatia, 2013). Proliposomes provide stable alternatives to liposome that are known to be unstable during storage (Payne et al., 1986). The use of liposomes as drug carriers in nasal delivery for local or systemic effects has been investigated and regarded promising compared to other nanosystems (Chen et al., 2013).

The use of polysaccharide such as chitosan for coating liposomes has been reported to obtain desirable characteristics, better targeting and controlled drug release (Takeuchi et al., 1996; Janes et al., 2001). The use of polymeric mucoadhesive coat on liposomes by mixing the polymer with the aqueous dispersion of liposomes can manipulate the characteristics of liposomes and enhance their storage stability (Takeuchi et al., 2000). Natural polymers (e.g. alginate and chitosan), synthetic polymers (e.g. polyvinyl alcohol) and other polysaccharides have been used to manipulate the surface properties of liposomes (Cheng et al., 2006; Takeuchi et al., 2000).

Natural cationic polymers such as chitosan coat the liposome vesicles by interacting with the negatively charge diacetyl phosphate in the phospholipid, resulting in enhanced bioavailability of the liposome-entrapped drug and improved permeation by opening the tight junctions between the cells (Takeuchi et al., 1996).

1.9.1 Classification of liposomes

Based on their size and morphology, liposomes might be classified into Multilamellar liposome vesicles (MLVs), Small unilamellar vesicles (SUVs), Large unilamellar vesicles (LUVs), Oligolamellar vesicles (OLVs) and Multivesicular liposomes (MVLs) (Fig. 1.13).

i) Multilamellar vesicles

MLVs consist of several phospholipid bilayers and size is larger than 500 nm (Laouini et al., 2012) (Figure 1.13). Rotary evaporator is used to prepare a thin lipid film in around bottomed flask while the organic solvent (e.g. chloroform) evaporated and collected via a condenser for disposal or reuse. Rehydration of the thin film above the transition temperature (T_m) of the phospholipid takes place by addition of water with shaking to form MLVs (Shek et al., 1983).

ii) Small unilamellar vesicles

These consist of a single phospholipid bilayer enclosed in an aqueous volume. SUVs range in size between 25 and 100 nm (Fig. 1.13). They are prepared either by gentle sonication of lipid dispersion for 5 to 10 minutes using probe tip or bath sonicator, or by sonication of multi-lamellar vesicles (Pitcher Iii and Huestis, 2002).

iii) Large unilamellar vesicles

This type of liposome is similar to SUVs and consists of a single phospholipid bilayer but vesicles have a larger size in the range of 0.1 μm to 1 μm (Figure 1.13). It provides a high loading efficiency of hydrophilic drugs compared to MLVs. To formulate LUVs, ethereal phospholipid solution is added to a previously heated aqueous phase above the T_m of phospholipid (Deamer and Bangham, 1976).

iv) Oligolamellar vesicles

Oligolamellar vesicles (OLVs) are MLVs possessing two or three phospholipid bilayers (Fig. 1.13). The OLVs are in the range of 100 - 500 nm (Laouini et al., 2012). They are prepared by the reverse phase evaporation method, which produces a mixture of OLVs and LUVs (Szoka and Papahadjopoulos, 1978). Ethanol-based proliposome method also generates OLVs (Perrett et al., 1991). Ethanol-based proliposomes are concentrated ethanolic solutions of phospholipid that generate liposomes upon addition of aqueous phase and shaking (Perrett et al., 1991).

v) Multivesicular liposomes

MVLs are liposomes enclosing a group of liposomes (Kim et al., 1983) (Figure 1.13). MVLs could be used for sustained release action when prepared by reverse phase evaporation technique (Jain et al., 2005). This technique may increase entrapment efficiency by 3 to 6 times compared to the conventional MLVs. Jain et al (2005) have reported 70% of acyclovir was released over 96 hours, whereas 80% of the drug was released from the conventional MLVs within 16 hour.

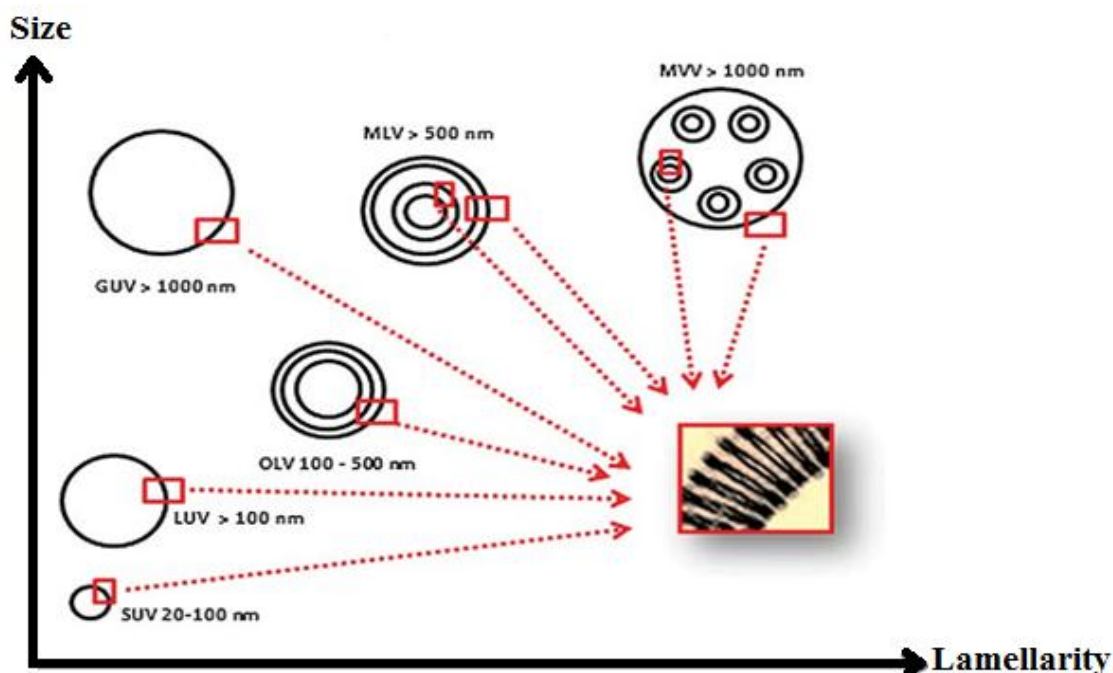


Figure 1. 13: Liposome classification based on residue size and morphology (Adapted from Laouini et al., 2012).

1.9.2 Liposomes in nasal drug delivery

Intranasal drug delivery using liposomes has been employed since 1992 by Alpar et al., (1992), who studied the immunogenicity of Tetanus toxoid loaded liposomes using distearoyl phosphatidylcholine (DSPC) and cholesterol (1:1) and compared the immune response to that elicited by the free antigen. Liposome loaded antigen significantly improved the immune response compared to the free antigen after intranasal delivery.

Vyas et al (1995) prepared multilamellar liposomes loaded with nifedipine. When bioadhesive agents were included in the formulation, nifedipine bioavailability improved and the plasma drug concentration was maintained over a prolonged time.

The rapid onset and sustained release of levonorgestrel using liposomes was demonstrated by Ding et al. (2007) who studied the pharmacokinetics and pharmacodynamics of levonorgestrel following intranasal administration. The relative bioavailability obtained using liposomes was 100%. Another study by Chen et al. (2009) demonstrated the improvement of salmon calcitonin absorption using ultradeformable liposomes via nasal delivery in rat.

Benefits of liposomes for nasal delivery of peptide vaccines together with anti-CD40 antibody has also been reported (Ninomiya et al., 2002). Formulation of DNA-hsp65 vaccine complexed with cationic liposomes allowed a 16-fold reduction in the DNA dose when given intranasally to elicit a cellular immune response (Rosada et al., 2008).

The attracting applications of liposomes for targeting of the drug to the brain have been studied. Armugam et al. (2008) demonstrated that intranasal administration of rivastigmine loaded liposome significantly passed to the brain with longer half-life compared to the drug given as solution.

The addition of bioadhesive agents to liposomal formulations delivered intranasally enhanced bioavailability and prolonged residence time of the drug at site of absorption. Alsarra et al. (2008) demonstrated that acyclovir loaded liposomal in mucoadhesive nasal gel formulation may significantly increase drug bioavailability (60.72%) compared to liposome free gel formulation (5.3%). Using rats, Qiang et al (2012) investigated the effect of incorporating chitosan into liposome formulations loaded with fexofenadine on the systemic absorption profile of the drug. Intranasal delivery chitosan-coated liposome significantly increased the bioavailability of fexofenadine with a prolonged effect compared to powder and uncoated liposome formulation.

1.10 Parkinson's disease and restless legs syndrome

Parkinson's disease is a common neurodegenerative disorder of the central nervous system (Jankovic, 2008). It is named after James Parkinson the English doctor who published the first detailed description in "An Essay on the Shaking Palsy" (1817). Its symptoms resulting the death of dopamine generating cells of the midbrain (Olanow et al., 2001). Shaking, rigidity, slowness of movement and difficulty in walking are equivalent in patients suffering from Parkinson's disease. Symptoms also include sensory, sleep and emotional problems (Jankovic, 2008). It occurs in 0.3% of the population and it is common in elderly people of 60 years of age or over by 1% (Olanow et al., 2001; Samii et al., 2004). It is idiopathic and the cause is not known. Levodopa (L-dopa) and dopamine agonists are the main treatments used to control the signs and symptoms of Parkinson's disease. Using these drugs for a long period may cause marked motor complications such as motor fluctuations and dyskinesia. It has been shown that after 4 - 6 years of levodopa therapy that nearly 40% of Parkinson's

disease patients may suffer from these adverse effects (Ahlskog and Muentner, 2001), and this percentage increases over time (Alves et al., 2008). Using of non-ergoline dopamine receptor agonists may reduce motor fluctuations in patients with advanced Parkinson's disease such as ropinirole, and pramipexole (Brooks, 2000).

Restless legs syndrome (RLS) is a neurological disorder characterised by irresistible urge to move the body to stop uncomfortable sensations. Legs, arms, and torso are affected and the movement modulates the sensation providing relief temporarily. These symptoms are alleviated by movement and are more common at rest, especially in the evening and at night. The sensations are similar to itching and tickling that does not stop. Limb jerking during sleep is an objective physical marker and disrupts restful sleep. This disease impairs the neurological functions (Allen et al. 2002). In the human populations approximately 5-10% suffer from RLS, however only a small proportion seek medical treatment (Phillips et al., 2000; Rothdach et al., 2000). The efficacy of L-dopa with a peripheral decarboxylase inhibitor has been established from the range of dopaminergic agents available (Brodeur et al., 1988). There is a high incidence of long-term side effects, which increase the severity of the symptoms (Allen & Earley 1996). An effective and well tolerated treatment has been found by using of ropinirole for the treatment of restless legs syndrome with improved sleep and cognitive functioning (Trenkwalder et al., 2004).

1.11 Ropinirole hydrochloride

Ropinirole hydrochloride (RH), commonly used for Parkinson's and restless legs syndrome, is administered orally as dopamine receptor agonist. Ropinirole hydrochloride is identified chemically as 4-[2-(dipropylamino) ethyl]-1,3-dihydro-2H-indol-2-one hydrochloride. The chemical structure of RH is shown in Figure 1.14. It has a molecular mass of 296.84 (260.38 free base) and its molecular formula is $C_{16}H_{24}N_2 \cdot HCl$.

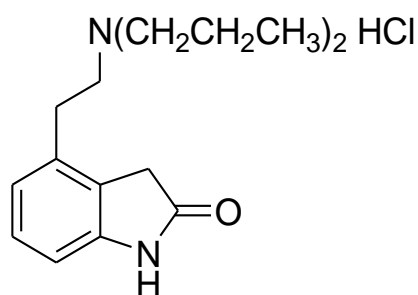


Figure 1. 14: Chemical structure of ropinirole hydrochloride.

RH is a white to yellow solid with a melting point in the range of 243 - 250°C and an aqueous solubility of 133 mg/ml. The tablet formulation of this drug contains 0.29 mg, 0.57 mg, 1.14 mg, 2.28 mg, 3.42 mg, 4.56 mg, or 5.70 mg RH equivalent to ropinirole, 0.25 mg, 0.5 mg, 1 mg, 2 mg, 3 mg, 4 mg, or 5 mg respectively (GlaxoSmithKline, 2009).

As mentioned above, Ropinirole is used to treat Parkinson's disease by alleviating the dopamine deficiency. It is a non-ergoline dopamine D₂/D₃ receptor agonist that stimulates striatal dopamine receptors (Matheson and Spencer, 2000). Ropinirole binds to central and peripheral dopamine receptors with an order of receptor affinity similar to that of dopamine (Jost and Angersbach, 2005). It is highly selective D₃ rather than D₂. Ropinirole is 20 times more selective for D₃ receptors than D₂ receptors and about 50 times more selective for D₃ than D₄ receptors, with negligible affinity for D₁ receptors (Matheson and Spencer, 2000). It has little or no affinity for β-adrenoceptors or adrenergic, serotonergic, GABA or benzodiazepine receptors. Ropinirole acts on postsynaptic dopamine receptors in the CNS associated with Parkinson's disease (Matheson and Spencer, 2000).

Ropinirole has about 50% bioavailability since it undergoes first pass effect after absorption. The main metabolic pathway is the cyto-chrome P450 (CYP) isozyme CYP1A2, with a minor contribution from CYP3A. 10% of a ropinirole dose is excreted unchanged in urine (Kaye and Nicholls, 2000). The distribution volume of ropinirole is 7 L/kg, with plasma protein binding of 10–40%. Ropinirole has an average elimination half-life of approximately 6 hours (DrugBank, 2013).

1.12 Devices used for nasal delivery

Variety of devices can be used for the nasal administration of dosage forms. Nasal drops and nasal sprays are delivery devices for liquids formulations, while nasal insufflators are delivery devices for powders.

1.12.1 Nasal drops

Nasal drops are the most traditional nasal devices for intranasal administrations of liquids owing to their low manufacturing cost. The main disadvantages of nasal drop devices are lack of precision in the administered dose and the risk of contamination during treatment. An issue that is overlooked is the special expertise required during use of nasal drops. For maximum benefit the patient should keep the nostril uppermost and the administration angle at 90° angle (angle between subject's head and nasal drop device) while instilling the dose. The head is swirled from side to side after application of drops to nostrils (Washington et al., 2001).

i) Drops delivered with a pipette

In this type of nasal drops, the quantity of dose administered depends on pulling a volume of the formulation into a glass dropper followed by placing the tip of the dropper into the nostril and squeezing the rubber top to release the formulation as drops (Figure 1.15a) (Djupesland, 2013). Clinical efficacy of fluticasone formulation using single dose pipette has been reported to be significantly higher than that using a nasal pump in patients with nasal polyps (Penttilä et al., 2000).

ii) Squeeze bottles

Squeezing bottles and nasal drops with pipette are recommended for exerting local therapeutic effects such as those used for delivery of liquid nasal decongestant formulations (Figure 1.15b). Squeezing a plastic bottle causes the release of air inside the bottle from a narrow orifice. This generates a small spray volume into the frontal region of the nostril. The drawback of this device is air pulled back into the container following the release of the dose which may pull part of the nasal secretions into the bottle, resulting in contamination of the formulation (Djupesland, 2013). The droplet size and dose accuracy are strongly dependent on the force applied on the plastic bottle to release the medication (Djupesland, 2013) resulting in poor control over the delivered

dose. Thus, this device is not recommended for use in children (Kublik and Vidgren, 1998).

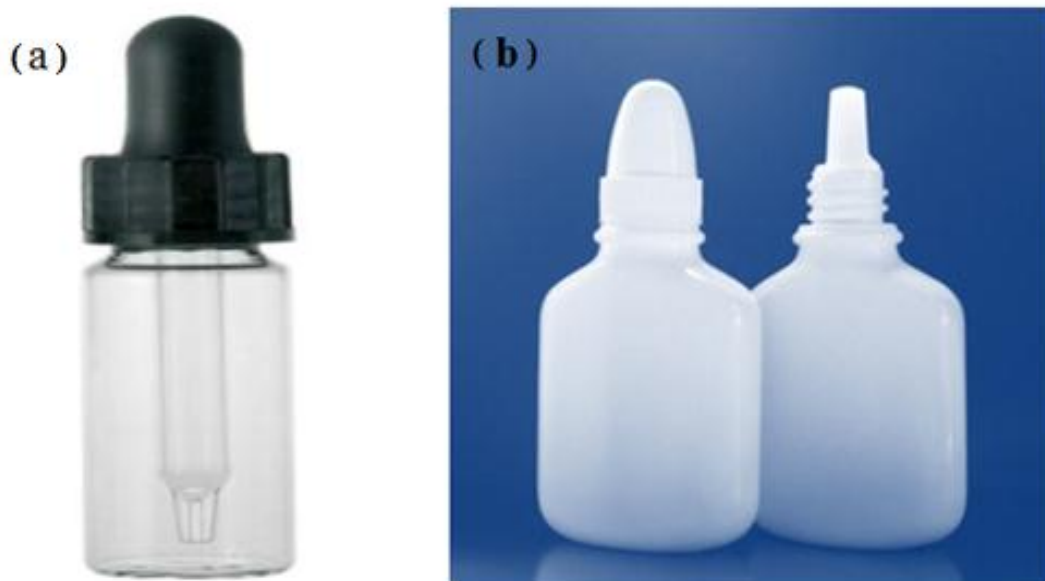


Figure 1. 115: (a) Nasal drops with pipette (www.adelphi-hp.com), and (b) nasal squeeze bottles (www.webpackaging.com).

1.12.2 Nasal Sprays

Nasal spray system consists of a chamber, a piston and an operating actuator. Unlike nasal drops, nasal spray generates precise doses (25 - 200 μl) per spray due the presence of pumps and actuators. *In vitro* studies have shown nasal sprays to produce consistent doses and reproducible plume geometry. Particle size of the generated drops, spray pattern, dose accuracy are affected by the formulation properties such as thixotropic behaviour, viscosity and surface tension (Kublik and Vidgren, 1998). The applied force, orifice size, design of the pump and formulation can all affect the droplet size and plume geometry of the spray (Djupesland, 2013). Doses are delivered by nasal sprays either by using metered-dose spray pumps or pressurized metered dose inhalers (pMDIs).

i) Metered- dose spray pumps

Spray pumps operate by replacing the generated liquid spray with air. Hence, preservatives are needed to prevent microbial contamination of the formulation. Priming and repriming are required before starting the delivery and when keeping it for a long

time to maintain consistency of the delivered dose. Different types of spray systems have been developed by manufacturers to overcome the risk of contamination and minimise irritation caused by inclusion of preservatives in the formulations. This was achieved either by designing a movable piston, collapsible bag or compressed air (carbon dioxide or nitrogen) to replace the vacuum created by the emitted volume. The pump prevents air from being pulled into the container during the generation of the spray (Kublik and Vidgren, 1998) (Figure 1.16). These systems generate reproducible spray regardless of the position of the device and spraying angle, offering convenience for use by children and patients confined to bed (Djupesland, 2013).

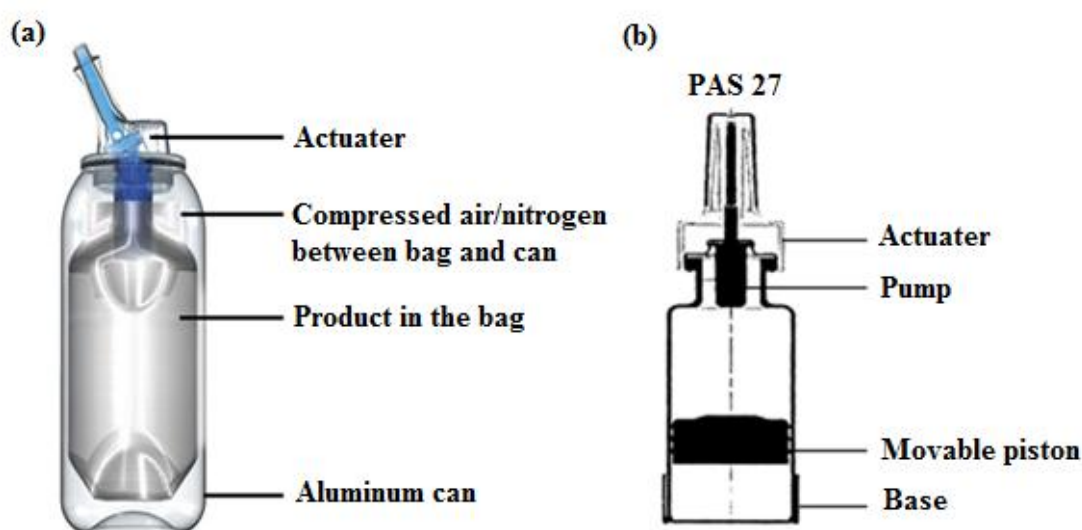


Figure 1. 16: (a) Airless nasal device with collapsible bag (Bag on valve system) (Adapted from www.aptar.com), and (b) airless nasal device with sliding piston (PAS 27, Valois S.A., Le Neubourg, France) (Adapted from Kublik and Vidgren, 1998).

Another system (Figure 1.17a), is preservative-free and operates by employing an aseptic filtration system, hence the air is pulled into the container while dose is emitted and filtered, resulting in prevention of microbial contamination (Kublik and Vidgren, 1998). Single and double-dose spray device (Figure 1.17b) is more useful than metered dose spray pumps for drugs that have narrow therapeutic index. Examples of this system are Zomig[®] (Zolmitriptan) nasal spray and Migranal[®] (dihydroergotamine mesylate, USP) nasal spray which are used for the treatment of migraine headaches (Djupesland, 2013).

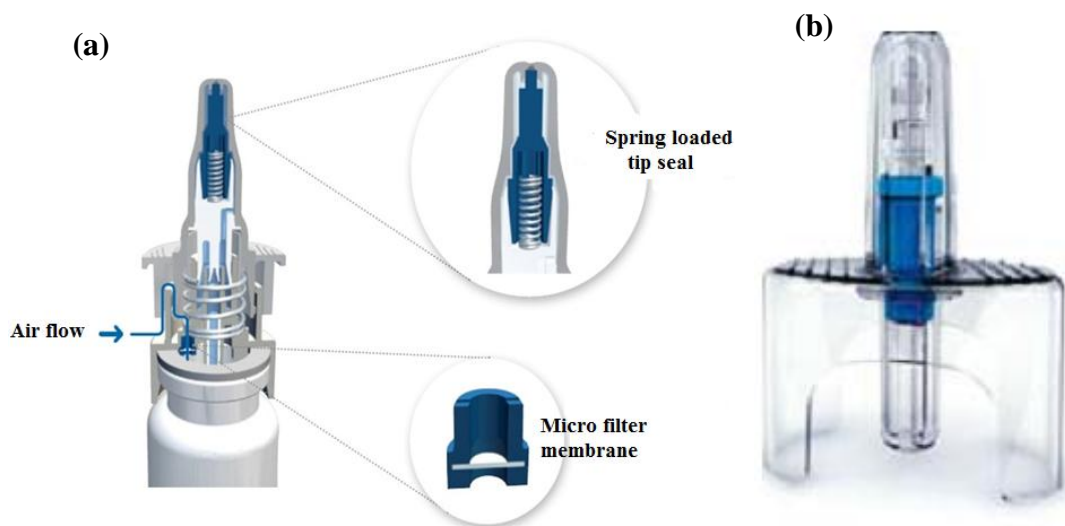


Figure 1. 17: (a) Preservative free pump with air filter (Adapted from www.aptar.com), and (b) nasal unit-dose system with glass container (www.aptar.com).

ii) Nasal pressurized metered-dose inhalers

Nasal pressurized metered-dose inhalers (pMDI) systems have been used for eliciting local therapeutic effects in the nose. The major sites of dose deposition are the anterior non ciliated regions of the nasal vestibule and anterior parts of the narrow nasal valve. Chlorofluorocarbon propellants cause irritation and dryness to the nasal mucosa. Moreover, the speeds of particles are much higher than those emitted from spray pumps. For these reasons, chlorofluorocarbon propellants have been replaced by hydrofluoroalkane propellants (Djupesland, 2013). Examples of pMDIs are budesonide and beclometasone dipropionate, which are used for the treatment of allergic rhinitis.

1.12.3 Delivery devices of powdered nasal formulations

Several designs of devices are available for delivery of nasal powders consisting of two pieces connected to each other, the mouthpiece and the nosepiece. When the patient blows air into the mouthpiece, particles are delivered to the nosepiece and then to nasal passage. Other systems operate by allowing the patient to sniff the powder stored in capsule or a blister placed within larger devices. Compressible compartments might be employed to expel the powders into the nostril with the aid of air pressure (Djupesland, 2013). The most commonly used devices for delivery of nasal powders are nasal insufflators.

i) Nasal insufflators for experimental purposes

Nasal insufflators or powder aerosolizers are tube-like containers in which powdered drug formulations can be stored. Alternatively, these tubes are connected with syringes or air pump to blow the powder into the nostril (Figure 1.18).

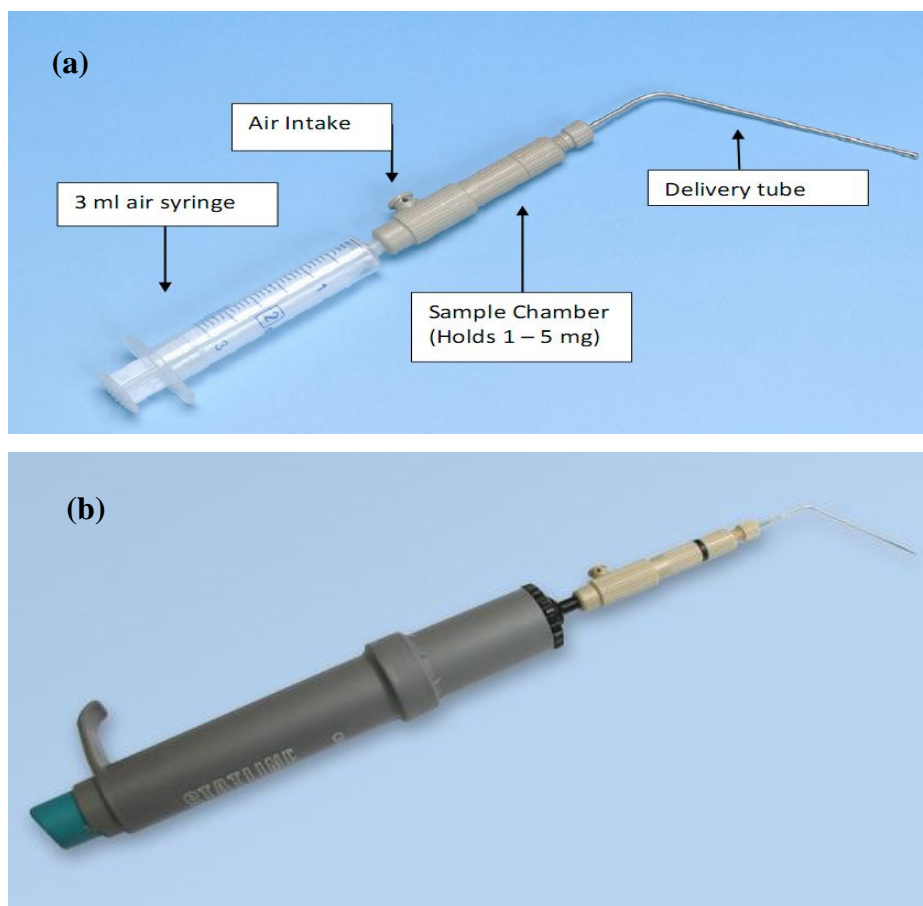


Figure 1. 18: (a) Penn-Century Dry Powder Insufflator™ - Model DP-4 connected with commercial syringe, (b) Dry Powder Insufflator™ Air Pump Assembly (www.penncentury.com).

ii) Bi-Directional™ nasal insufflators

Bi-Directional™ nasal insufflators have been developed by OptiNose breath-powered nasal delivery technology. This design consists of mouthpiece and nosepiece (Figure 1.19a). The breathing force carries particles from prefilled gelatin capsule with powder doses into nostril, while soft palate separates the nose from the throat. This device offers potential particle distribution into deep part of the nose, resulting in minimized lung deposition and enhanced powder targeting of the drug to the sinus ostia (Dhakar et al., 2011). Sumatriptan powder is an example that is currently in phase III clinical trials using the Bi-Directional™ nasal insufflator to treat acute migraine.

iii) Miat[®] monodose nasal insufflator

Miat[®] monodose nasal insufflator has been developed by Miat S.P.A Milan, Italy and consists of compressible pump, a revolving chamber with a grip tab, a nozzle, a two-push-button (pin) and a protective cap (Figure 1.19). Upon squeezing the pump the compressible compartment creates a stream of air that passes through an in-let puncture in the capsule made by two opposite pins, resulting in particle delivery to the nostril by means of air stream (Cocozza, 1989). The delivery of powder dose from the monodose insufflator is evaluated by the weight of capsule before and after each puffing (Patil and Sawant, 2011). The delivery performance was evaluated by Patil and Swant, (2011), who reported that more than 98% of the dose was delivered after three puffs.

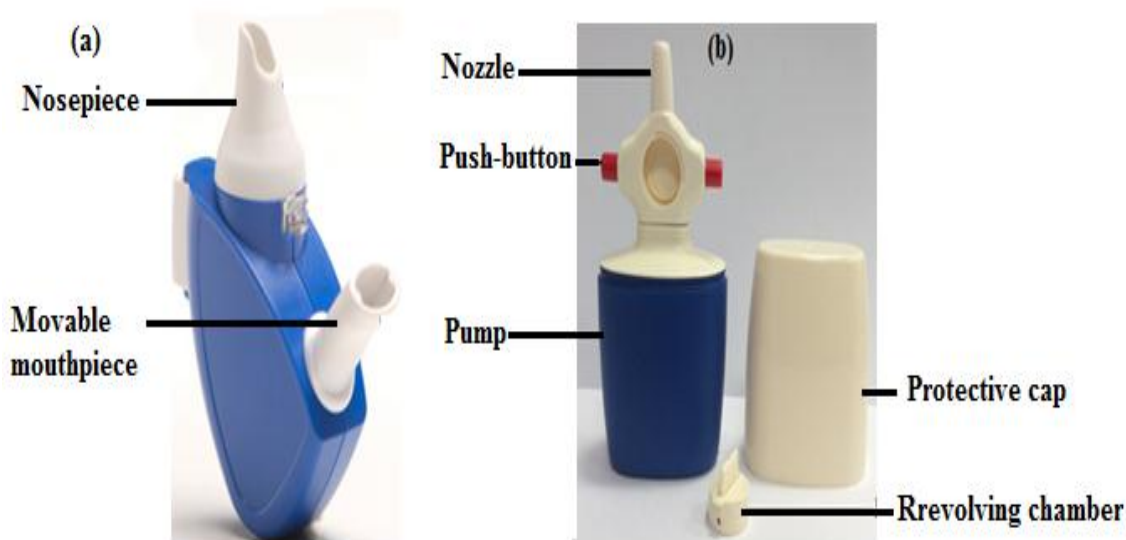


Figure 1. 19: (a) Optinose Bi-Directional[™] nasal insufflator (www.optinose.com), and (b) Miat[®] monodose nasal insufflator.

iv) Monopowder P[®] insufflator

The Monopowder P[®] insufflator developed by Valois Dispray, France consists of a pump, a nasal adaptor and a powder reservoir. The piston actuates a stream of air to expel the powder into the nasal pathway (Sacchetti et al., 2002). Deposition and particle size of the delivered powder depends on formulations and actuator performance. Moreover, a multi-dose dry powder device has been developed to improve patient compliance (Kublik and Vidgren, 1998). For example, the multi dose system of budesonide powder (Rhinocort Turbuhaler[®]; www.az.com) has been marketed by Astrazeneca, to treat allergic rhinitis (Agertoft et al., 1993).

1.13 Hypothesis and objectives

Despite of the advantages offered by delivering drugs via the nasal route for various therapeutic applications, the duration of therapeutic activity following intranasal administration is short owing to rapid mucociliary clearance in the nose. Inclusion of bioadhesive agents into formulations improves drug absorption and possibly controls the rate of drug release. Amongst drug carriers, microspheres are considered effective at prolonging the contact time between the drug and mucosal membrane and increasing drug permeation, hence, this may improve the therapeutic effect of the drug. In a similar manner liposomes are highly promising carriers for drug targeting to the applications site, owing to the ability of liposomes to entrap hydrophilic and hydrophobic therapeutic agents and enhance the residence time of the liposome entrapped drug at the application site, hence this can improve the permeation and bioavailability of drug.

Encapsulating of the anti-Parkinson drug ropinirole hydrochloride (RH), into mucoadhesive microparticles or liposomes may improve the management of Parkinson's disease and restless legs syndrome when the drug is administered via the nose.

The main aims of this study were to prepare formulations of RH loaded into mucoadhesive agents (e.g. chitosan glutamate or low viscosity sodium alginate) via spray drying and ropinirole loaded liposomes via ethanol-based proliposome technology for intranasal delivery using appropriate medical devices, and to study the potential of mucoadhesive microspheres and liposomes as drug carriers for delivery of the microspheres using Miat[®] nasal insufflator and to spray liposomes as liquid dispersion using a range of nasal spray devices.

Objectives of the study:

- To conduct preformulation studies in order to investigate the interactions between the drug and polymer (e.g. chitosan or sodium alginate).
- To prepare optimum RH loaded mucoadhesive microsphere formulations from chitosan glutamate and low viscosity sodium alginate via spray drying.
- To examine the properties of RH loaded mucoadhesive formulations.
- To investigate the physical properties of encapsulated drug in relation to polymer to drug ratio.
- To conduct toxicological study for the best performing RH loaded mucoadhesive microspheres using isolated sheep nasal mucosa.

- To study device performance in relation to microsphere formulations using Miat[®] nasal insufflator and investigate the cloud produced from the device.
- To formulate optimum RH loaded liposome formulations using proliposome technology.
- To examine liposome properties in relation to inclusion of different mucoadhesive agents.
- To study nasal spray devices performance in relation to liposome formulations and investigate the cloud generated from the sprayed liposome formulations.
- To analyze the data obtained and present them as PhD thesis.

CHAPTER 2

GENERAL METHODOLOGY

2.1 Materials

Chitosan Glutamate salt, Protasan Up G113 (Ch G2113) (mW: <200 kDa, DD: 75-90% (degree of deacetylation)), and Protasan up G213 (Ch G213) were supplied by Novamatrix/FMC biopolymer (Sandvika, Norway). The carboxymethyl chitosan (CM ch) was supplied by Santacruz Biotechnology, USA. Ropinirole hydrochloride (RH) USP-grade was supplied by Shanghai Yancui (China), Soya phosphatidylcholine (SPC; Lipoid S 100) was obtained from Lipoid (Steinhausen, Switzerland). Low viscosity sodium alginate (LVSA) and medium viscosity sodium alginate (MVSA), cholesterol (99%), sucrose ($\geq 99.5\%$ GC), absolute ethanol, sodium phosphate monobasic, sodium hydroxide and deoxycholate hydrate were purchased from Sigma Aldrich, UK. Acetonitrile (HPLC grade), High performance liquid chromatography (HPLC) grade water, and 1-butanol were all purchased from Fisher Scientific Ltd, UK. Miat[®] monodose insufflator was kindly supplied by Miat, Milan, Italy (Figure 1.19b) and three different multi-dose nasal spray devices were used in this study: device A (Zolmist nasal spray, Cipla Ltd; Batch No. K21137, India), device B (Model V04.2480, Costerpharm) was kindly provided by Costerpharm, Italy and device C (Model VP3/93, Valois) from a Beconase[®] aqueous nasal spray (Figure 2.1).



Figure 2. 1: Nasal spray devices used in this study.

2.2 Compatibility studies

The compatibility study between RH and polymers were conducted using Thin Layer Chromatography (TLC) and Fourier transform infrared spectroscopy (FTIR) to detect any drug decomposition or drug-excipient interactions before and after spray drying.

To determine decomposition or interaction of ropinirole hydrochloride (RH) and polymer using TLC, the solution of RH crude material and solution of RH loaded into microsphere formulation in a specific concentration equivalent to 400 µg/ml RH were prepared and spotted separately onto TLC plate and then dried using a laboratory "hair-style" drier. TLC chamber that contains the mobile phase consisted of methanol and acetonitrile (80:20 v/v) and one drop of glacial acetic acid was added to the mobile phase to prevent tailing of the spot was prepared before and left at room temperature for 20 minutes to saturate the chamber with the mobile phase before running the TLC sheet. The spotted TLC was placed into the chamber; it was left for sufficient running time and dried at room temperature. The UV chamber was used to detect the spots of the drug (Patel and Chaudhari, 2012).

Compatibility studies between the drug and polymer were carried out using FTIR spectroscopy analysis. The IR spectra of the formulations and physical mixture of the drug and polymer were then analyzed in comparison with the spectrum of RH raw material to determine the compatibility of formulations. A small quantity of RH as raw material, physical mixture of the drug and polymer, or RH loaded into microsphere formulation (polymer: RH, 50:50 w/w) were analyzed using FTIR (Thermo Scientific, NICOLET is10, USA). The scan was collected at the range of 400 – 4000 cm⁻¹ using OMNIC software to analyze the data. The experiment was conducted in triplicate.

2.3 Standard calibration curve of ropinirole hydrochloride

A stock solution was prepared by weighing 10 mg of RH accurately on the electronic sensitive balance (Ohaus Corporation, USA) followed by dissolution in 100 ml HPLC water. Aliquots were pipetted out (0.5 ml, 1 ml, 2 ml, 3 ml, 4 ml, 5 ml, 6 ml, 7 ml, 8 ml, 9 ml and 10 ml) to prepare a number of samples from the stock solution into a series of 10 ml volumetric flasks and made up to level mark with HPLC water in order to get concentrations in the range of 5 to 90 µg/ml. Quantities of 2 ml from every diluted

solution were placed into small vials and arranged in ascending order from low to higher concentrations using HPLC (Agilent Technology 1200 Series, USA) and C18 column 250 x 4.6 mm, 5 μ m. The temperature of the column was set at 40°C, and the mobile phase comprising phosphate buffer pH 6.0 and acetonitrile HPLC grade in a ratio 50:50 v/v was used, and the flow rate was set up at 0.5 ml/min and the detection wavelength was adjusted to 249 nm (Sreekanth et al., 2009). Figure 2.2 shows the calibration curve of ropinirole hydrochloride.

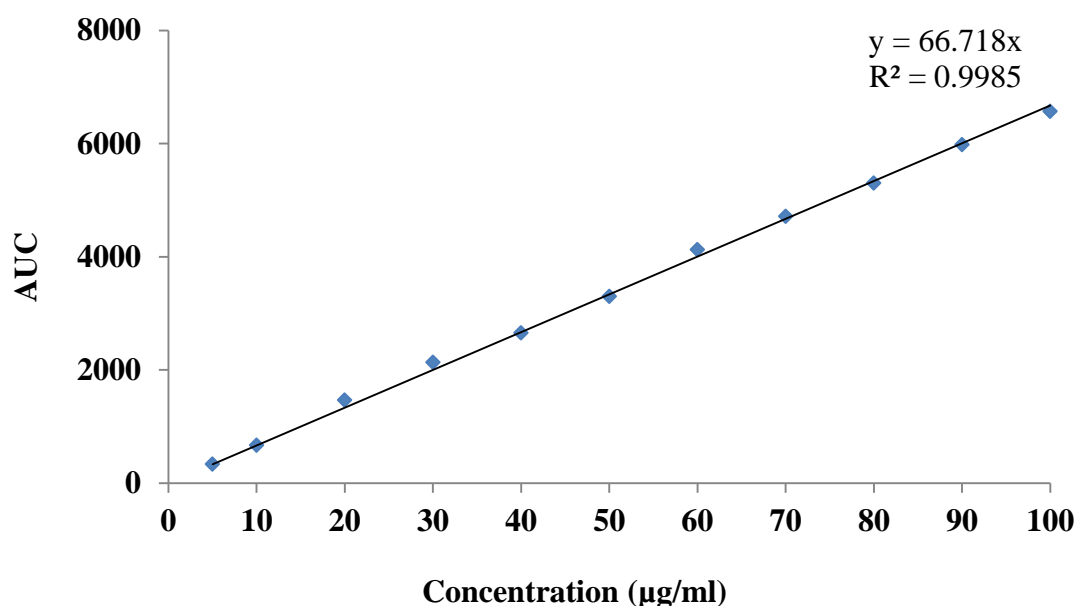


Figure 2. 2: Calibration curve of ropinirole hydrochloride.

2.4 Preparation of phosphate buffers (pH 6 and 6.5)

Sodium dihydrogen orthophosphate (6.8 g) (British Pharmacopoeia, 2011) was weighed accurately and dissolved in HPLC grade water to produce 1000 ml, solutions 10M NaOH was used to adjust the pH to 6 using Corning pH meter (Corning Science Products, UK).

Sodium dihydrogen phosphate monohydrate (13.8 g) was weighed accurately and dissolved in 900 ml of HPLC grade water. Solution of 10M NaOH was used for adjusting the pH to 6.5, and then diluted to 1000 ml with HPLC water.

2.5 Preparation of microspheres

Spray drying is widely used to prepare solid particles, dry powders, granules and microparticles. It is a rapid one step technique of drying with high reproducibility of production of spherical particle with micro size range. The principle of spray drying is based on three steps; atomization of the feeding liquid with aid of nitrogen gas, drying of the droplets containing solid particles within a drying chamber and collection of dried powder by the effect of gravity within a collecting vessel (Figure 2.3).

A Büchi -290 Mini Spray-Drier (Büchi Laboratories, Switzerland) was used to prepare the microsphere formulations. Four formulations of the polymer (chitosan or low viscosity sodium alginate) and the drug (RH) were prepared using various polymer to drug ratios (Table 2.1). The formulations were compared with drug free microspheres (% 0.5 w/v polymer). The method was adapted from the study conducted by Alhalaweh et al., (2009). The feed solutions were prepared by dissolving the specified quantity of the polymer and the drug in 100 ml of HPLC water using a magnetic stirrer to enhance the dissolution. The feed solution was atomized under 0.7 mm nozzle size, and inlet temperature was set at 160°C. The outlet temperature was varying between 75 to 80°C. The feed rate was 5 - 6 ml per minute, atomizing air flow rate and aspiration rate were kept at 357 L/h and 100% respectively. After evaporation of the solvent from atomized droplets, dried microparticles passed through the cyclone and were collected in the collecting vessel by the effect of gravity. For each batch, 200 ml of solution was processed in triplicate.

Table 2. 1: Formulation composition of mucoadhesive microparticles.

Weight ratio (polymer: RH)	Polymer (mg)	RH (mg)	Total weight (mg)/100ml
100:0	500	0	500
90:10	450	50	500
70:30	350	150	500
50:50	250	250	500
30:70	150	350	500

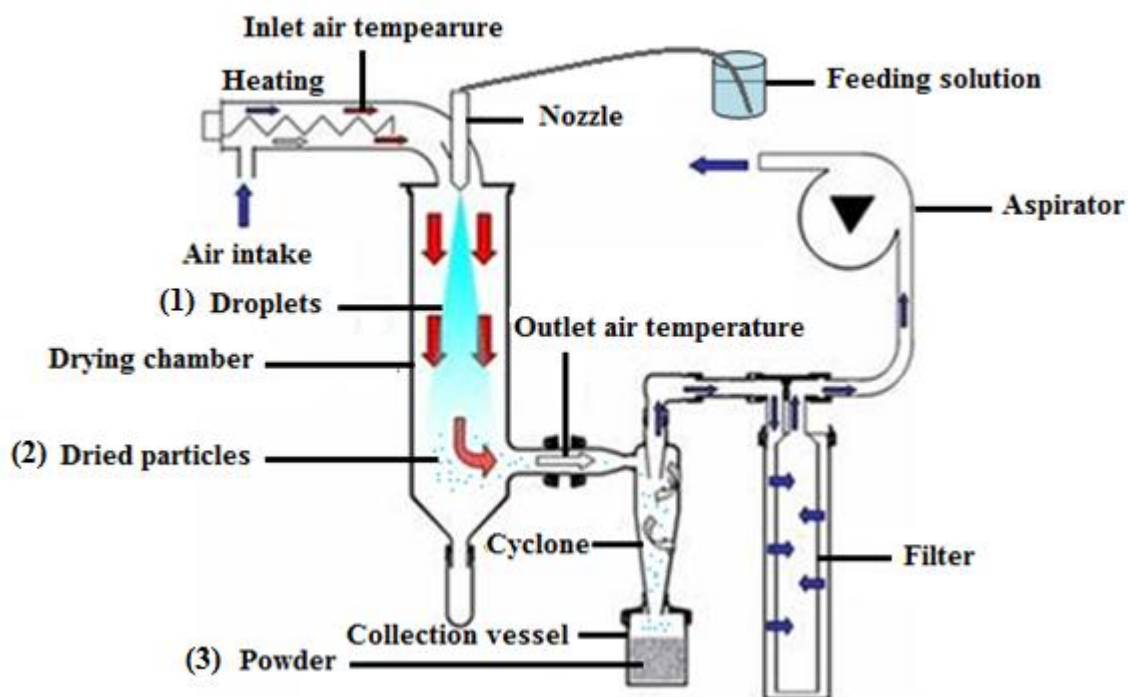


Figure 2. 3: A schematic presentation of spray drying (Adapted from Büchi -290 Mini Spray-Drying, Büchi Laboratories, Switzerland).

2.5.1 Viscosity measurements of feeding solution

Anton Paar's viscometer (Figure 2.4) is commonly used in pharmaceutical and biotechnology industries as an alternative to the traditional type of capillary viscometer due to its calibrated system, small volume of sample required (150 μl), no sample/air contact (close measuring system), and highly precise and reproducible measurements.

The measurement is based on Stoke's law (Eq. 2.1). To determine the viscosity of a liquid, the required time to roll a ball in a sloping cylindrical tube filled with sample liquid under the influence of gravity was determined (Figure 2.4b). The travelling time taken by the ball for fixed distance is measured using two sensors. The viscosity of the known sample can be expressed as dynamic viscosity (mPa.s) and kinematic viscosity (mm^2/s) for each ball rolling time.

$$\frac{dy}{dx} = \frac{d^2 (p_i - p_e)g}{18\eta} \quad (\text{Eq. 2.1})$$

Where dy/dx is the settling rate of particle, d is the diameter of the particle, ρ_i is the density of the particle, ρ_e is the density of the liquid, g is the constant of gravity, and η is the viscosity of the liquid.

This study used a microviscometer (AMVn Automated Microviscometer, Anton Paar, Austria) at 20°C to determine the viscosity of the solution. Density of the solution was measured with DMA 35N density meter (Anton Paar, Austria). A special glass capillary tube was used to measure the viscosity. A small ball was introduced into the capillary tube which was then filled with the sample solution using a syringe to draw up the sample solution from a beaker. The capillary tube was completely free of air bubbles. The tip of the capillary was dried with a tissue and closed with the sealing cap before being placed into the Automated Microviscometer to measure the viscosity of the solutions.

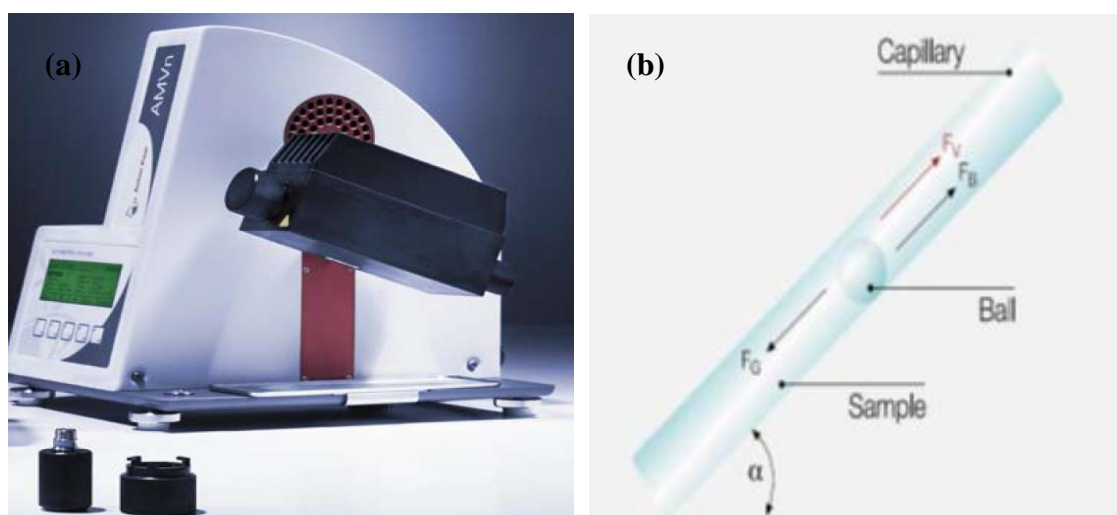


Figure 2. 4: (a) Automated Microviscometer, (b) cylindrical tube (Adapted from AMVn Automated Microviscometer, Anton-Paar) (www.anton-paar.com).

2.6 Characterizations of mucoadhesive microspheres

2.6.1 Production yield

The production yield was calculated as the weight percentage of the final product with respect to the total amount of the drug and polymer originally being used in the beginning of the experiments (Harikarnpakdee et al. 2006). The following equation was used:

$$\% \text{ Yield} = \left(\frac{W_1}{W_2} \right) * 100 \quad (\text{Eq. 2.2})$$

Where W1 is the weight of dried microspheres and W2 is the initial dry weight of starting materials.

2.6.2 Particle size measurement

Microspheres (5 mg) generated by spray drying were suspended in 3 ml of 1-butanol and sonicated for 15 seconds to deaggregated the microparticles. The resultant microsphere dispersion was diluted further with 1-butanol and size was measured using laser diffraction (Malvern Mastersizer 2000, UK) (Figure 2.5). The equipment was thoroughly cleaned with distilled water after each sample measurement, in order to eliminate cross-contamination. For liposome formulations aqueous media was used as a dispersion medium for particulate sample suspension. The average value of particle size was expressed as the volume mean diameter (D0.5). Polydispersity was expressed as a Span:

$$\text{Span} = \frac{(D_{0.9} - D_{0.1})}{D_{0.5}} \quad (\text{Eq. 2.3})$$

where D0.9, D0.5 and D0.1 are 90% undersized, 50% undersize and 10% undersize respectively (Gavini et al. 2006).

Mastersizer 2000 software analyses the data to determine the size and size distribution of particles based on measuring the angular variability and intensity of the laser beam scattered by a series of photosensitive detectors. When laser beams pass through a dispersed particulate sample, the scattering of light depends on particles size in the sample; larger particles gives smaller angles of scattering while smaller particles give larger angles of scattering (Figure 2.5) (Manual of Malvern Instrument). The laser diffraction instrument in this study employed “Mie theory” to analyze the size of

particles. This theory relies on the refractive indexes of dispersed particles and the dispersion medium (manufacturer personal communication). Deionized water and butanol-1-ol were used as dispersion medium and their refractive index were 1.33 and 1.3993 respectively.

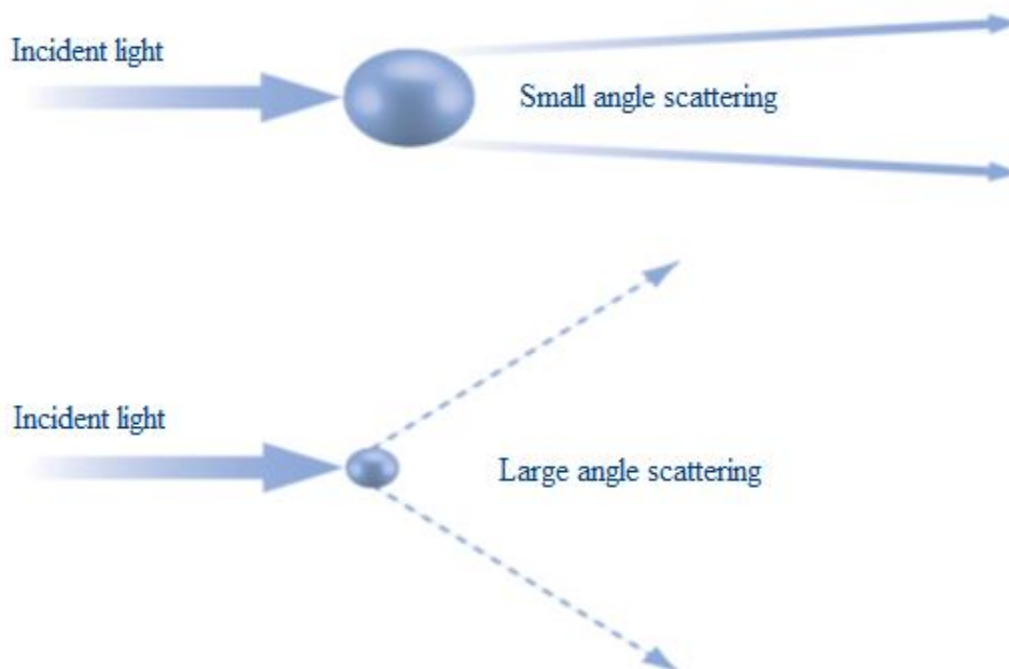
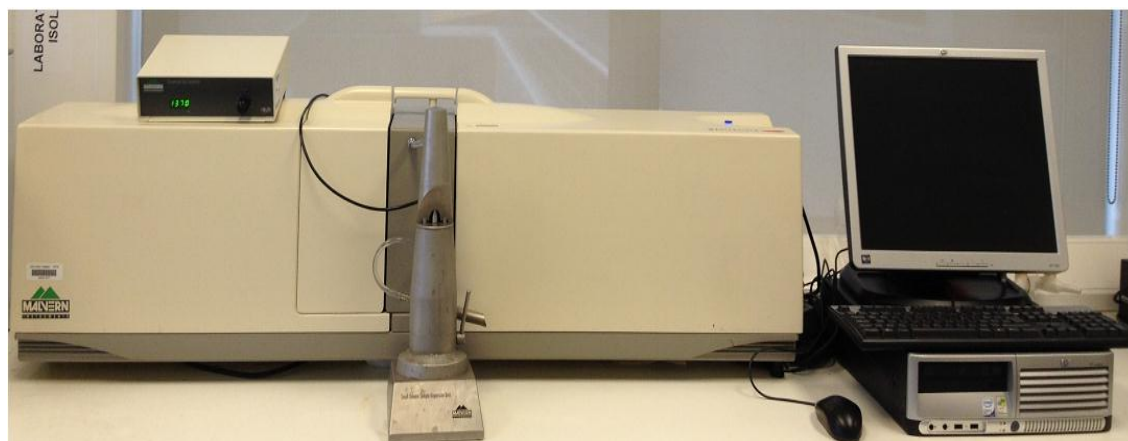


Figure 2. 5: The Malvern Mastersizer instrument used in the present study (upper picture) and a schematic illustration of light scattering from small and large particles (lower picture) (Malvern-Instruments Ltd, 2012) (www.malvern.com).

2.6.3 Zeta potential analysis

A Zetasizer Nanoseries (Malvern Instruments Ltd., UK) (Figure 2.6) was used to measure the surface charge of liposomes. Liposomal suspension was vigorously shaken and Gilson pipette was used to place 70 μl of formulations into a disposable polystyrene zeta cell (Malvern Instruments Ltd., UK). The analysis was carried out after equilibrium time of 2 min at 25°C.

To measure the zeta potential of microspheres formulations, 1 ml of phosphate buffer solutions (pH 6.5; 0.001 M) was added to 5 mg of the formulations and 70 μl of the dispersion was placed into the zeta cell. The difference in potential between a conducting liquid and the surface of a dispersed vesicle in the liquid is the zeta potential (Maherani et al., 2012).



Figure 2. 6: Malvern Zetasizer Nanoseries 2000 used in the present study.

2.6.4 Powder tapped and bulk density measurement

Tap density of mucoadhesive microspheres was measured by using Tapped density meter (ERWEKA[®] GmbH, D-63150 Heusenstamm/ Germany). A known quantity of powder was poured into 5 ml cylinder. The volumes occupied by the powder before and after tapping were recorded. The tapped density of microparticles was determined until

no further change in the powder volume was observed (6 min). Measurements were repeated in triplicate. Bulk density (BD) and tapped density (TD) for microparticles were calculated by using equation 2.4 and 2.5. Hausner's ratios were used to determine the powder flow properties of mucoadhesive microspheres as follows (Eq. 2.6) (Allamneni et al., 2012):

$$BD = \left(\frac{W}{V}\right) \quad (\text{Eq. 2.4})$$

$$TD = \left(\frac{W}{V_t}\right) \quad (\text{Eq. 2.5})$$

$$\text{Hausner ratio} = V/V_t \quad (\text{Eq. 2.6})$$

$$\text{Carr's Index} = \left[1 - \left(\frac{\text{Bulk density}}{\text{Tapped density}}\right)\right] * 100 \quad (\text{Eq. 2.7})$$

Where D = density of the powder (g/ml), BD = Bulk density (g/ml), TD = tapped density (g/ml), W = weight of powder (g), V = volume of powder before tapping (ml), V_t = tapped volume of powder.

2.6.5 Encapsulation efficiency and drug loading

Total amount of the drug within the microspheres was estimated by weighing 4 mg of microspheres followed by microsphere dispersion into 30 ml phosphate buffer solution (pH 6.5). This was left for 5 h, then vortexed for 1 minute to extract the entrapped drug. The solution was then filtered through micro filter paper (0.22 μm) in size and quantified using High Performance Liquid Chromatography (Agilent 1200, Agilent technology Ltd, USA) to determine the encapsulation efficiency (EE) and drug loading (DL) present within the microspheres (Parul et al. 2008) using equation 2.8 and 2.9.

$$EE(\%) = \left(\frac{\text{Amount of encapsulated drug}}{\text{Theoretical drug content}}\right) \times 100 \quad (\text{Eq. 2.8})$$

$$DL(\%) = \left(\frac{\text{Weight of drug loaded in microspheres}}{\text{Total Weight of microspheres}}\right) \times 100 \quad (\text{Eq. 2.9})$$

2.6.6 Swelling index

The swelling ability of mucoadhesive microparticle formulations intended for intranasal delivery is correlated to their mucoadhesive properties. The swelling capacity of the microspheres was calculated by measuring the extent of swelling of microspheres to their equilibrium in phosphate buffer (pH 6.5). The experiment was performed by dispersing microparticle formulations (15 mg) in the buffer solution followed by allowing them to swell for up to 4 hours, to ensure complete equilibrium of swelling. Excess amount of water was removed from the surface of swollen microparticles by gentle blotting using a soft tissue. A digital balance (Ohaus electronic balance, Ohaus Corporation, USA) to an accuracy of 0.00001g was used to weigh the swollen sample. The swelling index was calculated according equation 2.10 (Patil and Sawant, 2011). The experiment was repeated three times.

$$\alpha = \frac{W_s - W_o}{W_o} \quad (\text{Eq. 2.10})$$

Where α = Degree of Swelling, W_s = weight of swollen microspheres, and W_o = weight of dry microspheres.

2.6.7 Scanning electron microscopy

Microparticles were scanned after mounting on to a carbon pad (Agar Scientific, UK). Spray air was used to remove excess amount of powder, then microparticles were coated by thin layer of gold using a sputter coater apparatus (Bio-Rad, England) under vacuum. The shape and surface characteristics of the microparticles were observed under vacuum using scanning electronic microscopy (SEM) using a voltage of 20kV (Quanta 200, Czech Republic).

2.6.8 X-Ray Diffraction

Physical states of RH, chitosan glutamate and RH loaded microspheres were determined by X-ray diffractometry (Equinox 2000 Inel, France). The powder samples were spread on metal sample holders, and glass slide was used to press and smooth the powder surfaces. The diffraction intensity was recorded at 2-theta and a run time was 20 min. The current and voltage generator were set at 28 mA and 32 kV, respectively.

2.6.9 Differential scanning calorimetry

Differential scanning calorimetry (DSC) is a thermo analysis technique; it can be used in various fields; pharmaceutical research, biotechnology, food, polymer, and nanomaterial products. DSC determines the thermal change events of a given material by measuring enthalpy and onset of the thermal event, or by determining the melting point of the crystalline material and glass transition temperature of the amorphous material (Figure 2.7). This instrument generates data that can be useful to understand the physical behaviour of materials (e.g. crystalline or amorphous form) (Gill et al., 2010). During sample analysis the reference pan (empty) and the test pan which contains the sample for thermal analysis are heated at constant heat flow. The detector records thermal changes happen to the sample either when absorbing or evolving heat (www.ami.ac.uk).

Differential scanning calorimetry (DSC823e, Mettler Toledo, Switzerland) was used to determine the thermal behaviour of the pure drug and drug loaded microspheres as powder samples. DSC was calibrated before the experiment was performed using indium and zinc oxide. The analysis was done for pure drug, chitosan, and drug-loaded microspheres. A weight between 3.5 to 4 mg was placed into an aluminium pan (40 μ l) and the pan was sealed using the sealing press apparatus. The samples were heated at a rate of 10°C/min, and the scanning was performed between 35 and 300°C.

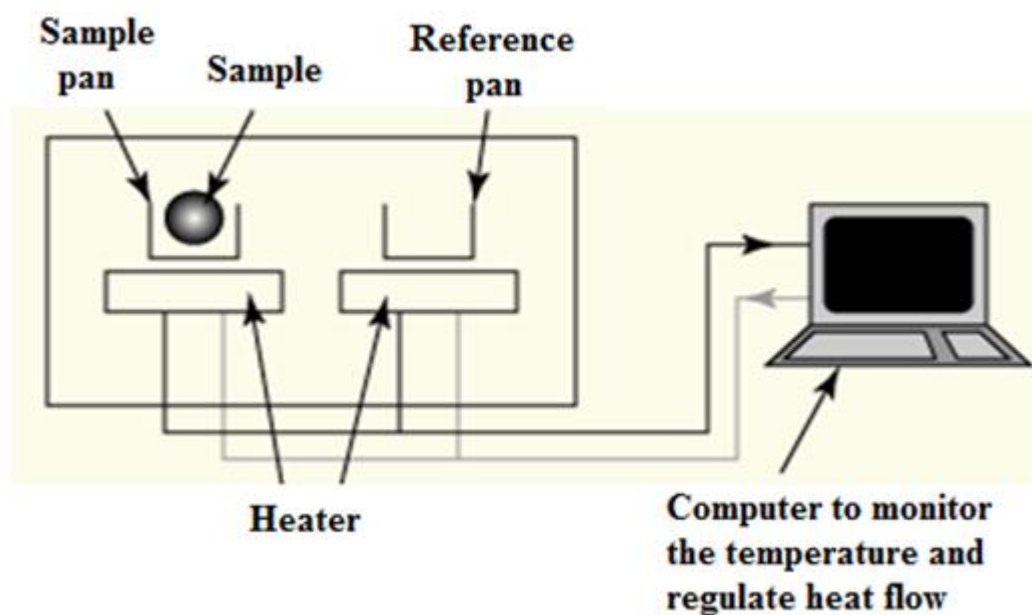


Figure 2. 7: Schematic presentation showing the principal components of a DSC equipment (Adapted from www.ami.ac.uk).

2.6.10 Thermogravimetric analysis

The weighed sample in crucible or aluminium pan was placed into the thermogravimetric (TGA) analyzer connected to a highly sensitive balance to determine the mass change of the sample during heating at a constant heating rate under purge of nitrogen gas. Difference in mass (decreasing or increasing) may indicate sample degradation (Figure 2.8).

Thermogravimetric analysis (TGA) was used to detect the weight lost as function of temperature (TGA/SDTA851e, Mettler Toledo, Switzerland). The equipment was calibrated before analysing the samples using indium and zinc oxide. Approximately 4.5 to 5.3 mg of the microsphere formulations were placed in to the aluminium pan (40 μ l) and sealed with a sealing pressure of crucible. A hole was made at the top of the cover using a pin to allow evaporation of moisture during heating process under a purge of N_2 gas. The sample was then placed onto the highly sensitive balance of 0.01 mg in accuracy and the equipment was set at a heating rate of $10^\circ\text{C}/\text{min}$ from 20 to 300°C . The change in mass of the powder formulation was determined as percentage of weight lost when no more weight loss of the sample was detected by the TGA instrument. The percentage of weight loss was determined when the temperature reached 120°C .

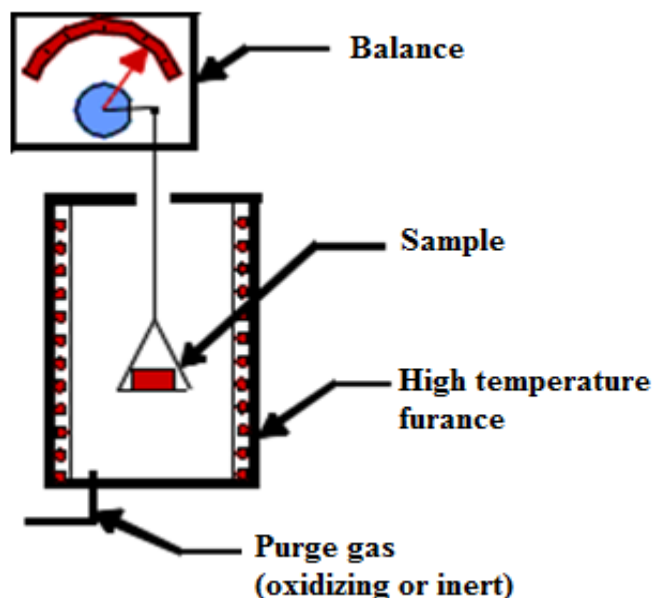


Figure 2. 8: Schematic diagram of a TGA equipment (www.ami.ac.uk).

2.6.11 *In vitro* drug release

Microsphere formulations containing 2 mg of RH were dispersed into 70 ml phosphate buffer (pH 6.5) in glass bottle, and the temperature was maintained at $37^{\circ}\text{C} \pm 0.20$ and continuous shaking was provided in a water bath at a rate of 100 rpm. Samples were taken at different time intervals (0.5, 1, 2, 5, 10, 20, 30, 60 and 90 min) and in order to keep a sink condition the taken sample was replaced by the same volume of formulation-free dissolution medium. The amount of drug released per time was analyzed using HPLC. These studies were conducted in triplicate and the results were expressed as average values (Huh et al., 2010).

2.6.12 Histopathological study

Freshly isolated nasal mucosa was taken immediately after sacrificing a healthy eight months in age Makui sheep. The sample was used to conduct the histopathological study (Seju et al., 2011). This experiment was conducted at the College of Pharmacy-Hawler Medical University, Erbil-Iraq according to their ethical regulations. The nasal mucosa was sectioned into four pieces. Each piece was treated for 2 hours with drug loaded-microspheres dispersion containing 2 mg/ml of RH from either drug-loaded chitosan microspheres (90:10 polymer to drug ratio) and drug-loaded alginate

microspheres (90:10 polymer to drug ratio), drug solution (2 mg/ml) in phosphate buffer solution (pH 6.5), phosphate buffer solution (pH 6.5) as a negative control and sodium deoxycholate (1% w/v) solution as a positive control. Samples were taken out and washed with NaCl (0.9%) and the tissue was fixed in 10% buffer formalin and embedded in paraffin wax for 4 h. Paraffin sections 7 - 5 mm were cut onto glass slides and stained with haematoxylin and eosin (Sigma Aldrich, UK). Sections were examined by light microscopy (Olympus microscope) to detect any damage during incubation. The examination was carried out by a pathologist who was not involved in the formulation work and by assigning numbers to the samples to minimise bias. Examination of the tissue included the observation of all essential components of the respiratory epithelial cells such as goblet cells, ciliated cells, mucosal and sub mucosal layers, sero-mucinous glands. The possible epithelial necrosis was examined and sloughing of the epithelial cells and inflammatory cells were also studied.

2.7 Characterization of microspheres emitted from a nasal device

2.7.1 Quantative determination of dose uniformity

To determine the consistency of the dose discharged from nasal insufflator, the Miat[®] nasal insufflator (provided as a gift from MIAT S.P.A. Milan, Italy) was used and gelatin capsule No.3 was filled with accurately weighed 5 mg, 10 mg or 20 mg powdered microsphere formulations using Ohaus electronic balance (Ohaus Corporation, USA). The capsule was placed into revolving chamber and introduced into the body of nasal insufflator. Sufficient pressure was added to the ends of capsule to pierce it with a needle, and then the powder was sprayed by squeezing the rubber bulb of the insufflator. The shot weight was determined based on weight difference of the capsule after each puff for a total of three puffs. The experiment was conducted in triplicate (Patil and Sawant, 2011).

2.7.2 Qualitative analysis of spray pattern of microsphere formulations

The qualitative study for the microspheres powder to be delivered via nasal route included spray investigations of the pattern and plume geometry. To perform spray pattern and plume geometry of the microspheres, MIAT[®] A.S.P Milan, Italy nasal insufflator was used. The technique was used to determine the plume geometry which is the same technique used for nasal spray. The resultant images were characterized in

terms of shape of the powders emitted from insufflator, plume angles and spray time. To determine spray pattern, blue pressure sensitive tape was used instead of TLC plates. It was placed 3 cm away from the tip of nasal insufflator (Figure 2.9). The microspheres were fired towards it, then the resultant images were analyzed for maximum and minimum diameters (D_{Max} and D_{Min}) and ovality ratio (D_{Max}/ D_{Min}) (Pringels et al., 2006).

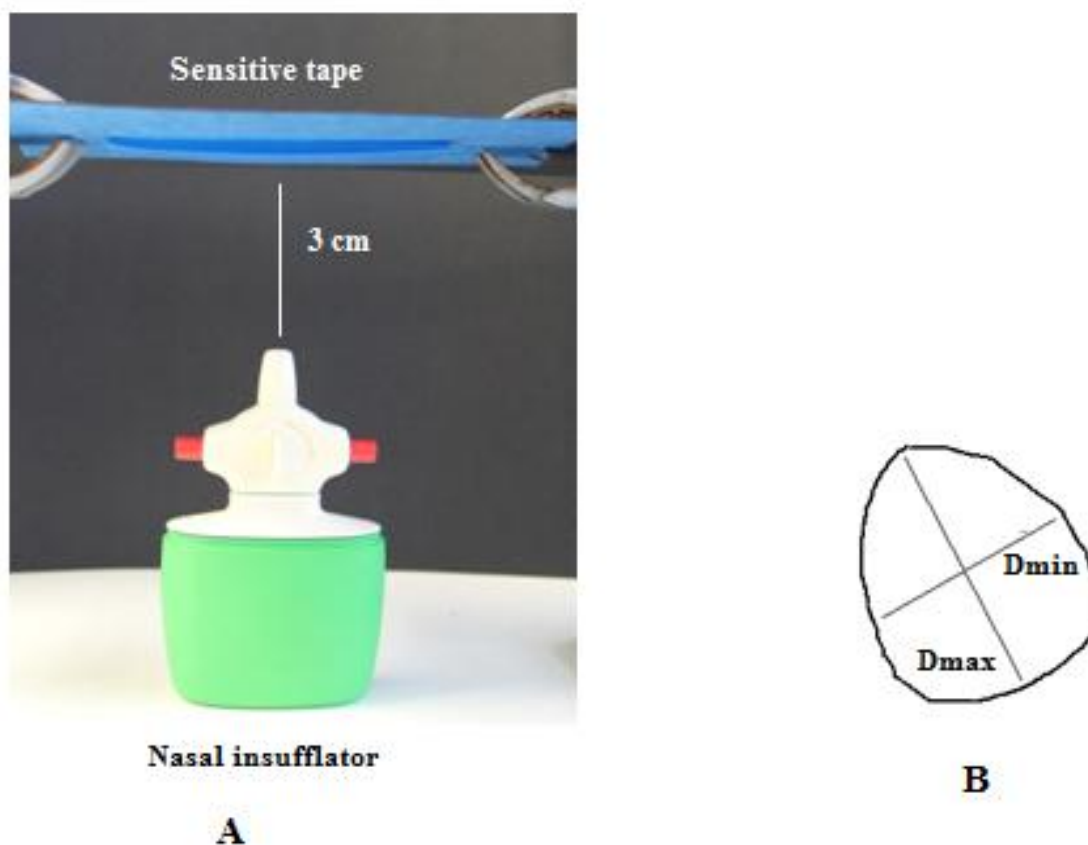


Figure 2. 9: An illustration of (A) technique used to determine spray pattern of powder, and (B) an example of spray pattern.

2.8 Liposome formulations

Several liposome formulations have been investigated and the details are given below.

2.8.1 Ethanol-based proliposomes

Ethanol-based proliposomes were used to prepared ropinirole hydrochloride loaded liposomes by adapting the method used by Perrett and co-workers (1991). Proliposomes were made by adding 60 mg ethanol (equivalent to 76 μ l) to 10 ml glass vial containing 50 mg of lipid phase (soya phosphatidylcholine (SPC) and cholesterol, 2:1 mole/mole) at 70°C for two minutes to obtain a clear lipid solution (i.e. proliposomes). RH (0.5 ml) in concentrations of 0.5, 1, 2, 4 or 8 mg/ml were quickly added to the lipid solution and vortexed for two minutes using the Whirl Mixer TM (Fisherbrand, Fisher, and UK). This resulted in the generation of concentrated liposomal suspensions (primary hydration step). The rest of HPLC water (4.5ml) was added to the concentrated liposomal suspension and vortexed again for two minutes (secondary hydration step) to yield the final liposome suspensions which were left at room temperature for 1 hour to anneal.

2.8.2 Polymer-coated liposomes

In this study 5 types of mucoadhesive agents were used: Protasan up G113 and Protasan up G213, Carboxymethyl chitosan, Low viscosity of sodium alginate or Medium viscosity of sodium alginate (0.2% w/v). The polymers were separately dissolved in 4.5 ml HPLC water. Vortex mixing enhanced the rate of dissolution of the polymer then addition of mucoadhesive solutions in secondary hydration step of the ethanol-based and again vortexed for two minutes generated liposomes coated with mucoadhesive polymer.

2.8.3 Drug entrapment studies

To separate the entrapped drug from un-entrapped drug, liposome dispersion was placed into centrifuge tube for centrifugation at 50,000 rpm (251,818 x g) for 20 minutes at 6°C using Beckman ultracentrifuge (Beckman LM-80, Beckman Coulter Instruments, UK). After centrifugation, the supernatant was collected and liposome pellets were redispersed in 5 ml of HPLC water to remove the drug adsorbed onto the surface of liposomes. Centrifugation was repeated for 20 min at the same condition, and then supernatant collected. The un-entrapped drug from the supernatants was measured by

HPLC (Agilent 1200 series, USA). The area under curve of the un-entrapped drug was used to quantify the amount of free drug present in the supernatant to determine the drug entrapment efficiency in liposomes. Equation 2.11 was used to calculate the entrapment efficiency (EE) (Elhissi et al., 2006).

$$EE(\%) = \left(\frac{\text{Total drug} - \text{Unentrapped drug}}{\text{Total drug}} \right) \times 100 \quad (\text{Eq. 2.11})$$

2.8.4 Liposome morphology study using transmission electronic microscopy

Transmission electron microscopy (TEM) offers highly resolution microscopic images of micro and nano structures. To carbon-coated copper grids (400 mesh) (TAAB Laboratories Equipment Ltd., UK), a drop of the liposome dispersion was spotted and negatively stained with 1% w/v phosphotungstic acid (Elhissi et al., 2006), then viewed and a number of high resolution images were taken by a Philips CM120 Bio-Twin transmission electron microscope (Philips Electron Optics BV, Netherlands). This study was conducted at the University College London.

2.8.5 Size analysis of droplets emitted from nasal devices using laser diffraction

Laser diffraction is a non-aerodynamic based method that measures droplet size in air. Moreover, laser diffraction provides the percentage of transmission (%T) and Span ((D0.9 – D0.1)/D0.5). The data obtained from laser diffraction was used to study each plume by three phases: formation phase, fully developed phase and dissipation phase. Droplet size change is consistent with the changes of percentage transmission (%T) or changes in obscuration, the settling values of droplet sizes and the settlement of obscuration or %T are observed within approximate time period (CDER, 2003).

Liposomes (5 ml) prepared using the ethanol-base technique proliposomes were centrifuged at 50,000 rpm using the Beckman ultracentrifuge at 6°C. The supernatant was discarded and replaced with 5 ml of fresh HPLC water to redisperse the liposome pellet with aid of vortexing. Rehydrated liposomal suspension (5 ml) was placed into the nasal spray device and spray was generated while holding the device perpendicularly 5 cm away from the beam of the Malvern Spraytec (Malvern Instruments Ltd., Model 3321 Aerodynamic Particle Sizer® (APS) Spectrometer UK) (Figure 2.10). Prior to particle size measurement, each formulation loaded into different

nasal devices was firstly primed by actuation of the pump of nasal device for seven times. When the sample unit discharged from the nasal device, geometric droplet size based on laser diffraction was determined using laser diffraction. The data was analyzed in terms of volume median diameter (VMD) and size distribution (Span).

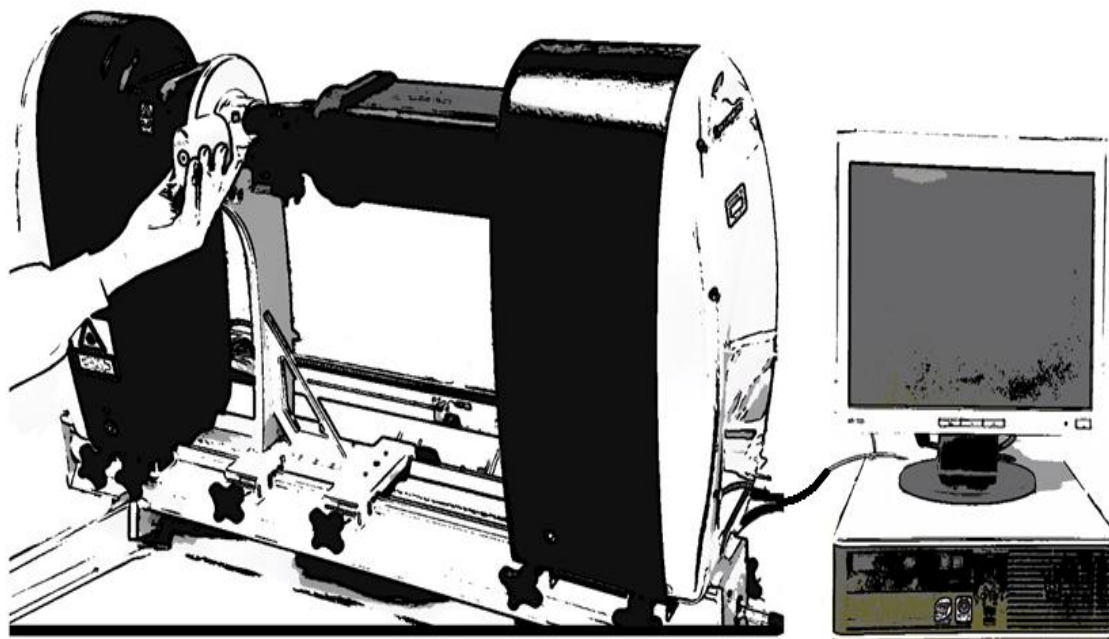


Figure 2. 10: The Malvern Spraytec system used to characterize particles since delivered from nasal sprays or insufflators.

2.8.6 Determination of shot weight and spray content uniformity

According to FDA recommendation, multiple metered dose nasal spray should be analysed for the amount of the spray discharged via actuation at the beginning to the end of the experiment for the individual nasal device used (CDER, 2002).

Prior to the experiment, a number of actuations (priming actuations) are required to purge the air off the system and dip tube used to generate the full dose. The number of actuations required to prime on initial used, number of actuations at fully developed phase and numbers of the actuations at the tail-off phase were determined for multiple metered dose nasal sprays. The accuracy of discharged volume from the nasal devices was determined. Low volumes of solutions within nasal devices might lead to generation of low discharged volumes of spray, compromising the content uniformity of the dose. This is referred to as “tailing-off” (Schultz, 1995), that continues until no

spray is discharged upon actuation. The phenomenon of tailing-off for the various nasal formulations and devices was recorded and the number of actuations required to obtain full actuation delivery was determined.

For shot weight measurement the spray pump devices were weighed prior and after each actuation using Ohaus electronic balance to accuracy 0.00001g (Ohaus Corporation, USA). This was referred to as delivered dose per single actuation of the nasal device (Guo and Doub, 2006).

Centrifuged liposome formulations were redispersed (5 ml) and placed in the nasal devices then the number of actuations required to prime, the number of full actuations discharged from devices, and the number of actuations in the tailing-off phases for the different nasal devices were determined.

2.9 Nasal spray characteristics

To determine the characteristics of nasal spray, droplet size and size distribution, spray pattern and plume geometry were analyzed (Guo and Doub, 2006). According to the guidelines of Centre for Drug Evaluation and Research (2003), two techniques are available to determine and analyze the spray pattern, impaction and non-impaction techniques (CDER, 2003). Impaction technique was used in this study to determine and characterize the discharged spray after actuation from the nasal devices.

Spray pattern was characterized after impaction onto TLC. It was performed at the specific distance from the tip of the nasal device to determine the shape of aerosol delivered from nasal device upon actuation. Spray pattern may give an indication of the site of deposition of the delivered dose in the nose. Before each experiment, each nasal spray was actuated 5 - 7 times to waste to ensure the device is primed. Solution (5 ml) was coloured with 3 drops of natural food colour (foodfinders Ltd, UK) to visualize the splatter pattern on the TLC sheet. For this purpose, nasal spray device was placed 3 cm in distance away from collection surface of the TLC sheet (Figure 2.11). Liposome formulation was fired toward TLC sheet (Guo and Doub, 2006). The image of the spray pattern on the TLC was taken immediately after actuation of the nasal device using a professional digital camera (LSH Canon 550 D 55 mm – 08, Cannon Ltd., Tokyo). Maximum diameter (D_{Max}), minimum diameter (D_{min}) and ovality ratio (D_{Max}/D_{min}) of the spray pattern shape were determined according to CDER guidelines (2003). Ovality

ratio gives indication of the shape of the impaction spray which is round, irregular or ellipsoid shape.

Plume geometry describes the shape of the discharged sample parallel to the axis of plume after actuation of nasal pump device. Two techniques are available to visualize plume geometry; (1) laser light sheet and high speed digital camera and (2) high-speed photography according to Center for Drug Evaluation and Research (CDER) guidelines (2003).

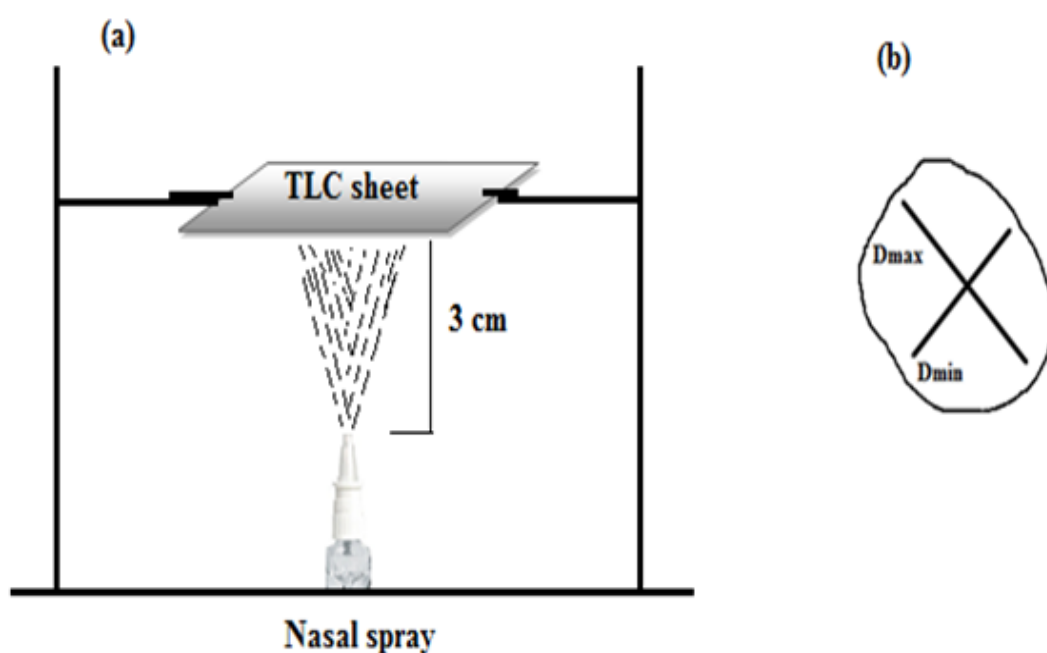


Figure 2. 11: Schematic illustration of (a) the technique used to determine spray pattern, and (b) an example of spray pattern.

To study plume geometry, actuations were fired upward and recording was conducted by placing the digital video camera (Full HD, JVC Ltd., Malaysia) in front of the nasal spray device, while keeping a black background at the opposite side at the back of the nasal device (Figure 2.12). The digital video camera was used to record the spray cloud generation while the sample proceeded to evolve from the tip of the nasal device. The recording videos were transferred to personal computer and the elapsed recording time was framed at different rates using AVs Video Editor software. The fully developed phase was printed and characterized for the three stages; at the early stage upon formation (formation phase), during an intermediate time of spray (fully developed

phase) and when the plume spray started to separate from the nasal device tip (dissipation phase). Studies were also performed to determine plume angle and widest horizontal distance of spray clouds after actuation of the nasal pump devices for the different samples using protractor from the printout images, while longest vertical distanced (plume height). The distance that was derived by the spray samples from the tip of devices was determined according to previously made graduation on the background using a ruler. According to the regulatory guidelines of CDER (2002; 2003), the image analysis was carried out at the fully developed phase while the spray cloud was still in contact with the tip of the nasal device.

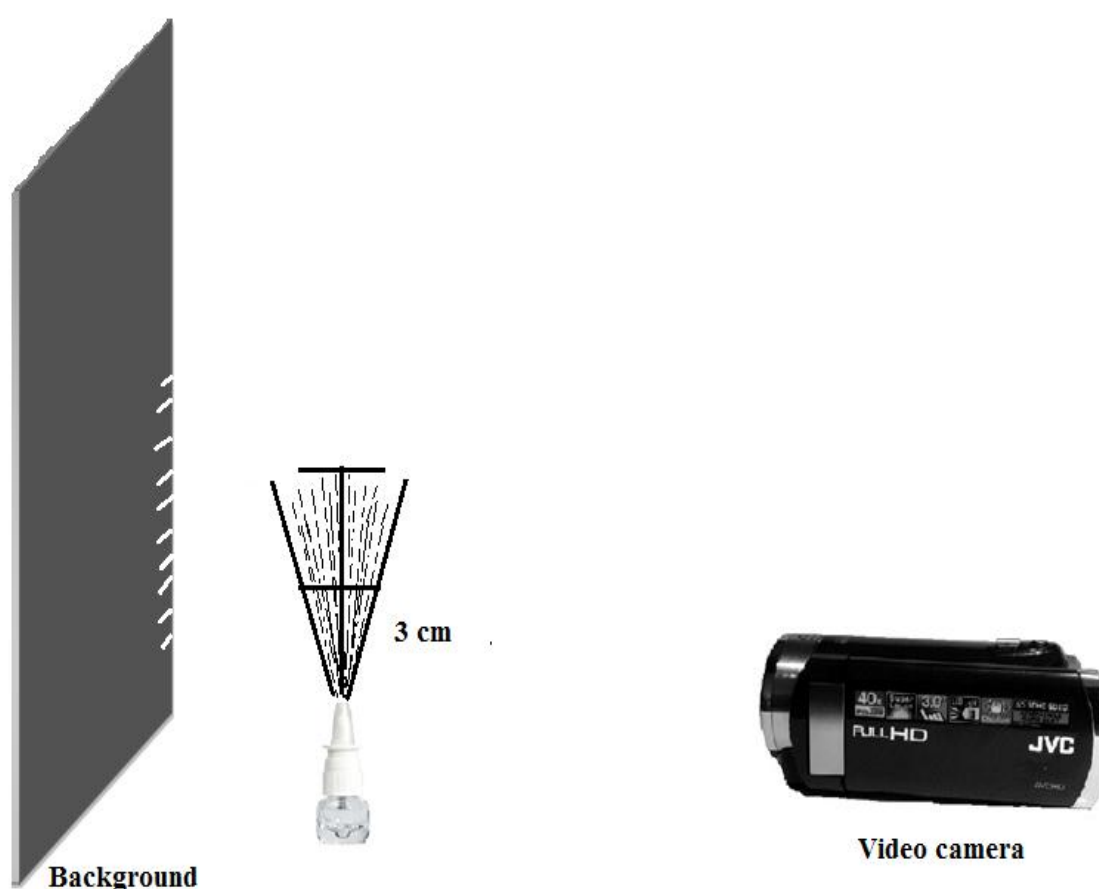


Figure 2. 12: Schematic illustration of the technique used to monitor the plume geometry.

2.10 Statistical analysis

All experiments were carried out in triplicates; One-way Analysis of Variance (ANOVA) and student's t-test were used for statistical data analysis to compare more than two groups of data and two groups of data respectively. Values were expressed as mean \pm standard deviations and p -value <0.05 indicated that difference between the groups were statistically significant.

CHAPTER 3

PREPARATION OF ROPINIROLE HYDROCHLORIDE LOADED CHITOSAN MICROPARTICLES VIA SPRAY DRYING

3.1 Introduction

Mucoadhesive systems incorporate bioadhesive agents to enhance the drug absorption by prolonging the period of contact between the drug and the cellular mucosa (Jain et al., 2004). Nasal delivery is a promising route for delivery of drugs, which are susceptible to enzymatic, acidic or first pass effect for treating systemic or nasal diseases because nasal mucosa may offer higher drug permeability compared to other mucosal membranes. Intranasal drug delivery has been investigated for treating CNS conditions such as brain tumour (Hashizume et al., 2008; Shingaki et al., 2010). This route is particularly attractive due to relatively high vascularity, which results in high absorption rates for small molecules, peptides and proteins that are difficult to be administered by other delivery routes (Illum et al. 2001; Vyas et al. 2005). Additional advantages include high surface area of the nasal cavity which provides rapid onset of drug action, convenience of using nasal formulations by patients, avoidance of first pass metabolism by the liver, and lower enzymatic activity in the nose compared to the GIT (Illum et al. 2001; Vyas et al. 2005). Targeting drug to the brain also circumvents the brain blood barrier (Graff and Pollack, 2005); therefore it is considered a smart route for drug targeting to the brain.

Mucociliary clearance is a barrier that plays an important role at clearing the nose from foreign particles. Hence, the use of bioadhesive polymers for the preparation of drug loaded microspheres could lead to enhanced residence time of the drug in the nasal cavity, thus increasing drug absorption (Soane et al., 1999).

Nasal formulations in powder form offers advantages over nasal drops and nasal sprays in terms of stability, hence offering a preservative-free alternative (Huang et al., 2004; Jadhav et al., 2007). The expediency of the powder formulation is however highly dependent on solubility, particle size, aerodynamic properties and nasal irritation of the active drug and/or excipients (Aurora, 2008).

Drug carriers such as mucoadhesive microspheres consist of a drug and natural or synthetic biodegradable excipients (e.g. chitosan) used to improve drug absorption by enhancing residence time in the nose, opening tight junctions between cells, increasing concentration at the site of absorption or providing protection from enzymatic degradation (Wang et al., 2006; Duan and Mao, 2010).

Chitosan prepared from chitin by alkaline deacetylation is a cationic polysaccharide. This is considered to be a second copious polymer next to cellulose (Singla and Chawla, 2001). Chitosan is insoluble in water but is soluble in dilute acids (pH less than 6.5) (Chandy and Sharma, 1990). In contrast, chitosan salts such as glutamate and hydrochloride are water soluble (Alhalaweh et al., 2009). The wide use of chitosan in pharmaceutical formulations is attributed to its safety, biodegradability and biocompatibility (Singla and Chawla, 2001). The polycationic property of chitosan facilitates its interaction with mucin and other negatively charged ions in the nasal mucosa resulting in prolonged retention time within the nasal cavity and enhanced drug permeability (Fernandez-Urrusuno et al., 1999). Abdel Mouez et al. (2014) have reported that verapamil hydrochloride loaded chitosan microparticles enhanced bioavailability significantly (58.6%) compared to the drug solution after intranasal administration (4.8%) and oral drug solution (13%) in rabbit animal model. Chitosan can also act as a permeation enhancer to promote the rate of drug transfer through nasal mucosa, hence improving bioavailability (Fernandez-Urrusuno et al., 1999).

Ropinirole hydrochloride (RH) is a non-ergot dopamine D₂-agonist used in the management of Parkinson's disease alone or as an adjunct to reduce 'on-off' fluctuations in levodopa response (Pahwa et al., 2004). When used orally only approximately 50% is absorbed since it undergoes extensive first pass effect (DrugBank, 2013). Beside to pramipexole and gabapentin, FDA has approved RH for use in patients with restless legs syndrome (Kurlan et al., 2006).

Hydrophilic drugs have difficulty in crossing the nasal epithelium due to their large size in tight junctions hence absorption via the transcellular pathway is difficult. The incorporation of polar drugs into chitosan microspheres may improve their absorption by transiently opening the tight junctions in the cellular membranes and enhancing the contact time of the drug with the site of absorption (Illum, 2002).

RH loaded chitosan microsphere formulations were prepared in this study using spray drying. Various characterization techniques were used to select the best performing formulation for subsequent studies. Thus, histopathological study using isolated nasal sheep mucosa, physical particle size analysis using laser diffraction, plume geometry and spray pattern using impaction method were all investigated.

3.2 Methodology

3.2.1 Compatibility studies

The methods used to study the compatibility of the drug with polymer were outlined in section 2.2.

3.2.2 Preparation of chitosan microspheres

Ropinirole hydrochloride-loaded chitosan microsphere formulations were prepared as described in section 2.5, by adapting the method used by Alhalaweh et al. (2009). Five formulations of the drug-loaded microspheres were prepared including drug free microspheres for comparison (Table 3.1). Chitosan glutamate (Chg) and RH were dissolved in HPLC-grade water and the solution was made up to 100 ml in a volumetric flask. Automated microviscometer was used to determine the viscosity of the resultant solutions. Spray drying was performed using a Büchi-290 Mini Spray-dryer (Büchi Laboratories, Switzerland). The peristaltic pump fed the solution (5 - 6 ml/min) into the nozzle (0.7 µm in diameter). The inlet air temperature was 160°C, which is the optimum inlet air temperature for chitosan microspheres prepared from its aqueous solution (He et al., 1999). Other spray drying parameters were: outlet air temperature 75 - 80°C, aspiration rate 100%, and gas flow 357L/h. For each batch of microspheres 200 ml of feed-solution was used.

Table 3. 1: Microsphere formulations using various ratios of chitosan to drug.

Formulation	Ratio (w/w) (Chg: RH)	Chitosan glutamate (mg)	RH (mg)	Total weight (mg)/100 ml
F1	100:0	500	0	500
F2	90:10	450	50	500
F3	70:30	350	150	500
F4	50:50	250	250	500
F5	30:70	150	350	500

3.2.3 Characterization of microspheres

The percentage yield, particle size, size distribution, entrapment efficiency, zeta potential, bulk density, swelling index, physical state of the drug in formulations, thermal behaviour of the formulations, powder morphology, drug release profile, and histopathological characteristics of the nasal epithelium using animal tissue were studied. For selected formulations, characterizations were conducted for emitted powder (e.g. physical particle size, plume geometry and spray pattern) using nasal insufflator. Methods used were described in related sections in chapter two.

3.3 Results and discussion

3.3.1 Compatibility studies

The pre-formulation studies are essential to detect undesirable interaction between the active ingredient and excipients which can affect the stability or bioavailability of the active ingredient, hence affecting the safety and/or efficacy of the formulation (Taylor and Zografis, 1997; Verma and Garg, 2005). A suitable excipient is required to prepare a stable and effective formulation (de Carvalho et al., 2006). To investigate the interaction between the formulation ingredients, a number of experimental techniques have been used such as FTIR spectroscopy, DSC, X-Ray diffraction and HPLC (Drebushchak et al., 2006; Bozdağ-Pehlivan et al., 2011).

The FTIR spectra of pure drug, physical mixture and spray dried formulations are shown in Figure 3.1. The FTIR data confirmed that the frequency of RH did not change significantly when drug-loaded microspheres were compared with the physical mixture formulation. Sharp peaks at 1241.19, 1455.36, 1702.18 and 3068.95 cm^{-1} for (C-N), (C=C stretching), (C=O stretching) and (N-H stretching) functional groups respectively were found for pure RH (Table 3.2). When infrared spectrum of pure RH was compared to the spectrum of RH in mixture form and spray dried RH loaded microspheres, no significant band-shift in wave number was observed between the spectra, indicating that the drug consistency and absence of significant interaction, modification or loss in drug characteristics (Figure 3.1). Thin layer chromatography study showed one spot for every run sample; RH as raw material, physical mixture of RH and chitosan glutamate (50:50 w/w), and co-spray dried microparticles all had similar R_f values ($R_f=0.55$), indicating no interaction between chitosan glutamate and RH had occurred.

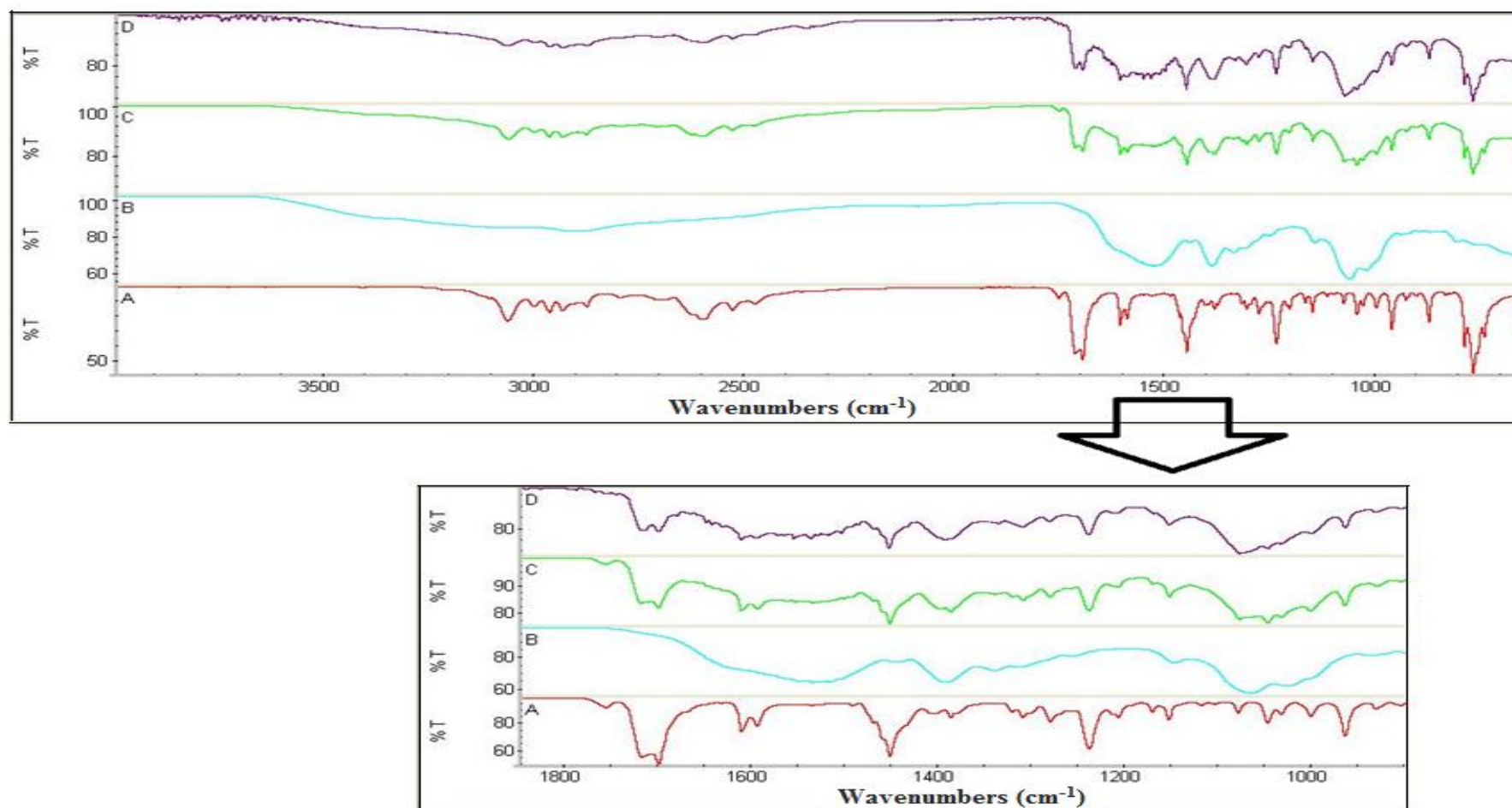


Figure 3. 1: FTIR spectrum of (A) RH, (B) chitosan glutamate, (C) physical mixture of chitosan 50% w/w and RH 50% w/w, and (D) RH loaded microspheres. The lower graph magnifies the wave numbers area between 900 and 1850 cm^{-1} .

Table 3. 2: Frequency of functional groups of pure RH physically mixed with polymer and drug-loaded microspheres.

Functional groups	Frequencies of pure RH (cm ⁻¹)	Frequencies of RH in physical mixture (cm ⁻¹)	Frequencies of RH in microspheres (cm ⁻¹)
C-N	1241.19	1241.92	1242.24
C=C stretching	1455.36	1455.56	1456.39
C=O stretching	1702.18	1702.97	1703.52
N-H stretching	3068.95	3068.45	3071.91

3.3.2 Percentage yield

The percentage yield of powder collected ranged from 70.5% \pm 0.45 to 76.9% \pm 1.01, thus spray drying was characterized by generating high product yield. However, the percentage of yield increased significantly ($p < 0.05$) when RH and chitosan glutamate were co-sprayed, whilst increasing the drug to polymer ratio in subsequent formulations significantly decreased the production yield (70.5% \pm 0.45) (Figure 2), possibly due to adherence of the drug powder to the drying chamber of the spray drier. It was confirmed when the spray drying was performed for RH (raw material) 0.5% w/v, the percentage yield was only 49.84%.

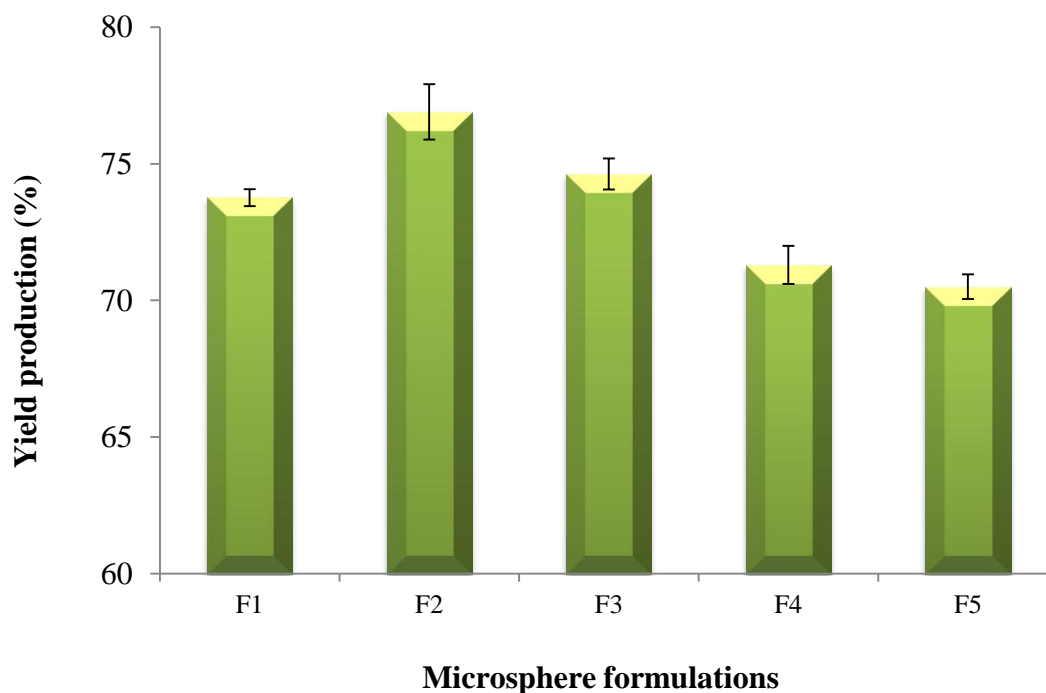


Figure 3. 2: Percentage yield of chitosan microsphere formulations (F1 – F5) for formulation composition refer to table 3.1. Data represent mean \pm S.D (n=3).

3.3.3 Particle size and distribution

Particle size for various spray dried mucoadhesive microspheres was between $1.98 \pm 0.09 \mu\text{m}$ and $3.66 \pm 0.04 \mu\text{m}$ (Figure 3.3). As the ratio of the drug to chitosan glutamate increased particle size was increased ($p < 0.05$). It is possible that at low drug to chitosan glutamate ratio, low drug concentration was available per particle, whilst increasing the ratio of the drug may lead to an increase in the amount of the dispersed drug molecules within the microparticles. In contrast, size distribution (Span) decreased significantly as the drug concentration was increased compared to the blank formulation. Span values for microspheres were ranged from 4.11 ± 0.92 to 1.10 ± 0.04 . The decreasing in Span may be due to the solution viscosity of the formulations, which was higher in F1 formulation and decreased significantly as the ratio of chitosan decreased in formulation F5 (Figure 3.4).

Figure 3.5 illustrates the relationship between viscosity of the feeding solution and particle size and size distribution. The viscosity decrease could be due to lower intermolecular entanglement, resulting in increasing the freedom of movement of individual chains of chitosan in solutions (Graessley, 1974), and possibly the formation

of uniform droplets during atomization within spray drier. Oliveira et al. (2005) have reported larger particle with wider size distribution were obtained with spraying viscous chitosan solution. These results agree with those reported by Learoyd et al. (2008a) who prepared respirable particles of beclometasone dipropionate encapsulated by chitosan via spray drying. In this study, particle size of RH as a raw material and spray dried were $59.72 \pm 3.07 \mu\text{m}$ and $23.62 \pm 4.66 \mu\text{m}$, whereas Span was 1.63 ± 0.14 and 1.84 ± 0.48 respectively.

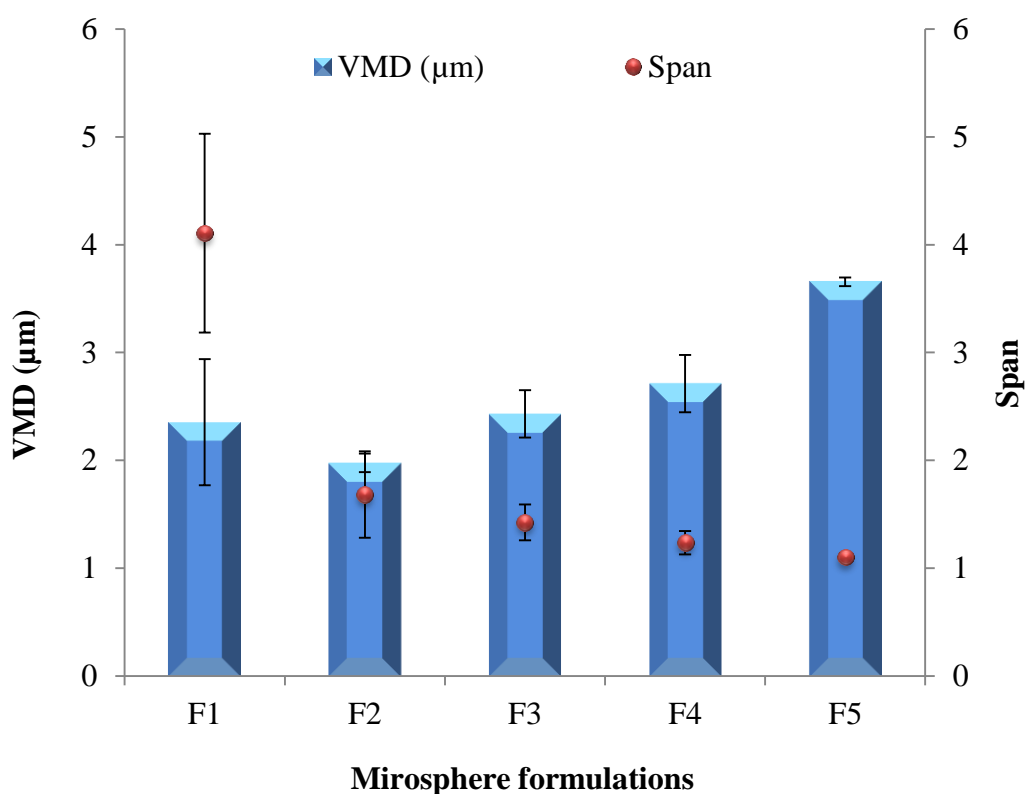


Figure 3. 3: Particle size and size distribution of RH-chitosan microparticles. Data represent mean \pm S.D (n=3).

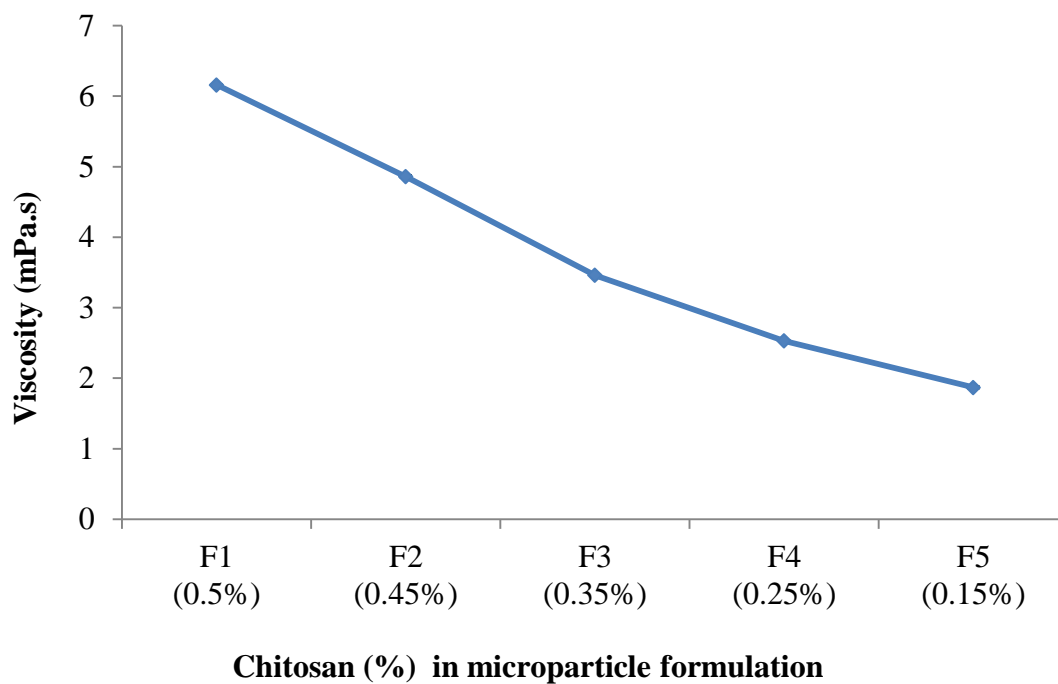


Figure 3. 4: Relationship between chitosan concentration and viscosity of the solution. Data represent mean \pm S.D (n=3).

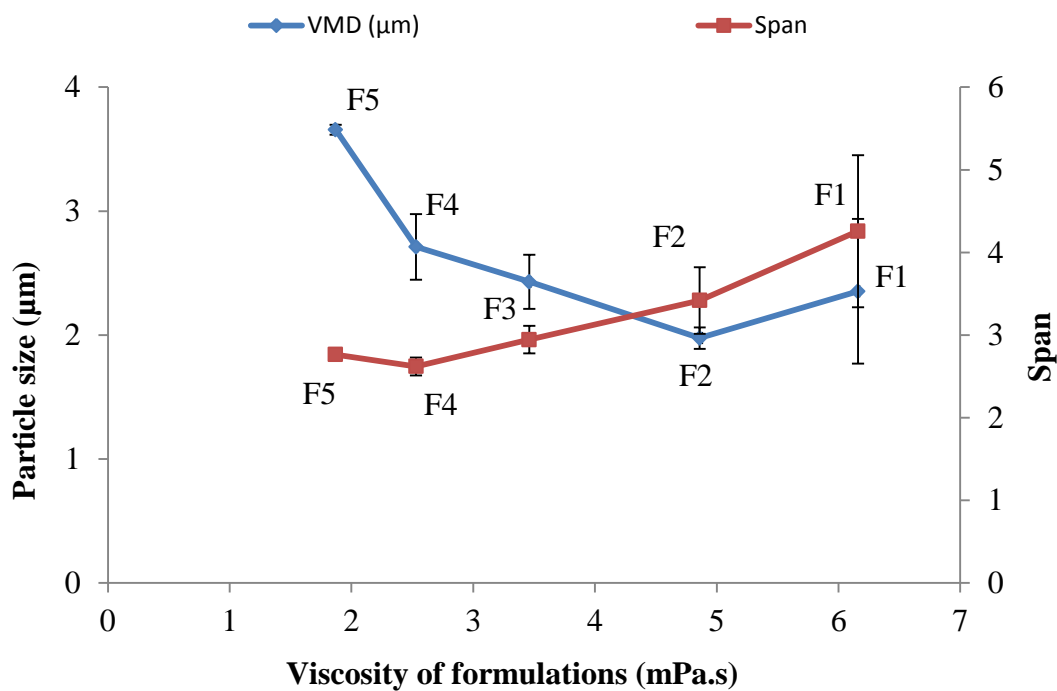


Figure 3. 5: Relationship between viscosity of the solution and particle size and size distribution (Span).

3.3.4 Zeta potential

Zeta potential of particles may influence adhesiveness onto the surface of mucous membranes. Free amino groups confer positive surface charge to the chitosan microparticles (Berthold et al., 1996). The positive charge of chitosan microspheres enhances the bioadhesion upon the strong interaction between the particles and negatively charged moieties of the membranes (e.g. mucin) (Illum et al., 1994).

In this study the positive charge of the microspheres decreased significantly ($p < 0.05$) with increasing the ratio of drug to chitosan from 52.13 ± 1.15 mV to 32.93 ± 2.5 mV (Figure 3.6). This may be attributed to the decrease in free amino groups responsible for positive charge in chitosan microparticles as the concentration of chitosan decreased (Berthold et al., 1996). Oliveira et al. (2005), have shown that the zeta potential of the particles is positive (53.7 mV) when 0.5% concentration of chitosan was used with spray drying. Dhawan et al. (2004) showed that chitosan microparticle preparation method may have a great effect on the zeta potential, and values were in the range of 20.7-50.2 mV when thermal cross-linking, emulsification and ionotropic gelation methods were used for preparation of microparticles.

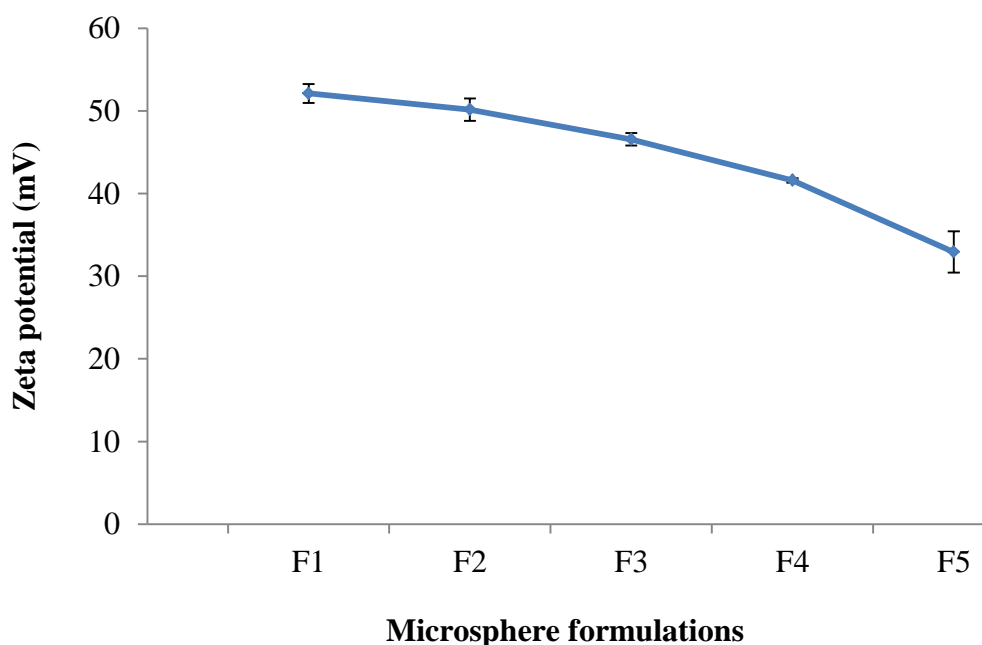


Figure 3. 6: Zeta potential of chitosan microparticles. Data represent mean \pm S.D (n=3).

3.3.5 Entrapment efficiency (EE) and drug loading (DL)

The encapsulation efficiency (%) and drug loading (%) values are shown in Figure 3.7. Almost all microsphere formulations were characterized by offering high drug encapsulation efficiencies; these were $93.28\% \pm 1.66$ for F2 and $98.91\% \pm 0.98$ for F5. Significant increase in the entrapment efficiency ($p < 0.05$) was found upon increasing the drug to polymer ratio as observed for formulations F2 and F5. The high drug loading supports the use of spray drying, since the actual drug content was close to the theoretical drug amount. Mahajan et al. (2008), Alhalaweh et al. (2009) and Gavini et al. (2008) support the conclusion that spray drying is reliable for the preparation of chitosan microspheres with high encapsulation efficiencies. For example, the entrapment efficiency values were 89-98% for ondansetron hydrochloride when loaded in microspheres (Mahajan et al., 2008), 93-105 % for zolmitriptan-chitosan microparticles (Alhalaweh et al., 2009) and 94.5 to 100% for metoclopramide microspheres (Gavini et al., 2008).

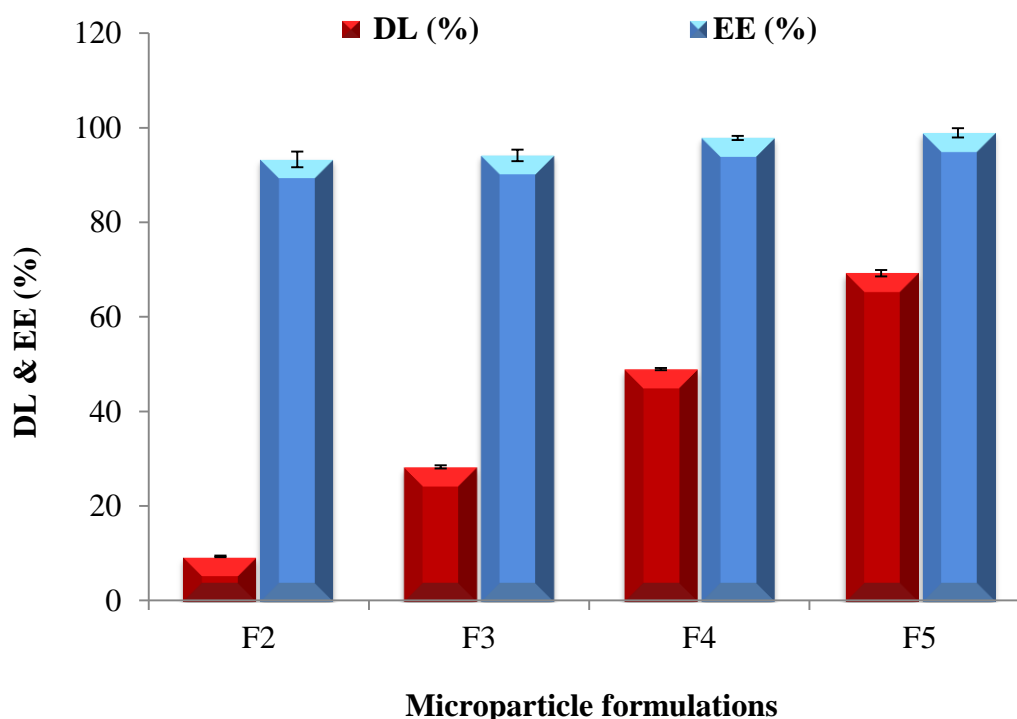


Figure 3. 7: Drug loading (DL) and entrapment efficiency (EE) in spray-dried microspheres at various drug/polymer ratios. Data represent mean \pm SD (n=3).

3.3.6 Tapped and bulk density

Tapped density and particle size are required for theoretical estimation of the powder flow properties (Kilian and Müller, 1998) which are essential for optimum delivery from the device to the desired site of deposition. Hausner's ratio is useful to determine the powder flow properties which may influence the delivery of drug from the device. Powders with Hausner's ratio <1.19 have good flow property; this is influenced by a number of parameters such as size, size distribution and cohesiveness of the particles (Copley, 2008).

Results of bulk and tapped density with Hausner's ratio are shown in Figure 3.8. The bulk density was relatively high for the formulations F2, F3, and F4, due to smaller particles compacting more closely compared to larger particles leading to lower volume to mass ratio. Larger microparticles have poorer packing properties with higher volume to mass ratio, agreeing with the finding of Sun et al. (2009). A significant difference in the tapped density amongst formulations is evident. The tapped density was greatest for F2 formulation, probably due to the highest Span values owing to the fact that the particles were much more compact than the drug-free formulation (F1). In contrast, F3, F4 and F5 formulations had lower Span values and larger particle size measurements, and hence they had more voids causing reduction in the tapped powder density to a level that was lower than that of F2 formulation. Hausner's ratio for F2, F3, and F4 formulation was between 1.26-1.34, indicating acceptable flow properties.

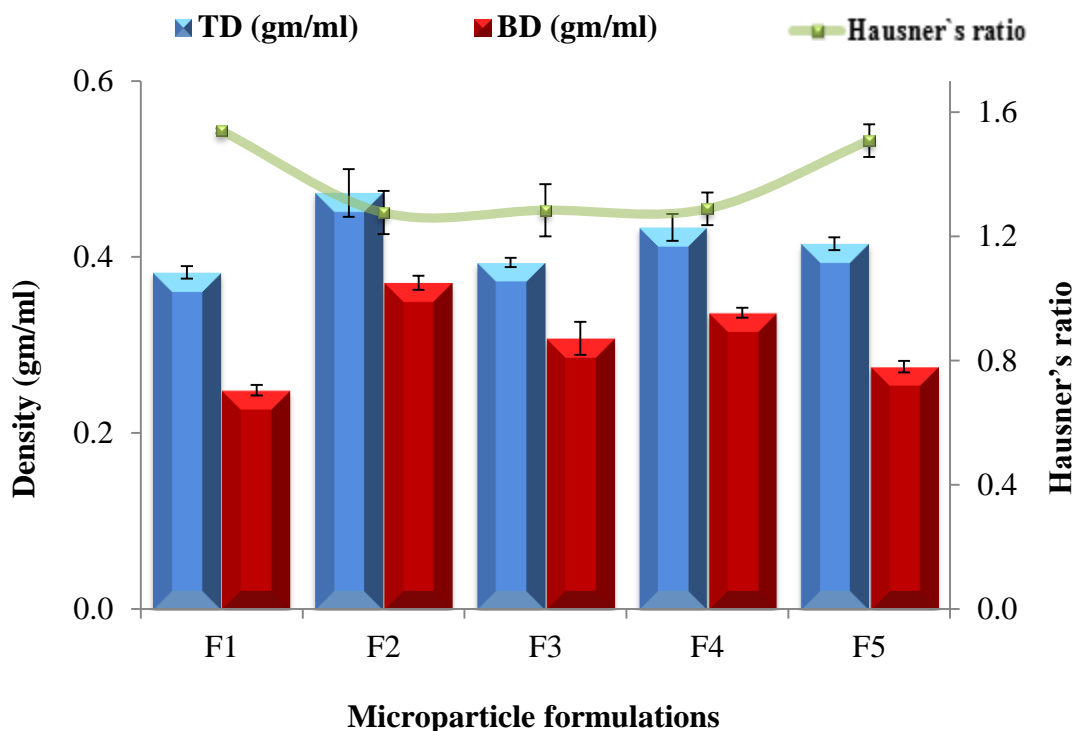


Figure 3. 8: Bulk density (BD), tapped density (TD) and Hausner's ratio of RH free and RH-loaded chitosan formulations. Data represent mean \pm SD (n=3).

3.3.7 Swelling index

Chitosan glutamate showed good swelling properties in phosphate buffer (pH 6.5) and could take up several times of its weight of water. This rapid swelling was followed by dissolution. The swelling index equilibrium depended on the amount of chitosan present in the microsphere formulation. The chitosan ratio in microspheres had a direct effect on the swelling ability in phosphate buffer (pH 6.5). As the ratio of chitosan to drug decreased the swelling index decreased significantly ($p < 0.05$), possibly due to reduced number of the positively charged amino groups, hence capturing less water (Roy et al., 2009). The high swelling property of chitosan microspheres may uncoil the polymer chains into extended and flexible chains (Agarwal and Mishra, 1999), which increases interpenetration and entanglement into mucous, hence improving mucoadhesion (He et al., 1998). Significant difference ($p < 0.05$) was observed in swelling ability as a result of decreased polymer/drug ratios (Figure 3.9). Oliveira et al. (2005) have reported that microspheres had higher swelling capacity when prepared from the more concentrated and viscous chitosan solution using spray drying. Linear relationship was observed between swelling index and surface charge of the microparticles (Figure 3.10).

Consequently, increasing drug-loading into microspheres may lead to a decrease in the swelling properties and zeta potential, possibly this would affect the mucoadhesion properties of the microspheres and drug bioavailability.

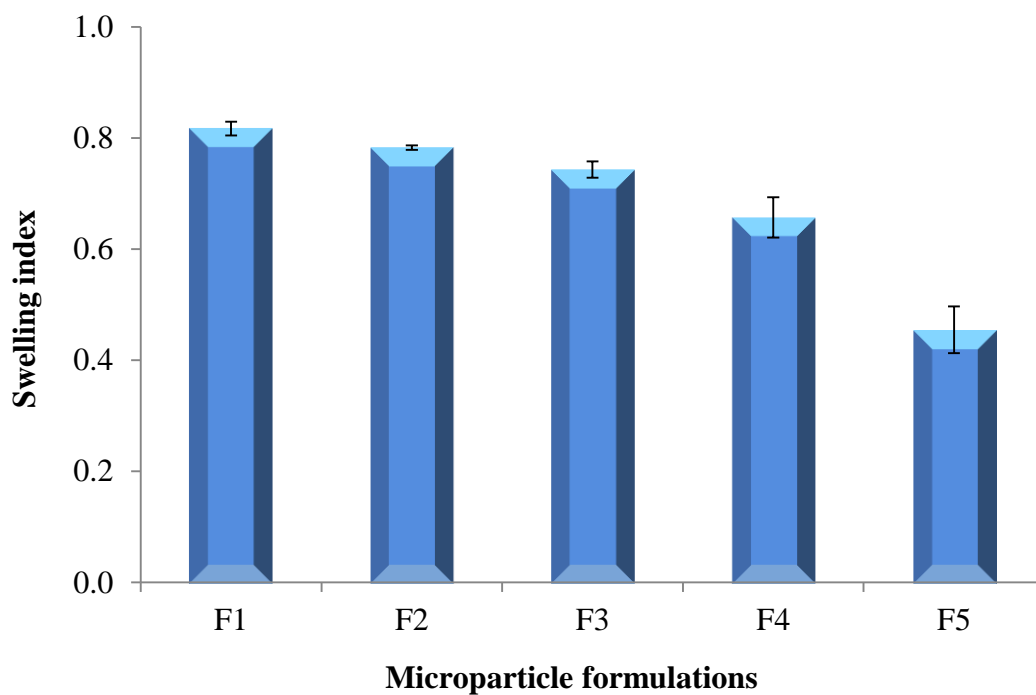


Figure 3. 9: Swelling index of RH free microspheres and RH-loaded chitosan microspheres. Data represent mean \pm SD (n=3).

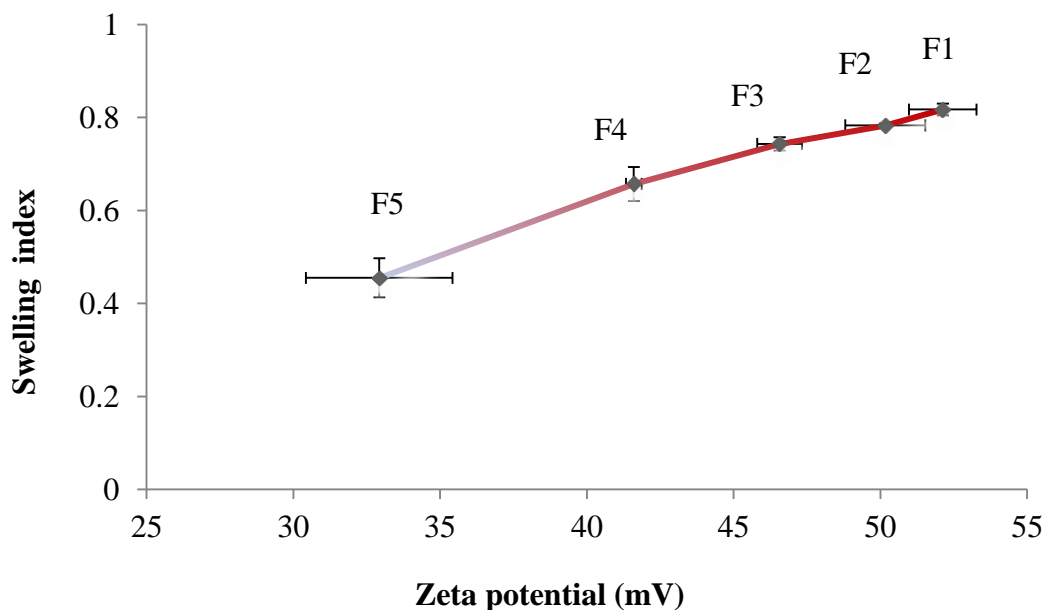


Figure 3. 10: Relationship between swelling index and zeta potential of spray dried particles. Data represent average values (n=3).

3.3.8 Mucoadhesion

In vitro study of the formulate mucoadhesive properties are needed to predict the *in-vivo* performance of mucoadhesive microspheres used for intranasal delivery (Gad, 2008). A number of *in vitro* methods have been developed to assess the mucoadhesiveness of formulations. Many research groups documented the bioadhesive properties of chitosan formulations (He et al., 1998; Harikarnpakdee et al., 2006; Sun et al., 2009). As the ratio of chitosan to drug increases the mucoadhesion increases, which can be attributed to the larger number of free positively charged amino groups that interact strongly with the negatively charged mucous glycoprotein and sialic acid of the mucous membrane (Martinac et al., 2005; Patil and Murthy, 2006; Hafner et al., 2007).

The interaction between mucin and microparticles is conveniently measured and may help for the prediction of the *in vitro* performance of mucoadhesive microparticle formulations (He et al., 1998). The amount of the drug loaded into the polymeric structure of the microspheres may influence bioadhesion (Gavini et al., 2008). The mucoadhesive properties of chitosan are attributed to the flexibility of its backbone which facilitates its entanglement into mucosal layer whilst its polycationic nature contributes to the electrostatic interaction between the polymer and the negatively

charged contribution of the epithelium (e.g. mucin and anions present in the mucous membrane like sialic acid (Harikarnpakdee et al., 2006; Robinson et al., 1987).

In this study, the intensity of chitosan adsorption onto the surface of mucin decreased significantly ($p < 0.05$) as the ratio of chitosan was decreased from formulation F1 to formulation F5 (Figure 3.11). This observation was accompanied by a decrease in the intensity of the negative zeta potential of mucin to reach neutrality when formulation F5 was included and revert to positive values upon increasing the concentration of chitosan in microparticle formulations (i.e. by using formulations F4, F3, F2 and F1). Reduced adsorption is due to lower chitosan concentration, resulting in less positively charged particles for interaction with mucin (Sun et al., 2009). Rapid swelling of small microparticles may provide a more powerful mucoadhesive system than larger particles (El-Hameed and Kellaway, 1997). Pereswetoff-Morath (1998) has report that microspheres can swell and take liquid up upon coming in contact with mucous membranes, resulting in dehydration of the epithelial cells with subsequent shrinkage. This may eventually cause the tight junctions to open, causing enhanced drug permeation.

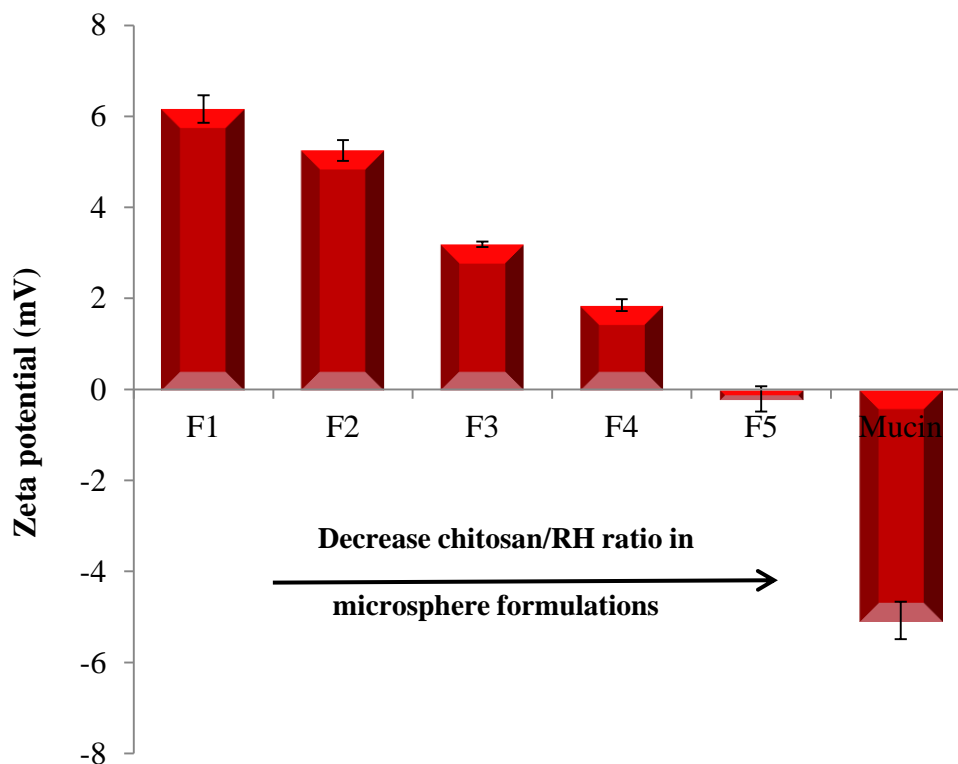


Figure 3. 11: Zeta potential of the mucin and the mixture of mucin from porcine stomach (Type II) with the microsphere formulations. Data represent mean \pm SD (n=3).

3.3.9 Surface morphology of microparticles

The morphology of drug-free and RH loaded microspheres were examined using scanning electron microscopy (SEM) (Figures 3.12, 3.13 and 3.14). RH particles had irregular shape before and after spray drying (Figure 3.12). Incorporation of chitosan glutamate in various ratios into RH solutions followed by spray drying made the microparticles spherical irrespective to the polymer: drug ratio, (Figures 3.13 and 3.14). Optimization of particle size, morphology and powder flowability is necessary to reduce the risk of nasal irritation and improve deposition in the nasal cavity (Behl et al., 1998).

Furthermore, SEM images showed absence of crystals and irregular shapes on the surface of microparticles, indicating that all drug particles were encapsulated within the polymeric structure of chitosan. These properties of microparticles may decrease mucosal irritation, enhance deposition pattern and improve drug absorption following intra-nasal delivery. Gavini et al. (2006) have reported improved nasal bioavailability of carbamazepine upon preparation of drug-loaded chitosan glutamate microspheres via

spray drying. Overall, SEM images indicated that RH-loaded chitosan microparticles are likely to be amorphous and efficiently encapsulated drugs since it is established that spray drying technology predominantly generates amorphous powders (Corrigan, 1995; Learoyd et al., 2008b).

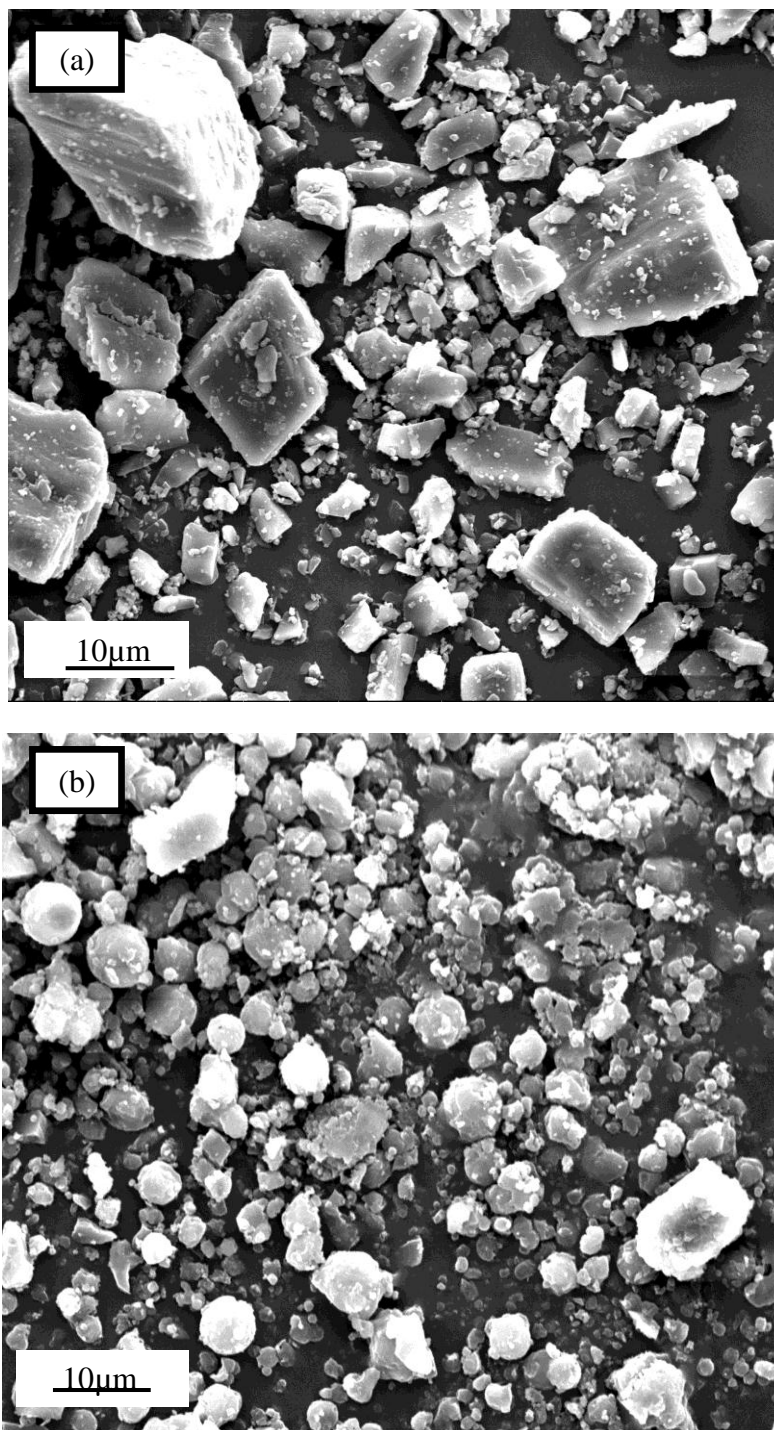


Figure 3. 12: SEM images of RH (a) before spray drying and (b) RH after spray drying. Magnification: 750x (a) and 1200x (b).

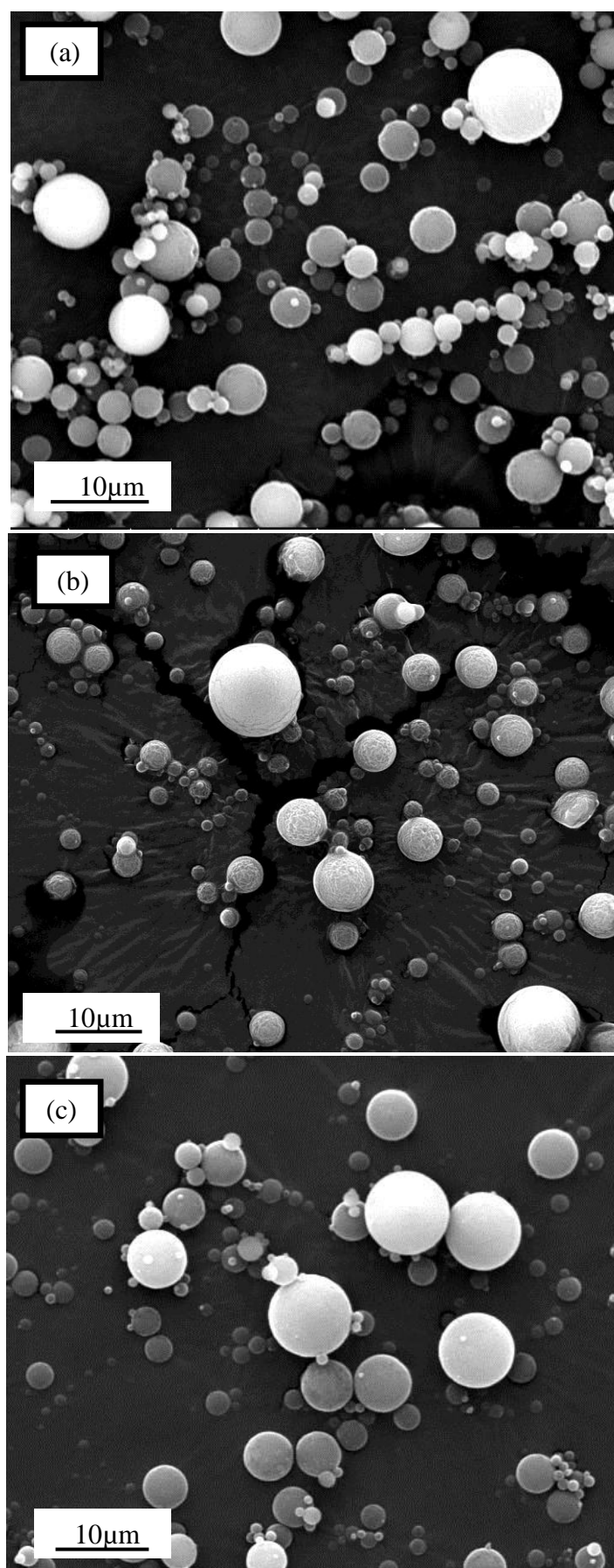


Figure 3. 13: SEM images of (a) the blank microspheres F1, (b) F2, and (c) F3. Magnification: 2500x.

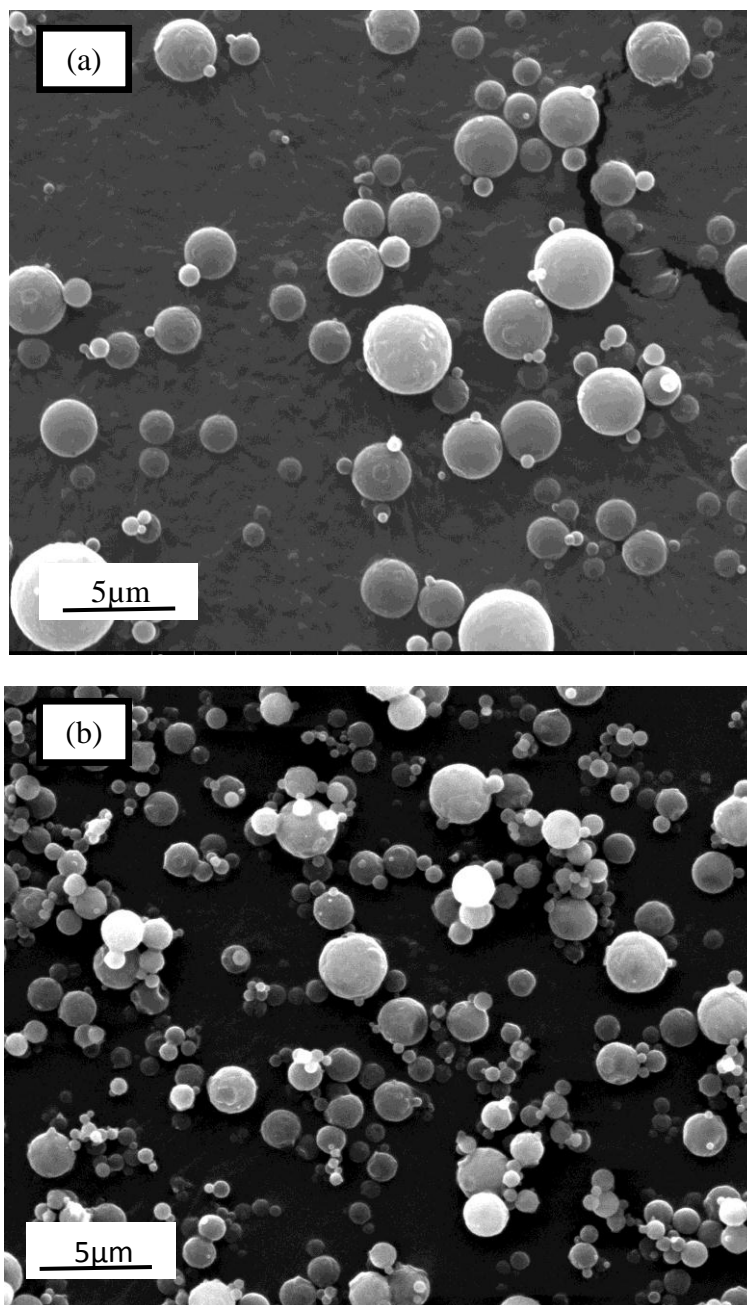


Figure 3. 14: SEM images of (a) is F4 and (b) is F5. Magnification: 2500x.

3.3.10 X-Ray diffraction

X-ray diffractogram of RH, drug-free microparticles, drug-loaded microspheres and the physical mixture of RH and chitosan glutamate are shown in Figure 3.15. The diffractogram of RH raw material showed sharp peaks at different angles, indicating the crystalline nature of the drug. The absence of crystal peaks for RH in chitosan formulations F2 and F3 (Figure 3.15h and f) indicates that the drug was converted into amorphous form and was uniformly dispersed into the polymeric network of chitosan. On the other hand, the intensity of the peak decreased in formulations F4 and F5, (Figure 3.15d and c), indicating some of the drug remained in the crystalline form and was only partially converted into amorphous. These findings agree with previous investigations by Shahi et al. (2011) using atenolol-loaded spray-dried bioadhesive microspheres. Generally, the amorphous form of a given material has better dissolution than its corresponding crystalline form (Craig et al., 1999). However, amorphous form is less stable and has a tendency to revert to crystalline form during storage, causing changes in the physical properties of the formulations (Learoyd et al., 2008a).

The stability study of microsphere formulations following storage in the fridge ($5^{\circ}\text{C} \pm 1$) and room temperature ($20^{\circ}\text{C} \pm 2$) over two months demonstrated no change in amorphicity of the encapsulated RH was observed (Figure 3.16), which agree with Learoyd et al. (2008a) who prepared respirable powders of beclometasone dipropionate loaded into chitosan microparticles via spray drying. Administration of an amorphous powder via insufflations could be advantageous owing to the ability of chitosan to form a mucoadhesive gel following hydration of the microspheres within the nose and hence this may improve drug bioavailability.

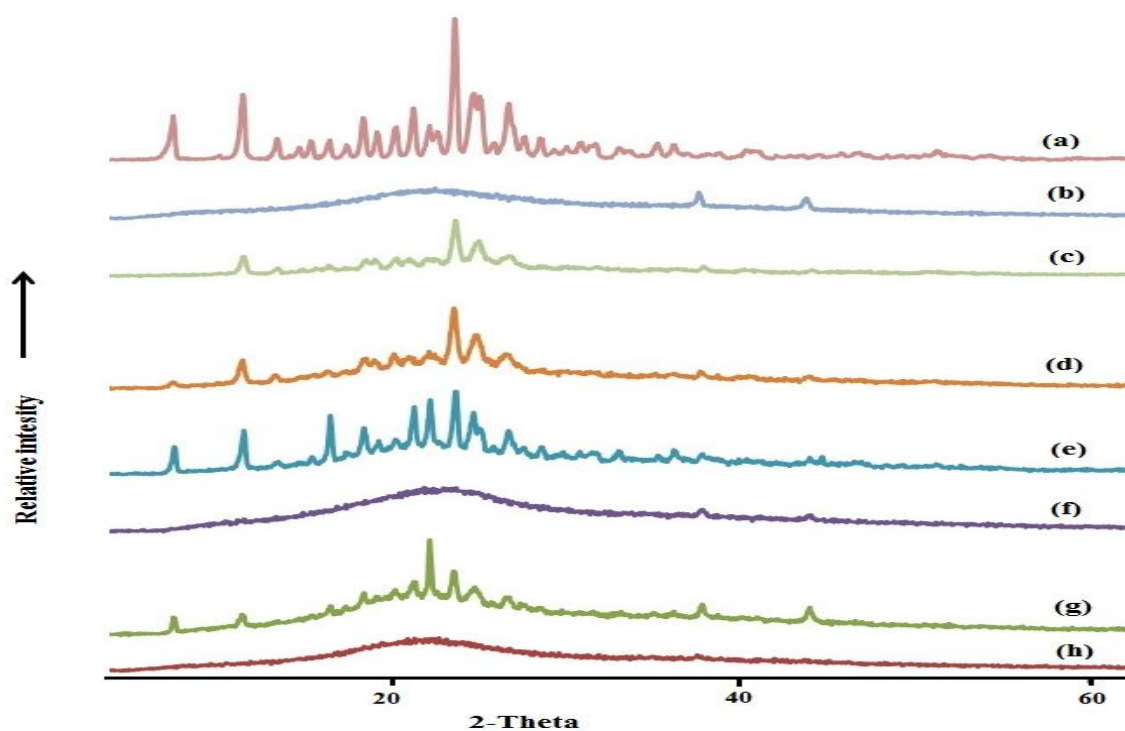


Figure 3. 15: X-Ray spectra of (a) pure RH and mucoadhesive formulations of (b) drug free microspheres (F1), (c) F5, (d) F4, (e) physical mixture (co-ground) of chitosan and RH, 70:30 ratio, (f) F3, (g) physical mixture (co-ground) of chitosan and RH, 90:10 ratio, and (h) F2.

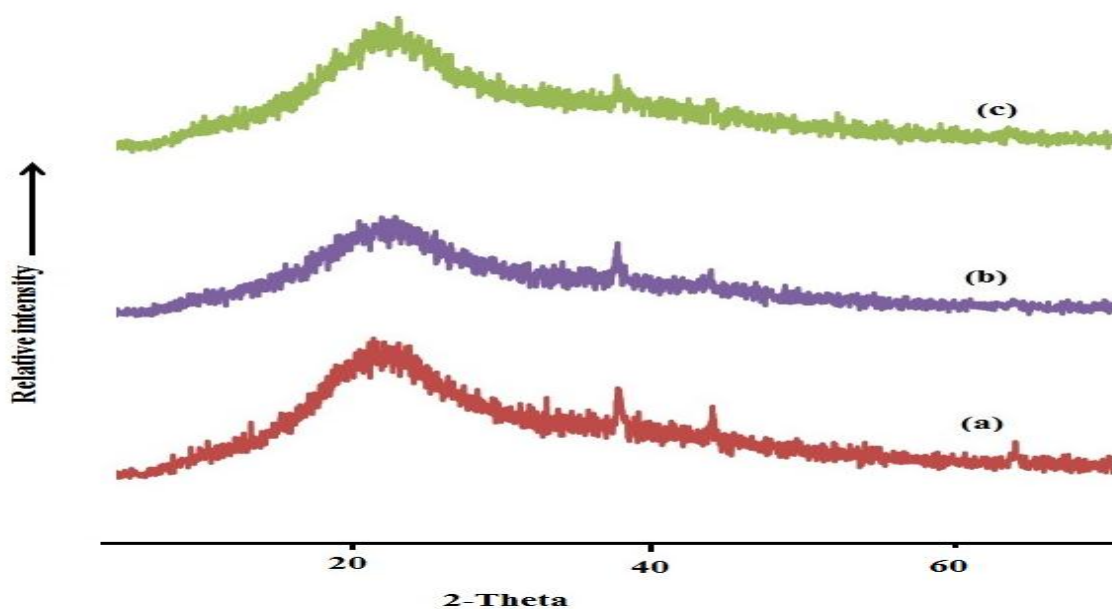


Figure 3. 16: X-Ray spectra of (a) fresh F2 formulation, (b) F2 formulation stored at fridge and (c) F2 formulation stored at room temperature for two months.

3.3.11 Thermo Gravimetric analysis (TGA)

Moisture content (%) of spray dried microsphere formulations may give an indication of the dispersion properties of the particles following intranasal delivery. Dispersion of small hygroscopic particles prior to inhalation might be negatively influenced by the tendency of particles to agglomerate following adsorbing some moisture from the surrounding environment (Ståhl et al., 2002). In the present study, the percentage weight loss ranged from $1.82\% \pm 0.18$ to $5.76\% \pm 0.23$ for formulations F5 and F1 respectively (Figure 3.17). The moisture content was not statistically different ($p > 0.05$) when F1, F2, and F3 were compared, whilst it was statistically different ($p < 0.05$) when F4 and F5 were included in the comparison. This is attributed to the higher ratio of chitosan glutamate to RH in F1, F2 and F3 formulations, since the higher polymer content may reduce water evaporation during spray drying process. These findings are comparable to Ståhl et al. (2002) who prepared spray dried insulin powder via spray drying.

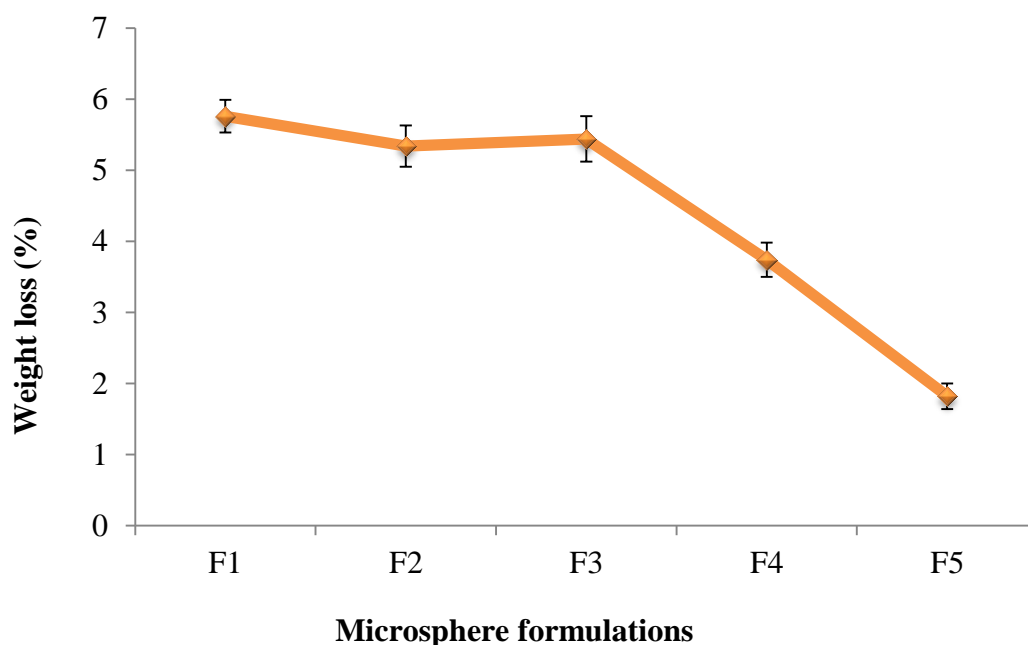


Figure 3. 17: Weight loss of chitosan microparticle formulations. Data represent mean \pm SD (n=3).

3.3.12 Differential scanning calorimetry (DSC)

Behaviour of drug within microparticles was evaluated by conducting DSC analysis. Chitosan microparticles showed broad endothermic peak between 150 and 180°C, which might be attributed to the salt of glutamate. The same observation was reported by other authors (Genta et al., 2003; Maestrelli et al., 2004) (Figure 3.18). Thermogram of RH raw material revealed a single sharp endothermic peak at 248.5°C, with endothermic energy of 117.36 J/g, indicating the crystallinity of the drug and it is corresponding to its melting point (243-250°C) (DrugBank, 2013). Endothermic peak of the drug in the physical mixture was closer to the peak of pure drug when the drug content increased (Figure 3.18), indicates the amount of crystalline RH in physical mixture increased as the ratio of the drug to polymer increased. However, endothermic peak of RH loaded microspheres disappeared for formulation F2, indicating that the drug molecules were dispersed in the polymeric matrix at the molecular level. By contrast, a dramatic decreased in the crystalline peak was observed for F3, F4 and F5 at 202.13, 210.3 and 224.25°C respectively. Additionally, the enthalpy measures the degree of crystallinity for melting materials, showing lowered enthalpy of encapsulated RH form 117.36 J/g to 6.79 J/g for F3, 8.8 J/g for F4 and 48.44 J/g for F5 formulations. These results suggested that the encapsulated drug was partially converted to amorphous form. The decomposition of chitosan was observed next to the melting of the drug at 253.88°C. However, an exothermic peak was observed for F3, and may be attributed to recrystallization of the drug at 238.82°C (i.e. the amorphous form reverted to crystalline). These DSC findings were in accordance with the results by Avachat et al. (2011) who prepared sustained release RH loaded microspheres using emulsion-solvent evaporation method from combination of ethylcellulose and poly-ethylene glycol (PEG) 6000.

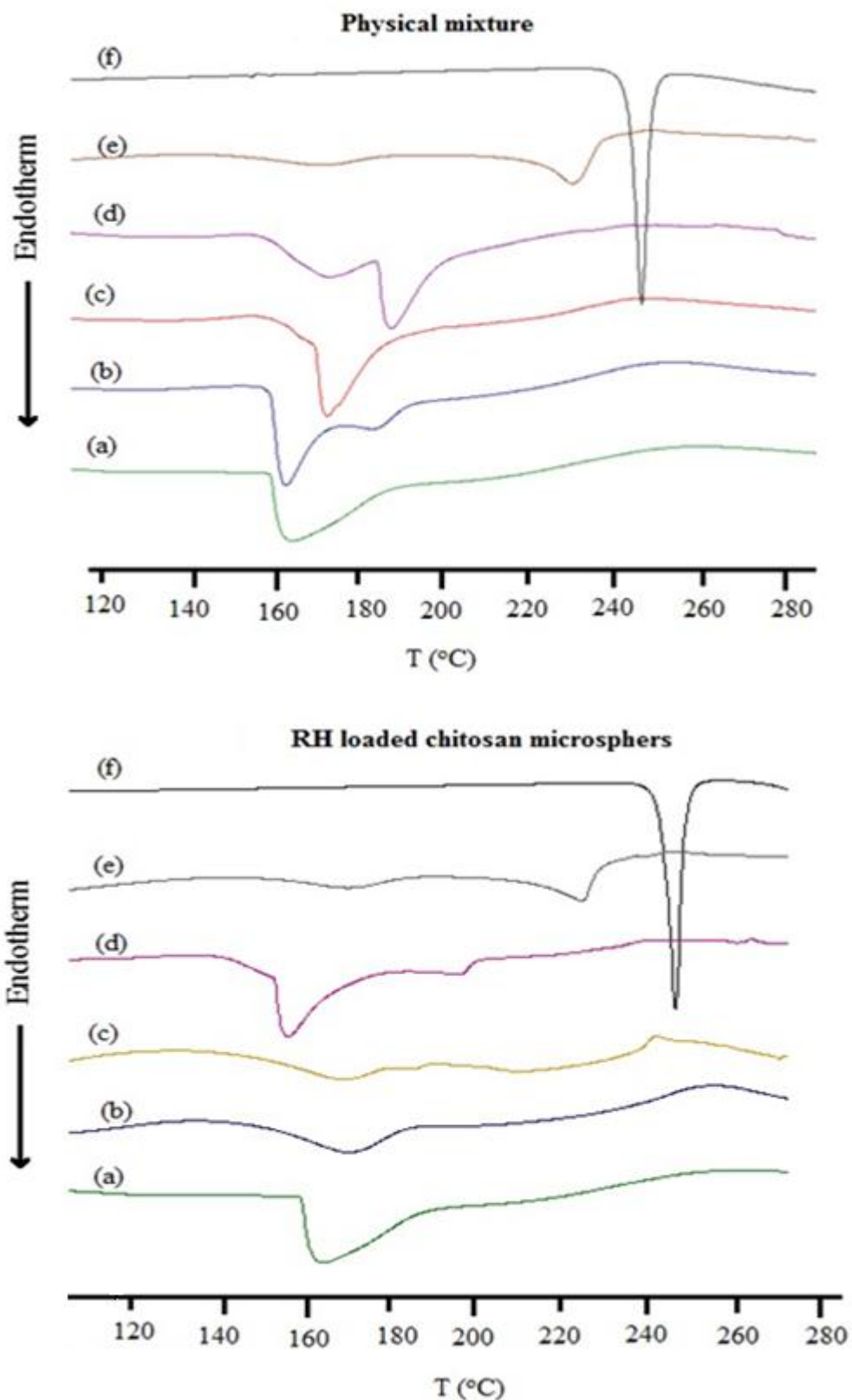


Figure 3. 18: DSC thermograms of (a) drug free microsphere, physical mixture of chitosan-RH; (b) 90:10, (c) 70:30, (d) 50:50, (e) 30:70 and RH loaded chitosan microspheres; (b) F2, (c) F3, (d) F4, (e) F5 and (f) pure drug.

3.3.13 Drug release from microspheres

In vitro drug release study was carried out in PBS (pH 6.5), similar to the pH of the nose. The drug alone had very fast dissolution rate, due to its high solubility in water. However, the release rate from microsphere formulations was dependent on the amount of chitosan present in the formulation. The time required to obtain maximum drug concentration (T_{max}) was observed at 60 and 20 min for formulations F2 and F3 respectively, whilst for formulations F4 and F5 the total amount of the drug recovered was found to be at 5 and 10 min respectively (Figure 3.19). This suggests that the drug diffusion rate from the microspheres into the medium was controlled by formation of a boundary gel layer around the microparticles. The viscosity and thickness of this layer were dependent on drug loading and polymer concentration in the microparticles, suggesting that higher levels of drug loading can provide faster drug release. Genta et al. (1995) have reported drug loaded into non-cross-linked spray dried chitosan microparticles offered rapid drug release which was ascribed to rapid swelling and dissolution of microspheres upon contacting water. The results were in accordance with those reported by Alhalawa and co-workers (Alhalaweh et al., 2009) for zolmitriptan loaded chitosan microspheres prepared by spray drying for nasal delivery. Rapid methotrexate release from spray dried chitosan microspheres has been reported by Sun et al. (2009).

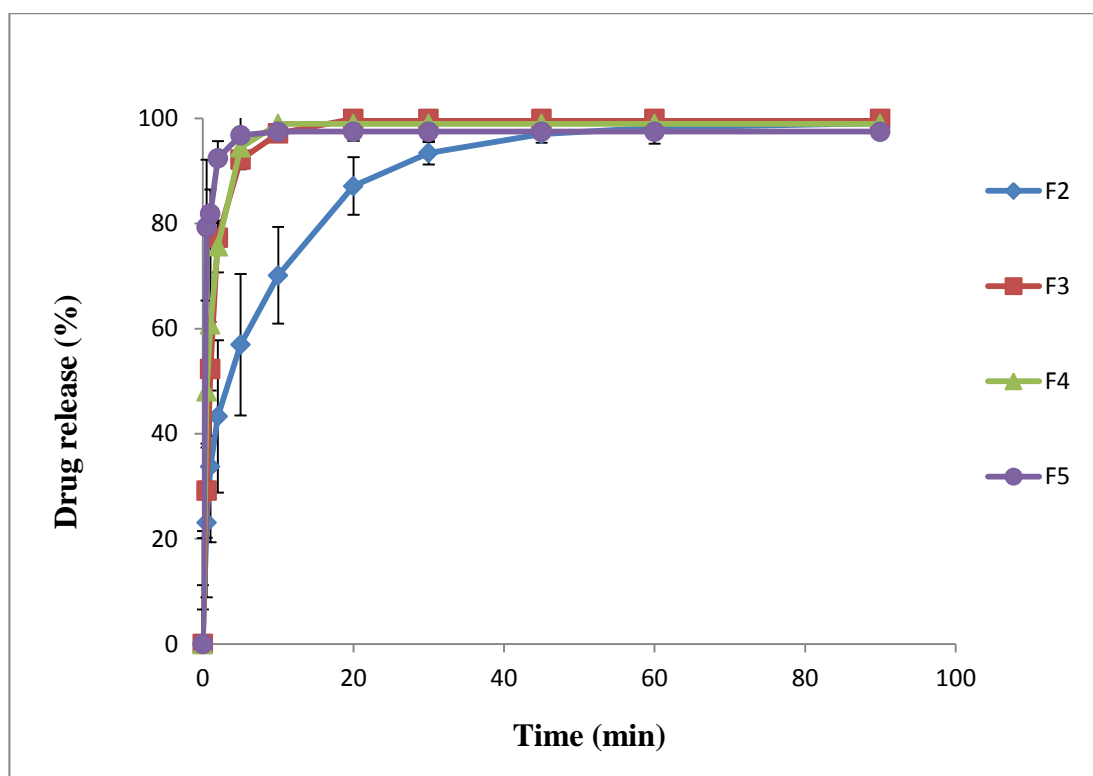


Figure 3. 19: *In-vitro* dissolution profiles of spray dried RH loaded chitosan microsphere formulations carried out in phosphate buffer solution (pH 6.5). Data represent mean \pm SD (n=3).

3.3.14 Toxicity of RH-loaded chitosan microspheres

Drug formulations designed for nasal delivery to give local or for systemic effects should not cause damage to the nasal mucosa or interfere with the normal mucociliary clearance. Hence, a histopathological study is necessary to evaluate the safety of formulations designed for intranasal applications (Hermens and Merkus, 1987). Microscopic images showed nasal mucosa of a sheep treated with PBS (pH 6.5) and used as negative control (Figure 3.20a), and sodium deoxycolate which was used as positive control (Figure 3.20b). In the same experiment, the histological characteristics of RH-loaded microsphere dispersions (F2) (Figure 3.21a), chitosan glutamate microspheres (Figure 3.21b) and RH solution (Figure 3.21c) were investigated. It was observed that the entire cilia became detached when the nasal mucosa was treated by the positive control. In contrast focal sloughing of cilia was observed when the nasal mucosa was treated with the negative control, drug solution, chitosan and RH-loaded chitosan dispersion. The details of the histopathological studies are given in Table 3.3. Previous studies have reported chitosan is non-toxic to mucosal membranes, strongly supporting its suitability and safety as a mucoadhesive carrier for delivery of drugs to

the nose (Islam et al., 2012). The results revealed no necrosis or major changes of the integrity of nasal mucosa upon the treatment with RH loaded microspheres. Goblet cells, Sero-mucinous glands and ciliated cells remained intact with very little focal sloughing of cells being detected. The study was in agreement with results obtained by several research groups (Nanda and Murthy, 2007; Seju et al., 2011; Shah et al., 2011; Mahajan et al., 2012). The microscopic results indicated that RH-loaded microparticles had no harmful effect on the nasal mucosa. The safety of RH was also documented by Khan and co-workers, using thermogel formulations of the drug for brain targeting (Khan et al., 2010).

Table 3. 3: The comparative histopathological evaluation of nasal mucosa treated with a range of formulation.

Treated nasal mucosa	Necrosis	Ciliated cells	Goblet cells	Inflammatory cell infiltrate in the sub mucosa	Sero-mucinous glands
Phosphate Buffer solution (pH 6.5) (Negative control)	Absent	Intact with focal sloughing	Not affected	Mild sub mucosal inflammation and increased intraepithelial lymphocytes	Not affected
Sodium deoxycholate solution (positive control)	Severe	Mostly sloughed	Present	Sever sub mucosal inflammation and increased number of intraepithelial lymphocytes	Inflamed
Drug-free chitosan microparticle	Absent	Intact with focal sloughing	Not-affected	Mild sub mucosal inflammation	Not affected
RH solution	Absent	Detached focally but still present	Not-affected	Mild sub mucosal inflammation	Not affected
Chitosan: RH (90:10) F2	Absent	Focal sloughing of the cilia	Not-affected	Mild sub mucosal inflammation	Not affected

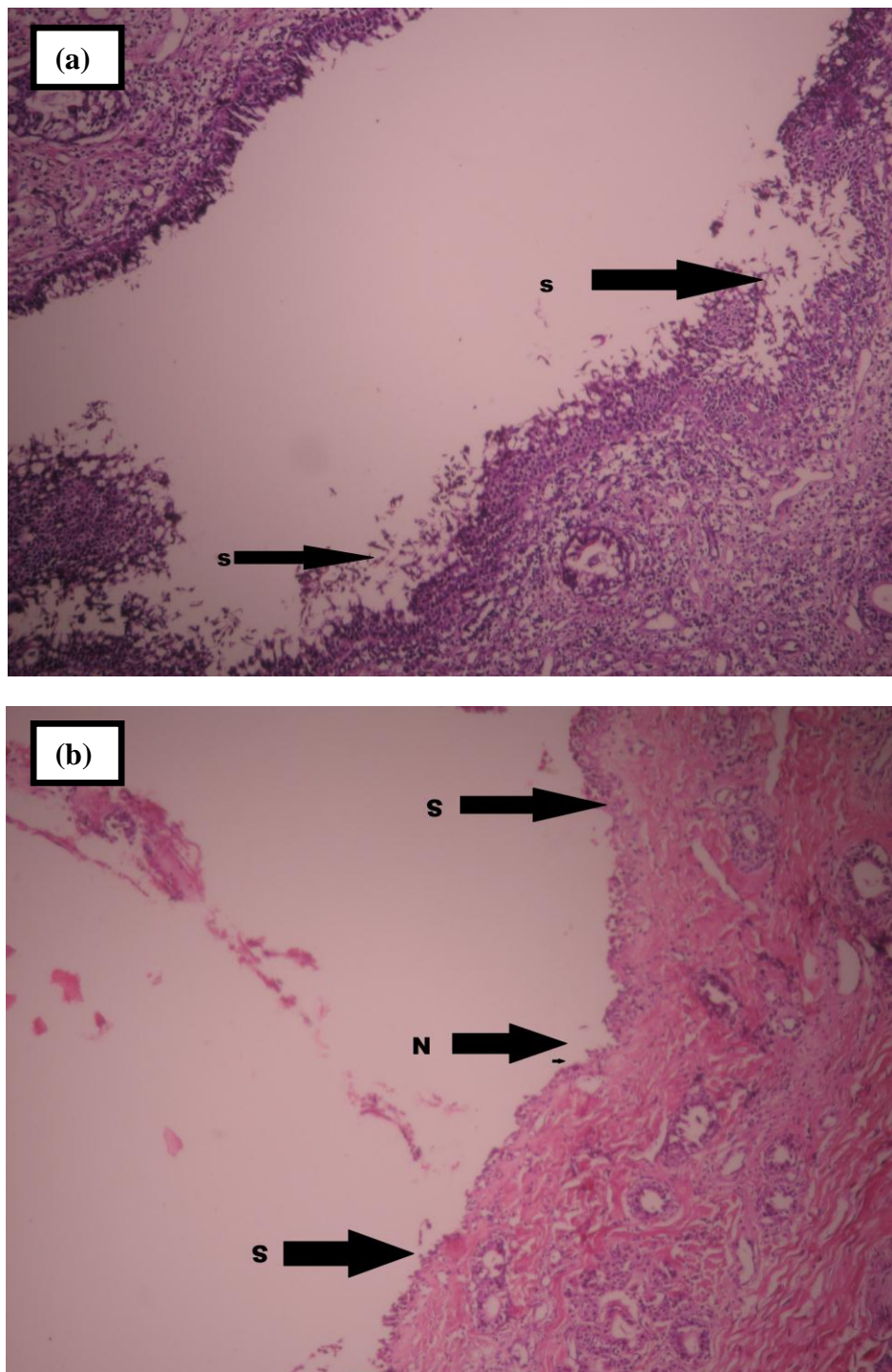


Figure 3. 20: Microscopic (Olympus) images of sheep nasal mucosa treated by; (a) negative control (phosphate buffer pH 6.5) (10 x 10 magnification, n=3) and (b) positive control (Sodium deoxycollate) (10x 10 magnification, n=3). "S" means sloughed, "N" means necrosis, "I" means inflammation.

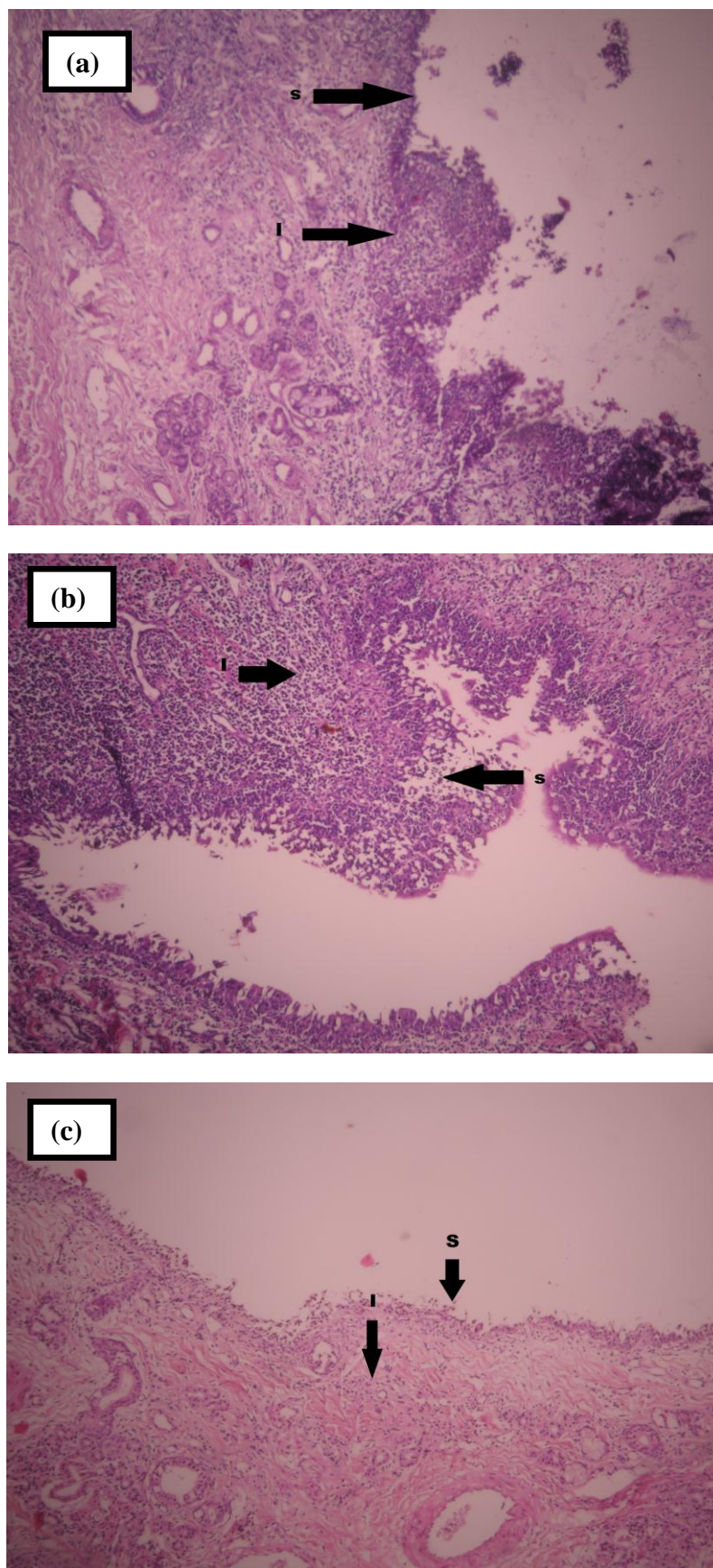


Figure 3. 21: Microscopic (Olympus) images of sheep nasal mucosa treated by (a) formulation F2, (b) drug-free microspheres and (c) RH solutions (10 x 10 magnification, n=3). "S" means sloughed, "N" means necrosis, "I" means inflammation.

3.3.15 Characterization of RH loaded chitosan microspheres delivered using Miat[®] nasal device

Delivery of powder to the nasal cavity is not well explored and little has been done on characterization of powder spray pattern, plume geometry and deposition using nasal insufflators. Passive and active systems are the main delivery systems that have been used to deliver powders into the nose. Active systems involve devices designed to emit powder originally loaded by using air pressure, whilst passive systems rely solely on inhalation power of the patient to deliver the powder to the nose. Most devices in the market are active devices (Kozłowski, 2012). A Valios Monopowder insufflator (Valios pharmaceutical division, France) has been experimented for delivery of anthrax vaccine powder (10 mg) to the nasal cavity of rabbit (Klas et al., 2008). Deposition of powders in the nasal cavity is influenced by powder formulation and type of nasal device used.

Unit dose nasal devices can be used for delivery of vaccines (Wang et al., 2012), biotechnology products (Lochhead and Thorne, 2012) and other active molecules (Ghimire et al., 2007; Djupesland and Docekal, 2010) into the nasal cavity either for local, systemic or CNS effect. In this study, Miat[®] Monopowder device (Miat, Milan, Italy) was investigated to determine the spray pattern and plume geometry (i.e shot weight, mean particle size, spray cone angle, plume width, plume length and spray velocity) (CDER, 2003). These *in vitro* studies are recommended by FDA to characterize the device performance and give information relating to drug bioavailability (CDER, 2002).

3.3.15.1 Determination of shot weight (Fraction of delivered formulation)

In this study, the effect of loading dose on the fraction of formulation delivered was determined. For this purpose three different weights of powder (5, 10 and 20 mg) were used. During spraying the movement of the powder within the capsule was affected by the void volume of the powder formulation and air turbulence within the device reservoir. These were responsible for emitting the powder from the capsule (De Ascentiis et al., 1996).

The quantitative delivery of RH loaded chitosan microspheres from Miat[®] nasal insufflator was determined by calculating the difference between the weight of the device reservoir (gelatin capsule) after each puff. It has been observed from the second puff that more than 94% of the powder formulation was emitted from the device with

the aid of air force, whilst after the third puff more than 96% of the powder was delivered (Table 3.4).

Results showed that the loading quantity had no effect on the fraction of formulation delivered following the first, second and third puffing using F2 formulation with various weights. Similar findings were recorded by De Ascentiis and co-workers who studied the delivery of β -Cyclodextrin powders using nasal insufflators (De Ascentiis et al., 1996). Results were also in accordance with Patile and Sawant (2011). Therefore, the uses of Miat[®] nasal device can be useful when the drug dose is very small such as in case of using potent drug formulations.

Table 3. 4: Percentage of RH loaded chitosan microspheres delivered using Miat[®] nasal insufflator. Data represent mean \pm SD (n=3).

Loading weight (mg)	Cumulative dose delivered (%)		
	First Puff	Second Puff	Third Puff
5	89.6 \pm 0.26	94.21 \pm 1.11	96.88 \pm 1.43
10	90.36 \pm 0.67	94.83 \pm 0.41	96.77 \pm 0.36
20	90.96 \pm 1.76	95.64 \pm 1.47	96.97 \pm 1.63

3.3.15.2 Physical particle size analysis using laser diffraction

The most important consideration for nasal delivery is the determination of physical particle size. The compactness of the cloud produced from the emitted powder may be affected by particle size, which can affect the impaction of the powder in nasal cavity following intranasal administration. VMD, particle size <10 μ m (%) and Span were determined using the Spraytech instrument (Malvern Instruments Ltd, UK) and found to be 76.02 \pm 4.57 μ m, 14.37 \pm 1.85 μ m and 3.96 \pm 1.3 respectively. Most nasal pumps used to deliver liquid formulations produce droplets in the range of 20 - 120 μ m. Increasing particle size and Span might be observed if cohesion between particles causes agglomeration, which might be useful for deposition in the nasal cavity. If particle size produced by the nasal delivery device is more than 10 μ m, the deposition in the upper respiratory tract may predominate, whereas particles between of 5 –7 μ m might be retained in the nasal cavity (Donovan and Huang, 1998). However, particles with size larger than 0.5 μ m may deposit in the nose due to filtration of the inspired air

by the nasal vibrissae (Burgess et al., 2004). In principle, the likelihood of particle deposition into the lower respiratory tract decreases as particle size increases, however particles having physical size below 5 μm are likely to deposit in the olfactory region (Keldmann, 2005).

3.3.15.3 Determination of plume geometry and spray pattern

Improving nasal bioavailability has been related to type of delivery device, physical status of the formulation (liquid, semi-liquid or solid) and the technique of administration. These factors may affect the site and pattern of spray deposition in the nose, consequently effecting drug bioavailability (Arora et al., 2002). Spray pattern investigation can help to determine the site of powder deposition after administration and give reliable prediction of nasal bioavailability.

Spray pattern is a useful quality control test for determining the bioequivalence of formulations and/ or feasibility of nasal devices (CDER, 2003). The representative image of spray pattern using impaction method (section 2.7.2) for F2 formulation, at the distance of 3cm was investigated. The longest diameter (D_{max}), shortest diameter (D_{min}) and ovality ratio ($D_{\text{max}}/D_{\text{min}}$) were 15.67 ± 0.52 mm, 14 ± 0.89 mm and 1.12 ± 0.04 respectively (Figure 3.22). The image showed spherical and intense spray pattern of F2 formulation (chitosan glutamate to RH, 90:10 w/w ratio).

Investigations of spray cloud demonstrated the required spray time to reach the fully developed phase was 0.16 sec whilst the total spray time to deliver 10 mg of RH loaded microparticles was 0.32 sec, indicating rapid delivery of the powder from the Miat[®] device (Figure 3.23).

Powder particles were ejected from the monopowder delivery device at an angle of 14.3 ± 1.03 and the plume width was 11.3 ± 1.03 at 3cm distance from the tip of the nasal device. It has been reported that anterior deposition of the emitted dose from nasal devices predominates when the spray has large angle ($60 - 70^\circ$), whereas deposition in posterior part of the nasal cavity happens when the plume cone is small (around 30 to 35°) (Pringels et al., 2006). Thus, deposition of the delivery dose at the anterior region may increase when the plume angle is increased. Conversely, the decrease in plume angle enhances the likelihood of targeting the turbinate region of the nose (Foo et al., 2007).

Powder formulation released from the monodose nasal insufflator was observed as an elongated puff with a homogeneous core, indicating the effective distribution pattern of the delivered microspheres. The compactness of the clouds might be affected by powder particle size, with small particles generating clouds that fluffy and homogeneous in density, whereas large particles may produce clouds with visible individual particle trajectories (De Ascentiis et al., 1996).



Figure 3. 22: Spray pattern of RH-chitosan microparticles (90:10 w/w, chitosan glutamate to RH) at 3cm distance from the nasal device tip (n= 4).

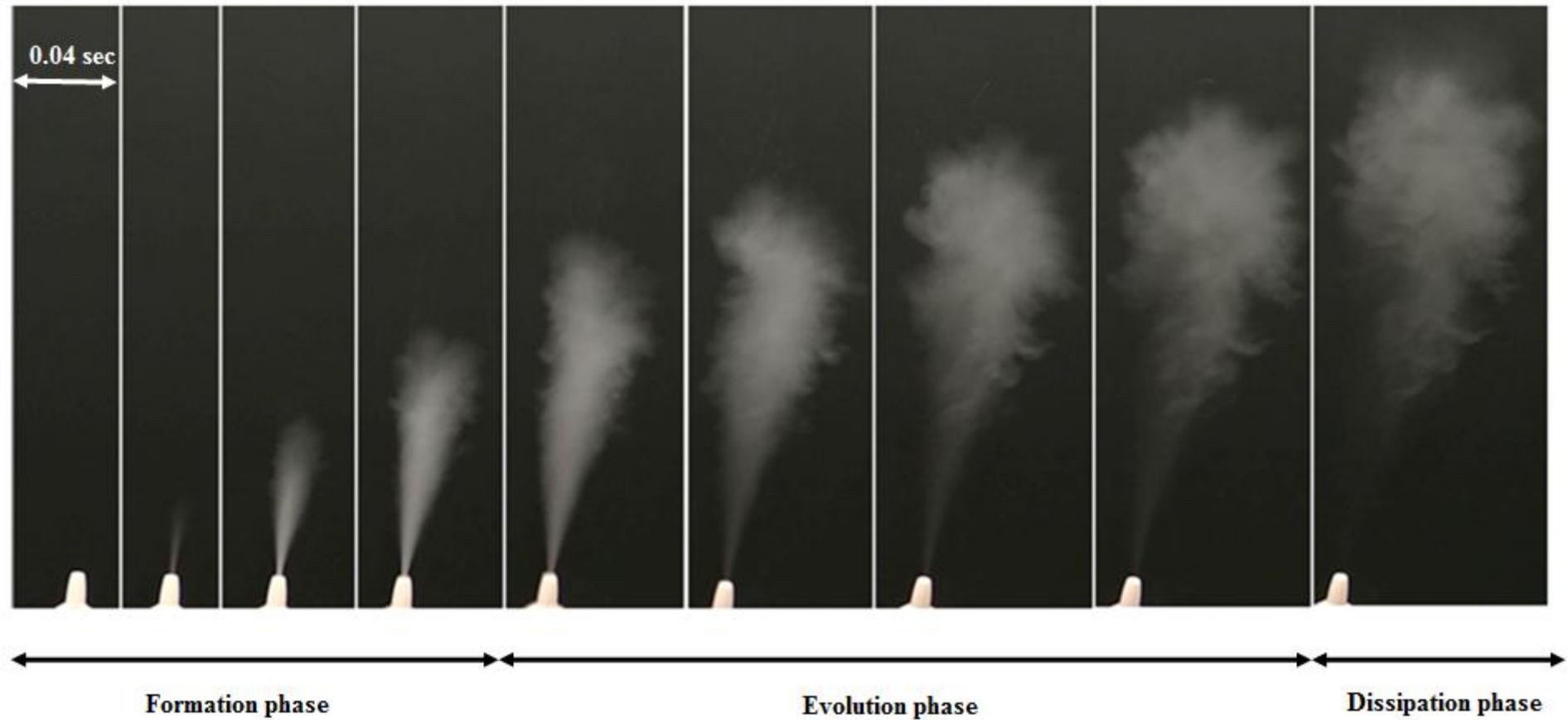


Figure 3. 23: RH-chitosan microspheres (F2) delivery sequences from Miat® monodose insufflator monitored by videography (n= 4).

3.4 Conclusions

Results of this study supports the theory that chitosan-based microspheres are promising drug delivery systems for nasal administration of RH by using Miat[®] nasal insufflator devices. FTIR spectra revealed no interaction between RH and chitosan glutamate. The ratio of polymer to drug in formulations had a crucial effect on particle size, size distribution, intensity of positive charge of the microparticles and swelling index. Improvements in the drug particle morphology and powder flowability were obtained by co-spraying the drug with chitosan. X-ray spectra and DSC demonstrated chitosan to drug ratio had remarkable effect on the physical state of the entrapped drug. Absence of crystal peak in formulation 90:10, polymer to drug ratio indicates that the drug was molecularly dispersed within the polymeric matrix. TGA revealed that the humidity content (%) was minimized as the ratio of chitosan/drug decreased. The release study demonstrated that chitosan to drug ratio has controlled the rate of drug released. Histopathology study revealed RH-chitosan microspheres formulations are relatively safe for intranasal administration.

The Miat[®] monopowder insufflator efficiently delivered nearly 90% upon first actuation regardless of the weight of the powder. Laser diffraction study of the cloud demonstrated that the sprayed particles were less likely to deposit in the lower respiratory tract, owing to particle agglomeration. The generation of homogeneous cloud with narrow plume angle might enhance powder deposition in the nasal cavity and particularly in the olfactory region of the nose where direct drug delivery to CNS may occur. Thus, particle agglomeration in this study was advantageous since it is expected to maximize the drug deposition in the nasal cavity (i.e. minimize deposition in the lower respiratory system) and enhance targeting properties to the olfactory region and the proportion of the drug available for absorption into the systemic circulation. The microsphere powder formulations prepared in this study, taking into account the therapeutic effects of RH, is suggested for nasal administration to treat Parkinson's disease and restless legs syndrome. Further *in vivo* studies are needed to explore the validity of this hypothesis.

CHAPTER 4

ROPINIROLE HYDROCHLORIDE LOADED SODIUM ALGINATE MICROPARTICLES PREPARED BY SPRAY DRYING

4.1 Introduction

Microparticles represent a powerful drug delivery technology for incorporating drugs into polymeric excipients prepared as spherical particles. These delivery systems modulate release and improve drug absorption due to the high surface area to volume ratio of the microparticles (Gavini et al., 2006).

Formulation of drugs as microparticulate powder dosage forms has been suggested to enhance chemical stability of drugs and excipients. Powder formulations are free from preservatives and can be administered in larger doses, and can be used for peptide and conventional drug molecules (Chaturvedi et al., 2011). The bioavailability of drug can be improved when it is administered in powder formulations compared to liquid dosage forms via the nose (Ishikawa et al., 2001).

As mentioned in chapter 3 the nasal route is characterized by its relatively high permeability, larger surface area (150 cm^2) and high blood supply. Therefore, it is highly appropriate for drugs that undergo extensive first pass metabolism, because the drug is directly absorbed to the circulation without passing through portal vein to the liver (Chaturvedi et al., 2011). The nasal route takes advantage of the neuronal connection between the nose and brain to elicit effects in the CNS (Wen, 2011; Kumar et al., 2013). This strategy may minimize systemic side effects of drug (Kumar et al., 2013). Nasal route is well established for administration of drugs to treat local diseases such as rhinitis and nasal congestions and CNS diseases such as migraine.

The drug is cleared rapidly from the nasal cavity towards nasopharynx by mucociliary process within 15 min when applied as a solution (Mao et al., 2004). Bioadhesive polymers interfere with the ciliary movement, hence drug loaded into microspheres may have prolonged contact with the mucous membranes compared to the corresponding drug solution (Illum, 2003).

Bioadhesive polymers are natural, synthetic or semi synthetic intended to carry, protect and prolong the residence time of the drug. Mucoadhesive agents may prolong the drug contact with the absorption site in the nose for up to 3-5 h, depending on type of mucoadhesive polymer. This may be particularly useful for enhancing absorption of drugs with poor bioavailability (Rai et al., 2008). Enhancement of carvedilol absorption and bioavailability improvement have been reported when the drug was encapsulated

into sodium alginate microspheres prior to administration into the nose (Patil et al., 2012).

Sodium alginate is a natural polyanionic polymer used for controlled drug release. It is relatively inexpensive, non-toxic and biodegradable (Farid et al., 2012). The mucoadhesive properties are directly proportional to the polymer's molecular weight and are influenced by the polar groups (Kharenko et al., 2009). Mucoadhesive properties of sodium alginate are ascribed to formation of hydrogen bonds as a result of carboxyl-hydroxyl interactions with mucin (Patil et al., 2012). This interaction ensures success of this polymer as a vehicle for drug absorption through the nasal epithelium (Farid et al., 2012). A wide range of active constituents have been encapsulating into alginate microparticles such as peptides, proteins (Coppi et al., 2002) and small therapeutic molecules (e.g. metoprolol tartarate) (Rajinikanth et al., 2003).

Ropinirole hydrochloride (RH) is non-ergoline antiparkinson drug, which may elicit therapeutic effect due to the selective agonistic activity on the D₂ dopamine-like receptors (DrugBank, 2013). RH is widely used in the management of Parkinson's disease, either alone or in combination with other drugs to minimize on-off fluctuation in response to levodopa (Tulloch, 1997). The drug is inactivated by the liver, hence its oral bioavailability is only around 50% (DrugBank, 2013).

This study hypothesises that intranasal administration of alginate microspheres of RH prolongs the contact between the formulation and nasal epithelium and facilitates the uptake of the drug to the brain, hence avoiding fluctuating plasma levels of the drug due to on-off phenomenon in Parkinson's disease.

This study aimed to design and develop microspheres based on sodium alginate polymer as a delivery carrier system using spray drying. In this study the effect of inlet temperature of the spray dryer on the microparticulate powder characteristics including particle shape, product yield, and particle size and size distribution were investigated to select the optimum inlet air temperature. Spray drying parameters were optimised and used to develop RH-sodium alginate microspheres, and full characterization of the formulations was conducted. The best performing formulations were further investigated using nasal insufflators.

4.2 Methodology

4.2.1 Compatibility Study

The compatibility between RH and sodium alginate was investigated by preparation of RH loaded alginate microspheres (50:50 w/w) using spray drying. FTIR spectroscopy and TLC were used to detect interaction or formation of new bonds between the drug and polymer as described in section 2.2.

4.2.2 Optimization of sodium alginate microsphere formulation

i) Preparation of sodium alginate microspheres (0.5%)

To optimize the formulation and spray drying parameters for the preparation of RH loaded sodium alginate microspheres, an aqueous solution of the polymer (600 ml; 0.5% w/v) was prepared by dissolving 500 mg in 100 ml HPLC water with magnetic stirrer to enhance the rate of dissolution. The resultant solution was divided into three equal volumes, each was atomized using certain spray drying conditions (Table 4.1) and using the Büchi-290 Mini Spray-Drying (Büchi Laboratories, Switzerland). The experiments were conducted three times and the microspheres were characterized for yield, particle size, size distribution and morphology as described in the section 2.5.

Table 4. 1: Conditions for the preparation of sodium alginate microspheres.

Condition	Inlet Temperature (°C)	Outlet Temperature (°C)	Aspiration rate (%)	Gas flow rate (L/h)	Pump rate (%)
1	160	72-81	100	357	17
2	140	64-71	100	357	17
3	120	56-58	100	357	17

ii) Characterization of sodium alginate microspheres

The production yield (%) of microspheres at different conditions, size and size distribution of alginate microparticles and morphology of spray dried sodium alginate microparticles were determined as described in chapter 2.

4.2.3 Preparation of RH loaded alginate

Four formulations using low viscosity sodium alginate and RH were prepared using a range of polymer to drug ratios (Table 4.2). Drug-free microspheres were prepared (0.5% w/v) for comparison using the same spray drying conditions. The feed solutions were prepared by dissolving sodium alginate and the drug in 100 ml of HPLC water. Automated microviscometer was used to measure viscosity of the solutions before spray drying. The feed solution was atomized through 0.7 mm nozzle. The spray dry conditions used were as follows: inlet temperature 140°C, outlet temperature 64 - 71°C, aspiration rate 100%, gas flow rate 357 L/h and pump ratio 17% (5 - 6 ml/min). Solution (200 ml) was prepared for each batch and each experiment was repeated three times.

Table 4. 2: Composition of sodium alginate microparticle formulations.

Formulation code	Ratio (w/w) (polymer: RH)	Sodium alginate (mg)	RH (mg)	Total weight (mg) in 100ml
A1	100:0	500	0	500
A2	90:10	450	50	500
A3	70:30	350	150	500
A4	50:50	250	250	500
A5	30:70	150	350	500

4.2.4 Characterization of RH loaded alginate microparticles

Microsphere formulations prepared in this study were investigated and characterized for powder yield, microscopic morphology, physical state using X-ray crystallography, and thermal behaviour using DSC and TGA. Following dispersion of the formulations, particle size, size distribution, zeta potential, drug entrapment efficiency, and *in vitro* drug release were investigated. As described in section 2.6.11, histopathological studies were conducted to evaluate the safety of microspheres for nasal administration. Using the best performing formulation, fraction output, VMD, size distribution, spray pattern and plume geometry were studied as explained in sections 2.7 and 2.8.5.

4.3 Results and discussion

4.3.1 Compatibility study

This study detected the interactions between the drug and polymer. It provided information on physicochemical properties of the drug and excipients since undesirable interactions could affect the stability of formulation, efficacy or dissolution behaviour of the drug (Taylor and Zografi, 1997). In this experiment drug-excipient interaction was studied using thin layer chromatography (TLC) and FTIR spectroscopy.

i) Thin layer chromatography (TLC)

The R_f values of RH as a co-spray dried, physical mixture and pure drug were similar ($R_f = 0.55$). No extra spot was observed in the TLC plate, suggesting no chemical interaction between drug and polymer.

ii) FTIR spectrum

FT-IR spectrum of RH, sodium alginate, physical mixture of RH and sodium alginate and spray dried formulations (1:1 ratio w/w) were compared to investigate possible interactions between drug and polymer (Figure 4.1). Sharp peaks of RH were found at 1241.19, 1455.36, 1702.18 and 3068.95 cm^{-1} for C-N, C=C stretching, C=O stretching and N-H stretching functional groups respectively, whilst the IR spectrum of sodium alginate showed peaks at 3273.05, 1595.09 1408.25 and 1026.88 cm^{-1} for O-H stretching, C=O stretching, COO- and C-O-C stretching respectively (Figure 4.2). When IR spectrum of pure RH was compared to the IR spectrum of physical mixture and spray dried RH loaded alginate microspheres, no remarkable band-shifts of wave number were observed. Hence, FTIR data confirmed no merging of peaks of RH with sodium alginate occurred, indicating no interaction between RH and sodium alginate.

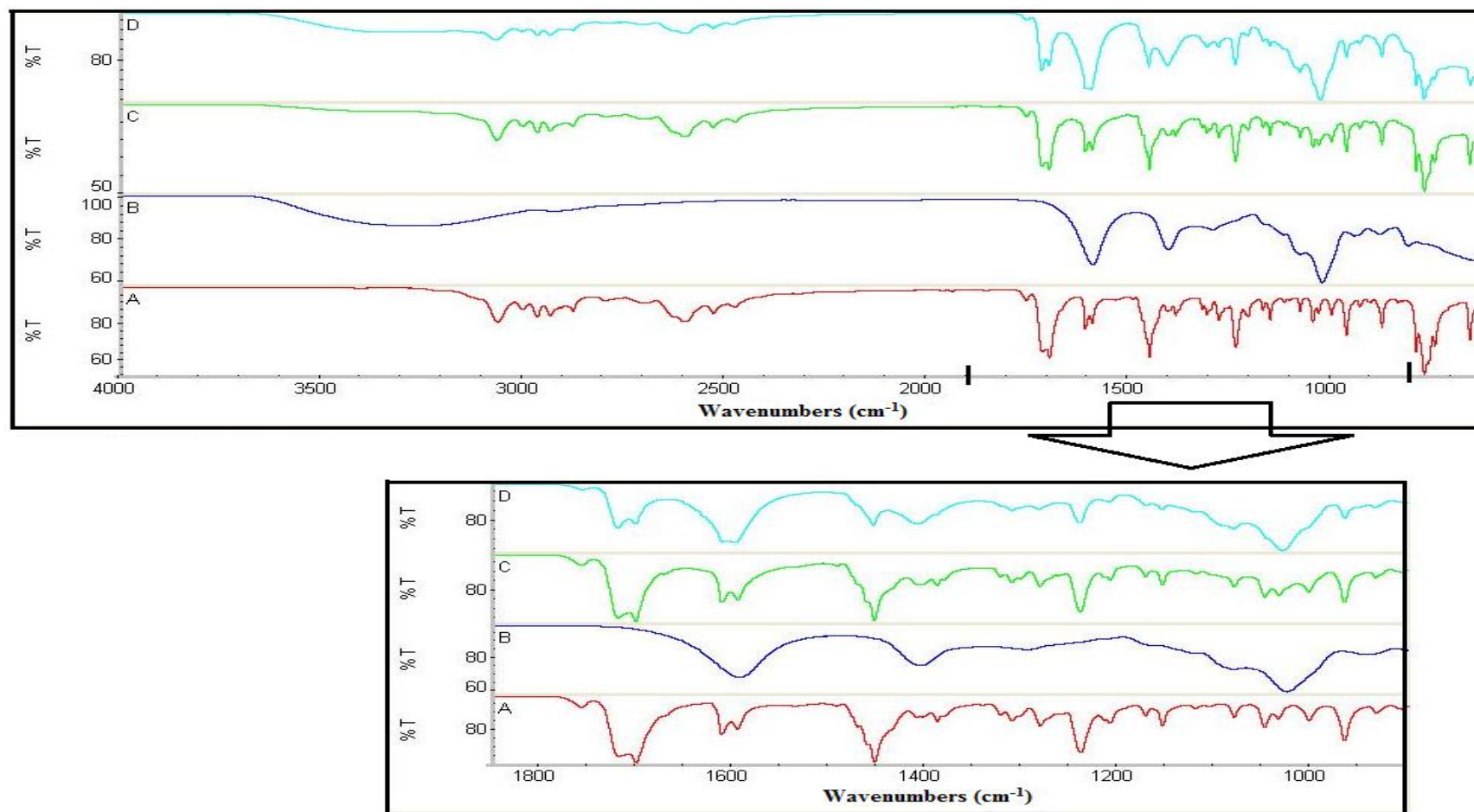


Figure 4. 1: FTIR spectra of (A) RH, (B) sodium alginate, (C) physical mixture of sodium alginate and RH (1:1) ratio, and (D) spray dried RH loaded sodium alginate microparticles. The lower graph magnifies the wave numbers area between 900 and 1900 cm^{-1} .

4.3.2 Optimization of sodium alginate microparticles

i) Production yield

Sodium alginate solutions (0.5% w/v) were spray-dried at different inlet air temperatures. The production yield decreased significantly ($p < 0.05$) from 70.27 ± 1.26 to 58.87 ± 2.95 as the inlet temperature was decreased from 160°C to 120°C , resulting in a decrease in the outlet air temperature from $77.2^{\circ}\text{C} \pm 2.7$ to $59.2^{\circ}\text{C} \pm 2$ respectively. This may be attributed to less heat energy available in the drying chamber, which is required to dry the atomized droplets quickly before non-dried droplets leave the drying chamber with vacuum. A positive relationship between inlet temperature and yield of product was found up to a point depending on the properties of the material used. When the inlet air temperature increased the process of drying the droplets also increased, resulting in yield promotion (Rathananand et al., 2007). However, no significant difference ($p > 0.05$) in yield was seen when comparing the inlet temperatures 140°C and 160°C (Figure 4.2). Rathananand et al. (2007) reported that evaporation of solvent in droplets depends on the latent heat, whereas an incremental change of inlet temperature can lead to a slight difference in the outlet temperature, resulting in minor effect on solvent evaporation at the surface of the droplet (Rathananand et al., 2007). Aspiration rate has a positive impact on the outlet air temperature, whilst the feeding rate (i.e. pump rate) has a negative effect on the outlet air temperature and so on the production yield. Tee et al. (2012) reported that the production mass of maltodextrin coated *Piper betle L.* (Sirih) decreased when the feed rate (pump speed) was increased. High inlet temperature increases outlet temperature, thus enhancing the solvent evaporation efficiency from the sprayed droplets, which reduces droplet deposition on the walls of the drying chamber and improves droplet drying, resulting in promoting the production yield (Maury et al., 2005). These experiments agree with those reported by Amaro et al. (2011) for maximizing the production yield of spray-dried trehalose and raffinose from methanol (80%)/n-butyl acetate (20%) v/v using laboratory-scale spray dryers.

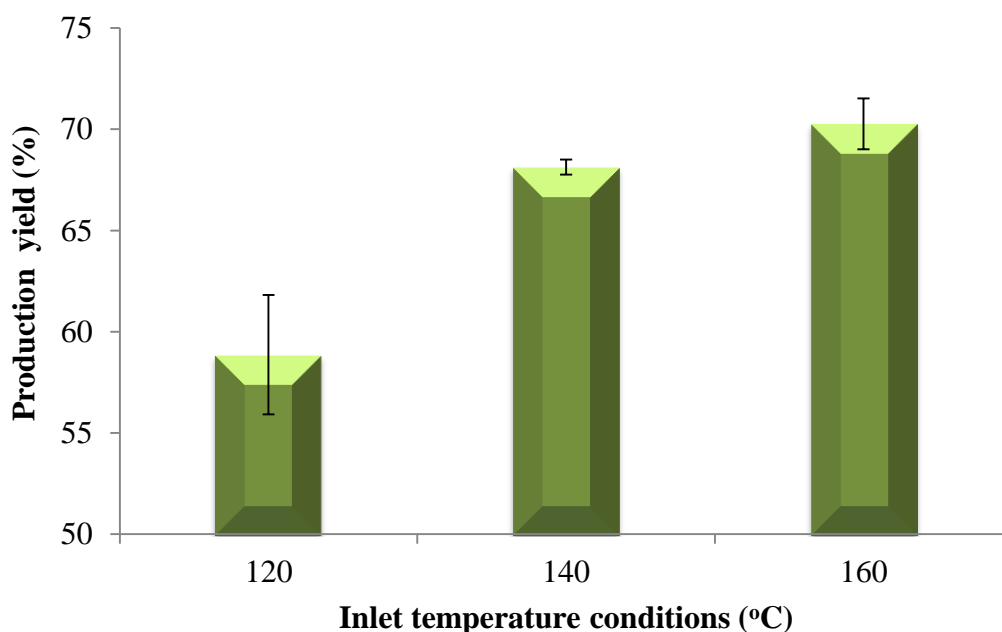


Figure 4. 2: Relationship between inlet air temperature and the production yield (%). Data represent mean \pm SD (n=3).

i) Particle size and size distribution

Particle size and size distribution (Span) of sodium alginate microparticles prepared at different inlet temperatures are shown in Figure 4.3 and Figure 4.4. The size ranged from 2.35 ± 0.10 to 2.58 ± 0.06 μm and the Span was in the range of 2.11 ± 0.53 to 2.71 ± 0.02 for microparticles produced at 120°C and 140°C respectively. Statistically no effect of the inlet air temperature was observed ($p > 0.05$) on particle size when the inlet temperature decreased from 160 to 120°C . The decreasing trend for particle size prepared under 120°C inlet temperature might be ascribed to low efficiency of heat vaporization in the drying chamber. These results disagreed with Tee et al. (2012) who have prepared Sirih coated by maltodextrin via spray drying. The conflicting findings might be due to the difference of the properties of excipients used. However, the size distribution (i.e. Span) of particles prepared using 120°C , 140°C and 160°C inlet temperatures did not significantly change ($p > 0.05$) (Figure 4.4).

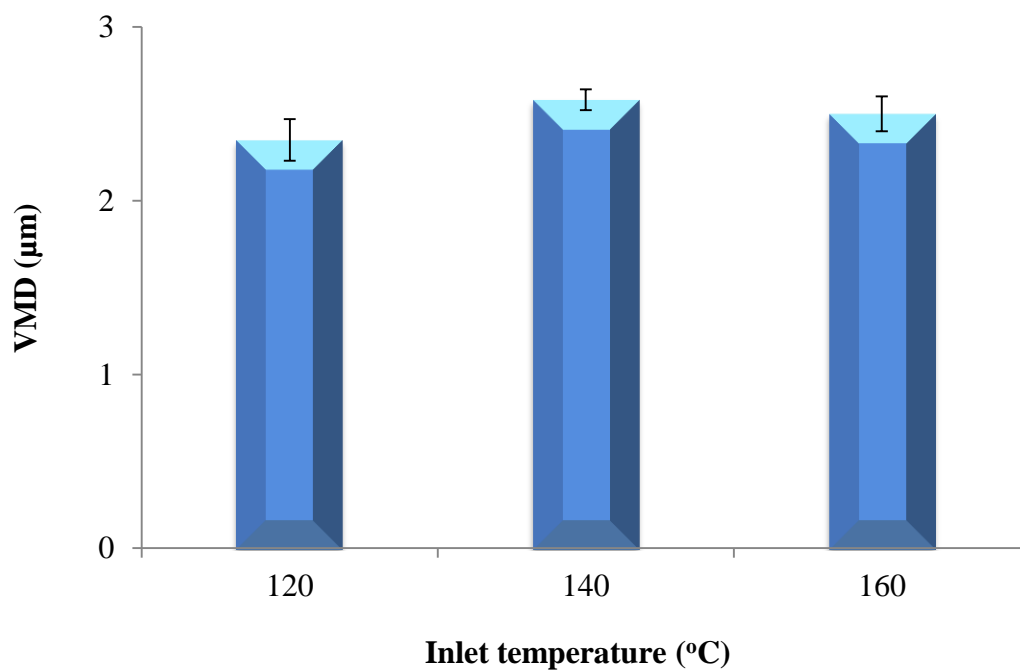


Figure 4. 3: Relationship between inlet air temperature (°C) and particle size (VMD) of sodium alginate microparticles. Data represent mean \pm SD (n=3).

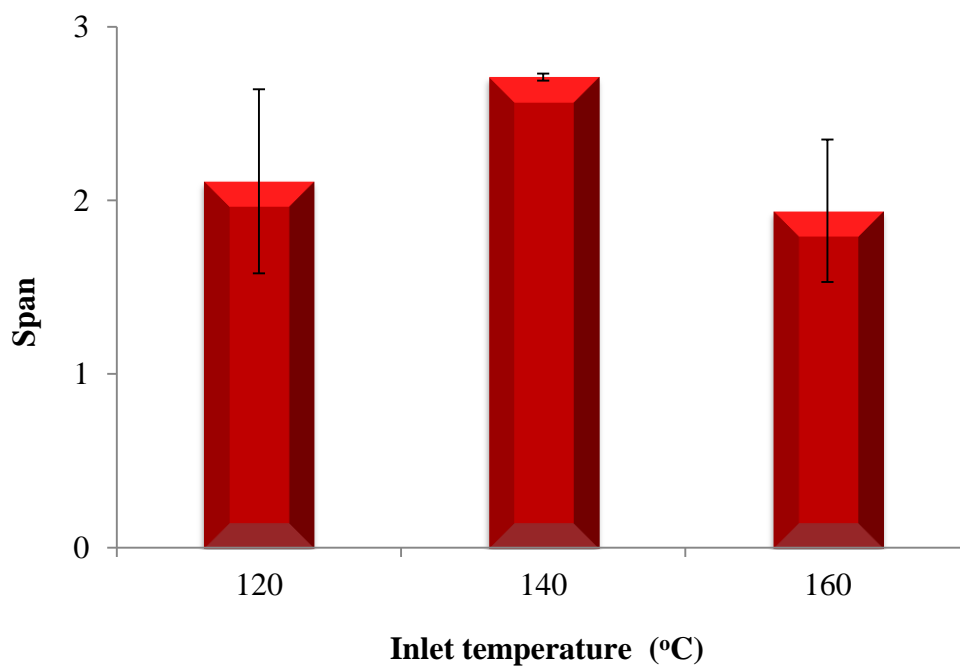


Figure 4. 4: Relationship between inlet air temperature (°C) and Span of sodium alginate microparticles. Data represent mean \pm SD (n=3).

ii) Morphology

Particle morphology influences particle size determination, bulk density, powder flowability and surface area. Furthermore, powder used for targeting specific regions of the respiratory tract depends on particle size and shape (Chegini and Taheri, 2013). Shape and residual solvent in particles produced by spray drying can be controlled via the optimization of inlet/outlet air temperatures. Rate of solvent evaporation from the droplet and formulation may affect morphology of the particles produced by spray drying. For example, particles may have defective shapes if drying occurs rapidly (Chegini and Taheri, 2013). The shapes of microparticles spray dried using the three drying conditions (120, 140 and 160°C) are shown in Figure 4.5. SEM images demonstrated that larger fractions of particles generated at 160°C inlet temperature were dimpled and holed. In contrast, the shape of particles became spherical, and surface was observed to have fissures/cracks as the inlet air temperature was decreased to 120°C. This might be attributed to incomplete water evaporation from the atomized droplet (Figure 4.5c). SEM images revealed that changing the inlet temperature had a great effect on the surface morphology of spray dried sodium alginate microspheres.

Based on these experiments, inlet air temperature of 140°C was selected to prepare various formulations of RH loaded sodium alginate microparticles, as round shaped particles are believed to improve powder flow and possibly can cause less irritation to the nasal mucosa.

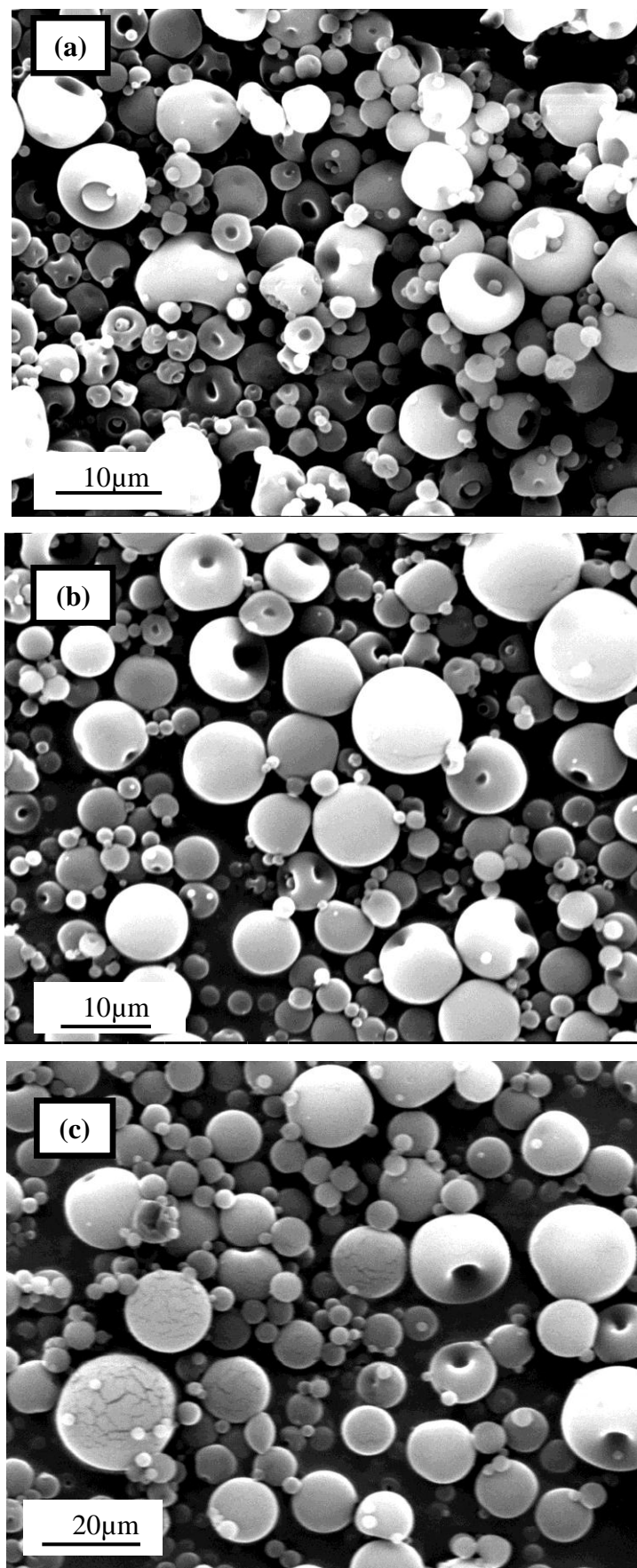


Figure 4. 5: SEM images of sodium alginate microparticles where inlet air temperatures were: (a) 160°C (magnification: 5000x), (b) 140°C (magnification: 5000x), and (c) 120°C (magnification: 2500x).

4.3.3 Characterization of RH loaded sodium alginate

4.3.3.1 Product yield

The product yield was relatively high (approaching 70%) and the increase of drug to polymer ratio did not affect ($p>0.05$) the powder yield (Figure 4.6).

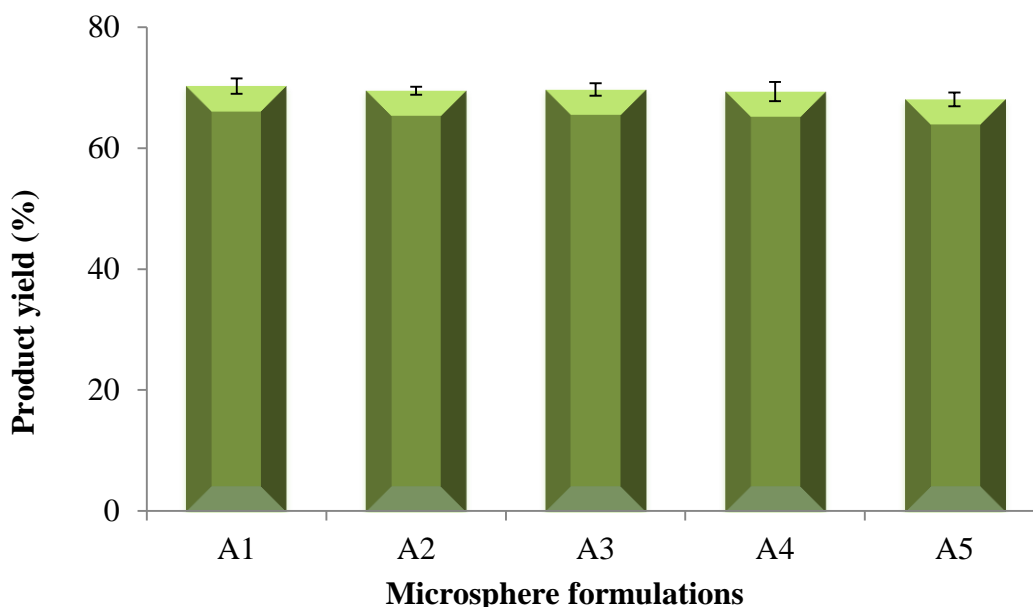


Figure 4. 6: Production yield (%) of sodium alginate microsphere formulations. Data represent mean \pm SD (n=3).

4.3.3.2 Size and size distribution of microparticles

Generally, particle size of the powders obtained by spray drying depends on the proportion of atomized droplets. Droplet size is directly proportional to concentration, viscosity and feed rate of the feeding solution, and inversely proportional to gas flow rate (Chegini and Taheri, 2013).

Particles size determines the final dosage form performance for oral, parenteral and pulmonary delivery (Thanoo et al., 1995). Particle size affects surface area of the particles; this influences the rate and duration of drug release at the site of absorption (Narayani and Panduranga Rao, 1996). The smaller the size of microsphere the larger its surface area, thus the release of insoluble drug from microspheres can be controlled owing to high surface area to volume ratio of the small particles (Sinha et al., 2004).

Particle size of RH-sodium alginate microspheres (Table 4.3) was $2.58 \pm 0.35 \mu\text{m}$ and $4.37 \pm 0.29 \mu\text{m}$ for formulations A2 and A5 respectively. As the ratio of drug to sodium alginate increased the particle size also increased significantly ($p < 0.05$). With regard to size distribution, Span values ranged from 1.52 ± 0.03 to 4.13 ± 1.19 .

Table 4. 3: Particle size, size distribution and viscosity of alginate microparticle formulations. Data represent mean \pm SD (n=3).

Formulation	VMD (μm)	Span	Viscosity (mPa.s)
A1	2.60 ± 0.03	2.71 ± 0.01	6.52 ± 0.001
A2	2.58 ± 3.35	1.72 ± 0.06	5.60 ± 0.003
A3	3.05 ± 0.53	1.52 ± 0.03	4.04 ± 0.002
A4	3.87 ± 0.17	2.11 ± 0.04	2.80 ± 0.003
A5	4.37 ± 0.29	4.13 ± 1.19	2.05 ± 0.001

Size distribution was affected by formulation ($p < 0.05$), possibly due to the change in solution viscosity, resulting in effects on atomized droplets during spray drying. The significant decrease in feed solution viscosity ($p < 0.05$) might be attributed to the decrease in the intermolecular entanglement, resulting in promoting the freedom of individual polymer chains movements in solution (Graessley, 1974); thus the change in feed composition and viscosity has produced larger droplets with broader size distribution during atomization (Figure 4.7 and Figure 4.8). Interestingly, particle size and Span of RH as a raw material were $59.72 \pm 3.07 \mu\text{m}$ and 1.63 ± 0.14 respectively. However, following spray drying they became respectively $23.62 \pm 4.66 \mu\text{m}$ and 1.84 ± 0.48 . However, for the large standard deviations to be reduced, the experiment needs to be repeated for more times in the future.

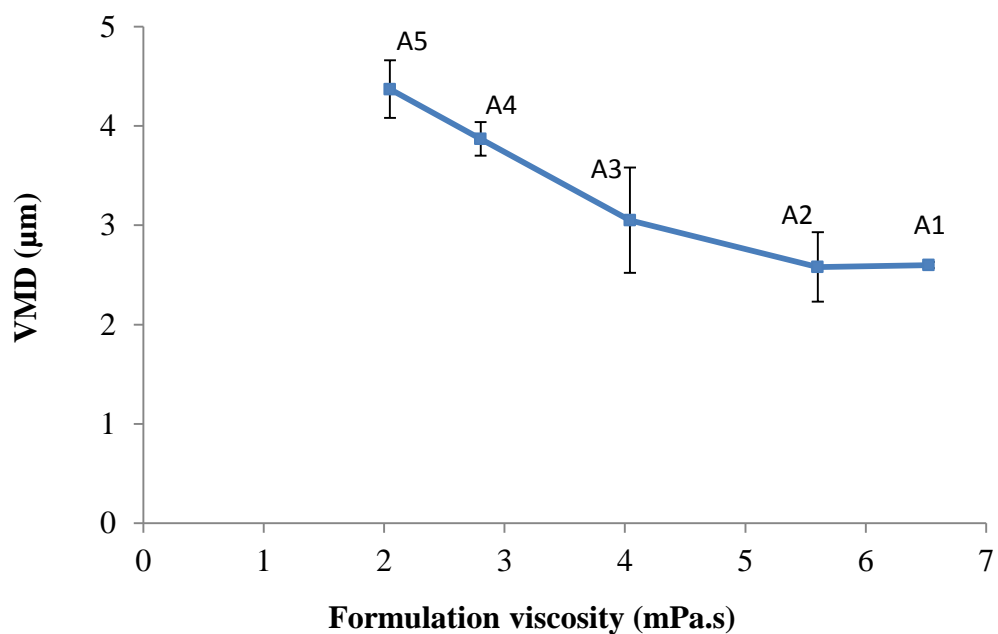


Figure 4. 7: Relationship between viscosity of formulations and particle size of spray-dried RH loaded sodium alginate microspheres.

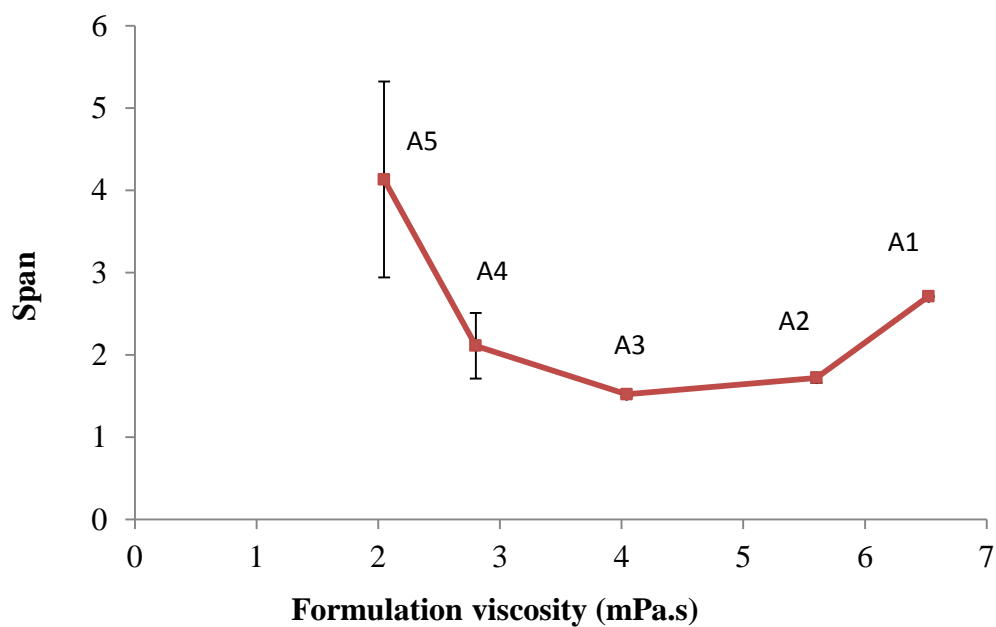


Figure 4. 8: Relationship between viscosity of formulations and size distribution of spray-dried RH loaded sodium alginate microspheres.

4.3.3.3 Drug loading and entrapment efficiency

The percentage loading and encapsulation efficiency for RH in sodium alginate microsphere formulations are shown in Figure 4.9. Almost all microsphere formulations had high encapsulation efficiencies and drug loading; these were respectively $101.55\% \pm 3.18$ and $10.46\% \pm 0.34$ for A2, and $106.99\% \pm 1.77$ and $73.66\% \pm 0.030$ for A4 formulations. Drug loading is the amount of the drug loaded into microparticles to the total weight of microparticles. The data showed drug loading was increased with increasing the ratio of RH in the formulations. These results are in agreement with Alhalaweh et al. (2009) who reported 93-105% entrapment for zolmitriptan-loaded into chitosan microspheres for nasal delivery. Spray drying provides formulations that have high drug loading due to the rapid evaporation of solvent from the droplets in the drying chamber, leading to enhance drug entrapment via excipient solidification (Rathananand et al., 2007).

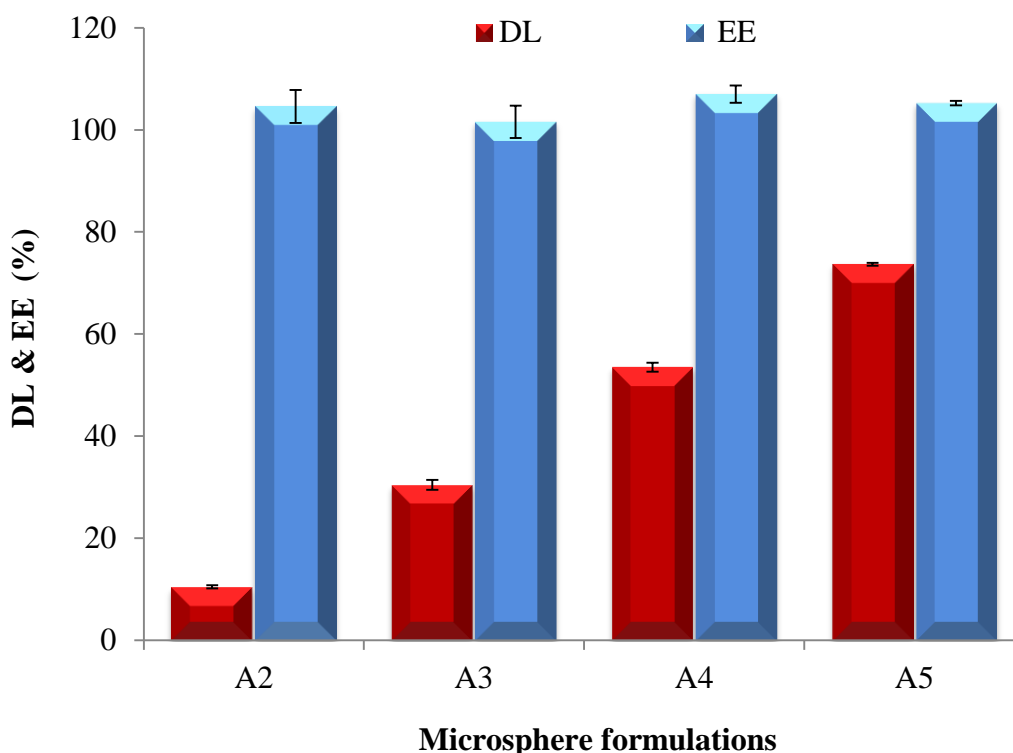


Figure 4. 9: Drug loading and entrapment efficiency of spray-dried microspheres at various drug to sodium alginate ratios. Data are mean \pm SD (n=3).

4.3.3.4 Zeta potential of microparticles

Zeta potential profoundly influences the bioadhesiveness of microparticles. Alginate is negatively charged due to ionization of the carboxyl moiety, resulting in the formation of hydrogen bonds or Vander Waals interactions with mucin or sialic acid of the epithelium (Patil et al., 2012). Zeta potential of the formulations ranged from -70.07 ± 0.73 mV to -39.82 ± 2.38 mV. The results demonstrated that negative zeta potential values of alginate microparticle formulations decreased significantly ($p < 0.05$) as the concentration of the polymer decreased (Figure 4.10).

The *in vitro* study of the mucoadhesive properties of polymeric microspheres is useful for predicting the *in-vivo* performance of nasal formulations (Gad, 2008). The bioadhesive characteristics of sodium alginate formulations is well established (Farid et al., 2012; Mali et al., 2010), and may take place by formation of hydrogen bonds and polymer chain penetration into the mucosa (Kolsure and Raj Kapoor, 2012). It has also been reported by Chickering and Mathiowitz (1995) and Yadav et al. (2010) that bioadhesion of poly anionic polymers (e.g. alginates) is more powerful than that of polycationic and non-ionic polymers due to the presence of strong hydrogen groups (-OH, -COOH) in the structure of anionic polymers. Bioadhesion may depend on charge density of the particles.

Hanna et al. (2013) demonstrated that the bioadhesion of gabapentin-loaded alginate decreased as the polymer to drug ratio decreased, which is in agreement with Allamneni et al. (2012) who evaluated the mucoadhesion performance of glipizide-loaded alginate microparticles.

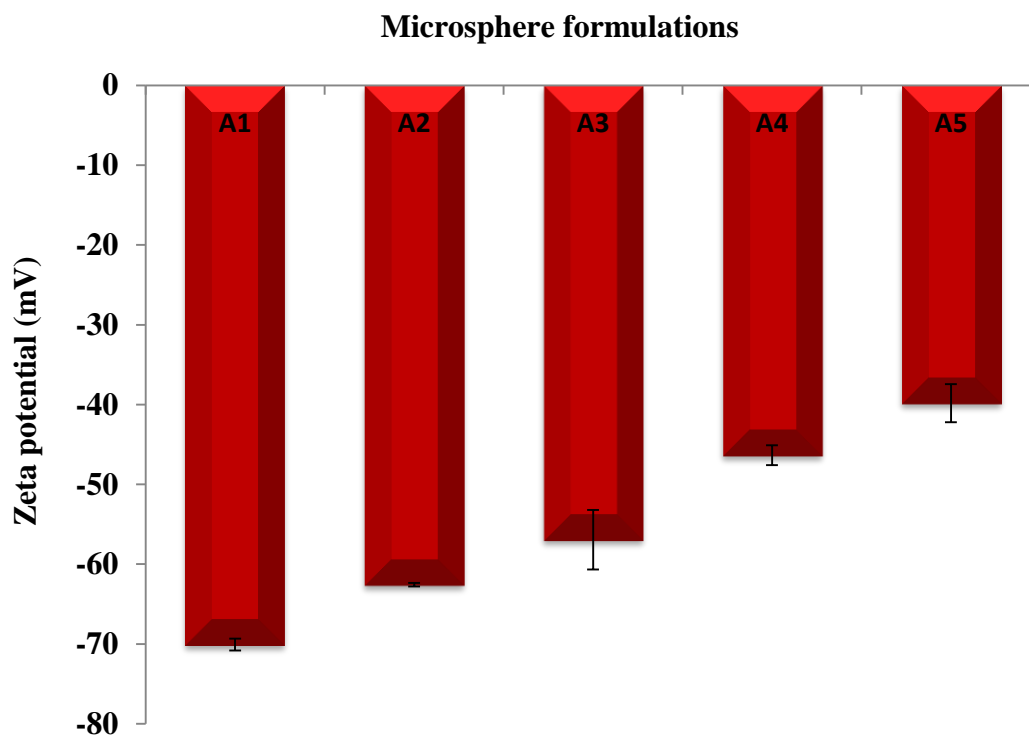


Figure 4. 10: Zeta potential of sodium alginate microparticle formulations. Data represent mean \pm S.D (n=3).

4.3.3.5 Surface morphology of microparticles

SEM images of RH before and after spray drying are shown in Figure 4.11. The shape and surface morphology of RH was improved and became spherical, by co-spray drying with sodium alginate compared to the spray drying of RH raw material alone without polymer (Figure 4.12, and Figure 4.13).

As the ratio of the polymer to drug decreased the proportion of perforated particles also decreased. This remarkable change was seen clearly in formulation A3 (Figure 4.11c), indicating that formulation in terms of polymer to drug ratio had major effect on particle morphology. Further decrease in the polymer to drug ratio made the particles spherically shaped and increased their surface roughness. The optimization in terms of particle size and morphology of powder dosage forms intended for nasal use are necessary to reduce the risk of nasal irritation, improve nasal deposition and promote powder flowability (Behl et al., 1998). Furthermore, the absence of irregular shape in the SEM images indicates that RH was efficiently encapsulated by sodium alginate.

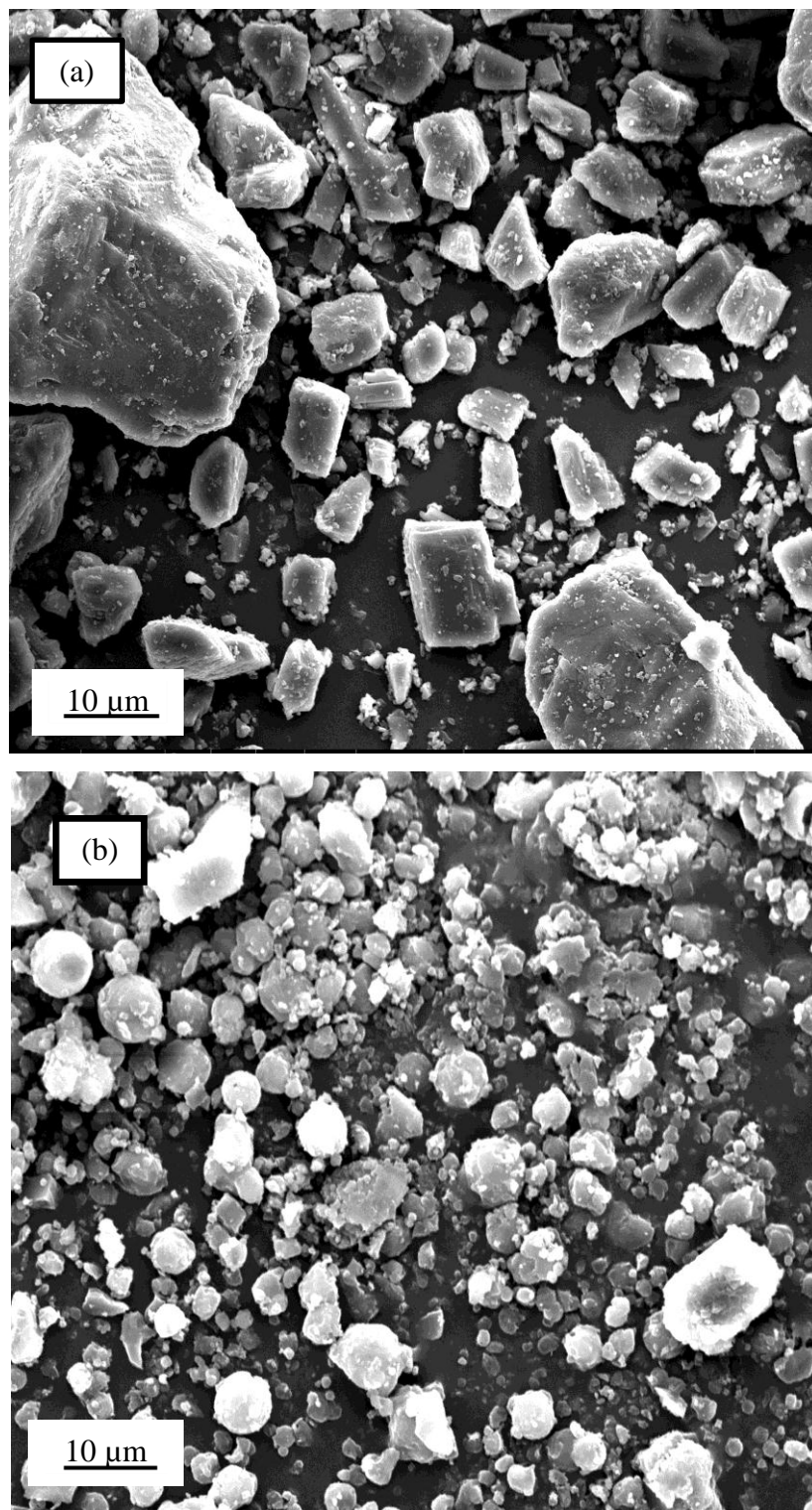


Figure 4. 11: EM images of RH (a) before spray drying (magnification: 750x) and (b) after spray drying (magnification: 1200x).

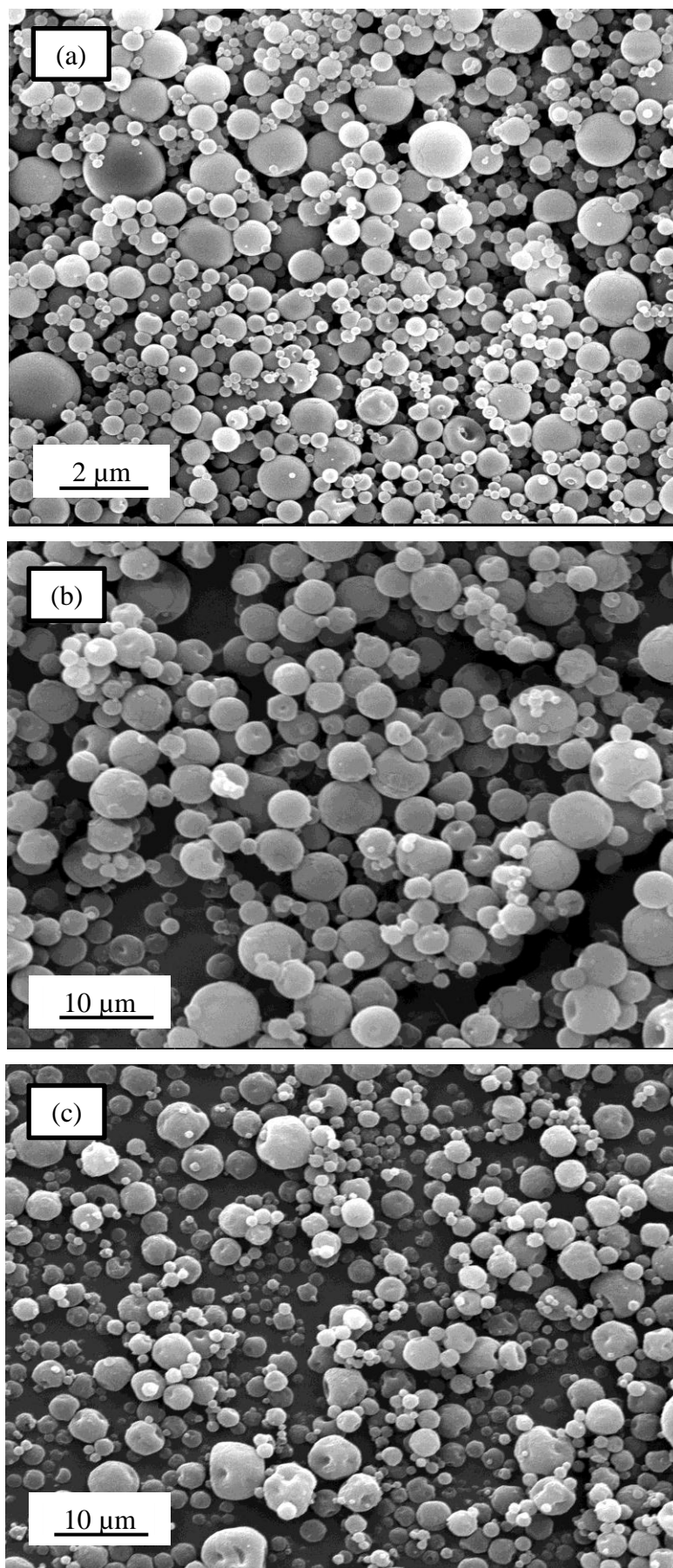


Figure 4. 12: SEM images of (a) drug-free microspheres, (b) A2 and (c) A3. Magnification: 3000x.

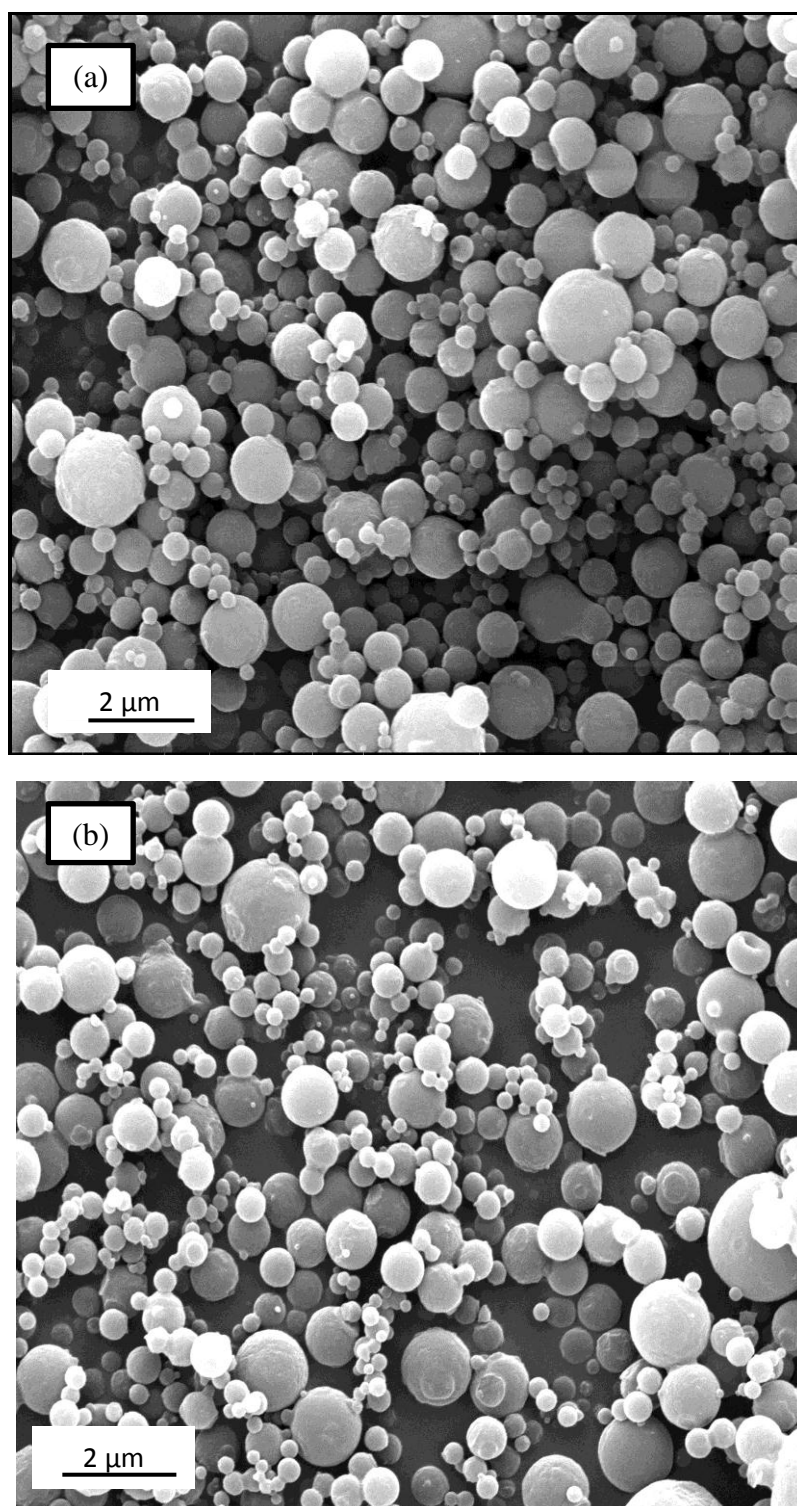


Figure 4. 13: SEM images of (a) A4 and (b) A5. Magnification: 3000x.

4.3.3.6 X-Ray diffraction

The physical behaviour and crystallinity of the spray-dried drug formulations were studied using X-ray diffractometry. X-ray diffraction spectra for RH, drug-free microparticles, drug-loaded microsphere formulations and physical mixture of RH and sodium alginate are shown in Figure 4.14. The diffractogram of RH raw material showed sharp peaks at different angles, indicating that the drug was highly crystalline (Figure 4.14g). The intensity of the crystal peaks decreased for the spray-dried RH-alginate formulations and the decrease was proportional to the polymer to drug ratio, with complete disappearance of the peaks when the alginate to RH ratio was 90:10 (i.e. for A2 formulation) (Figure 4.14b). This indicates that the drug has converted to amorphous form and was molecularly dispersed into the polymeric network (Mahajan et al., 2012). X-ray spectra were in accordance with results reported by Alanazi (2007) using a different hydrophilic polymer for improving the dissolution rate of albendazole via spray drying. For any material the amorphous form has a higher dissolution than the corresponding crystalline form (Craig et al., 1999). Conversion of crystalline form to amorphous state upon spray drying is attributed to rapid solvent evaporation from the droplet. Hence the drug molecules are not given the time to rearrange in the long range ordered crystalline form (Corrigan, 1995). Amorphous form is less stable and have tendency to recrystallize upon storage, causing changes in the physical properties of the formulation (Learoyd et al., 2008c). The stability of RH-alginate microspheres (A2) upon storage for two months was investigated at fridge ($5^{\circ}\text{C} \pm 1$) and at room temperatures ($20^{\circ}\text{C} \pm 2$). Experiments revealed that microsphere formulations had no marked changes in the X-ray spectra regardless of the temperature and over the time course of investigation (Figure 4.15).

Administration of amorphous powders via insufflations may provide advantages, since formation of a mucoadhesive gel as a result of hydration of microspheres within nose may improve drug bioavailability; this might be facilitated by the affinity of the amorphous powder to absorb moisture and have higher dissolution rate. *In vivo* studies are needed to confirm whether this hypothesis is achievable.

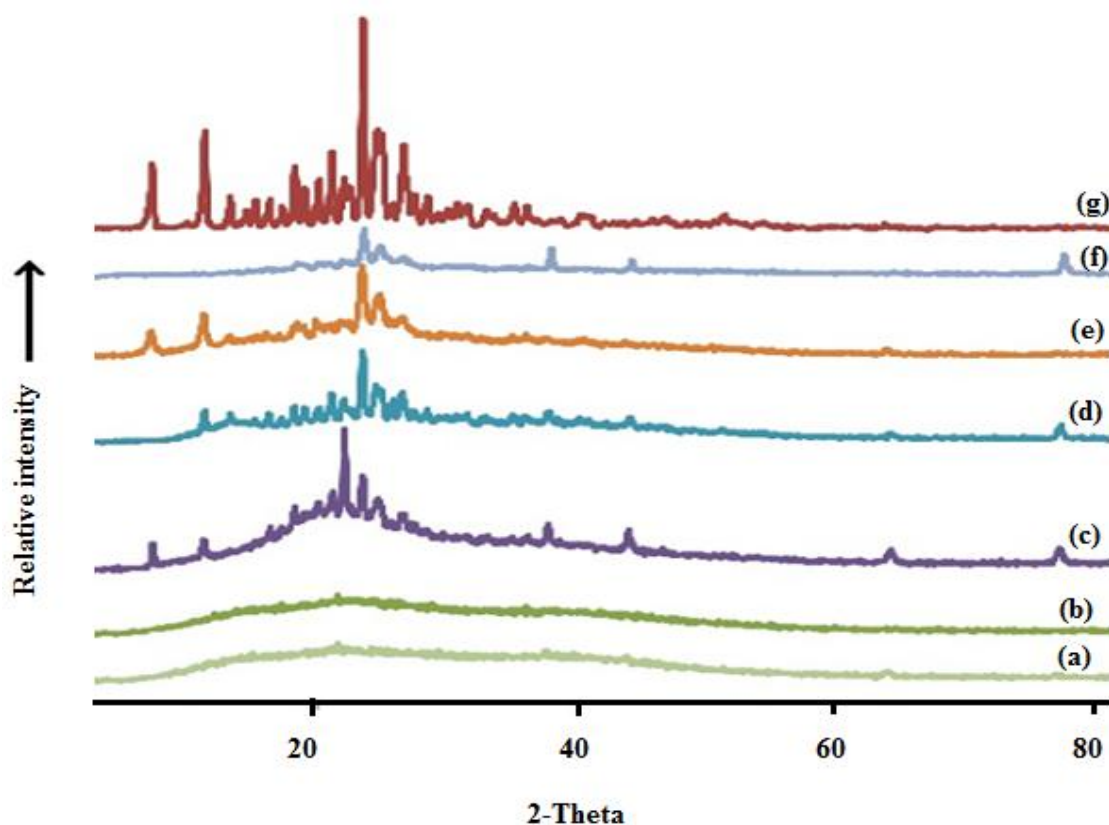


Figure 4. 14: X-Ray diffractogram of (a) drug free microparticles, (b) A2, (c) A2 physical mixture, (d) A3, (e) A4, (f) A5, and (g) RH raw material. For composition of formulations refer to Table 4.2.

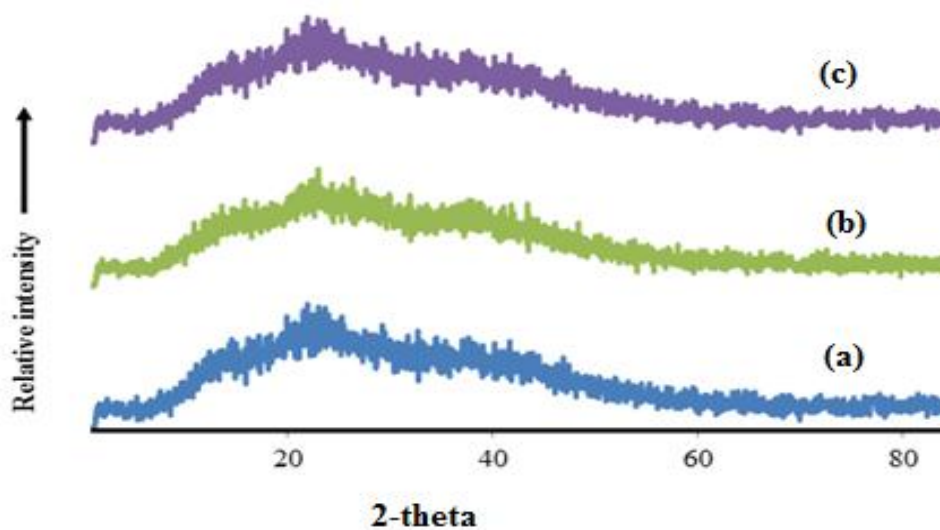


Figure 4. 15: X-Ray diffractogram of (a) fresh A2 formulation, (b) A2 formulations stored at fridge (5 ± 1) and (c) A2 formulations stored at room temperature (20 ± 2) for two months.

4.3.4 Thermo gravimetric analysis (TGA)

The percentage of moisture present in spray dried microsphere formulations gives an indication of the dispersion of particles and their stability. The dispersion of small hygroscopic particles prior to inhalation is not easy, which is attributed to particle agglomeration as a result of adsorbing moisture from air (Ståhl et al., 2002). The moisture content correlates with the long term stability of drug and excipients (Ståhl et al., 2002). In spray drying, moisture content of the product might be affected by the inlet and outlet air temperatures, feed content and feeding rate (Chegini and Taheri, 2013). In this study, TGA revealed that the amount of residual water was in the range of 4.54 ± 0.69 (%) to 18.03 ± 0.65 (%), depending on polymer to drug ratio (Figure 4.16). It was observed that with decreasing polymer to drug ratio, the moisture content decreased significantly ($p < 0.05$). Sodium alginate could retain water within the particle matrix and reduce water evaporation during spray drying.

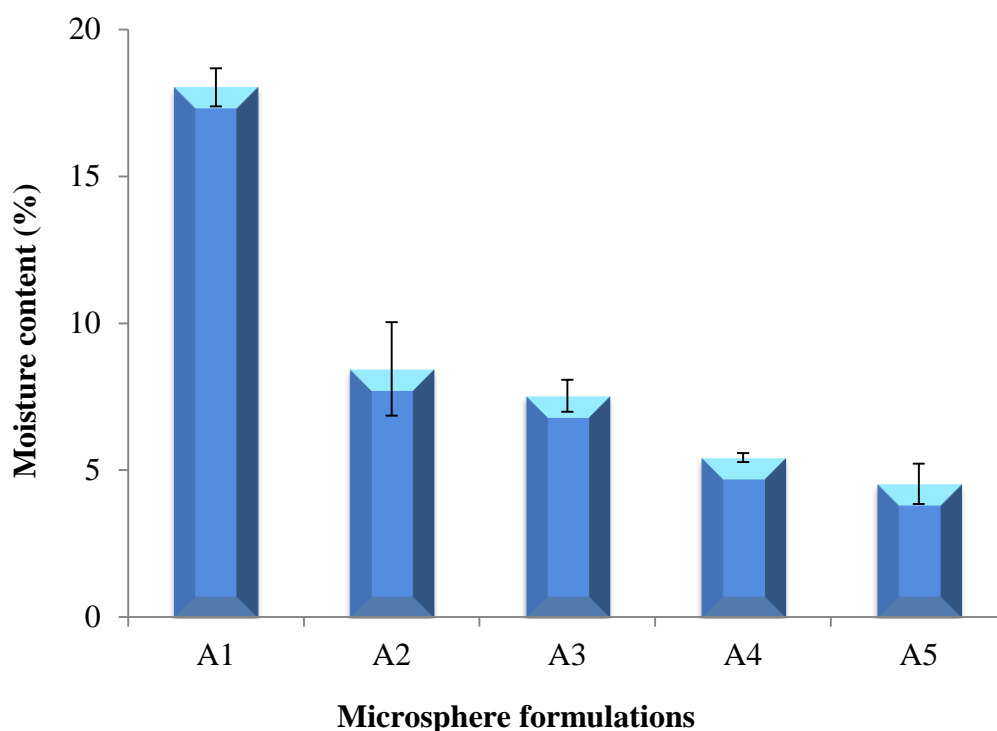


Figure 4. 16: Moisture content (%) of sodium alginate microparticle formulations. Data represent mean \pm SD (n=3).

4.3.4.1 Differential Scanning Calorimetry (DSC)

The state of the drug and its interaction with excipients can possibly be determined by DSC. The thermograph of RH raw material, drug free microparticles, physical mixture of sodium alginate and RH with different ratios (90:10, 70:30, 50:50, and 30:70) and RH loaded sodium alginate microparticle formulations (A2, A3, A4 and A5) are presented in Figure 4.17. An endothermic peak around 100°C was observed for sodium alginate due to dehydration, then an exothermic peak appeared at 239-260°C due to decomposition of the polymer (Soares et al., 2004). The exothermic peak was absent at low polymer to drug ratio. The endothermic sharp peak was observed for RH raw material at 248.57°C ($\Delta H = 117.35$ J/g) corresponding to its melting point, indicating a highly crystalline nature. The sharp endothermic peak for RH has been reported previously (Avachat et al., 2011). The DSC thermogram for RH formulations (Figure 4.17B) showed a decrease in the sharpness of crystalline peak especially as the concentration of the polymer increased and the onset temperature shifted forward (224.88 to 212.58°C), indicating partial loss of crystallinity of RH upon loading in the microspheres. The peak was absent in formulation A2, indicating that the drug existed in amorphous form and was uniformly distributed within the polymeric matrix (Corrigan, 1995). The results agreed with those shown by Alanazi et al (2007), when they aimed to enhance dissolution of albendazole by loading into microparticles using spray drying. The endothermic peak of the drug may disappear when the drug is uniformly distributed in the microparticle matrix at the molecular level (Das and Senapati, 2008).

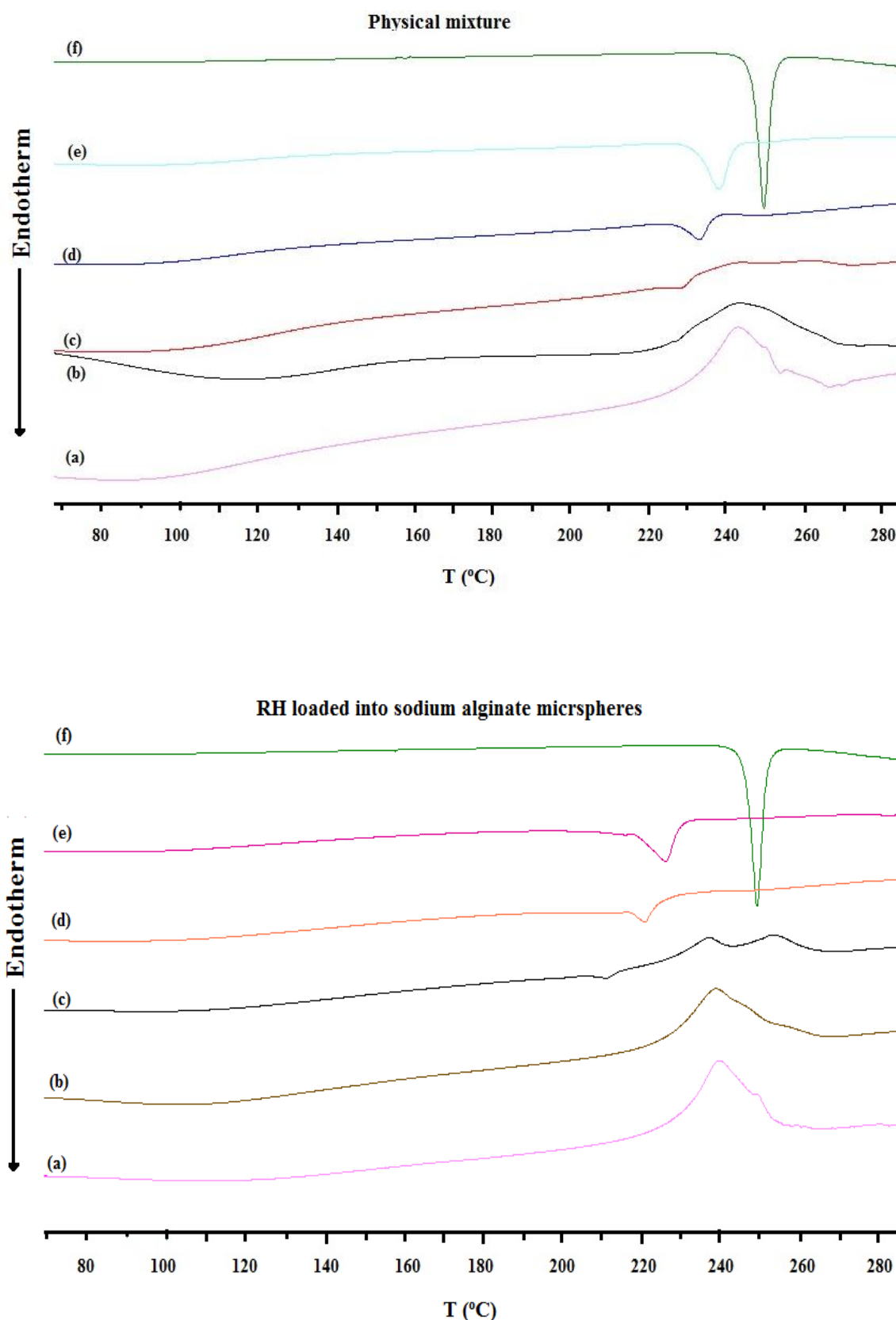


Figure 4. 17: DSC thermograms of (a) drug-free microsphere, physical mixture of alginate-RH; (b) 90:10, (c) 70:30, (d) 50:50, (e) 30:70, RH loaded alginate microspheres; (b) A2, (c) A3, (d) A4, (e) A5 and (f) pure drug.

4.3.4.2 Dissolution test

In vitro drug release study was carried out in phosphate buffer with pH 6.5 within the physiological pH range of the nose. The cumulative drug release (%) from formulation A2, A3, A4 and A5 at different time intervals is presented in Figure 4.18. The time required for maximum drug release (>95%) were 60, 30, 10 and 1 minutes for A2, A3, A4 and A5 formulations respectively. Rapid drug released is ascribed to the solubility of sodium alginate and RH in aqueous media and smaller particle size of the formulations. Decreasing the particle size increased the surface area, hence the rate of dissolution is increased (Kondo et al., 1993). Polymer to drug ratio plays an important role in the drug release rate. As the ratio of polymer to drug was decreased from A2 to A5 formulations the rate of microparticle dissolution increased. This might be ascribed to the drug diffusion through shorter path length of microsphere layer. The drug release mechanism from the polymeric matrix occurs by diffusion through the matrix and erosion as the polymeric particles are dissolved by the dissolution medium. Rathananand et al., (2007) determined the release rate of levocetirizine from chitosan microparticles, and reported slower drug release at high polymer concentrations. Rapid release of RH from alginate microparticle formulations confirmed no interaction happened between the drug and polymer, whereas Gavini et al. (2005) reported a possible interaction between sodium alginate and metoclopramide hydrochloride caused prolonged drug released (>3hr).

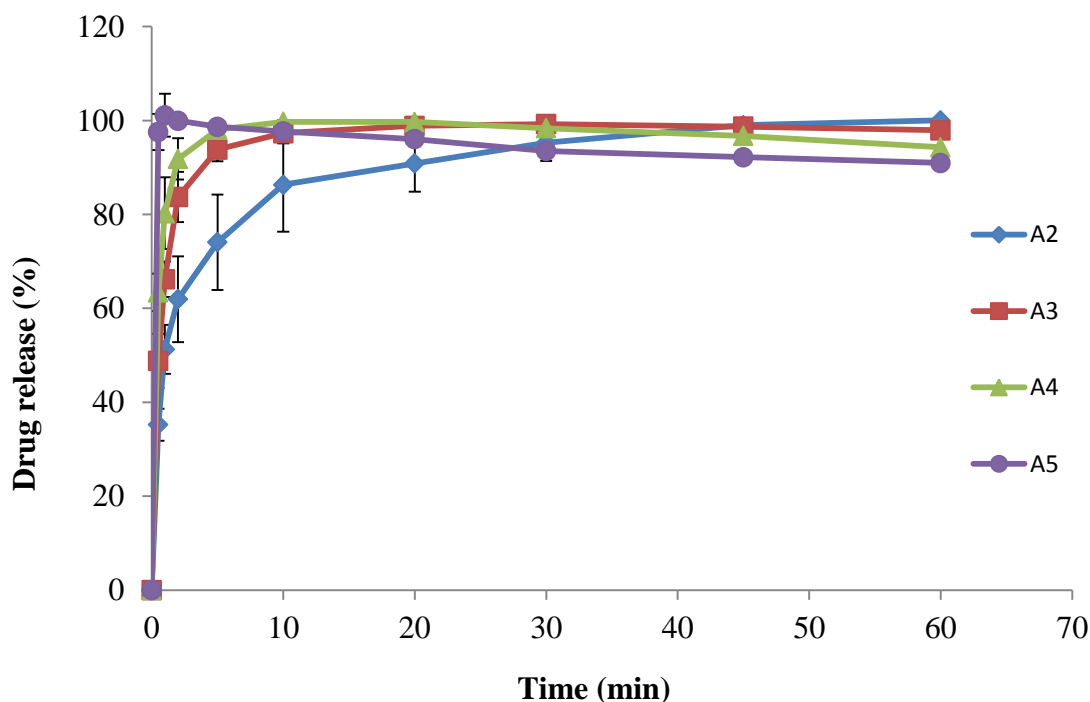


Figure 4. 18: Dissolution profile of various spray dried RH-loaded sodium alginate microsphere formulations carried out in phosphate buffer solution (pH 6.5). Data represent mean (n=3).

4.3.4.3 Histopathological study of RH-loaded sodium alginate

The *ex-vivo* toxicity for the best performing formulation RH-sodium alginate microparticles (A2) was investigated on isolated nasal sheep mucosa, to evaluate the safety of formulation for nasal delivery. This experiment was adapted from the protocol of investigation used by Hermens and Merkus (1987). Microscopic images of RH loaded alginate microparticles (A2) and drug free microparticles did not show remarkable effect on the overall appearance of the sheep nasal mucosa (Figure 4.19a, b) compared to positive control (Figure 4.19c) as previously discussed in section 3.3.14. The cilia lining mucosa and its components were normal, and necrosis was not found as compared to the sample treated with the positive control (sodium deoxycholate % w/v). Goblet cell, sero-mucinous glands and ciliated cell were intact with only little focal sloughing of cells being detected (Table 4.4). These results were in agreement with Kolsure and Raj Kapoor (2012) using nasal gels of zolmitriptan and with Patil et al. (2012) using carvedilol-sodium alginate microspheres for intranasal delivery. Microscopic results in this study indicated that optimized RH-loaded sodium alginate microsphere formulations have no harmful effects on the nasal mucosa, and RH loaded microspheres are safe and can potentially applicable for nasal delivery.

Table 4. 4: The comparative histopathological evaluation of nasal mucosa treated with a range of formulations and RH-loaded sodium alginate microparticles.

Treated nasal mucosa	Necrosis	Ciliated cells	Goblet cells	Inflammatory cell infiltrate in the sub mucosa	Sero-mucinous glands
Phosphate Buffer solution (PH 6.5) (Negative control)	Absent	Intact with focal sloughing	Not affected	Mild sub-mucosal inflammation and increased intraepithelial lymphocytes	Not affected
Sodium deoxycholate solution (positive control)	Severe	Mostly sloughed	Present	Severe sub mucosal inflammation and increased intraepithelial lymphocytes	Inflamed
Alginate microparticle dispersion	Absent	Intact with focal sloughing	Not affected	Mild sub mucosa inflammation	Not affected
RH solution	Absent	Detached focally but still present	Not affected	Mild sub-mucosa inflammation	Not affected
Alginate: RH (90:10) (A2)	Absent	Focal sloughing	Not affected	Mild sub-mucosa inflammation	Not affected

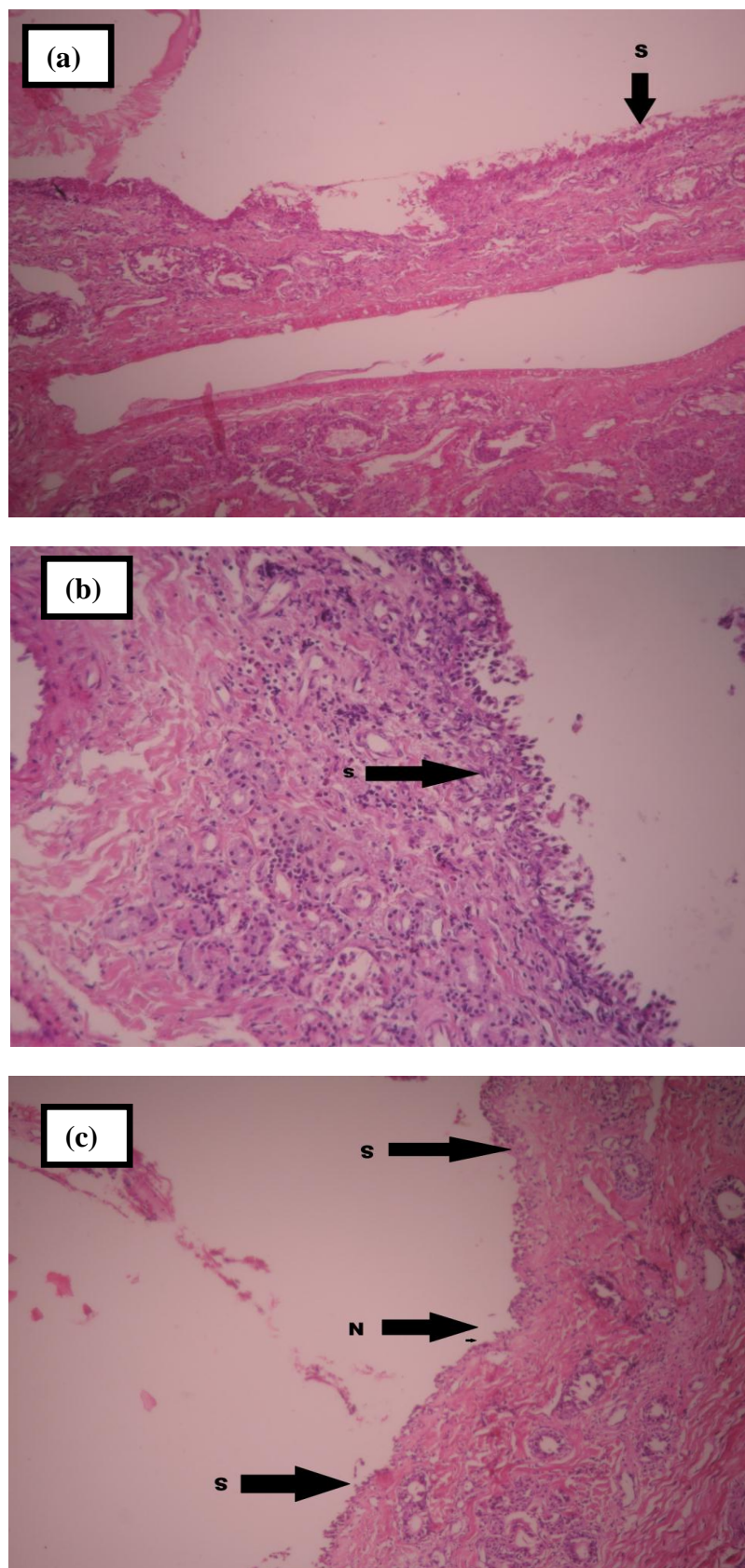


Figure 4. 19: Microscopic (Olympus) images of sheep nasal mucosa treated with (a) A2 formulations, (b) drug free microparticles, and (c) positive control (10 x 10 magnification, n=3). "S" means sloughed, "N" means necrosis, "I" means inflammation.

4.3.5 Characterization of delivered RH loaded sodium alginate microspheres using Miat[®] nasal device

Powder delivery to the nasal cavity has not been explored in terms of studying and characterization of spray pattern, plume geometry and deposition of powder dosage forms using nasal insufflators. The deposition of powders in nasal cavity depends on the powder formulation properties and type of nasal device used (Djupesland, 2013).

Miat[®] Monopowder device was used for spray pattern and plume geometry investigations. Powder spray characteristics such as shot weight, mean particle size, spray cone angle, plume width and spray velocity were all investigated (CDER, 2003). These *in vitro* tests are required by FDA to characterize the device performance and may give useful information relating to the bioavailability of the drug given in nasal formulations (CDER, 2002).

4.3.5.1 Determination of shot weight

Miat[®] monodose powder insufflator was used to determine the fraction delivered of RH-sodium alginate microspheres (Alginate: RH, 9:1 w/w) by calculating the difference in weight of powder in the device before delivery and after each puff. This study investigated the effect of loading dose on the fraction of powder delivered. Three weights of powder (5, 10 and 20 mg) were used.

Quantitative delivery of RH-sodium alginate microspheres from the Miat nasal insufflator is shown in Table 4.5. When the device was actuated the first time (i.e. first puff) around 90% of the formulation was released, regardless of formulation weight. The second and third puffs have forced marked fractions of the remaining powder (i.e. the remaining 10%) to leave the device, resulting in slight but significant ($P < 0.05$) increases in the total weight released. The Miat[®] device was highly efficient single dose insufflator since most of the loaded dose was emitted by the first puff. The emitted dose of powder was dependent on the number of puffs rather than the amount of powder loaded into the device.

Various loads were compared (5 mg, 10 mg and 20 mg) and a significant fraction of the dose was released by the second puff when 20 mg loading dose was compared to 5 and 10 mg. The loading dose has effected the delivery of RH-sodium alginate microspheres (A2). Results of this experiment disagreed with De Ascentiis et al. (1996) and Patil and

Sawant (2011), who studied the delivery of chitosan microparticles using the Miat nasal device. The conflicting findings might be due to formulation properties (e.g. moisture content).

Table 4. 5: Fraction delivered of RH-loaded chitosan microspheres using Miat[®] nasal insufflator. Data represent mean \pm SD (n=3).

loading weight (mg)	Fraction of powder delivered (%)		
	First Puff	Second Puff	Third Puff
5	88.61 \pm 0.44	90.78 \pm 0.67	91.63 \pm 0.99
10	89.26 \pm 1.36	90.53 \pm 0.42	92.07 \pm 0.92
20	90.28 \pm 0.44	93.11 \pm 0.56	94.2 \pm 0.62

4.3.5.2 Particle size analysis using laser diffraction

Particles in the micrometres range may agglomerate owing to their high surface area. In the context of nasal drug delivery, particle agglomeration might be useful to increase the overall size of particles to be suitable for nasal deposition and minimize possible travelling of the particles to the lower respiratory tract. The weakly agglomerating particles may deagglomerate to a smaller size of particles during delivery, enhancing the surface area of the particles and obtaining a size range that is suitable for absorption by the nasal epithelium (De Ascentiis et al., 1996). The VMD, percentage of particle size $<10 \mu\text{m}$ and Span value of A2 formulation were determined by the Spraytech aerosol size analyser and were $87.25 \mu\text{m} \pm 7.54$, $22.65 \mu\text{m} \pm 1.65$ and 4.02 ± 0.37 respectively. De Ascentiis et al. (1996) have found that the size of beta-cyclodextrin particles was around $100 \mu\text{m}$ upon delivery for nasal deposition using the Miat[®] monodose device. This suggest that RH-sodium alginate (A2) formulation is less likely deposit in the respiratory region when delivered by the Miat[®] nasal device insufflator.

Previous reports on the particle size and impaction in the nose are conflicting. The nasal mucosa can efficiently filter out particles larger than $3\text{-}10 \mu\text{m}$ because it is covered by a protective mucous layer from the posterior part to the nasal valve which can effectively

trap particles and microorganisms from the inspired air (Djupesland, 2013). Donovan and Huang (1998) have reported that particles in the size range of 5–7 μm might be retained in the nasal cavity. Particle deposition in the nose increases when particle size is larger than 10 μm , and anterior deposition is most prominent for larger particles, and velocity of inhaled particles and the turbulence in the air flow determine the deposition site of smaller particles in the nose (Rai et al., 2008). Particles larger than 0.5 μm deposit intranasally via inertial impaction (Burgess et al., 2004). In contrast, the deposition of particles less than 0.5 μm is dominated by diffusional mechanism (Foo, 2007). The probability of particle deposition into the lower respiratory tract may decrease as the particle size increases, However, particles below 5 μm have greater possibility to deposit in the olfactory region (Keldmann, 2005).

4.3.5.3 Determination of plume geometry and spray pattern

Improving nasal bioavailability is related to the delivery device, physical form of the formulation (liquid, viscous or solid) and technique of administration (Arora et al., 2002). Figure 4.21 shows representative images of spray pattern for A2 formulation, at a distance of 3cm from the nasal device tip. The longest diameter (D_{max}), shortest diameter (D_{min}) and ovality ratio ($D_{\text{max}}/D_{\text{min}}$) were 13.33 ± 1.03 mm, 10.67 ± 0.52 mm and 1.25 ± 0.04 respectively. Spherical spray pattern and the agglomeration of particles were seen on the impact sheet, as shown from the ejected powder formulations (Figure 4.20).

Spray time required to reach fully developed phase was 0.16 sec, whilst the total spray time to deliver 10 mg of RH loaded alginate microparticles was 0.32 sec, indicating rapid delivery of the powder (Figure 4.21). The spray cone angle and width 3cm distance from the tip of the device were $14.67^\circ \pm 0.52$ and 10.67 ± 0.52 mm respectively. The powder particles were characterized by elongated puff with visible individual particles as they emitted from the device. De Ascentiis et al. (1996) have reported the compactness of the clouds to be affected by powder particle size; small particle size generated fluffy clouds which are homogeneous in density, whereas larger particles may produce clouds with visible individual particle trajectories. Pringels et al. (2006) reported the anterior deposition of the emitted dose from the device to be more predominant when the spray had larger angle ($60 - 70^\circ$), whereas deposition in posterior part of the nasal increased as the plume cone angle was smaller (30 to 35°). The

decrease in the plume angle increases the probability of targeting the turbinate region in the nose (Foo et al., 2007). Overall, the results of this study suggested deposition of RH loaded sodium alginate might be more prominent in the turbinate region which may improve absorption.



Figure 4. 20: Spray pattern of formulation A2 at 3cm distance from the insufflator device tip (n= 4).

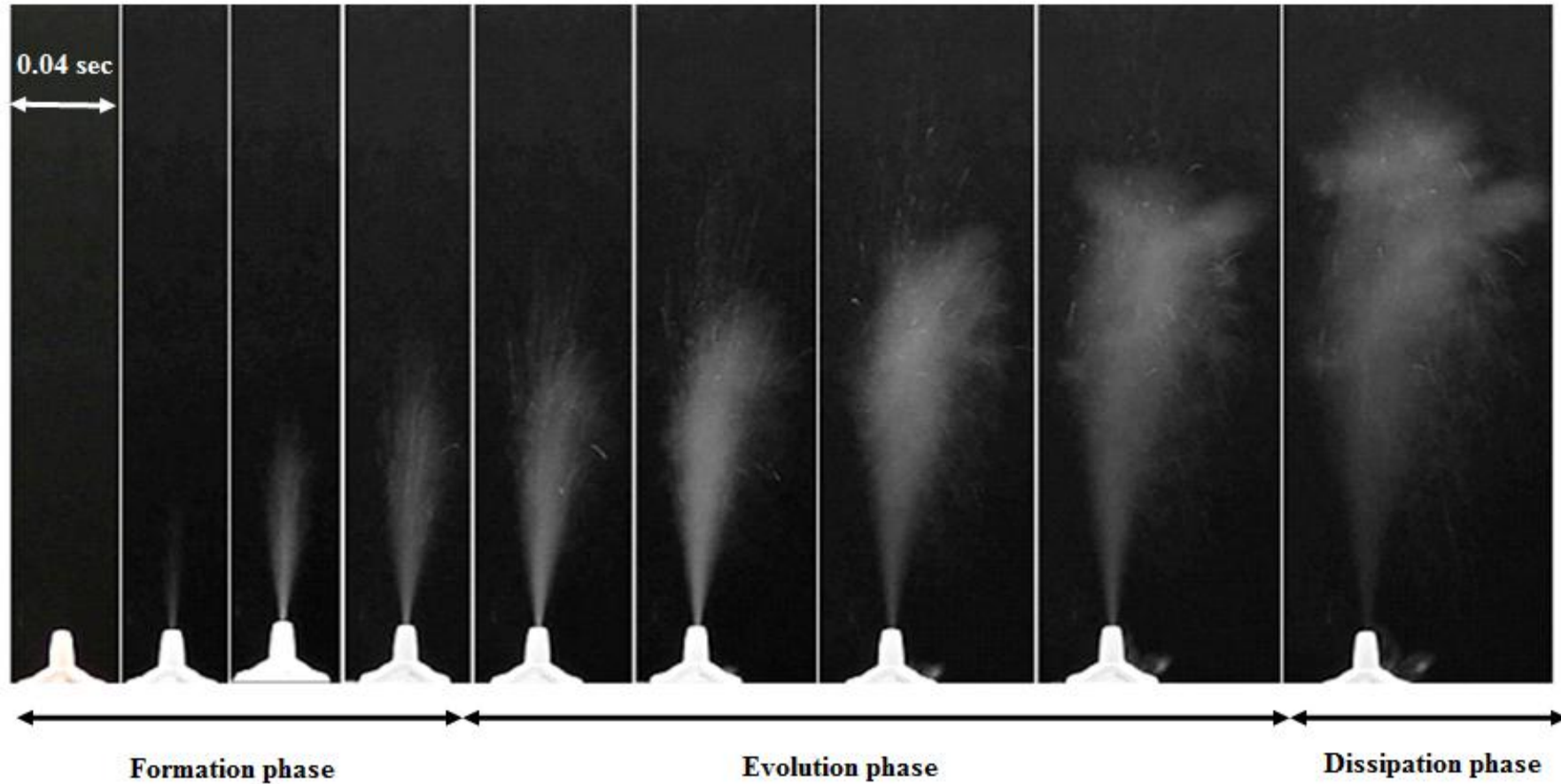


Figure 4. 21: RH-sodium alginate microspheres delivery from Miat® monodose insufflator as monitored using videography (n= 4).

4.4 Conclusions

This study demonstrated that spray drying is a powerful technique for producing RH loaded sodium alginate microspheres. Inlet temperature had remarkable effect on the particle morphology and yield percent of sodium alginate microspheres. The optimum inlet temperature to produce RH-alginate microparticles was 140°C. FTIR revealed that no interaction occurred between polymer and RH. The characterization studies demonstrated that the composition of the feed solution had a remarkable effect on the particle shape, size and size distribution. The findings of this study represented that alginate to drug ratio of 90:10 (w/w) was the best performing formulations. X-ray diffractogram demonstrated that crystallinity of the encapsulated drug decreased and was completely converted to amorphous phase when the polymer and drug were co-sprayed in the ratio of 90:10 (w/w). Additionally, X-ray study revealed RH loaded alginate microspheres was stable over two months. DSC thermograms demonstrated drug molecules were molecularly dispersed in microparticles when polymer to drug ratio was 90:10 (w/w). Histopathological study showed RH loaded sodium alginate is non-toxic to nasal epithelium. Investigation of the device performance using Miat[®] nasal insufflator demonstrated that fraction delivered (%) was affected by loading weight. Cloud study using laser diffraction demonstrated that the sprayed particles are less likely to deposit in the lower respiratory tract. Videography showed that the cloud is most likely to deposit in the nasal cavity and particularly in the olfactory region. *In-vivo* studies are required in the future to determine the amount of the drug that may reach the brain, CSF and blood circulation after administration of RH-sodium alginate microspheres in the forms of nasal powders.

The study demonstrated that the percentage of yield for F2 formulation (76.9%±1.01) to be higher than A2 formulation (69.5±0.68) which might be attributed to the difference in the inlet air temperature between the two formulations. RH loaded chitosan glutamate microparticles were spherical, whereas dimpled particles were present in the spray dried sodium alginate formulation; this difference is ascribed to the different properties of the polymers used. Comparison of the drug entrapment efficiency obtained from spray dried sodium alginate with drug has shown that entrapment provided by A2 formulation (104.59% ± 3.23) was higher than that of chitosan based microspheres (i.e. F2) 93.28% ± 1.66), which might be attributed to the affinity of the cationic drug (RH) to sodium alginate polymer which has a negative charge whilst chitosan glutamate has a positive charge.

The emitted amount using 10 mg of F2 formulation ($94.83\% \pm 0.41$) was more than that using A2 formulation ($90.53\% \pm 0.42$) after the second puff of the nasal insufflator; this difference might be related to the difference in percentage of humidity content of the formulations. Hence, F2 formulations produced elongated homogenous cloud, whereas, visible individual particles were found in the plume produced by A2 formulation.

CHAPTER 5

FORMULATION OF ROPINIROLE HYDROCHLORIDE LOADED LIPOSOMES USING ETHANOL-BASED PROLIPOSOME METHOD

5.1 Introduction

Since their discovery in 1960s, liposomes have been of great interest to use in drug delivery. The interest in using liposomes is attributed to the convenience of their preparation and their desirable properties such as biocompatibility, non-toxicity, and non-immunogenicity, because they are made from natural phospholipids or similar synthetic phospholipid molecules (Ahn et al., 1995). The amphiphilic properties of phospholipids make the encapsulation of hydrophilic and lipophilic drugs possible (Brandl, 2001). Particle size and surface properties of liposome can be manipulated upon addition of other materials during formulation of liposomes (Tran, 2011).

Nasal administration offers several advantages over oral delivery including rapid onset of action, evasion of first pass effect and blood brain barrier. However, the duration of drug contact with epithelial surfaces for drug is given via the nose is short due to the rapid removal of the drug from the site of absorption via the mucociliary clearance (Jadhav et al., 2007). For this reason incorporation of mucoadhesive agents into formulation is required to improve the drug absorption. Frequent dosing is required to maintain drug therapeutic concentration in the plasma might increase therapeutic cost. Thus, prolonging the retention time of the formulation at the site of absorption and extending the drug release time could improve the efficacy of drug and enhance patient compliance. Liposome drug delivery systems are capable of reducing the mucociliary clearance in the nose and provide sustained release properties (Gregoriadis and Florence, 1993; Ahn et al., 1995). Furthermore, liposomes coated with mucoadhesive agents may improve drug permeation through the nasal epithelium (Naderkhani et al., 2014).

Various strategies have been proposed to improve the delivery of peptide and non-peptide drugs to the nose by using microspheres, nanoparticles, liposomes and liposomes. Liposomes are suitable carrier systems for nasal delivery since they are made from biocompatible and biodegradable materials such as phospholipids which are similar to the natural components of the mucous membranes (Schnyder and Huwyler, 2005). Liposomes from hydrogenated soya phosphatidylcholine has been shown to be safe in animals, since no critical changes in the integrity of the respiratory tract cells were observed upon acute or chronic exposure to liposomes (Manca et al., 2012).

Liposomes are unstable upon storage when generated by conventional technique (e.g. thin film hydration method), hence the difficulty in producing on large scale. To

overcome this limitation proliposome technologies such as ethanol (solvent)-based proliposomes (Perrett et al., 1991) and particulate-based proliposomes (Payne et al., 1986) have been suggested. Furthermore, they can use for the large scale manufacture of stable liposome precursors. Depending on the hydration procedure of ethanol-based proliposomes the generated liposomes are either multilamellar (Turánek et al., 1997) or oligolamellar (Perrett et al., 1991). Polysaccharides have been used to change and modify liposome surface properties by improving the retention time of liposomes within the nasal cavity (Takeuchi et al., 2000; Cheng et al., 2006).

Ethanol based proliposome method was used to prepare liposomes incorporating the model hydrophilic drug RH. Parameters involved in the preparation were investigated to optimize the loading of RH in liposomes using various drug concentrations ranging from 0.5 to 8 mg /ml. In addition, the effect of inclusion of different types of mucoadhesive agents (0.2% chitosan G113, chitosan G213, carboxymethyl chitosan, low and medium viscosity sodium alginate) on liposomes was evaluated to establish an optimum liposome formulation for nasal administration. The resultant liposomes were characterised in terms of particle size, Span, zeta potential and percentage of drug entrapment. The delivery of liposome formulation was performed and studied using three different nasal spray devices.

5.2 Methodology

5.2.1 Manufacture of RH liposomes

Ethanol-based proliposome method was used to prepared RH loaded liposomes by adapting the procedure introduced by Arafat (Arafat, 2013) who developed a method to prepare liposomes loaded with protein or salbutamol sulphate for nasal delivery. Liposomes were generated by adding 60 mg ethanol (76 μ l) into a 10 ml glass vial containing 50 mg of lipid phase (SPC and cholesterol; 4:1 w/w) at 70°C to enhance the dissolution of cholesterol for two minutes to obtain a clear lipid solution (i.e. the proliposomes). Solutions of RH were prepared in HPLC water in a range of concentrations (0.5, 1, 2, 4, or 8 mg/ml). To this lipid solution, RH solution (0.5 ml) was added and vortexed for 2 minutes using a Whirl Mixer TM (Fisherbrand, Fisher, UK) to obtain a concentrated suspension of liposomes (the primary hydration step). To generate the final liposomal suspension, the rest of HPLC water (4.5ml) was added to the concentrated liposomal suspension and vortexed again for 2 minutes (the secondary

hydration step). Liposomes were kept at room temperature ($20^{\circ}\text{C} \pm 2$) for 1 hour to anneal before conducting subsequent studies.

5.2.2 Characterization of liposomes

Liposomes were characterized in terms of (i) particle size and Span (section 2.6.2), (ii) zeta potential (section 2.6.3), and (iii) drug entrapment efficiency (section 2.8.3).

5.2.3 Formulation of mucoadhesive liposome

Five types of mucoadhesive agents were used: Chitosan G113 (Ch G113), Chitosan G213 (Ch G213), Carboxymethyl chitosan (CM Ch), (Santacruz Biotechnology, USA), low viscosity sodium alginate (LVSA) and medium viscosity sodium alginate (MVSA) in a concentration 0.2% w/v. Mucoadhesive agents were dissolved in 4.5 ml HPLC water with aid of vortex mixing. The resultant mucoadhesive solutions were used in the secondary hydration step of the ethanol-based proliposomes to generate mucoadhesive liposomes. Formulations were left at room temperature ($20^{\circ}\text{C} \pm 2$) to anneal for 1 hour. The technique used in this study was adapted from that of Arafat (2013).

5.2.4 Liposome morphology study using Transmission Electronic Microscopy

A drop of liposome dispersion was spotted onto carbon-coated copper grids (400 mesh) (TAAB Laboratories Equipment Ltd., UK), and negatively stained with 1% w/v phosphotungstic acid (Elhissi et al., 2006), then viewed and imaged using a Philips CM 120 Bio-Twin transmission electron microscope (Philips Electron Optics BV, Netherlands) the voltage was 120 kV, as described in section 2.8.4..

5.2.5 Characterisation of liposomes after delivery using nasal spray devices

Size and size distribution analysis was performed for carboxymethyl chitosan coated RH loaded liposomes using three different devices (A, B and C) as previously explained in section 2.6.2. Zeta potential of liposomes was determined by using the Malvern Zetasizer (section 2.6.3). The entrapment efficiency (%) of RH was analyzed for samples before and after delivery from the nasal spray devices according to the HPLC method (section 2.9.3). Droplet size, size distribution and percentage of droplets less than $10\ \mu\text{m}$ were analysed by using the Malvern Spraytec instrument (Malvern Instruments Ltd, UK) following the generation of sprays from each device (section 2.8.5). The spray plume investigation was conducted for both spray pattern and plume geometry (section 2.9).

5.3 Results and Discussion

5.3.1 Characterization of RH loaded in liposomes

5.3.1.1 Size and size distribution of liposomes

The effect of RH concentration (0.5, 1, 2, 4 and 8 mg/ml) on the size and size distribution of liposomes produced from SPC and cholesterol (4:1 w/w) using ethanol-based proliposomes are shown in Figure 5.1 and Figure 5.2. Size and size distribution of RH loaded liposomes and drug-free vesicles were compared. Data showed that by adding drug in a concentration of 0.5 mg/ml to the formulation, VMD of the liposome increased significantly ($p < 0.05$; $4.80 \mu\text{m} \pm 0.54$) compared to the drug-free liposomes ($3.20 \mu\text{m} \pm 0.47$). Further increases in the RH concentration resulted in insignificant trend of increase in the VMD. For example the measured VMD was $4.85 \mu\text{m} \pm 0.54$ when the drug concentration was 0.5 mg/ml and was $5.74 \mu\text{m} \pm 0.74$ when the concentration was increased to 4 mg/ml. However, with regard to size distribution, expressed as Span, a significant difference ($p < 0.05$) was observed when the drug formulation (2 mg/ml) (Span = 2.66 ± 0.25) was compared to the drug-free formulation (Span = 1.68 ± 0.17). For all RH loaded liposome formulations no significant difference in the Span values was found (Figure 5.1). However, for the large standard deviations to be reduced, the experiment needs to be repeated for more times in the future.

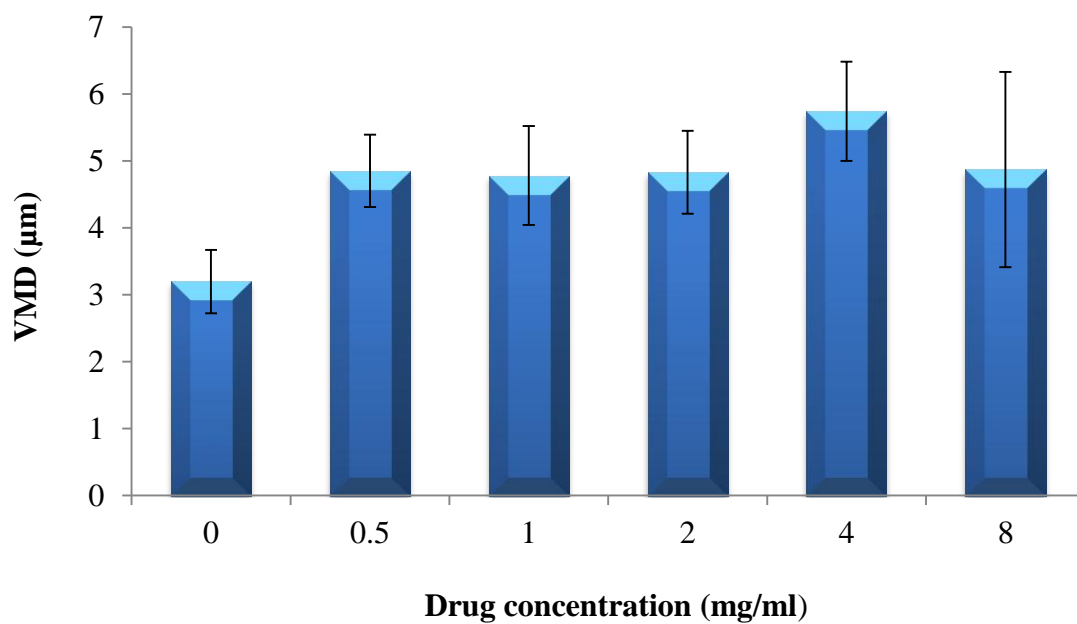


Figure 5. 1: Size (VMD) of liposomes generated from ethanol-based proliposomes using a range of RH concentrations (0 – 8 mg/ml).

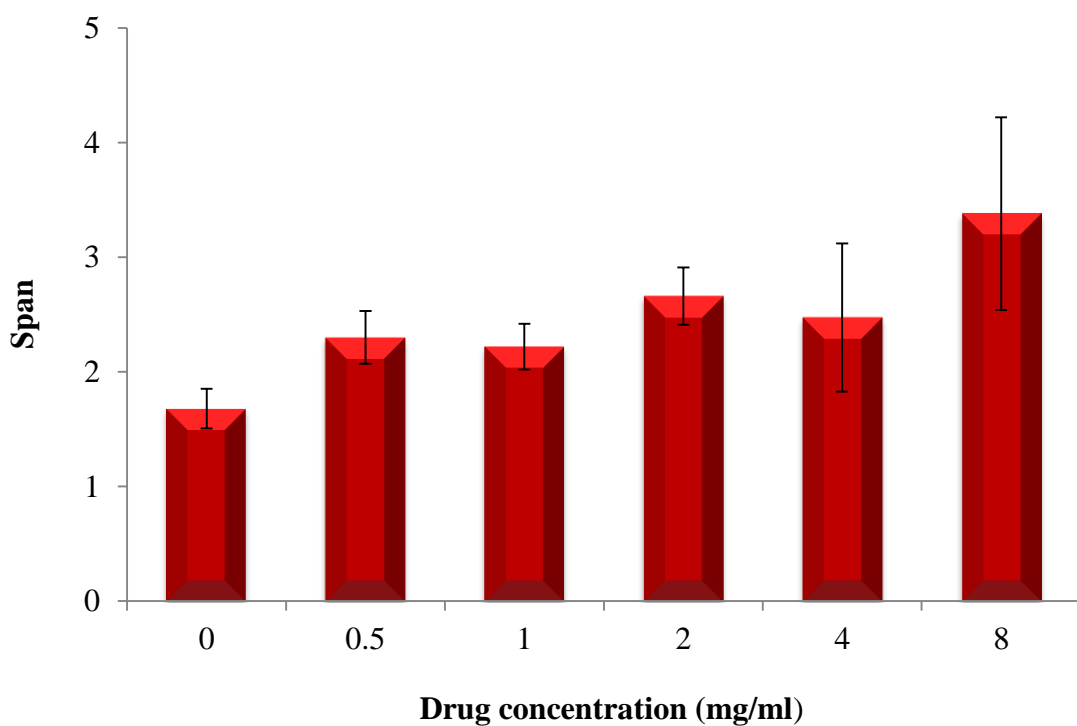


Figure 5. 2: Size distribution (Span) of liposomes generated from ethanol-based proliposomes using a range of RH concentrations (0 – 8 mg/ml).

5.3.1.2 Zeta potential measurement of liposomes

The zeta potential of the liposome formulations was measured after separation of the liposome pellets from un-entrapped drug using Beckman ultracentrifuge at 50,000 rpm (251,818 x g) for 20 minutes at 6°C and re-dispersed using 5ml HPLC water. Figure 5.3 shows the zeta potential measurements of the liposome formulations. The zeta potential of drug-free liposomes was -0.46 ± 0.08 mV, whilst after centrifugation and replacing the supernatant with a fresh dispersion medium it became -10.23 ± 0.70 mV. This indicates that a high centrifugation speed affected the packing and surface properties of liposome vesicles. As the concentration of the drug was increased, the negative surface charge of liposomes became less intense, and started to have a slightly positive charge at the drug concentration of 8 mg/ml (zeta potential = 1.09 ± 2.31 mV). This is an indication that the free drug in the supernatant has affected the surface charge of the vesicles. To the best knowledge of the author of this report, no studies in the literature have described the effect of water-soluble drugs on the zeta potential of liposomes, especially taking into account that the drug is not expected to be associated with the lipid bilayers. Interestingly, even when no drug was included within the liposome formulation, centrifugation to sediment liposomes followed by re-dispersion of the pelleted liposomes caused a significant change in the measured zeta potential of liposomes. Further investigations are required to understand the reason behind the different zeta potential of liposomes at different conditions.

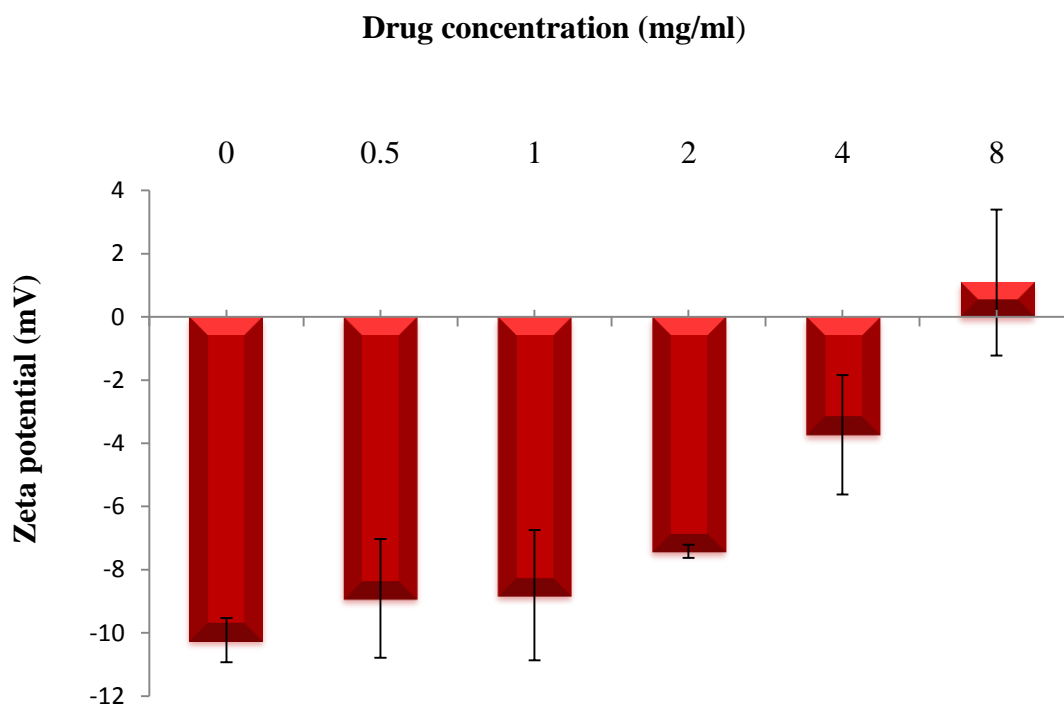


Figure 5. 3: Zeta potential of liposomes generated from ethanol-based proliposomes using a range of RH concentrations (0-8 mg/ml).

5.3.1.3 Entrapment efficiency of RH

The entrapment efficiency of RH loaded in liposomes was analyzed using HPLC following the separation of the liposome-entrapped fraction of the drug. Figure 5.4 shows the entrapment efficiency of RH versus drug concentration in the liposome formulations. These findings demonstrate that the percentage of drug entrapped in liposomes was dependent on the drug concentrations and entrapment efficiency was decreased with higher drug concentration (i.e after 2mg/ml). The maximum drug entrapment was $23.3\% \pm 0.26$ for 2 mg/ml drug concentration and minimum was $12.63\% \pm 2.46$ for 8 mg/ml drug concentration. The entrapment efficiency values were lower than those found by Elhissi et al. (2006) and Arafat (2013), who reported entrapment efficiency to be approximately 62% and 60% respectively, when they generated salbutamole sulphate loaded liposomes via the ethanol-based proliposome method. The differences of entrapment findings might be attributed to the differences in the physical properties of the drugs. However, for the large standard deviations to be reduced, the experiment needs to be repeated for more times in the future.

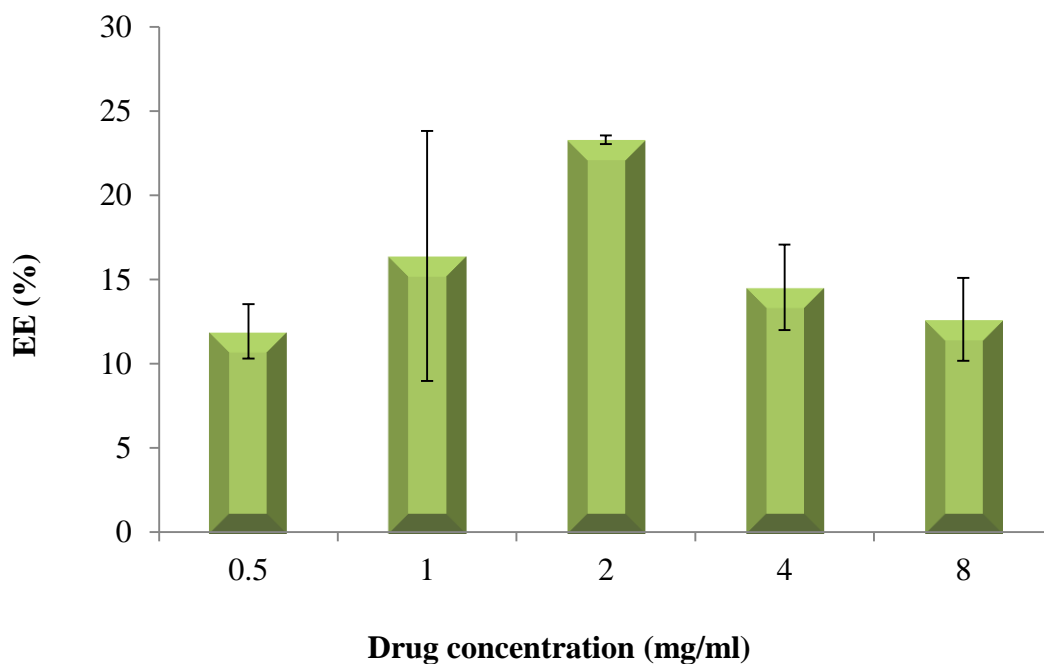


Figure 5. 4: Entrapment efficiency (%) of RH loaded into liposomes generated from ethanol-based proliposome formulations in relation to drug concentration. Data represent mean \pm SD (n=3).

5.3.2 Effect of inclusion of mucoadhesive agents in liposome formulations

Five types of water soluble mucoadhesive agents (0.2%) was included into the selected liposome formulation to promote the mucoadhesive properties of liposomes. Chitosan and sodium alginate are natural polysaccharides which can enhance the mucoadhesive properties of liposomes thus improve drug permeability through biological membranes (Chen et al., 2013).

The reason behind using natural polymers is attributed to the facts that they are non-toxic and can provide strong mucoadhesion owing to their ionizable groups which can form electrostatic or hydrogen bonds with mucin molecules. The use of bioadhesive agents in pharmaceutical formulations may increase the duration of drug contact with nasal mucosa (Carvalho et al., 2010) and hence enhance drug permeation by opening the tight junctions between cells (Chaturvedi et al., 2011; Smith et al., 2004), resulting in improved absorption of small polar drug molecules, proteins and peptides through nasal mucosa and enhanced drug bioavailability and efficacy (Illum et al., 1994).

Furthermore, inclusion of mucoadhesive agents could potentially reduce the tendency of liposomes to fuse together and hence formation of larger vesicles and subsequent phase separation are retarded (Wu et al., 2004; Laye et al., 2008; Mady and Darwish, 2010). Chitosan concentrations in the range of 0.1 to 0.5% have been studied by Wu et al., (2004). They demonstrated that chitosan concentration and molecular weight both had significant effects on the hypoglycaemic activity of liposome-entrapped insulin following oral delivery of the formulation. Insulin-based liposomes when coated with chitosan (0.2%), gave high drug entrapment efficiency ($75.90\% \pm 4.90$).

Controversial reports on the mucoadhesive efficiency of chitosan and sodium alginate exist. Chen et al., (2013) reported chitosan coated liposome vesicles may have significantly higher mucoadhesive properties than alginate coated liposomes due to interactions between positively charged ions of chitosan with the negatively charged ions of sialic acid.

In this study, the effect of different types of mucoadhesive polymers (0.2%) on liposome size, size distribution and zeta potential was investigated and the loading efficiency of RH studied.

5.3.2.1 Size and size distribution of liposomes

The effect of inclusion of 0.2% (w/v) mucoadhesive agent on the size and size distribution of liposomes with RH of 2mg/ml are demonstrated in Figure 5.5. Mucoadhesive agents increased the particle size by a small amount compared to non-coated liposome. However, the size of liposomes was unaffected by the type of mucoadhesive agent. Size distributions of the polymer-coated liposomes are shown in Figure 5.6. Findings indicate that regardless of the bioadhesive polymer type, inclusion of the bioadhesive had no effect on the Span values ($p > 0.05$) compared to the uncoated vesicles.

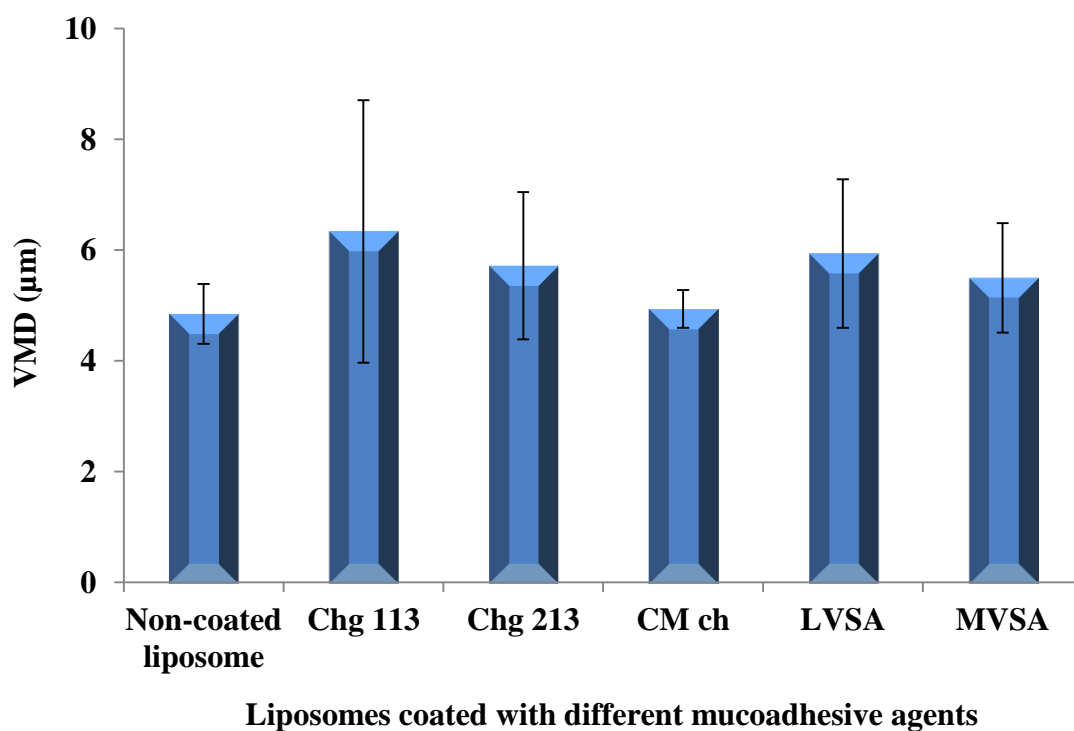


Figure 5. 5: Size of liposomes containing drug (2 mg/ml) in relation to the inclusion of different mucoadhesive agents in concentration of 0.2%. Data represent mean \pm SD (n=3).

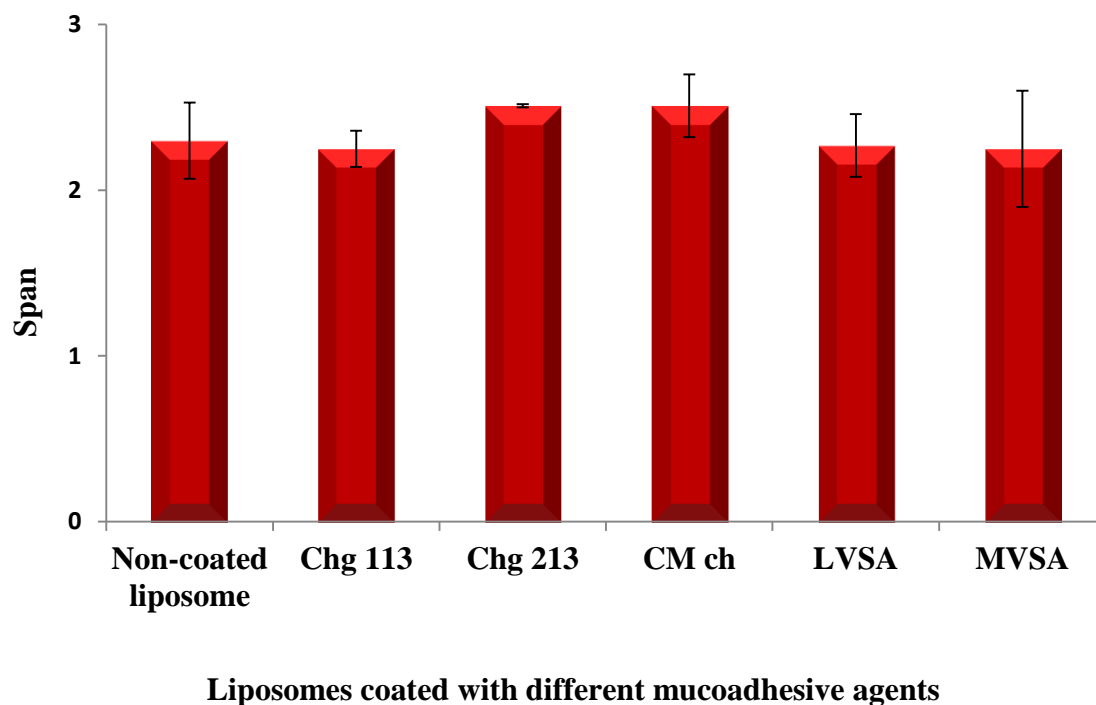


Figure 5. 6: Size distribution (Span) of liposomes containing drug (2 mg/ml) in relation to the inclusion of different mucoadhesive agents in concentration of 0.2%. Data represent mean \pm SD (n=3).

5.3.2.2 Zeta potential

Figure 5.7 shows the zeta potential of liposomes in relation to inclusion of mucoadhesive agents. The findings demonstrated remarkable changes ($p < 0.05$) in zeta potential of the liposomes from -7.42 ± 0.21 mV toward neutrality since chitosan G113 and G213 included into formulations caused the zeta potential to become -0.53 ± 1.82 mV and -0.18 ± 1.5 mV respectively (Figure 5.7) due to the positive charges caused by chitosan adsorption on the surface of the liposomes (Liu and Park, 2010; Mady and Darwish, 2010). The liposome and polymer interactions are due to the electrostatic forces between the oppositely charged ions of chitosan and lipid (Laye et al., 2008) and/or the formation of H-bonding between the polymer and phospholipid headgroups (Perugini et al., 2000). This favours the adsorption of chitosan onto the surface of liposomes and increasing the zeta potential. Zeta potentials of vesicles became more intensely negative ($p < 0.05$) upon addition of low viscosity sodium alginate (zeta potential = -13.41 ± 0.19 mV), medium viscosity sodium alginate (-13.56 ± 0.6 mV) and carboxymethyl chitosan (-11.58 ± 0.44 mV), indicating successful coating by these anionic polymers onto the liposomes. The zeta potential values in this experiment are an indication that the formulation are stable, as high values regardless of charge type enhance the repulsion forces between the similarly charged particles, thus reducing particle aggregation (Mady and Darwish, 2010).

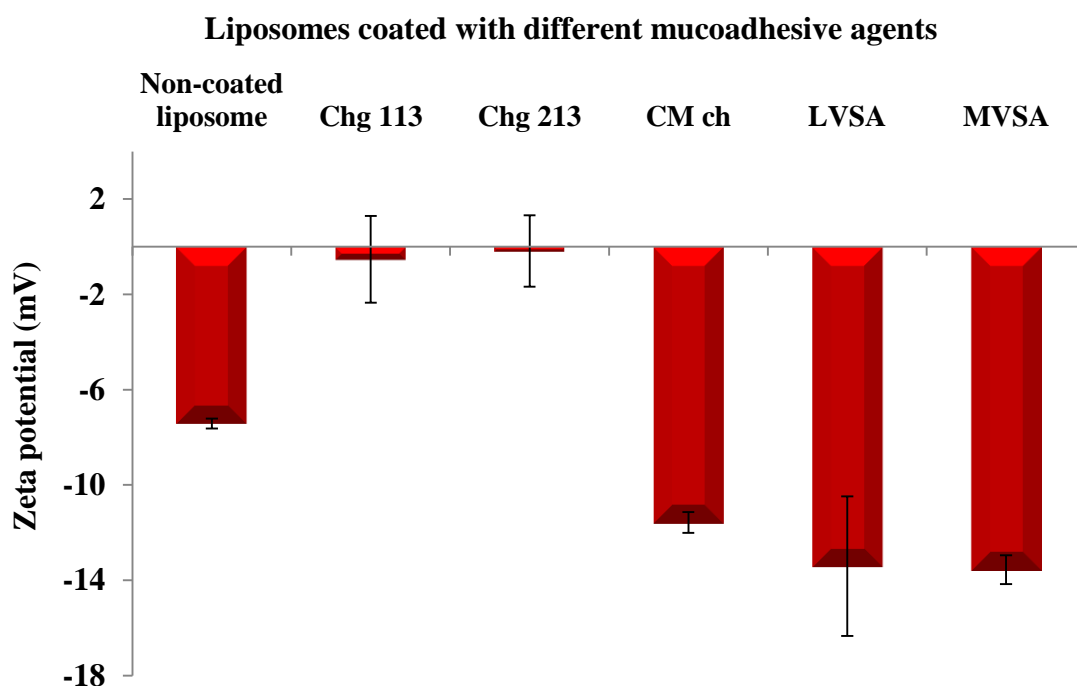


Figure 5. 7: Zeta potential of liposomes containing drug (2 mg/ml) in relation to the inclusion of different mucoadhesive agents in concentration of 0.2%. Data represent mean \pm SD (n=3).

5.3.2.3 Drug entrapment efficiency

There is some controversy amongst researchers in literature regarding entrapment efficiency in relation to inclusion of bioadhesive agents. Many research groups have reported that inclusion of chitosan significantly increases drug entrapment (Perugini et al., 2000; Albasarah et al., 2010). In contrast, other researchers reports have documented that coating the liposomes with chitosan decreased the drug entrapment efficiency (Wu et al., 2004; Zhuang et al., 2010). Liu and Park, (2010) have found that chitosan concentration had no effect on the entrapment efficiency of vitamin C. Whilst Goyal et al., (2011) have found that increasing alginate to liposome ratio caused an increase in drug entrapment efficiency. To resolve these controversies further investigations were conducted. Figure 5.8 showed that the effect of inclusion of mucoadhesive agents (0.2%) on RH entrapment efficiency. The entrapment efficiency of RH was $23.3\% \pm 0.27$, whilst after inclusion of mucoadhesive agents the entrapment efficiency decreased significantly ($p < 0.05$) using chitosan G113 (EE= $7.36\% \pm 4.48$) and medium viscosity sodium alginate (EE= $11.16\% \pm 4.69$) and chitosan G213 (EE= $10.35\% \pm 4.07$). In contrast the inclusion of carboxymethyl chitosan did not affect the drug entrapment efficiency (EE= $25.97\% \pm 3.86$) (Figure 5.8). However, low viscosity sodium alginate

decreased the entrapment efficiency but not significantly ($p>0.05$). Disagreements between findings might be attributed to the variations in the properties of different types of mucoadhesive agents employed. Guo et al., (2003) have reported a decrease in the drug entrapment whilst mucoadhesive agents included in the formulations might be attributed to the polymer and phospholipid interactions interfering with drug entrapment. Chitosan has a positive charge and affinity to phospholipid thus it may compete with the cationic drug RH for phospholipids which are negatively charge. Subsequently chitosan may reduce the entrapment efficiency of the drug, hence lower entrapment efficiency observed for chitosan compared sodium alginate and carboxymethyl chitosan.

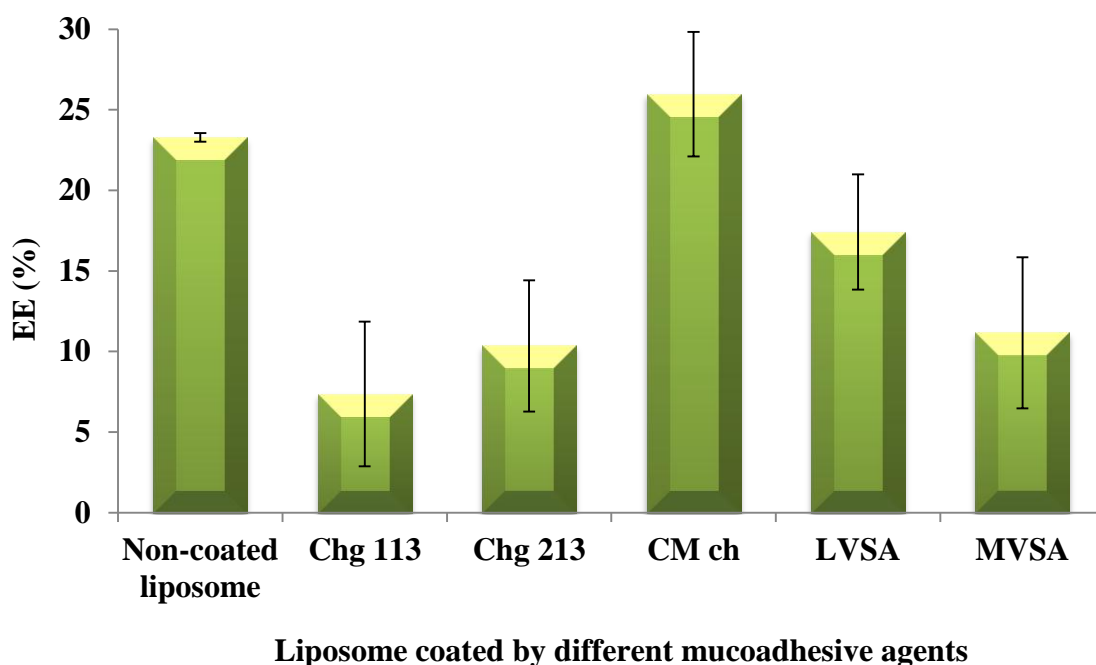


Figure 5. 8: Drug entrapment (%) by liposomes in relation to the inclusion of different mucoadhesive agents in a concentration of 0.2%. Data represent mean \pm SD (n=3).

5.3.3 Transmission electron microscopy study

Liposome morphology was studied using TEM (Figure 5.9). Regardless of drug or bioadhesive polymer inclusion, liposomes were OLVs. The strong adsorption of the polymer to the liposomal bilayers might have resulted in making no apparent difference between coated and uncoated liposomes. The same finding has been previously reported (Zhuang et al., 2010).

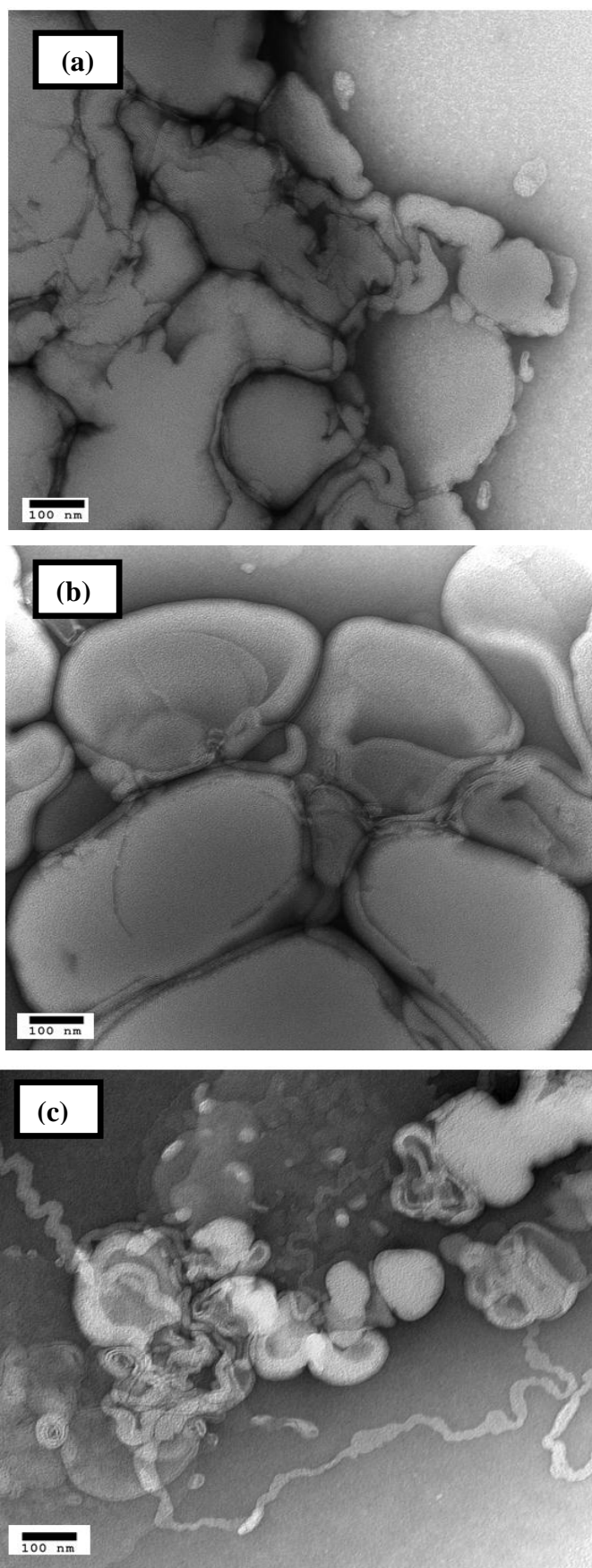


Figure 5. 9: TEM images of (a) drug free liposomes, (b) drug loaded liposome, and (c) carboxymethyl chitosan-coated drug free liposomes. Magnification: 93000x.

5.3.4 Influence of nasal spray device on the spray cloud characteristics

5.3.4.1 Determination of priming, tail off and shot weight

Several tests are recommended by FDA for development of new nasal products such as mean delivered dose (shot weight), dose content uniformity, droplet size and size distribution and characterization of the spray plume (spray pattern and plume geometry) (CDER, 2002). To determine nasal spray performance, study of prime, full actuation and tail-off phases were conducted. Priming is the number of actuations which are required to reach the full actuation. It is useful to determine the number of actuations in the nasal spray device which generates reproducible dose. Figure 5.10 shows the characteristics of the spray using nasal spray devices such as priming, full actuation and number of actuations required in the tailing off phase using liposome formulations or deionised water.

Considering prime and tail off are necessary to assess multiple nasal spray doses performance, the required actuations to prime were 3-6 actuations. However, no difference was observed for each device to reach the prime when water and liposome formulation were compared, and in a similar manner no discernable difference ($p>0.05$) was observed between the nasal spray devices A, B and C. In contrast, a significant difference was observed in the number of full actuations between device A and B ($p<0.05$) and device B and C (Figure 5.10). The number of full actuations of water and liposome formulation delivered by the nasal spray device A was 27.00 ± 0.52 and 26.00 ± 0.52 actuations respectively. For device B the numbers of actuations were respectively 21.00 ± 1.37 and 19.00 ± 1.03 , and for device C they were 25.00 ± 1.03 and 22.00 ± 1.33 respectively.

The data showed significant differences for the number of actuations in the tail off phase between device A and B ($p<0.05$) and device B and C ($p<0.05$) (Figure 5.10). The total number of actuations for devices A, B and C were 37.00 ± 0.52 and 37.00 ± 0.52 , 41.00 ± 1.79 and 39.00 ± 0.52 and 39.00 ± 0.52 and 39.00 ± 1.37 using water and liposomes respectively. A difference ($p<0.05$) was observed when the total number of actuations of water for devices A and C was compared to those of device B. Nasal spray device A had larger number of full actuations among other devices, as it had lower number of total number of actuations. These differences between devices may be due design characteristics of the device, pump performance, orifice design and metering

chamber of the devices (Dayal et al., 2004). In contrast nasal spray B had lower number of full actuations, as it had larger number of actuations.

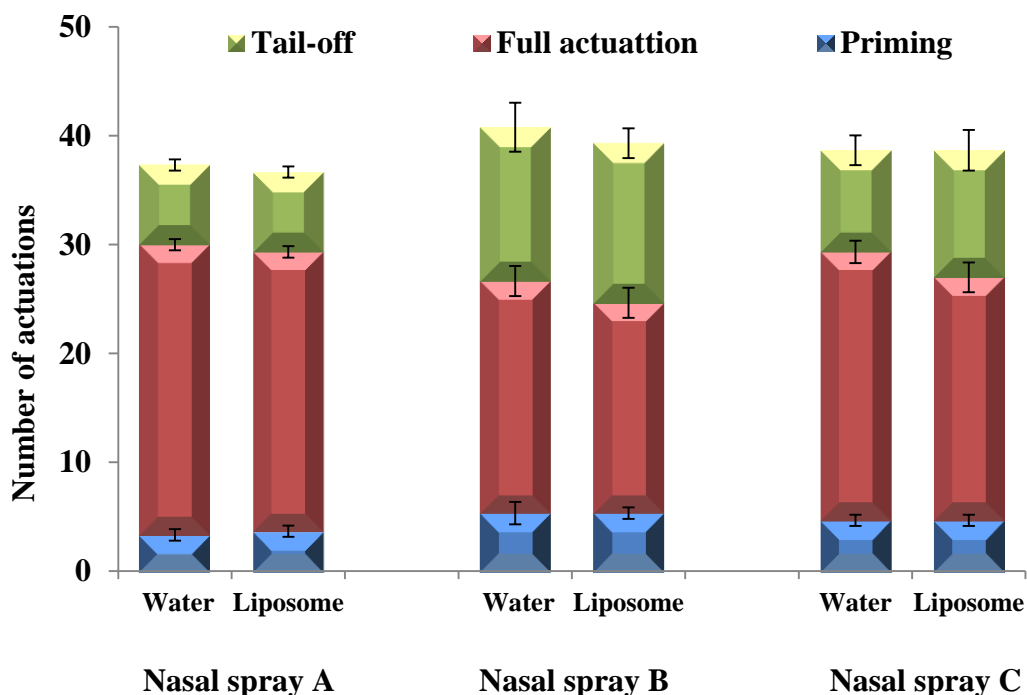


Figure 5. 10: Number of actuations required for priming the devices, full actuations delivered and the number of actuations in the tail off phase. Data represent mean \pm SD (n=3).

Investigation of dose consistency was conducted by studying the weight measurement of the spray devices before and after actuation. Data indicate all three nasal spray devices delivered approximately 100 μ l per actuation at the fully actuation phase and no remarkable difference ($p > 0.05$) in the mean delivered volume between the devices (Figure 5.11). Suman et al. (1999) have reported nasal spray pump design played a major role to deliver an accurate dose upon actuation. Overall, the findings of this study demonstrated the differences in performance of different devices owing to the difference in designed pump rather than formulation properties.

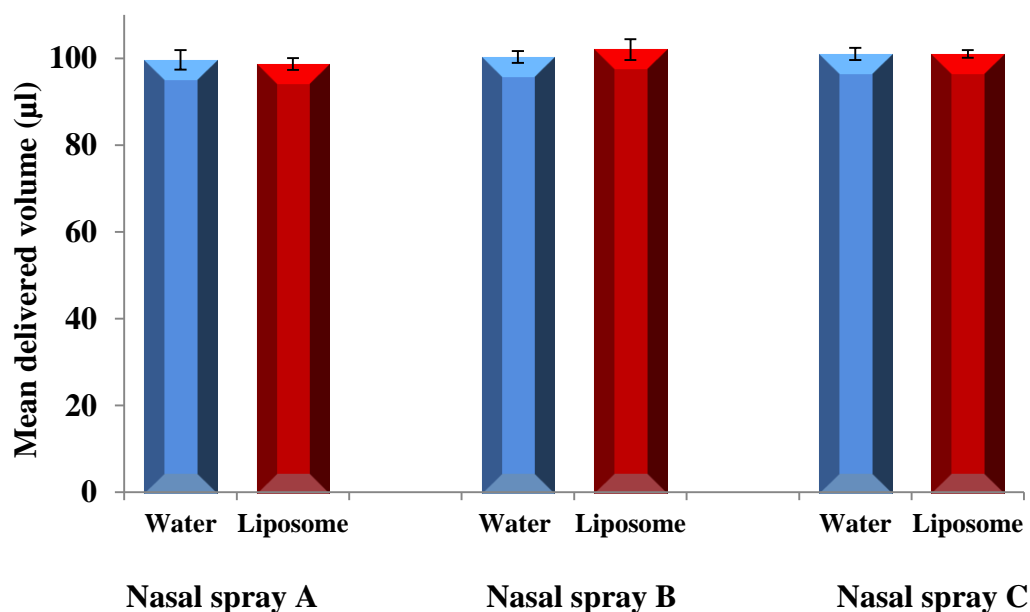


Figure 5. 11: Mean delivered volume (µl) by nasal spray devices at fully actuation state. Data were mean \pm SD (n=3).

Table 5.1 shows the effect of spraying on particle size, size distribution and surface charge of carboxymethyl chitosan coated RH liposomes using three different nasal spray devices was studied. No changes ($p>0.05$) were observed when liposomes before and after spraying were compared. Hence, these devices did not significantly affect the characteristics of the selected liposome formulation. Drug leakage from liposomes was absent ($p>0.05$) when drug entrapment after spraying was compared to before spraying (Figure 5.12). All nasal spray devices investigated in this study could potentially be used to deliver RH loaded liposomes to the nose, because the integrity of liposome formulations upon spraying was preserved. Unlike nasal sprays, previous investigations have shown nebulizers damage liposome structures, causing significant leakage of the originally entrapped drug (Taylor, 1990; Arafat, 2013).

Table 5. 1: Particle size (VMD), size distribution (Span) and zeta potential of carboxymethyl chitosan coated RH liposomes compared to non-sprayed liposomes using nasal spray devices A, B and C.

Conditions	VMD (μm)	Span	Zeta potential (mV)
Non-sprayed liposome	4.22 \pm 0.25	2.93 \pm 0.21	-11.28 \pm 3.26
Nasal spray A	4.01 \pm 0.23	2.79 \pm 0.14	-11.97 \pm 0.97
Nasal spray B	4.04 \pm 0.23	3.09 \pm 0.26	-12.02 \pm 1.5
Nasal spray C	3.94 \pm 0.33	3.11 \pm 0.22	-11.45 \pm 2.54

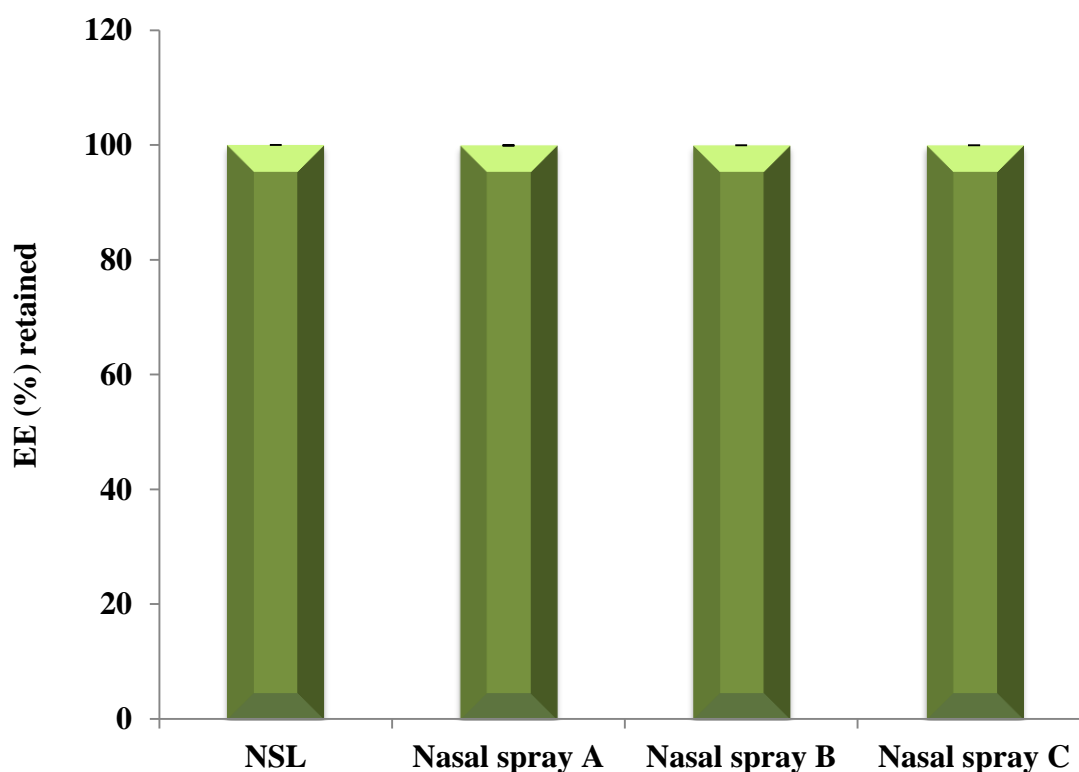


Figure 5. 12: Effect of spraying on the retained EE (%) of RH loaded liposomes coated by carboxymethyl chitosan compared to non-sprayed liposome (NSL) using nasal spray devices A, B and C. Data were mean \pm SD (n=3).

5.3.4.2 Droplet size distribution

Droplet size distribution (DSD) and fraction of droplets $<10\ \mu\text{m}$ are prime determinant of the location where the droplet is likely to deposit in the nasal cavity from nasal sprays, which might affect the bioavailability of the drug (Kippax et al., 2010). The droplet size, size distribution and the percentage of droplets less than $10\ \mu\text{m}$ were measured by using the Malvern Spraytec, at the fully developed phase using device A, B and C. FDA recommended the fully developed phase (stable phase) for spray cloud characterization, because at this phase consistent particle size is produced since the flow rate through the device nozzle is optimal, therefore the analysis is useful in comparing devices and formulations (CDER, 2003).

Control over the size of the sprayed droplets size is crucial to ensure that deposition in the nose rather than the pulmonary region because droplet size affects the deposition profile and retention time of sprayed particles (Kippax, 2009). Particles larger than $3\text{-}10\ \mu\text{m}$ are filtered out by the nose, minimizing the probability of lung deposition (Dahl and Mygind, 1998). Larger droplets may however drip out of the nose after administration whilst too small droplets may deposit in the lower respiratory regions (Kulkarni and Shaw, 2012).

Table 5.2 demonstrated that droplet size dramatically decreased ($p<0.05$) for chitosan coated liposomes compared to water using device A or device B, while no major changes were found for device C. This effect might be attributed to the thixotropic behaviour of liposomes. However, droplet size generated from nasal device A were smaller than from nasal devices B and C. Dayal et al., (2004) have demonstrated that the spray characteristics depend on the pump design and physicochemical properties of the drug formulation such as viscosity, density, thixotropic behaviour, elasticity and surface tension of the liquid. This finding agrees with Dayal et al., (2004), who reported that addition of surfactant (0.5 - 5% Tween 80) to the 2% carboxymethyl cellulose and shear thinning of carbopol formulation may reduce the droplet size, due to the alteration the rheological behaviour of formulation. Reducing the droplet size might be beneficial since smaller droplet size may provide better surface coverage of nasal cavity than large particles (Kundoor and Dalby, 2011, 2010).

In contrast to the droplet size, Span and percentage of droplets below $10\ \mu\text{m}$ for the sprayed liposome formulation using different devices were similar to that of water

($p > 0.05$). However, proportion of droplets $< 10 \mu\text{m}$ (%) generated by device C were smaller than those generated by other two devices, however droplets are unlikely to deposit in the respiratory region as the percentage of fraction droplets $< 10 \mu\text{m}$ was less than 5%. Overall, the droplet size in this study was within the optimal size range (10 to $50 \mu\text{m}$) for nasal delivery (Behl et al., 1998). Hence, liposomes coated with chitosan merits *in-vivo* investigations to evaluate their use as delivery carriers using these devices.

Table 5. 2: Droplet size, size distribution and percentage of droplets below $10 \mu\text{m}$ for RH loaded into liposome formulation coated by carboxymethyl chitosan.

Nasal spray devices	Water			Liposome formulation		
	VMD(μm)	Span	Droplets $< 10 \mu\text{m}$	VMD(μm)	Span	Droplets $< 10 \mu\text{m}$
A	41.13 \pm 1.02	1.35 \pm 0.09	7.04 \pm 1.19	30.69 \pm 1.3	1.45 \pm 0.12	9.11 \pm 1.81
B	55.87 \pm 4.35	1.78 \pm 0.1	6.79 \pm 0.85	44.7 \pm 1.94	2.86 \pm 1.02	8.16 \pm 0.43
C	49.5 \pm 3.32	1.68 \pm 0.25	4.03 \pm 0.46	47.85 \pm 3.29	2.4 \pm 0.85	3.94 \pm 2.3

5.3.4.3 Spray pattern and plume geometry studies

In addition to droplet size, both spray pattern and plume geometry of the spray may contribute to the determination of the possible site of spray deposition in the nose (Foo, 2007). Generally, deposition in the anterior region might be more dominant when the plume angle is high, whereas droplets tend to deposit in the turbinate region when the plume angle is lower (Foo et al., 2007).

As demonstrated in Table 5.3, formulation properties profoundly effected the plume generated. When water was sprayed, the plume angle differed using different devices ($p < 0.05$). The large difference was observed for plume width of the nasal device A ($p < 0.05$) as compared to the other two devices. When liposome dispersion and water sprayed using nasal devices A and C, it was observed that plume angle and the width of cloud generated from liposome dispersion were statistically ($p < 0.05$) larger than

compared water. Deposition of droplets in the anterior region of the nose increases when nasal device generated cloud with wide plume angle (Cheng et al., 2001).

The required time per actuation was also investigated for the nasal spray devices (Figure 5.13 - 5.15). The full spray time per actuation for water using devices A, B and C was 0.28 ± 0.00 , 0.20 ± 0.00 and 0.28 ± 0.00 sec respectively. Device B offered fast delivery of the dose (0.20 sec) compared to devices A and C. However, duration of formation phase (0.12 sec), evolution phase (0.12 sec) and dissipation phase (0.04 sec) of nasal spray pumps A and C were similar (Figure 5.13 and Figure 5.14). In contrary, nasal device B was characterized by short evolution phase (0.04 sec) and long dissipation phase (0.08 sec). The differences might be ascribed to the differences in the design of the nasal devices (Suman et al., 1999).

Additionally, the height of the spray cloud was measured before the cloud dissipated from the nasal device tip and was significantly lower ($p < 0.05$) for the liposome formulation compared to water for all three devices due to variation in the formulation properties. This means that both device design and formulation properties affected the cloud characterization.

Table 5. 3: Plume angle, width and height for sprays generated from nasal devices A, B and C.

Nasal spray devices	Deionised water			Liposomes		
	Plume angle	Plume width at 3 cm (mm)	Height (cm)	Plume angle	Plume width at 3 cm (mm)	Height (cm)
A	59.00±3.22	35.00±2.37	23.33±1.03	64.00 ±0.89	39.33±1.37	20.00±1.79
B	49.00±0.89	31.33±0.52	27.33±1.03	49.33±1.03	30.33±1.03	24.33±0.52
C	48.67±1.37	30.67±1.86	36.67±1.03	56.67±2.73	39.00±0.89	30.00±1.79

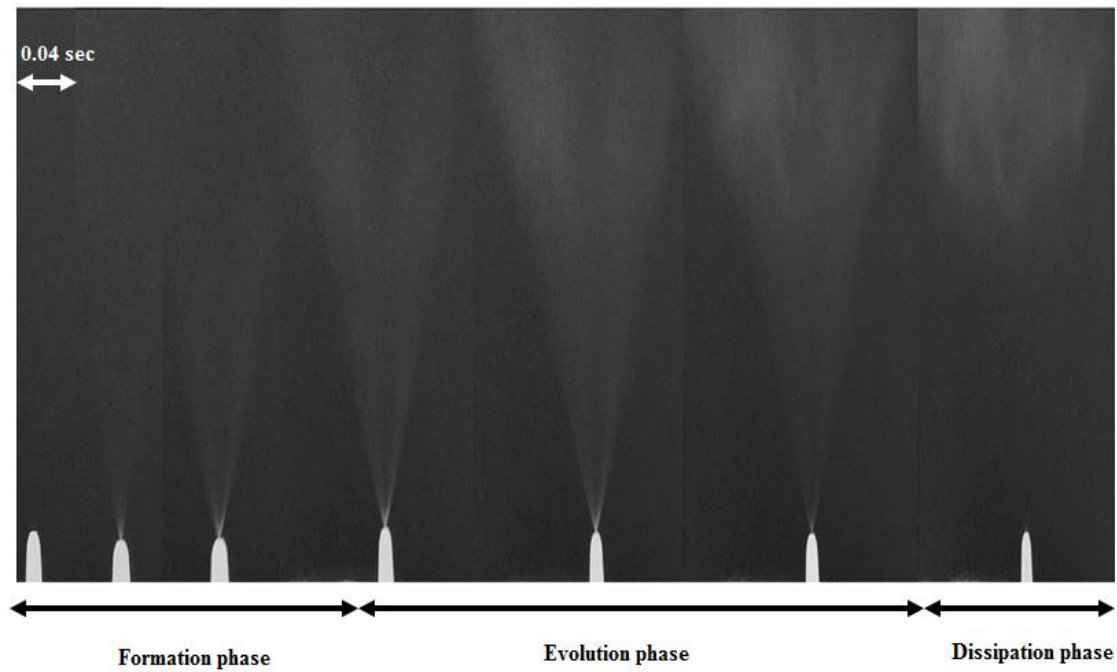


Figure 5.13: Generation of plume from nasal spray device A showing the different phases of spray cloud development as monitored by videography.

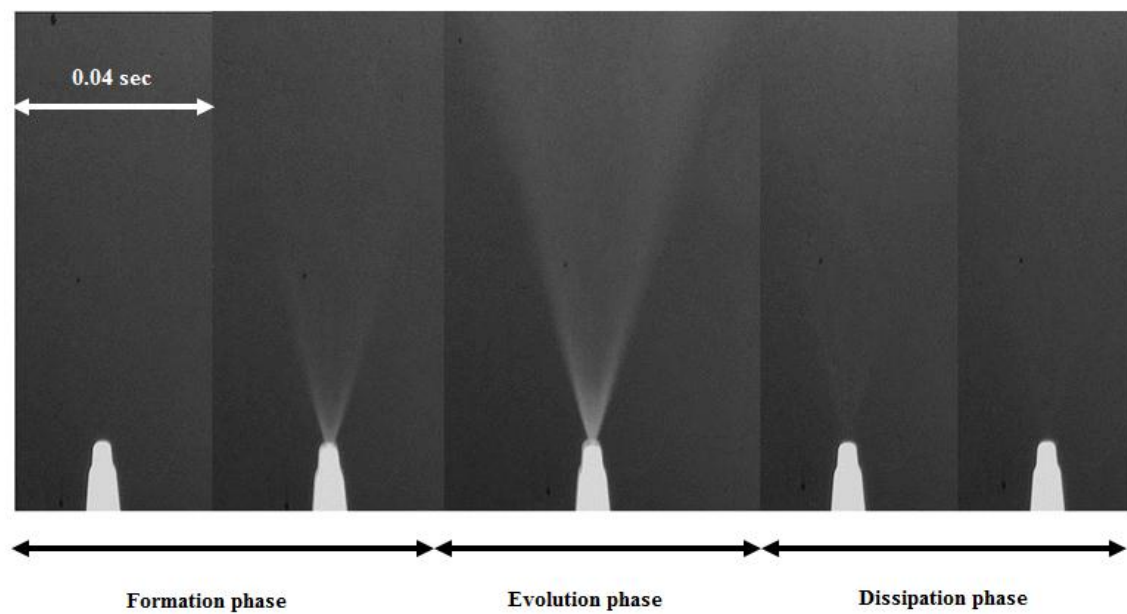


Figure 5.14: Generation of plume from nasal spray device B showing the different phases of spray cloud development as monitored by videography.

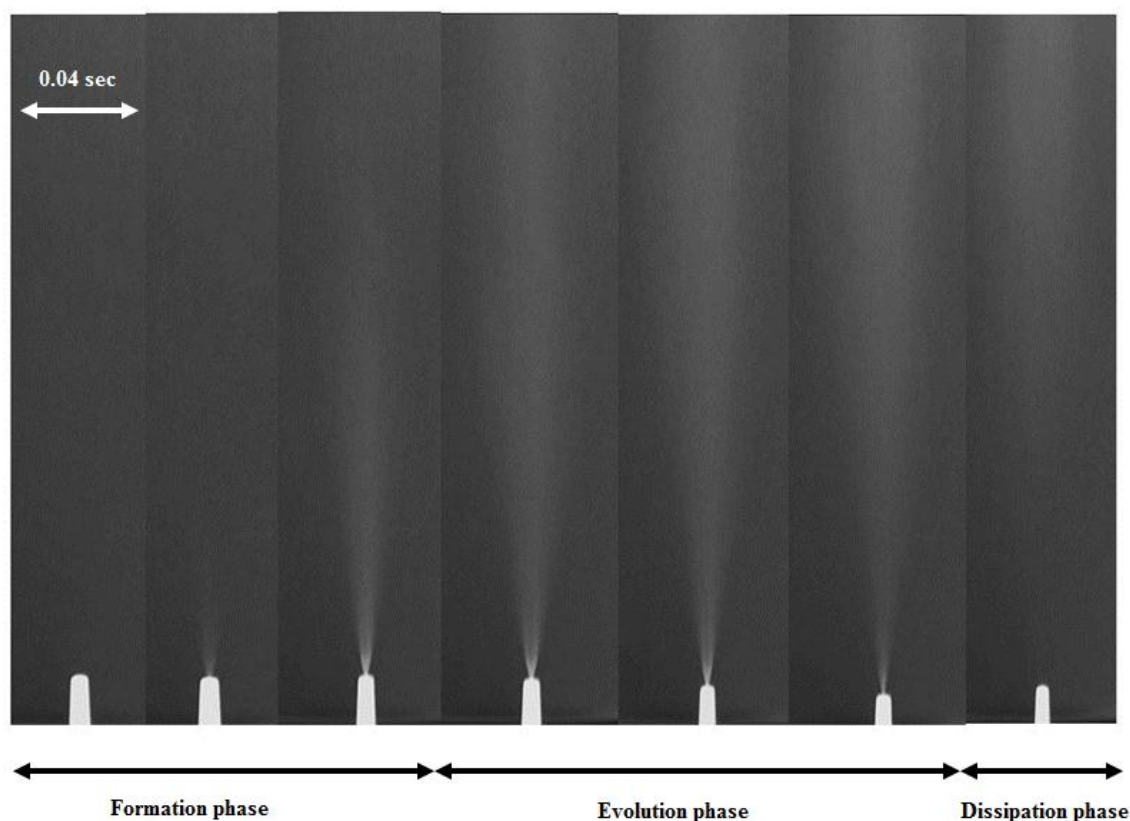


Figure 5. 15: Generation of plume from nasal spray device C showing the different phases of spray cloud development as monitored by videography.

A traditional technique was used to characterize the spray pattern of liposomes using impaction method. This was performed by spraying the liposome formulation to impact on a thin layer chromatography (TLC) surface positioned at 3cm distance from the orifice of the nasal spray device. The ovality ratios of the spray produced from different devices are shown in Table 5.4. Different shape of spray pattern might be attributed to the differences in the shape of the nozzle orifice of different devices (Figure 5.16). This finding is in agreement with the finding of a number of research articles (Dayal et al., 2004; Guo and Doub, 2006; Kundoor and Dalby, 2011). The ovality ratio of the spray was in the following order: device C > device A > device B (Figure 5.16). This study also found that the shape of the nozzle orifice has great effects on the shape of the spray pattern. Dayal et al. (2004) have reported that pump design is the determinant of the spray shape.

Large D_{\max} and D_{\min} of spray patterns were obtained ($p < 0.05$) from sprayed liposome dispersion when using all nasal devices. This might be attributed to the increase of plume cone and width of the sprayed aerosol compared to deionised water. The larger

the plume angle the larger the spray pattern, whereas smaller plume angles produced smaller spray pattern. The hollow-cone of the spray pattern generated from nasal devices may indicate the enhanced probability of spray deposition in the anterior and middle regions of the nasal cavity than the full-cone (non-hollow) spray and may reduce particle deposition in the respiratory tract (Inthavong et al., 2011).

In addition to the droplet size distribution (DSD), plume angle and spray pattern, administration angle between nasal spray unit and the head of patient also may play a role at the determination of the site of droplet deposition in the nose (Foo et al., 2007). When the angle of the plume is greater than 60° the deposition is more dominant in the nasal valve, whereas droplets could pass the nasal valve region when the plume angle is less than 45° (Kundoor and Dalby, 2011).

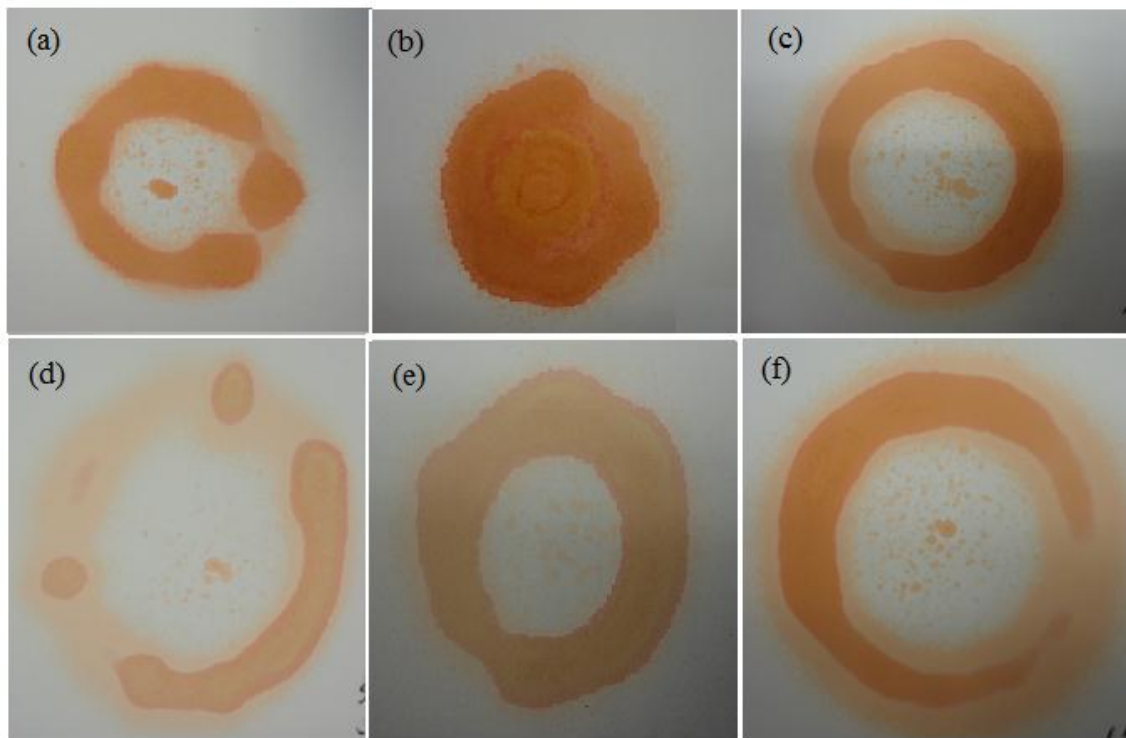


Figure 5. 16: Spray pattern images for water and liposome dispersion using nasal device A (a and d respectively), nasal device B (b and e respectively) and nasal device C (c and f respectively) using Conon EOS 550D digital camera.

Table 5. 4: Spray patterns (D_{\max} , D_{\min} and ovality ratio) generated from nasal spray devices A, B and C.

Nasal spray device	Water			Liposomes		
	D_{\max} (mm)	D_{\min} (mm)	Ovality ratio	D_{\max} (mm)	D_{\min} (mm)	Ovality ratio
A	40.67±1.86	35.67±1.86	1.14±0.01	46.67±2.58	41.67±1.37	1.12±0.04
B	33.00±1.79	27.67±1.03	1.19±0.08	38.33±3.14	33.33±2.58	1.15±0.05
C	41.33±1.37	40.00±0.89	1.03±0.01	48.67±1.03	47.33±1.37	1.03±0.01

5.4 Conclusions

This study explored the suitability of nasal spray device for delivery of liposome formulations. TEM images showed that ethanol based proliposomes have generated OLVs which could entrap maximum amount of the drug when 2mg/ml drug concentration was used. Inclusions of mucoadhesive agents into liposome formulations had major effects on the liposome properties. All bioadhesive agents used except carboxymethyl chitosan have decreased the drug entrapment efficiency. Changes in the surface zeta potential indicated liposome vesicles were coated with the bioadhesive polymers. Investigation of device performance demonstrated nasal pump design with formulation properties both affected the cloud height, plume angles and spray patterns. Integrity of RH loaded liposomes was not changed following spraying via a range of nasal devices, indicating all the devices investigated could be used for nasal delivery of RH loaded liposomes. Aerosol droplet size generated from all three devices was within the range for deposition in the nose. Overall, the analysis of the spray cloud generated by nasal spray device B was characterized by smaller plume angle, which may provide greater impaction in the vasculature area of the nasal cavity. Further studies are required to determine the site of droplet deposition in the nose and drug bioavailability following delivery of the liposome formulations *in vivo* using the same nasal spray devices used in this study.

CHAPTER 6

GENERAL CONCLUSIONS AND FUTURE WORK

6.1 Nasal insufflator system using bioadhesive polymers

Ropinirole hydrochloride loaded microparticles and liposomes were developed via spray drying technique and ethanol-based proliposome method respectively. Various *In vitro* characterizations were conducted to select the optimum formulations for subsequent studies. Investigations were also conducted for the spray cloud generated from either powder or dispersed liposomes using Miat[®] nasal insufflator or a range of nasal spray devices respectively.

This study showed that no chemical interaction between the drug and polymers (e.g. chitosan or sodium alginate) when they were co-spray dried as revealed by FTIR and TLC. Hence, the drug and excipients were compatible. The study showed spray drying is a satisfactory method to produce best performing microparticle formulations which entrapped large amount of RH in the range of 93–99%. Particle size analysis revealed that particle size increased as chitosan to drug ratio was decreased (VMD= 1.98 - 3.66 μm) however, the size distribution (i.e. Span value) decreased from 4.11 to 1.10. SEM studies revealed that spray dried microparticles were spherical regardless of polymer to drug ratio used, which improved powder flowability compared to drug-free microparticle formulation. X-ray diffraction and DSC studies revealed that the crystallinity of the RH after encapsulation into the microparticles was reduced. When the polymer to drug ratio was 90:10 (w/w), the drug was completely converted into its amorphous form. Formulations with high polymer to drug ratio (90:10) exhibited a maximum swelling capacity and prolonged drug release.

The best performing RH loaded microparticle formulation was produced when 90:10 (w/w), polymer to drug ratio was co-spray dried. *Ex vivo* histopathological study using sheep nasal mucosa proved that the RH loaded chitosan mucoadhesive microspheres for intranasal administration are safe.

Optimized spray drying conditions were developed to prepare sodium alginate microparticles loaded with RH. The inlet temperature was found to be a crucial parameter affecting the particle morphology. Inlet air temperature of 140°C produced spherical microparticles with high yield percent (approaching 70%). Similar findings were observed for RH loaded sodium alginate and RH loaded chitosan microparticles. Co-spray dried sodium alginate and drug were compatible and polymer to drug ratio had marked effect on the particle size (VMD= 2.60 - 4.37 μm), morphology and surface smoothness of the particles as shown by SEM. DSC thermograms revealed that the drug

was well dispersed in the microparticles when the polymer to drug weight ratio was 90:10. X-ray diffractogram demonstrated crystallinity of the encapsulated drug by sodium alginate reduced and completely converted into its amorphous form in the concentration of 90:10, polymer to drug ratio. *In vitro* drug release profile demonstrated concentration of sodium alginate in the formulation had crucial effect on the rate of drug release. In a similar manner, the best RH loaded sodium alginate microparticle formulation was achieved when the polymer to drug ratio was 90:10. The optimum formulation was safe to use for subsequent studies.

Following the manufacture of optimum formulations of RH loaded chitosan and sodium alginate microparticles, the potential delivery of the microparticle formulations via Miat[®] nasal insufflator and its performance were studied. Additionally, the properties of the cloud generated from sprayed RH loaded chitosan and sodium alginate microparticles were investigated using the Miat[®] powder insufflator device.

Studies revealed that Miat[®] nasal insufflator could deliver 90% of the dose (RH loaded chitosan) with the first puff regardless of loading weight and generated elongated homogenous cloud. In contrast, loading dose effected the dose delivered for the RH loaded sodium alginate formulation owing to agglomeration of the microparticles and caused the observation of trajectories of particle in the generated cloud using videography. These indicated that the spray cloud was not homogeneous. Laser diffraction study of the cloud demonstrated that aerosolized particle size was 76.02 μm for RH loaded chitosan and 87.25 μm for RH loaded alginate microparticles which is suitable for intranasal administration. Overall, the results of these studies suggested that deposition of intranasal delivery of RH loaded chitosan and sodium alginate are likely to be more prominent in the turbinate region and particles are less likely to deposit in the lower respiratory tract.

6.2 Nasal spray devices using proliposome technology

Ethanol-based proliposome technology produced OLVs liposomes as revealed by TEM. The maximum loading efficiency of RH was 23.3% when the drug concentration used was 2mg/ml. Studies using five different bioadhesive agents attempting to enhance local residence time of the drug at site of application were performed. Addition of any of these bioadhesive agents (0.2% w/v) caused a decrease in the drug entrapment except

for carboxymethyl chitosan which showed a slight increase in the drug entrapment from 23.3 to 25.97%. Liposome surface zeta potential was influenced by the inclusion of mucoadhesive agents. These changes indicated that the polymer has coated the liposome vesicles.

Studies to determine the potential delivery of RH-loaded liposomes and the effect of nasal spray devices on the liposome integrity were conducted. Nasal devices were shown to have no effect on liposome integrity (e.g. particle size, span, and drug loading efficiency), thus all devices investigated can be used to deliver RH-loaded liposomes coated with carboxymethyl chitosan. All nasal devices generated 100 μ l of the dispersed liposome formulations, indicating formulation composition had no effect on nasal device performance. Study of aerosol properties generated from liposome dispersion using a range of nasal sprays was investigated by laser diffraction which demonstrated that aerosol particles are unlikely to travel to the lower respiratory region.

6.3 Final conclusion of the thesis

Overall, this study demonstrated that generation of RH loaded mucoadhesive microparticles via spray drying and RH loaded liposomes via ethanol based proliposomes may offer promising delivery systems via the nose for potential management of Parkinson disease and Restless legs syndrome.

6.4 Future work

Whilst this study has revealed a number of interesting findings, inevitably as with any research project of this type involving drug delivery many questions still need to be answered and offer avenues for future research:

- Stability study of RH loaded microparticle formulations under different conditions is required in order to determine the physical state of the encapsulated drug since amorphous products are less stable and have tendency to revert to crystalline form.
- Investigations of plume geometry and spray patterns generated using non-impaction method by laser diffraction are required, since laser methods are much more precise than the traditional methods employed for characterization of the ejected spray cloud.

- Drug delivery to a nasal cast model would be helpful to determine the site of dose deposition in the nasal cavity. Hence, an investigation of the impaction site of emitted dose in the nose while using either nasal insufflator or nasal sprays might constitute an important field in the future investigations.
- *In vivo* studies are required in order to determine the amount of bioavailable drug particularly the proportion of the drug that may go directly to CNS and CSF after nasal delivery using an appropriate animal model.

CHAPTER 7

REFERENCES

- Abdel Mouez, M., Zaki, N.M., Mansour, S., Geneidi, A.S., 2014. Bioavailability enhancement of verapamil HCl via intranasal chitosan microspheres. *Eur J Pharm Sci* 51, 59–66.
- Abdel-Bar, H.M., Abdel-Reheem, A.Y., Awad, G.A.S., Mortada, N.D., 2013. Evaluation of brain targeting and mucosal integrity of nasally administrated nanostructured carriers of a CNS active drug, clonazepam. *J Pharm Pharm Sci* 16, 456–469.
- Agarwal, V., Mishra, B., 1999. Design, development, and biopharmaceutical properties of buccoadhesive compacts of pentazocine. *Drug Dev Ind Pharm* 25, 701–709.
- Agertoft, L., Wolthers, O.D., Fuglsang, G., Pedersen, S., 1993. Nasal powder administration of budesonide for seasonal rhinitis in children and adolescents. *Pediatr Allergy Immunol* 4, 152–156.
- Agu, R., Dang, H.V., Jorissen, M., Willems, T., Vandoninck, S., Van Lint, J., Vandenheede, J.V., Kinget, R., Verbeke, N., 2003. In vitro polarized transport of L-phenylalanine in human nasal epithelium and partial characterization of the amino acid transporters involved. *Pharm. Res.* 20, 1125–1132.
- Ahlskog, J.E., Muentner, M.D., 2001. Frequency of levodopa-related dyskinesias and motor fluctuations as estimated from the cumulative literature. *Movement Disorders* 16, 448–458.
- Ahn, B.-N., Kim, S.-K., Shim, C.-K., 1995. Proliposomes as an intranasal dosage form for the sustained delivery of propranolol. *J. Controlled Release* 34, 203–210.
- Alam, M.I., Baboota, S., Ahuja, A., Ali, M., Ali, J., Sahni, J.K., 2013. Intranasal infusion of nanostructured lipid carriers (NLC) containing CNS acting drug and estimation in brain and blood. *J. Controlled Release* 20, 247–251.
- Albasarah, Y.Y., Somavarapu, S., Stapleton, P., Taylor, K.M.G., 2010. Chitosan-coated antifungal formulations for nebulisation. *J. Pharm. Pharmacol.* 62, 821–828.
- Alhalaweh, A., Andersson, S., Velaga, S.P., 2009. Preparation of zolmitriptan-chitosan microparticles by spray drying for nasal delivery. *Eur J Pharm Sci* 38, 206–214.
- Allamneni, Y., Reddy, B.V.V.K., Chary, P.D., Rao N, V., Kumar, S., Kalekar, A., 2012. Performance evaluation of mucoadhesive potential of sodium alginate on microspheres containing an anti-diabetic drug: Glipizide. *International Journal of Pharmaceutical Sciences and Drug Research* 4, 115–122.
- Allen, R., Vallow, S., Abetz, L., Washburn, T., Earley, C., 2002. The impact of Restless Legs Syndrome (RLS) on patient Quality of Life: Results from a survey of RLS sufferers. *Sleep* 25, A253–A254.
- Allen, R.P., Earley, C.J., 1996. Augmentation of the restless legs syndrome with carbidopa/levodopa. *Sleep* 19, 205–213.
- Alpar, H.O., Bowen, J.C., Brown, M.R.W., 1992. Effectiveness of liposomes as adjuvants of orally and nasally administered tetanus toxoid. *Int. J. Pharm.* 88, 335–344.

- Alsarra, I.A., Hamed, A.Y., Alanazi, F.K., 2008. Acyclovir liposomes for intranasal systemic delivery: development and pharmacokinetics evaluation. *Drug Deliv* 15, 313–321.
- Alves, G., Forsaa, E.B., Pedersen, K.F., Dreetz Gjerstad, M., Larsen, J.P., 2008. Epidemiology of Parkinson's disease. *J. Neurol.* 255 Suppl 5, 18–32.
- Amaro, M.I., Tajber, L., Corrigan, O.I., Healy, A.M., 2011. Optimisation of spray drying process conditions for sugar nanoporous microparticles (NPMPs) intended for inhalation. *Int J Pharm* 421, 99–109.
- Amin, M.L., Jesmeen, T., Sutradhar, K.B., Mannan, M.A., 2013. Development and in vitro evaluation of diclofenac sodium loaded mucoadhesive microsphere with natural gum for sustained delivery. *Curr Drug Deliv* 10, 765–770.
- Arafat, B., 2013. Proliposome Technology for Protein Delivery. University of Central Lancashire, Preston, UK.
- Armugam, K., Subramanian, G.S., Surulivelrajan, M., Averineni, R.K., Reddy, M.S., Udupa, N., 2008. A study of rivastigmine liposomes for delivery into the brain through intranasal route. *Acta Pharm* 58, 287–297.
- Arora, P., Sharma, S., Garg, S., 2002. Permeability issues in nasal drug delivery. *Drug Discov. Today* 7, 967–975.
- Aurora, J., 2008. Development of Nasal Delivery Systems: A Review 2.
- Avachat, A.M., Bornare, P.N., Dash, R.R., 2011. Sustained release microspheres of ropinirole hydrochloride: effect of process parameters. *Acta Pharm* 61, 363–376.
- Balasubramaniam, J., Rao, V.U., Vasudha, M., Babu, J., Rajinikanth, P.S., 2007. Sodium alginate microspheres of metformin HCl: formulation and in vitro evaluation. *Curr Drug Deliv* 4, 249–256.
- Bangham, A.D., Standish, M.M., Watkins, J.C., 1965. Diffusion of univalent ions across the lamellae of swollen phospholipids. *Journal of Molecular Biology* 13, 238–IN27.
- Behl, C.R., Pimplaskar, H.K., Sileno, A.P., deMeireles, J., Romeo, V.D., 1998. Effects of physicochemical properties and other factors on systemic nasal drug delivery. *Advanced Drug Delivery Reviews* 29, 89–116.
- Belshe, R.B., Newman, F.K., Anderson, E.L., Wright, P.F., Karron, R.A., Tollefson, S., Henderson, F.W., Meissner, H.C., Madhi, S., Robertson, D., Marshall, H., Loh, R., Sly, P., Murphy, B., Tatem, J.M., Randolph, V., Hackell, J., Gruber, W., Tsai, T.F., 2004. Evaluation of combined live, attenuated respiratory syncytial virus and parainfluenza 3 virus vaccines in infants and young children. *J. Infect. Dis.* 190, 2096–2103.
- Berthold, A., Cremer, K., Kreuter, J., 1996. Preparation and characterization of chitosan microspheres as drug carrier for prednisolone sodium phosphate as model for anti-inflammatory drugs. *Journal of Controlled Release* 39, 17–25.
- Bitter, C., Suter-Zimmermann, K., Surber, C., 2011. Nasal drug delivery in humans. *Curr. Probl. Dermatol.* 40, 20–35.

- Blanco, M.D., Sastre, R.L., Teijón, C., Olmo, R., Teijón, J.M., 2005. 5-Fluorouracil-loaded microspheres prepared by spray-drying poly(D,L-lactide) and poly(lactide-co-glycolide) polymers: characterization and drug release. *J Microencapsul* 22, 671–682.
- Bogdanffy, M.S., 1990. Biotransformation enzymes in the rodent nasal mucosa: the value of a histochemical approach. *Environ. Health Perspect.* 85, 177–186.
- Bozdağ-Pehlivan, S., Subaşı, B., Vural, I., Unlü, N., Capan, Y., 2011. Evaluation of drug-excipient interaction in the formulation of celecoxib tablets. *Acta Pol Pharm* 68, 423–433.
- Brandl, M., 2001. Liposomes as drug carriers: a technological approach. *Biotechnol Annu Rev* 7, 59–85.
- Brandtzaeg, P., 2011. Potential of nasopharynx-associated lymphoid tissue for vaccine responses in the airways. *American Journal of Respiratory and Critical Care Medicine* 183, 1595–1604.
- British Pharmacopoeia, 2011. British Pharmacopoeia Commission, 6th ed.
- Brodeur, C., Montplaisir, J., Godbout, R., Marinier, R., 1988. Treatment of restless legs syndrome and periodic movements during sleep with L-dopa: A double-blind, controlled study. *Neurology* 38, 1845–1845.
- Brooks, D.J., 2000. Dopamine agonists: their role in the treatment of Parkinson's disease. *J Neurol Neurosurg Psychiatry* 68, 685–689.
- Bu, H., Kjøniksen, A.-L., Knudsen, K.D., Nyström, B., 2005. Effects of surfactant and temperature on rheological and structural properties of semidilute aqueous solutions of unmodified and hydrophobically modified alginate. *Langmuir* 21, 10923–10930.
- Burgess, D.J., Duffy, E., Etzler, F., Hickey, A.J., 2004. Particle size analysis: AAPS workshop report, cosponsored by the Food and Drug Administration and the United States Pharmacopeia. *AAPS J* 6, 23–34.
- Burt, D., Mallett, C., Plante, M., Zimmermann, J., Torossian, K., Fries, L., 2011. Proteosome-adjuvanted intranasal influenza vaccines: advantages, progress and future considerations. *Expert Rev Vaccines* 10, 365–375.
- Carvalho, F.C., Bruschi, M.L., Evangelista, R.C., Gremião, M.P.D., 2010. Mucoadhesive drug delivery systems. *Brazilian Journal of Pharmaceutical Sciences* 46, 1–17.
- CDER, 2002. Nasal spray and inhalation solution, suspension, and spray drug products. chemistry, manufacturing, and controls documentation. Department of Health and Human Services Food and Drug Administration, USA.
- CDER, 2003. Bioavailability and Bioequivalence Studies for Nasal Aerosols and Nasal Sprays for Local Action. Department of Health and Human Services Food and Drug Administration, USA.
- Chakraverty, R., 2011. Preparation and Evaluation of sustained release microsphere of Norfloxacin using Sodium alginate. *International Journal of Pharmaceutical Science and Research* 3, 293–299.

- Chandy, T., Sharma, C.P., 1990. Chitosan--as a biomaterial. *Biomater Artif Cells Artif Organs* 18, 1–24.
- Chaturvedi, M., Kumar, M., Pathak, K., 2011. A review on mucoadhesive polymer used in nasal drug delivery system. *J Adv Pharm Technol Res* 2, 215–222.
- Chegini, G., Taheri, M., 2013. Whey powder: Process technology and physical properties: A review. *Middle-East Journal of Scientific Research* 13, 1377–1387.
- Chen, K.H., Di Sabatino, M., Albertini, B., Passerini, N., Kett, V.L., 2013. The effect of polymer coatings on physicochemical properties of spray-dried liposomes for nasal delivery of BSA. *European Journal of Pharmaceutical Sciences* 50, 312–322.
- Chen, M., Li, X.-R., Zhou, Y.-X., Yang, K.-W., Chen, X.-W., Deng, Q., Liu, Y., Ren, L.-J., 2009. Improved absorption of salmon calcitonin by ultraflexible liposomes through intranasal delivery. *Peptides* 30, 1288–1295.
- Chen, X.-Q., Fawcett, J.R., Rahman, Y.-E., Ala, T.A., Frey II, W.H., 1998. Delivery of nerve growth factor to the brain via the olfactory pathway. *J. Alzheimers Dis.* 1, 35–44.
- Cheng, J., Zhu, J., Wen, N., Xiong, F., 2006. Stability and pharmacokinetic studies of O-palmitoyl amylopectin anchored dipyridamole liposomes. *Int J Pharm* 313, 136–143.
- Cheng, Y.S., Holmes, T.D., Gao, J., Guilmette, R.A., Li, S., Surakitbanharn, Y., Rowlings, C., 2001. Characterization of nasal spray pumps and deposition pattern in a replica of the human nasal airway. *Journal of Aerosol Medicine* 14, 267–280.
- Chickering, D.E., Mathiowitz, E., 1995. Bioadhesive microspheres: I. A novel electrobalance-based method to study adhesive interactions between individual microspheres and intestinal mucosa. *Journal of Controlled Release* 34, 251–262.
- Chien, Y.W., Su, K.S.E., Chang, S.-F., 1989. *Nasal systemic drug delivery*. M. Dekker.
- Christen, A.G., Swanson, B.Z., Glover, E.D., Henderson, A.H., 1982. Smokeless tobacco: the folklore and social history of snuffing, sneezing, dipping, and chewing. *J Am Dent Assoc* 105, 821–829.
- Cocozza, S., 1989. Insufflator for the administration of drugs in the form of a powder pre-dosed into opercola. US4884565 A.
- Copley, M., 2008. A test of quality [WWW Document]. URL http://www.manufacturingchemist.com/technical/article_page/A_test_of_quality/41488 (accessed 11.3.13).
- Coppi, G., Iannuccelli, V., Leo, E., Bernabei, M.T., Cameroni, R., 2002. Protein immobilization in crosslinked alginate microparticles. *J Microencapsul* 19, 37–44.
- Corrigan, O.I., 1995. Thermal analysis of spray dried products. *Thermochimica Acta* 248, 245–258.

- Costantino, H.R., Illum, L., Brandt, G., Johnson, P.H., Quay, S.C., 2007. Intranasal delivery: physicochemical and therapeutic aspects. *Int J Pharm* 337, 1–24.
- Craig, D.Q., Royall, P.G., Kett, V.L., Hopton, M.L., 1999. The relevance of the amorphous state to pharmaceutical dosage forms: glassy drugs and freeze dried systems. *International Journal of Pharmaceutics* 179, 179–207.
- Dahl, Mygind, 1998. Anatomy, physiology and function of the nasal cavities in health and disease. *Adv. Drug Deliv. Rev.* 29, 3–12.
- Das, M.K., Senapati, P.C., 2008. Furosemide-loaded alginate microspheres prepared by ionic cross-linking technique: Morphology and release characteristics. *Indian J Pharm Sci* 70, 77–84.
- Davis, 1999. Delivery of peptide and non-peptide drugs through the respiratory tract. *Pharm. Sci. Technol. Today* 2, 450–456.
- Davis, S.S., Illum, L., 2003. Absorption enhancers for nasal drug delivery. *Clin Pharmacokinet* 42, 1107–1128.
- Dayal, P., Shaik, M.S., Singh, M., 2004. Evaluation of different parameters that affect droplet-size distribution from nasal sprays using the Malvern Spraytec. *J Pharm Sci* 93, 1725–1742.
- De Ascentiis, A., Bettini, R., Caponetti, G., Catellani, P.L., Peracchia, M.T., Santi, P., Colombo, P., 1996. Delivery of Nasal Powders of β -Cyclodextrin by Insufflation. *Pharmaceutical Research* 13, 734 – 738.
- De Carvalho, L.A.E.B., Marques, M.P.M., Tomkinson, J., 2006. Drug–excipient interactions in ketoprofen: A vibrational spectroscopy study. *Biopolymers* 82, 420–424.
- Deamer, D., Bangham, A.D., 1976. Large volume liposomes by an ether vaporization method. *Biochimica et Biophysica Acta (BBA) - Biomembranes* 443, 629–634.
- Dhakar, R.C., Maurya, S.D., Tilak, V.K., Gupta, A.K., 2011. A review on factors affecting the design of nasal drug delivery system. *International Journal of Drug Delivery* 3, 194–208.
- Dhawan, S., Singla, A.K., Sinha, V.R., 2004. Evaluation of mucoadhesive properties of chitosan microspheres prepared by different methods. *AAPS PharmSciTech* 5, 122–128.
- Diesel, D.A., Lebel, J.L., Tucker, A., 1991. Pulmonary particle deposition and airway mucociliary clearance in cold-exposed calves. *Am. J. Vet. Res.* 52, 1665–1671.
- Ding, W.-X., Qi, X.-R., Fu, Q., Piao, H.-S., 2007. Pharmacokinetics and pharmacodynamics of sterylglucoside-modified liposomes for levonorgestrel delivery via nasal route. *Drug Delivery* 14, 101–104.
- Djupesland, P.G., 2013. Nasal drug delivery devices: characteristics and performance in a clinical perspective—a review. *Drug Deliv Transl Res* 3, 42–62.
- Djupesland, P.G., Docekal, P., 2010. Intranasal sumatriptan powder delivered by a novel breath-actuated bi-directional device for the acute treatment of migraine: A randomised, placebo-controlled study. *Cephalalgia* 30, 933–942.

- Dodane, V., Amin Khan, M., Merwin, J.R., 1999. Effect of chitosan on epithelial permeability and structure. *Int J Pharm* 182, 21–32.
- Donovan, M.D., Huang, Y., 1998. Large molecule and particulate uptake in the nasal cavity: the effect of size on nasal absorption. *Advanced Drug Delivery Reviews* 29, 147–155.
- Dos Santos, J., Dockal, E., Cavalheiro, E., 2005. Thermal behavior of Schiff bases from chitosan. *J. Therm. Anal. Calorim.* 79, 243–248.
- Drebushchak, V.A., Shakhtshneider, T.P., Apenina, S.A., Medvedeva, A.S., Safronova, L.P., Boldyrev, V.V., 2006. Thermoanalytical investigation of drug–excipient interaction. *J Therm Anal Calorim* 86, 303–309.
- DrugBank, 2013. Ropinirole (DB00268). DrugBank.
- Duan, X., Mao, S., 2010. New strategies to improve the intranasal absorption of insulin. *Drug Discovery Today* 15, 416–427.
- El-Hameed, M.D., Kellaway, I.W., 1997. Preparation and in vitro characterisation of mucoadhesive polymeric microspheres as intra-nasal delivery systems* 1. *European journal of pharmaceutics and biopharmaceutics* 44, 53–60.
- Elhissi, A.M.A., Karnam, K.K., Danesh-Azari, M.-R., Gill, H.S., Taylor, K.M.G., 2006. Formulations generated from ethanol-based proliposomes for delivery via medical nebulizers. *Journal of Pharmacy and Pharmacology* 58, 887–894.
- Farid, R., Etman, M., Nada, A., Ebian, A.-E., 2012. Sodium alginate-based microspheres of salbutamol sulphate for nasal administration: Formulation and evaluation. *Am. J. PharmTech Res* 2, 289–307.
- Fars K. Alanazi, M.E.-B., 2007. Improvement of Albendazole Dissolution by Preparing Microparticles Using Spray-Drying Technique. *Scientia Pharmaceutica* 75, 63–79.
- Fernandez-Urrusuno, R., Calvo, P., Remunan-Lopez, C., Vila-Jato, J., Alonso, M., 1999. Enhancement of nasal absorption of insulin using chitosan nanoparticles. *Pharm. Res.* 16, 1576–1581.
- Foo, M.Y., 2007. Deposition pattern of nasal sprays in the human nasal airway--- interactions among formulation, device, anatomy and administration techniques. ProQuest.
- Foo, M.Y., Cheng, Y.-S., Su, W.-C., Donovan, M.D., 2007. The influence of spray properties on intranasal deposition. *Journal of Aerosol Medicine* 20, 495–508.
- Frey, W.H., Liu, J., Chen, X., Thorne, R.G., Fawcett, J.R., Ala, T.A., Rahman, Y.-E., 1997. Delivery of 125 I-NGF to the brain via the olfactory route. *Drug Delivery* 4, 87–92.
- Fukunaga, M., Miller, M.M., Deftos, L.J., 1991. Liposome-entrapped calcitonin and parathyroid hormone are orally effective in rats. *Horm. Metab. Res.* 23, 166–167.
- Furubayashi, T., Kamaguchi, A., Kawaharada, K., Masaoka, Y., Kataoka, M., Yamashita, S., Higashi, Y., Sakane, T., 2007. Evaluation of the contribution of

- the nasal cavity and gastrointestinal tract to drug absorption following nasal application to rats. *Biol. Pharm. Bull.* 30, 608–611.
- Gad, S.C., 2008. *Pharmaceutical Manufacturing Handbook: Production and Processes*. John Wiley & Sons.
- García, A., Leonardi, D., Piccirilli, G.N., Mamprin, M.E., Olivieri, A.C., Lamas, M.C., 2013. Spray drying formulation of albendazole microspheres by experimental design. *In vitro-in vivo studies. Drug Dev Ind Pharm.*
- Gavini, E., Hegge, A.B., Rasso, G., Sanna, V., Testa, C., Pirisino, G., Karlsen, J., Giunchedi, P., 2006. Nasal administration of carbamazepine using chitosan microspheres: *in vitro/in vivo* studies. *International journal of pharmaceutics* 307, 9–15.
- Gavini, E., Rasso, G., Ferraro, L., Generosi, A., Rau, J.V., Brunetti, A., Giunchedi, P., Dalpiaz, A., 2011. Influence of chitosan glutamate on the *in vivo* intranasal absorption of rokitamycin from microspheres. *J. Pharm. Sci.* 100, 1488–1502.
- Gavini, E., Rasso, G., Muzzarelli, C., Cossu, M., Giunchedi, P., 2008. Spray-dried microspheres based on methylpyrrolidinone chitosan as new carrier for nasal administration of metoclopramide. *European journal of pharmaceutics and biopharmaceutics* 68, 245–252.
- Gavini, E., Rasso, G., Muzzarelli, C., Cossu, M., Giunchedi, P., 2008. Spray-dried microspheres based on methylpyrrolidinone chitosan as new carrier for nasal administration of metoclopramide. *European Journal of Pharmaceutics and Biopharmaceutics* 68, 245–252.
- Gavini, E., Rasso, G., Sanna, V., Cossu, M., Giunchedi, P., 2005. Mucoadhesive microspheres for nasal administration of an antiemetic drug, metoclopramide: *in-vitro/ex-vivo* studies. *j pharm pharmacol* 57, 287–294.
- Genta, I., Pavanetto, F., Conti, B., Giunchedi, P., Conte, U., 1995. Improvement of dexamethasone dissolution rate from spray-dried chitosan microspheres. *STP pharma sciences* 5, 202–207.
- Genta, I., Perugini, P., Modena, T., Pavanetto, F., Castelli, F., Muzzarelli, R.A.A., Muzzarelli, C., Conti, B., 2003. Miconazole-loaded 6-oxychitin–chitosan microcapsules. *Carbohydrate Polymers* 52, 11–18.
- Ghimire, A., Das, B.P., Mishra, S.C., 2007. Comparative efficacy of steroid nasal spray versus antihistamine nasal spray in allergic rhinitis. *Nepal Med Coll J* 9, 17–21.
- Gill, P., Moghadam, T.T., Ranjbar, B., 2010. Differential scanning calorimetry techniques: applications in biology and nanoscience. *J. Biomol. Tech. JBT* 21, 167.
- GlaxoSmithKline, 2009. **REQUIP (ropinirole tablets) (PRESCRIBING INFORMATION No. NC 27709)**.
- Gombotz, W.R., Wee, S., 1998. Protein release from alginate matrices. *Advanced Drug Delivery Reviews* 31, 267–285.

- Goyal, S., Vashist, H., Gupta, A., Jindal, S., Goyal, A., 2011. Development of alginate gel beads-entrapped liposome for colon specific drug delivery of Prednisolone. *Der Pharmacia Sinica* 2.
- Graessley, W.W., 1974. *The Entanglement Concept in Polymer Rheology*. Springer-Verlag, Berlin, Germany.
- Graf, E., 1986. Transnasal systemic medications, fundamentals, developmental concepts and biomedical assessments. *Pharmazie in unserer Zeit* 15, 62–62.
- Graff, C.L., Pollack, G.M., 2005. Nasal drug administration: potential for targeted central nervous system delivery. *J Pharm Sci* 94, 1187–1195.
- Gregoriadis, G., Florence, A.T., 1993. Liposomes in drug delivery. Clinical, diagnostic and ophthalmic potential. *Drugs* 45, 15–28.
- Guerrero, S., Muñíz, E., Teijón, C., Olmo, R., Teijón, J.M., Blanco, M.D., 2008. Ketotifen-loaded microspheres prepared by spray-drying poly(D,L-lactide) and poly(D,L-lactide-co-glycolide) polymers: characterization and in vivo evaluation. *J Pharm Sci* 97, 3153–3169.
- Gungor, S., Okyar, A., Erturk-Toker, S., Baktir, G., Ozsoy, Y., 2010. Ondansetron-loaded chitosan microspheres for nasal antiemetic drug delivery: an alternative approach to oral and parenteral routes. *Drug Dev Ind Pharm* 36, 806–813.
- Guo, C., Doub, W.H., 2006. The influence of actuation parameters on in vitro testing of nasal spray products. *J Pharm Sci* 95, 2029–2040.
- Guo, J., Ping, Q., Jiang, G., Huang, L., Tong, Y., 2003. Chitosan-coated liposomes: characterization and interaction with leuprolide. *International Journal of Pharmaceutics* 260, 167–173.
- Hafner, A., Filipović-Grcić, J., Voinovich, D., Jalsenjak, I., 2007. Development and in vitro characterization of chitosan-based microspheres for nasal delivery of promethazine. *Drug Dev Ind Pharm* 33, 427–436.
- Hanna, P.A., Gad, S., Ghonaim, H.M., Ghorab, M.M., 2013. Optimization of gabapentin release and targeting absorption, through incorporation into alginate beads. *British Journal of Pharmaceutical Research* 3.
- Harikarnpakdee, S., Lipipun, V., Sutanthavibul, N., Ritthidej, G.C., 2006. Spray-dried mucoadhesive microspheres: Preparation and transport through nasal cell monolayer. *AAPS PharmSciTech* 7, E79–E88.
- Hashizume, R., Ozawa, T., Gryaznov, S.M., Bollen, A.W., Lamborn, K.R., Frey, W.H., Deen, D.F., 2008. New therapeutic approach for brain tumors: Intranasal delivery of telomerase inhibitor GRN163. *Neuro Oncol* 10, 112–120.
- He, P., Davis, S.S., Illum, L., 1998. In vitro evaluation of the mucoadhesive properties of chitosan microspheres. *Int J Pharm* 166, 75–88. He, P., Davis, S.S., Illum, L., 1999. Chitosan microspheres prepared by spray drying. *Int J Pharm* 187, 53–65.
- Hermens, W.A., Merkus, F.W., 1987. The influence of drugs on nasal ciliary movement. *Pharm. Res.* 4, 445–449.

- Hinchcliffe, Illum, 1999. Intranasal insulin delivery and therapy. *Adv. Drug Deliv. Rev.* 35, 199–234.
- Horak, F., 2008. Effectiveness of twice daily azelastine nasal spray in patients with seasonal allergic rhinitis. *Ther Clin Risk Manag* 4, 1009–1022.
- Houtmeyers, E., Gosselink, R., Gayan-Ramirez, G., Decramer, M., 1999. Regulation of mucociliary clearance in health and disease. *European Respiratory Journal* 13, 1177–1188.
- Huang, J., Garmise, R.J., Crowder, T.M., Mar, K., Hwang, C.R., Hickey, A.J., Mikszta, J.A., Sullivan, V.J., 2004. A novel dry powder influenza vaccine and intranasal delivery technology: induction of systemic and mucosal immune responses in rats. *Vaccine* 23, 794–801.
- Huh, Y., Cho, H.-J., Yoon, I.-S., Choi, M.-K., Kim, J.S., Oh, E., Chung, S.-J., Shim, C.-K., Kim, D.-D., 2010. Preparation and evaluation of spray-dried hyaluronic acid microspheres for intranasal delivery of fexofenadine hydrochloride. *Eur J Pharm Sci* 40, 9–15.
- Ikechukwu Ugwoke, M., Kaufmann, G., Verbeke, N., Kinget, R., 2000. Intranasal bioavailability of apomorphine from carboxymethylcellulose-based drug delivery systems. *Int J Pharm* 202, 125–131.
- Illum, L., 2000. Transport of drugs from the nasal cavity to the central nervous system. *Eur J Pharm Sci* 11, 1–18.
- Illum, L., 2002. Nasal drug delivery: new developments and strategies. *Drug Discov. Today* 7, 1184–1189.
- Illum, L., 2003. Nasal drug delivery--possibilities, problems and solutions. *J Control Release* 87, 187–198.
- Illum, L., Farraj, N.F., Davis, S.S., 1994. Chitosan as a novel nasal delivery system for peptide drugs. *Pharm. Res.* 11, 1186–1189.
- Illum, L., Jørgensen, H., Bisgaard, H., Krogsgaard, O., Rossing, N., 1987. Bioadhesive microspheres as a potential nasal drug delivery system. *International Journal of Pharmaceutics* 39, 189–199.
- Inthavong, K., Ge, Q., Se, C.M.K., Yang, W., Tu, J.Y., 2011. Simulation of sprayed particle deposition in a human nasal cavity including a nasal spray device. *Journal of Aerosol Science* 42, 100–113.
- Ishikawa, F., Katsura, M., Tamai, I., Tsuji, A., 2001. Improved nasal bioavailability of elcatonin by insoluble powder formulation. *Int J Pharm* 224, 105–114.
- Islam, M.A., Firdous, J., Choi, Y.-J., Yun, C.-H., Cho, C.-S., 2012. Design and application of chitosan microspheres as oral and nasal vaccine carriers: an updated review. *Int J Nanomedicine* 7, 6077–6093.
- Jadhav, K.R., Gambhire, M.N., Shaikh, I.M., Kadam, V.J., Pisal, S.S., 2007. Nasal drug delivery system-factors affecting and applications. *Current drug therapy* 2, 27–38.

- Jain, S.K., Chourasia, M.K., Jain, A.K., Jain, R.K., Shrivastava, A.K., 2004. Development and characterization of mucoadhesive microspheres bearing salbutamol for nasal delivery. *Drug Deliv* 11, 113–122.
- Jain, S.K., Jain, R.K., Chourasia, M.K., Jain, A.K., Chalasani, K.B., Soni, V., Jain, A., 2005. Design and development of multivesicular liposomal depot delivery system for controlled systemic delivery of acyclovir sodium. *AAPS PharmSciTech* 6, E35–E41.
- Jankovic, J., 2008. Parkinson's Disease: Clinical Features and Diagnosis. *J Neurol Neurosurg Psychiatry* 79, 368–376.
- Jayakumar, R., Menon, D., Manzoor, K., Nair, S.V., Tamura, H., 2010. Biomedical applications of chitin and chitosan based nanomaterials—A short review. *Carbohydrate Polymers* 82, 227–232.
- Jiménez-castellanos, M.R., Zia, H., Rhodes, C.T., 1993. Mucoadhesive drug delivery systems. *Drug Development and Industrial Pharmacy* 19, 143–194.
- Jost, W.H., Angersbach, D., 2005. Ropinirole, a non-ergoline dopamine agonist. *CNS Drug Rev* 11, 253–272.
- Taylor, G.T., 1990. The stability of liposomes to nebulisation. *International Journal of Pharmaceutics* 57–61.
- Kandimalla, K.K., Donovan, M.D., 2005a. Carrier mediated transport of chlorpheniramine and chlorcyclizine across bovine olfactory mucosa: implications on nose-to-brain transport. *J Pharm Sci* 94, 613–624. doi:10.1002/jps.20284
- Kandimalla, K.K., Donovan, M.D., 2005b. Localization and differential activity of P-glycoprotein in the bovine olfactory and nasal respiratory mucosae. *Pharm. Res.* 22, 1121–1128.
- Kaye, C.M., Nicholls, B., 2000. Clinical pharmacokinetics of ropinirole. *Clin Pharmacokinet* 39, 243–254.
- Keldmann, T., 2005. Advanced simplification of nasal delivery technology: anatomy+innovative device =added value opportunity.
- Khan, S., Patil, K., Bobade, N., Yeole, P., Gaikwad, R., 2010. Formulation of intranasal mucoadhesive temperature-mediated in situ gel containing ropinirole and evaluation of brain targeting efficiency in rats. *J Drug Target* 18, 223–234.
- Kharenko, E.A., Larionova, N.I., Demina, N.B., 2009. Mucoadhesive drug delivery systems (Review). *Pharmaceutical Chemistry Journal* 43, 200–208.
- Kilian, N., Müller, D.G., 1998. The effect of a viscosity and an absorption enhancer on the intra nasal absorption of metoprolol in rats. *International Journal of Pharmaceutics* 163, 211–217.
- Kimura, R., Miwa, M., Kato, Y., Yamada, S., Sato, M., 1989. Nasal absorption of tetraethylammonium in rats. *Arch Int Pharmacodyn Ther* 302, 7–17.
- Kippax, P., 2009. Complementary techniques for nasal spray analysis.

- Kippax, P., Suman, J., Virden, A., Williams, G., 2010. Effects of viscosity, pump mechanism and nozzle geometry on nasal spray droplet size. Presented at the ILASS-Europe 201, 23rd Annual Conference on Liquid Atomization and Spray Systems, Brno, Czech Republic.
- Kirby, C., Clarke, J., Gregoriadis, G., 1980. Effect of the cholesterol content of small unilamellar liposomes on their stability in vivo and in vitro. *Biochem J* 186, 591–598.
- Kisel, M.A., Kulik, L.N., Tsybovsky, I.S., Vlasov, A.P., Vorob'yov, M.S., Kholodova, E.A., Zabarovskaya, Z.V., 2001. Liposomes with phosphatidylethanol as a carrier for oral delivery of insulin: studies in the rat. *Int J Pharm* 216, 105–114.
- Klas, S.D., Petrie, C.R., Warwood, S.J., Williams, M.S., Olds, C.L., Stenz, J.P., Cheff, A.M., Hinchcliffe, M., Richardson, C., Wimer, S., 2008. A single immunization with a dry powder anthrax vaccine protects rabbits against lethal aerosol challenge. *Vaccine* 26, 5494–5502.
- Kolsure, P.K., Raj Kapoor, B., 2012. Development of zolmitriptan gel for nasal administration. *Asian Journal of Pharmaceutical and Clinical Research* 5, 88–94.
- Kondo, N., Iwao, T., Masuda, H., Yamanouchi, K., Ishihara, Y., Yamada, N., Haga, T., Ogawa, Y., Yokoyama, K., 1993. Improved oral absorption of a poorly water-soluble drug, HO-221, by wet-bead milling producing particles in submicron region. *Chem. Pharm. Bull.* 41, 737–740.
- Kozlowski, P.A., 2012. *Mucosal vaccines: Modern concepts, strategies, and challenges*. Springer.
- Kublik, H., Vidgren, M., 1998. Nasal delivery systems and their effect on deposition and absorption. *Advanced Drug Delivery Reviews* 29, 157–177.
- Kulkarni, V., Shaw, C., 2012. Formulation and characterization of nasal sprays. *Inhalation* 10–15.
- Kumar, T.P., Sirisha, B., Raju, P.N., Reddy, G.N., 2013. Nasal drug delivery: A potential route for brain targeting 2, 77–85.
- Kundoor, V., Dalby, R.N., 2010. Assessment of nasal spray deposition pattern in a silicone human nose model using a color-based method. *Pharm. Res.* 27, 30–36.
- Kundoor, V., Dalby, R.N., 2011. Effect of formulation- and administration-related variables on deposition pattern of nasal spray pumps evaluated using a nasal cast. *Pharm. Res.* 28, 1895–1904.
- Kurlan, R., Richard, I.H., Deeley, C., 2006. Medication tolerance and augmentation in restless legs syndrome: The need for drug class rotation. *J Gen Intern Med* 21, C1–C4.
- Kushwaha, S.K., Keshari, R.K., Rai, A.K., 2011. Advances in nasal trans-mucosal drug delivery. *Journal of Applied Pharmaceutical Science* 1, 21–28.
- Lachman, L., Lieberman, H.A., Kanig, J.L., 1986. *The Theory and Practice of Industrial Pharmacy*, 3 Sub. ed. Lea & Febiger.

- Langley, J.M., Halperin, S.A., McNeil, S., Smith, B., Jones, T., Burt, D., Mallett, C.P., Lowell, G.H., Fries, L., 2006. Safety and immunogenicity of a Proteosome - trivalent inactivated influenza vaccine, given nasally to healthy adults. *Vaccine* 24, 1601–1608.
- Laouini, A., Jaafar-Maalej, C., Limayem-Blouza, I., Sfar, S., Charcosset, C., Fessi, H., 2012. Preparation, characterization and applications of liposomes: state of the art. *Journal of Colloid Science and Biotechnology* 1, 147–168.
- Lasic, D.D., 1988. The mechanism of vesicle formation. *Biochem J* 256, 1–11.
- Laye, C., McClements, D.J., Weiss, J., 2008. Formation of biopolymer-coated liposomes by electrostatic deposition of chitosan. *Journal of Food Science* 73, N7–N15.
- Learoyd, T.P., Burrows, J.L., French, E., Seville, P.C., 2008a. Modified release of beclometasone dipropionate from chitosan-based spray-dried respirable powders. *Powder Technology* 187, 231–238.
- Learoyd, T.P., Burrows, J.L., French, E., Seville, P.C., 2008b. Chitosan-based spray-dried respirable powders for sustained delivery of terbutaline sulfate. *European Journal of Pharmaceutics and Biopharmaceutics* 68, 224–234.
- Learoyd, T.P., Burrows, J.L., French, E., Seville, P.C., 2008c. Modified release of beclometasone dipropionate from chitosan-based spray-dried respirable powders. *Powder Technology* 187, 231–238.
- Lee, J.W., Park, J.H., Robinson, J.R., 2000. Bioadhesive-based dosage forms: the next generation. *J Pharm Sci* 89, 850–866.
- Lippmann, M., Yeates, D.B., Albert, R.E., 1980. Deposition, retention, and clearance of inhaled particles. *Br J Ind Med* 37, 337–362.
- Liu, N., Park, H.-J., 2010. Factors effect on the loading efficiency of Vitamin C loaded chitosan-coated nanoliposomes. *Colloids Surf B Biointerfaces* 76, 16–19.
- Lochhead, J.J., Thorne, R.G., 2012. Intranasal delivery of biologics to the central nervous system. *Adv. Drug Deliv. Rev.* 64, 614–628.
- Maa, Y.F., Nguyen, P.A., Andya, J.D., Dasovich, N., Sweeney, T.D., Shire, S.J., Hsu, C.C., 1998. Effect of spray drying and subsequent processing conditions on residual moisture content and physical/biochemical stability of protein inhalation powders. *Pharm. Res.* 15, 768–775.
- Mady, M.M., Darwish, M.M., 2010. Effect of chitosan coating on the characteristics of DPPC liposomes. *Journal of Advanced Research* 1, 187–191.
- Maestrelli, F., Zerrouk, N., Chemtob, C., Mura, P., 2004. Influence of chitosan and its glutamate and hydrochloride salts on naproxen dissolution rate and permeation across Caco-2 cells. *Int J Pharm* 271, 257–267.
- Mahajan, H., Gattani, S., Surana, S., 2008. Spray Dried Mucoadhesive Microspheres of Ondansetron for Nasal Administration. *International Journal of Pharmaceutical Sciences and Nanotechnology* 1, 267–274.

- Mahajan, H.S., Tatiya, B.V., Nerkar, P.P., 2012. Ondansetron loaded pectin based microspheres for nasal administration: In vitro and in vivo studies. *Powder Technology* 221, 168–176.
- Maherani, B., Arab-tehrany, E., Kheiriloomoom, A., Reshetov, V., Stebe, M.J., Linder, M., 2012. Optimization and characterization of liposome formulation by mixture design. *Analyst* 137, 773–786.
- Malhotra, M., Tomaro-Duchesneau, C., Saha, S., Prakash, S., 2013. Intranasal, siRNA Delivery to the Brain by TAT/MGF Tagged PEGylated Chitosan Nanoparticles. *Journal of Pharmaceutics* 2013.
- Mali, K.K., Dias, R.J., Ghorpade, V.S., Havaladar, V.D., 2010. Sodium alginate microspheres containing multicomponent inclusion complex of domperidone. *Latin American Journal of Pharmacy* 29.
- Manca, M.L., Sinico, C., Maccioni, A.M., Diez, O., Fadda, A.M., Manconi, M., 2012. Composition influence on pulmonary delivery of rifampicin liposomes. *Pharmaceutics* 4, 590–606.
- Mao, S., Chen, J., Wei, Z., Liu, H., Bi, D., 2004. Intranasal administration of melatonin starch microspheres. *International journal of pharmaceutics* 272, 37–43.
- Matheson, A.J., Spencer, C.M., 2000. Ropinirole: a review of its use in the management of Parkinson's disease. *Drugs* 60, 115–137.
- Mathias, N.R., Hussain, M.A., 2010. Non-invasive systemic drug delivery: developability considerations for alternate routes of administration. *J Pharm Sci* 99, 1–20.
- Mathiowitz, E., III, D.E.C., Lehr, C.-M., 1999. Bioadhesive formulations for nasal peptide delivery: Fundamentals, Novel Approaches, and Development, 1st ed. Informa Healthcare, New York.
- Maury, M., Murphy, K., Kumar, S., Shi, L., Lee, G., 2005. Effects of process variables on the powder yield of spray-dried trehalose on a laboratory spray-dryer. *European Journal of Pharmaceutics and Biopharmaceutics* 59, 565–573.
- McMartin, C., Hutchinson, L.E., Hyde, R., Peters, G.E., 1987. Analysis of structural requirements for the absorption of drugs and macromolecules from the nasal cavity. *J Pharm Sci* 76, 535–540.
- Merkus, Verhoef, Schipper, Marttin, 1998. Nasal mucociliary clearance as a factor in nasal drug delivery. *Adv. Drug Deliv. Rev.* 29, 13–38.
- Mestecky, J., Moldoveanu, Z., Michalek, S.M., Morrow, C.D., Compans, R.W., Schafer, D.P., Russell, M.W., 1997. Current options for vaccine delivery systems by mucosal routes. *Journal of controlled release* 48, 243–257.
- Morimoto, K., Katsumata, H., Yabuta, T., Iwanaga, K., Kakemi, M., Tabata, Y., Ikada, Y., 2001. Evaluation of gelatin microspheres for nasal and intramuscular administrations of salmon calcitonin. *Eur J Pharm Sci* 13, 179–185.
- Morimoto, K., Yamaguchi, H., Iwakura, Y., Miyazaki, M., Nakatani, E., Iwamoto, T., Ohashi, Y., Nakai, Y., 1991a. Effects of proteolytic enzyme inhibitors on the nasal absorption of vasopressin and an analogue. *Pharm. Res.* 8, 1175–1179.

- Morimoto, K., Yamaguchi, H., Iwakura, Y., Morisaka, K., Ohashi, Y., Nakai, Y., 1991b. Effects of viscous hyaluronate-sodium solutions on the nasal absorption of vasopressin and an analogue. *Pharm. Res.* 8, 471–474.
- Mu, L., Feng, S.S., 2001. Fabrication, characterization and in vitro release of paclitaxel (Taxol) loaded poly (lactic-co-glycolic acid) microspheres prepared by spray drying technique with lipid/cholesterol emulsifiers. *J Control Release* 76, 239–254.
- Na, D.H., Youn, Y.S., Park, E.J., Lee, J.M., Cho, O.R., Lee, K.R., Lee, S.D., Yoo, S.D., DeLuca, P.P., Lee, K.C., 2004. Stability of PEGylated salmon calcitonin in nasal mucosa. *J Pharm Sci* 93, 256–261.
- Na, L., Wang, J., Wang, L., Mao, S., 2013. A novel permeation enhancer: N-succinyl chitosan on the intranasal absorption of isosorbide dinitrate in rats. *European Journal of Pharmaceutical Sciences* 48, 301–306.
- Naderkhani, E., Erber, A., Skalko-Basnet, N., Flaten, G.E., 2014. Improved permeability of acyclovir: optimization of mucoadhesive liposomes using the phospholipid vesicle-based permeation assay. *J Pharm Sci*.
- Nagaraju, R., Pallavi, K., Deepthy, K., Haritha, M., 2013. Formulation and evaluation of niosomal nasal drug delivery system of folic acid for brain targeting. *Curr Drug Discov Technol*.
- Nagda, C., Chotai, N., Patel, S., Nagda, D., Patel, U., Soni, T., 2010. Chitosan microspheres of aceclofenac: in vitro and in vivo evaluation. *Pharmaceutical Development And Technology* 15, 442–451.
- Nagda, C.D., Chotai, N.P., Nagda, D.C., Patel, S.B., Patel, U.L., 2012. Preparation and characterization of spray-dried mucoadhesive microspheres of ketorolac for nasal administration. *Curr Drug Deliv* 9, 205–218.
- Nanda, B., Murthy, R.S.R., 2007. Preparation and characterization of chitosan lactate nanoparticles for the nasal delivery of enalaprilat. *Journal of Biomedical Nanotechnology* 3, 45–51.
- Narayani, R., Panduranga Rao, K., 1996. Gelatin microsphere cocktails of different sizes for the controlled release of anticancer drugs. *International Journal of Pharmaceutics* 143, 255–258.
- Ninomiya, A., Ogasawara, K., Kajino, K., Takada, A., Kida, H., 2002. Intranasal administration of a synthetic peptide vaccine encapsulated in liposome together with an anti-CD40 antibody induces protective immunity against influenza A virus in mice. *Vaccine* 20, 3123–3129.
- O'Hagan, D.T., Illum, L., 1990. Absorption of peptides and proteins from the respiratory tract and the potential for development of locally administered vaccine. *Crit Rev Ther Drug Carrier Syst* 7, 35–97.
- Olanow, C.W., Watts, R.L., Koller, W.C., 2001. An algorithm (decision tree) for the management of Parkinson's disease (2001): treatment guidelines. *Neurology* 56, S1–S88.
- Oliveira, B.F., Santana, M.H.A., Ré, M.I., 2005. Spray-dried chitosan microspheres cross-linked with d, l-glyceraldehyde as a potential drug delivery system:

- preparation and characterization. *Brazilian Journal of Chemical Engineering* 22, 353–360.
- Olson, J., 2008. Nose to brain is a promising path in Alzheimer's fight [WWW Document]. TwinCities.com. URL http://www.twincities.com/health/ci_8160098 (accessed 3.3.14).
- Ozsoy, Y., Gungor, S., Cevher, E., 2009. Nasal delivery of high molecular weight drugs. *Molecules* 14, 3754–3779.
- Pahwa, R., Lyons, K.E., Hauser, R.A., 2004. Ropinirole therapy for Parkinson's disease. *Expert Review of Neurotherapeutics* 4, 581–588.
- Park, J.-H., Jin, H.-E., Kim, D.-D., Chung, S.-J., Shim, W.-S., Shim, C.-K., 2013. Chitosan microspheres as an alveolar macrophage delivery system of ofloxacin via pulmonary inhalation. *Int J Pharm* 441, 562–569.
- Patel, C., Chaudhari, B., 2012. Study of Degradation Profile and Development of Stability Indicating Spectrophotometric Method for Ropinirole Hydrochloride under Acid/Base Hydrolytic and Oxidative Conditions. *International Journals For Pharmaceutical Research Scholars* 1, 27–.
- Patil, S., Murthy, R., 2006. Preparation and in vitro evaluation of mucoadhesive chitosan microspheres of amlodipine besylate for nasal administration. *Indian Journal of Pharmaceutical Sciences* 68, 64.
- Patil, S.B., Kaul, A., Babbar, A., Mathur, R., Mishra, A., Sawant, K.K., 2012. In vivo evaluation of alginate microspheres of carvedilol for nasal delivery. *J. Biomed. Mater. Res. Part B Appl. Biomater.* 100, 249–255.
- Patil, S.B., Sawant, K.K., 2008. Mucoadhesive microspheres: a promising tool in drug delivery. *Curr Drug Deliv* 5, 312–318.
- Patil, S.B., Sawant, K.K., 2011. Chitosan microspheres as a delivery system for nasal insufflation. *Colloids Surf B Biointerfaces* 84, 384–389.
- Payne, N.I., Timmins, P., Ambrose, C.V., Ward, M.D., Ridgway, F., 1986. Proliposomes: a novel solution to an old problem. *J Pharm Sci* 75, 325–329.
- Penttilä, M., Poulsen, P., Hollingworth, K., Holmström, M., 2000. Dose-related efficacy and tolerability of fluticasone propionate nasal drops 400 microg once daily and twice daily in the treatment of bilateral nasal polyposis: a placebo-controlled randomized study in adult patients. *Clin. Exp. Allergy* 30, 94–102.
- Pereswetoff-Morath, L., 1998. Microspheres as nasal drug delivery systems. *Advanced drug delivery reviews* 29, 185–194.
- Perrett, S., Golding, M., Williams, W.P., 1991. A simple method for the preparation of liposomes for pharmaceutical applications: characterization of the liposomes. *J. Pharm. Pharmacol.* 43, 154–161.
- Perugini, P., Genta, I., Pavanetto, F., Conti, B., Scalia, S., Baruffini, A., 2000. Study on glycolic acid delivery by liposomes and microspheres. *Int J Pharm* 196, 51–61.

- Perugini, P., Genta, I., Pavanetto, F., Conti, B., Scalia, S., Baruffini, A., 2000. Study on glycolic acid delivery by liposomes and microspheres. *International journal of pharmaceutics* 196, 51–61.
- Phillips, B., Young, T., Finn, L., Asher, K., Hening, W.A., Purvis, C., 2000. Epidemiology of restless legs symptoms in adults. *Arch. Intern. Med.* 160, 2137–2141.
- Pietrowsky, R., Thiemann, A., Kern, W., Fehm, H.L., Born, J., 1996. A nose-brain pathway for psychotropic peptides: evidence from a brain evoked potential study with cholecystokinin. *Psychoneuroendocrinology* 21, 559–572.
- Pires, A., Fortuna, A., Alves, G., Falcão, A., 2009. Intranasal drug delivery: how, why and what for? *J Pharm Pharm Sci* 12, 288–311.
- Pitcher Iii, W.H., Huestis, W.H., 2002. Preparation and analysis of small unilamellar phospholipid vesicles of a uniform size. *Biochemical and biophysical research communications* 296, 1352–1355.
- Porta, C., Dossena, S., Rossi, V., Pinza, M., Cremaschi, D., 2000. Rabbit nasal mucosa: nanospheres coated with polypeptides bound to specific anti-polypeptide IgG are better transported than nanospheres coated with polypeptides or IgG alone. *Biochim. Biophys. Acta* 1466, 115–124.
- Pringels, E., Callens, C., Vervaet, C., Dumont, F., Slegers, G., Foreman, P., Remon, J.P., 2006. Influence of deposition and spray pattern of nasal powders on insulin bioavailability. *Int J Pharm* 310, 1–7.
- Qiang, F., Shin, H.-J., Lee, B.-J., Han, H.-K., 2012. Enhanced systemic exposure of fexofenadine via the intranasal administration of chitosan-coated liposome. *Int J Pharm* 430, 161–166.
- Quraishi, M. s., Jones, N. s., Mason, J. d. t., 1997. The nasal delivery of drugs. *Clinical Otolaryngology & Allied Sciences* 22, 289–301.
- Rai, B., Gajbhiye, V., Kavita Rai, Jain, A., Jadon, R., Nayak, A., 2008. Drug delivery via nasal route. *Pharma Student Magazine*.
- Raj, N.K.K., Sharma, C.P., 2003. Oral insulin – a perspective. *Journal of Biomaterials Applications* 17, 183 –196.
- Rajinikanth, P.S., Sankar, C., Mishra, B., 2003. Sodium alginate microspheres of metoprolol tartrate for intranasal systemic delivery: development and evaluation. *Drug Deliv* 10, 21–28.
- Rathananand, M., Kumar, D., Shirwaikar, A., Kumar, R., Sampath Kumar, D., Prasad, R., 2007. Preparation of mucoadhesive microspheres for nasal delivery by spray drying. *Indian Journal of Pharmaceutical Sciences* 69, 651.
- Reis, C.P., Neufeld, R.J., Vilela, S., Ribeiro, A.J., Veiga, F., 2006. Review and current status of emulsion/dispersion technology using an internal gelation process for the design of alginate particles. *J Microencapsul* 23, 245–257.
- Robinson, J.R., Longer, M.A., Veillard, M., 1987. Bioadhesive polymers for controlled drug delivery. *Ann. N. Y. Acad. Sci.* 507, 307–314.

- Rosada, R.S., Torre, L.G., Frantz, F.G., Trombone, A.P., Zárata-Bladés, C.R., Fonseca, D.M., Souza, P.R., Brandão, I.T., Masson, A.P., Soares, É.G., Ramos, S.G., Faccioli, L.H., Silva, C.L., Santana, M.H., Coelho-Castelo, A.A., 2008. Protection against tuberculosis by a single intranasal administration of DNA-hsp65 vaccine complexed with cationic liposomes. *BMC Immunology* 9, 38.
- Rothdach, A.J., Trenkwalder, C., Habersack, J., Keil, U., Berger, K., 2000. Prevalence and risk factors of RLS in an elderly population: the MEMO study. *Memory and Morbidity in Augsburg Elderly. Neurology* 54, 1064–1068.
- Rowe, R.C., Sheskey, P.J., Quinn, M.E. (Eds.), 2009. *Handbook of pharmaceutical excipients*, 6th ed. ed. Pharmaceutical Press.
- Roy, S., Panpalia, S.G., Rai, V.K., Tyagi, L.K., Dey, S., Meena, K.C., 2009. Effect of Method Of Preparation on Chitosan Microspheres of Mefenamic Acid. *International Journal of Pharmaceutical Sciences and Drug Research* 1, 36–42.
- Sacchetti, C., Artusi, M., Santi, P., Colombo, P., 2002. Caffeine microparticles for nasal administration obtained by spray drying. *Int J Pharm* 242, 335–339.
- Samii, A., Nutt, J.G., Ransom, B.R., 2004. Parkinson's disease. *Lancet* 363, 1783–1793.
- Sarmiento, B., Ferreira, D., Veiga, F., Ribeiro, A., 2006. Characterization of insulin-loaded alginate nanoparticles produced by ionotropic pre-gelation through DSC and FTIR studies. *Carbohydrate polymers* 66, 1–7.
- Schipper, N.G., Vârum, K.M., Stenberg, P., Ocklind, G., Lennernäs, H., Artursson, P., 1999. Chitosans as absorption enhancers of poorly absorbable drugs. 3: Influence of mucus on absorption enhancement. *Eur J Pharm Sci* 8, 335–343.
- Schnyder, A., Huwyler, J., 2005. Drug transport to brain with targeted liposomes. *NeuroRX* 2, 99–107.
- Schultz, R.K., 1995. Drug delivery characteristics of metered-dose inhalers. *Journal of Allergy and Clinical Immunology* 96, 284–287.
- Seju, U., Kumar, A., Sawant, K.K., 2011. Development and evaluation of olanzapine-loaded PLGA nanoparticles for nose-to-brain delivery: In vitro and in vivo studies. *Acta Biomaterialia* 7, 4169–4176.
- Shah, V., Sharma, M., Parmar, V., Upadhyay, U., 2011. Formulation of sildenafil citrate loaded nasal microspheres: An in vitro, ex vivo characterization. *ijdd* 2.
- Shahi, S., Tribhuvan, S., Tadwee, I., Gupta, S., Nityanand, Z., Shivanikar, S., 2011. Formulation of Atenolol Mucoadhesive Microspheres for Nasal Delivery by Spray Drying Technique: In vitro/ Ex vivo Evaluation. *Pelagia Research Library Der Pharmacia Sinica*, 2011, 2 (5):54-63 2, 54–63.
- Shaikh, R., Raj Singh, T.R., Garland, M.J., Woolfson, A.D., Donnelly, R.F., 2011. Mucoadhesive drug delivery systems. *J Pharm Bioallied Sci* 3, 89–100.
- Shaji, J., Bhatia, V., 2013. Proliposomes: A brief overview of novel delivery system. *International Journal of Pharma & Bio Sciences* 4.
- Sharma, P., Chaudhari, P., Kolsure, P., Ajab, A., Varia, N., 2006. Recent trends in nasal drug delivery system - An overview. 2006 5.

- Sharma, S., Lohan, S., Murthy, R.S.R., 2013. Formulation and characterization of intranasal mucoadhesive nanoparticulates and thermo-reversible gel of levodopa for brain delivery. *Drug Dev Ind Pharm.*
- Shek, P.N., Yung, B.Y., Stanacev, N.Z., 1983. Comparison between multilamellar and unilamellar liposomes in enhancing antibody formation. *Immunology* 49, 37–44.
- Shin, B.S., Jung, J.H., Lee, K.C., Yoo, S.D., 2004. Nasal absorption and pharmacokinetic disposition of salmon calcitonin modified with low molecular weight polyethylene glycol. *Chem. Pharm. Bull.* 52, 957–960.
- Shingaki, T., Inoue, D., Furubayashi, T., Sakane, T., Katsumi, H., Yamamoto, A., Yamashita, S., 2010. Transnasal delivery of methotrexate to brain tumors in rats: A new strategy for brain tumor chemotherapy. *Mol. Pharmaceutics* 7, 1561–1568.
- Singh, A.K., Singh, A., Madhv, N.V., 2012. Nasal cavity, a promising transmucosal platform for drug delivery and research approaches from nasal to brain targeting. *Journal of Drug Delivery and Therapeutics* 2.
- Singh, D.J., Lohade, A.A., Parmar, J.J., Hegde, D.D., Soni, P., Samad, A., Menon, M.D., 2012. Development of chitosan-based dry powder inhalation system of cisplatin for lung cancer. *Indian J Pharm Sci* 74, 521–526.
- Singla, A.K., Chawla, M., 2001. Chitosan: some pharmaceutical and biological aspects-an update. *J. Pharm. Pharmacol.* 53, 1047–1067.
- Sinha, V., Singla, A., Wadhawan, S., Kaushik, R., Kumria, R., Bansal, K., Dhawan, S., 2004. Chitosan microspheres as a potential carrier for drugs. *Int. J. Pharm.* 274, 1–33.
- Smart, J.D., Kellaway, I.W., Worthington, H.E., 1984. An in-vitro investigation of mucosa-adhesive materials for use in controlled drug delivery. *J. Pharm. Pharmacol.* 36, 295–299.
- Smith, J., Wood, E., Dornish, M., 2004. Effect of chitosan on epithelial cell tight junctions. *Pharm Res* 21, 43–49.
- Soane, R.J., Frier, M., Perkins, A.C., Jones, N.S., Davis, S.S., Illum, L., 1999. Evaluation of the clearance characteristics of bioadhesive systems in humans. *Int J Pharm* 178, 55–65.
- Soane, R.J., Hinchcliffe, M., Davis, S.S., Illum, L., 2001. Clearance characteristics of chitosan based formulations in the sheep nasal cavity. *Int J Pharm* 217, 183–191.
- Soares, J.P., Santos, J.E., Chierice, G.O., Cavaleiro, E.T.G., 2004. Thermal behavior of alginate acid and its sodium salt. *Eclética Química* 29, 57–64.
- Soni, M.L., Kumar, M., Namdeo, K.P., 2010. Sodium alginate microspheres for extending drug release: formulation and in vitro evaluation. *International Journal of Drug Delivery* 2, 64–68.
- Ståhl, K., Claesson, M., Lilliehorn, P., Lindén, H., Bäckström, K., 2002. The effect of process variables on the degradation and physical properties of spray dried insulin intended for inhalation. *International Journal of Pharmaceutics* 233, 227–237.

- Steyn, D., du Plessis, L., Kotzé, A., 2010. Nasal delivery of recombinant human growth hormone: in vivo evaluation with Pheroid technology and N-trimethyl chitosan chloride. *J Pharm Pharm Sci* 13, 263–273.
- Suman, J.D., Laube, B.L., Dalby, R., 1999. Comparison of nasal deposition and clearance of aerosol generated by a nebulizer and an aqueous spray pump. *Pharm Res* 16, 1648–1652.
- Sun, Y., Cui, F., Shi, K., Wang, J., Niu, M., Ma, R., 2009. The effect of chitosan molecular weight on the characteristics of spray-dried methotrexate-loaded chitosan microspheres for nasal administration. *Drug Development and Industrial Pharmacy* 35, 379–386.
- Sun, Y., Gu, L., Gao, Y., Gao, F., 2010. Preparation and characterization of 5-fluorouracil loaded chitosan microspheres by a two-Step solidification method. *Chemical and Pharmaceutical Bulletin* 58, 891–895.
- Sunilbhai, P.A., Saikat, P., Ronakkumar Pravinbhai, P., 2014. Mucoadhesive microspheres containing anti-hypertensive agent: Formulation and characterization. *Curr Drug Deliv*.
- Swamy, N.G.N., Abbas, Z., 2012. Preparation and in vitro characterization of mucoadhesive polyvinyl alcohol microspheres containing amlodipine besylate for nasal administration. *Ind J Pharm Edu Res* 46.
- Swamy, N.G.N., Abbas, Z., 2012. Mucoadhesive in situ gels as nasal drug delivery systems: an overview. *Asian Journal of Pharmaceutical Sciences* 7, 168–180.
- Szoka, F., Papahadjopoulos, D., 1978. Procedure for preparation of liposomes with large internal aqueous space and high capture by reverse-phase evaporation. *Proc Natl Acad Sci U S A* 75, 4194–4198.
- Tafaghodi, M., Abolghasem Sajadi Tabassi, S., Jaafari, M.-R., Zakavi, S.R., Momen-Nejad, M., 2004. Evaluation of the clearance characteristics of various microspheres in the human nose by gamma-scintigraphy. *Int J Pharm* 280, 125–135.
- Takeuchi, H., Kojima, H., Yamamoto, H., Kawashima, Y., 2000. Polymer coating of liposomes with a modified polyvinyl alcohol and their systemic circulation and RES uptake in rats. *J Control Release* 68, 195–205.
- Takeuchi, H., Yamamoto, H., Niwa, T., Hino, T., Kawashima, Y., 1996. Enteral absorption of insulin in rats from mucoadhesive chitosan-coated liposomes. *Pharm. Res.* 13, 896–901.
- Taylor, L.S., Zografi, G., 1997. Spectroscopic characterization of interactions between PVP and indomethacin in amorphous molecular dispersions. *Pharm. Res.* 14, 1691–1698.
- Tee, H., Chuah, L., Pin, Y., Rshih, A., A., Y., 2012. Optimization of spray drying process parameters of Piper betle L.(Sirih) leaves extract coated with maltodextrin. *Journal of Chemical and Pharmaceutical Research* 4, 1833–1841.
- Tengamnuay, P., Sahamethapat, A., Sailasuta, A., Mitra, A.K., 2000. Chitosans as nasal absorption enhancers of peptides: comparison between free amine chitosans and soluble salts. *Int J Pharm* 197, 53–67.

- Thanoo, B.C., Doll, W.J., Mehta, R.C., Digenis, G.A., DeLuca, P.P., 1995. Biodegradable indium-111 labeled microspheres for in vivo evaluation of distribution and elimination. *Pharm. Res.* 12, 2060–2064.
- Tran, P.A., 2011. Nanotechnologies for Cancer Sensing and Treatment, in: Webster, T.J. (Ed.), *Nanotechnology Enabled In Situ Sensors for Monitoring Health*. Springer New York, pp. 1–39.
- Trenkwalder, C., Garcia-Borreguero, D., Montagna, P., Lainey, E., de Weerd, A.W., Tidswell, P., Saletu-Zyhlarz, G., Telstad, W., Ferini-Strambi, L., 2004. Ropinirole in the treatment of restless legs syndrome: results from the TREAT RLS 1 study, a 12 week, randomised, placebo controlled study in 10 European countries. *J. Neurol. Neurosurg. Psychiatr.* 75, 92–97.
- Tsuneji, N., Yuji, N., Naoki, N., Yoshiki, S., Kunio, S., 1984. Powder dosage form of insulin for nasal administration. *Journal of Controlled Release* 1, 15–22.
- Turánek, J., Záluská, D., Neca, J., 1997. Linkup of a fast protein liquid chromatography system with a stirred thermostated cell for sterile preparation of liposomes by the proliposome-liposome method: application to encapsulation of antibiotics, synthetic peptide immunomodulators, and a photosensitizer. *Anal. Biochem.* 249, 131–139.
- Ugwoke, M.I., Agu, R.U., Verbeke, N., Kinget, R., 2005. Nasal mucoadhesive drug delivery: background, applications, trends and future perspectives. *Adv. Drug Deliv. Rev.* 57, 1640–1665.
- Van Kampen, K.R., Shi, Z., Gao, P., Zhang, J., Foster, K.W., Chen, D.-T., Marks, D., Elmets, C.A., Tang, D.C., 2005. Safety and immunogenicity of adenovirus-vectored nasal and epicutaneous influenza vaccines in humans. *Vaccine* 23, 1029–1036.
- Vasir, J.K., Tambwekar, K., Garg, S., 2003. Bioadhesive microspheres as a controlled drug delivery system. *Int J Pharm* 255, 13–32.
- Verma, R.K., Garg, S., 2005. Selection of excipients for extended release formulations of glipizide through drug-excipient compatibility testing. *J Pharm Biomed Anal* 38, 633–644.
- Vyas, S.P., Goswami, S.K., Singh, R., 1995. Liposomes based nasal delivery system of nifedipine: Development and characterization. *International Journal of Pharmaceutics* 118, 23–30.
- Wang, L.-Y., Gu, Y.-H., Su, Z.-G., Ma, G.-H., 2006. Preparation and improvement of release behavior of chitosan microspheres containing insulin. *Int J Pharm* 311, 187–195.
- Wang, S.H., Kirwan, S.M., Abraham, S.N., Staats, H.F., Hickey, A.J., 2012. Stable dry powder formulation for nasal delivery of anthrax vaccine. *J Pharm Sci* 101, 31–47.
- Washington, N., Washington, C., Wilson, C.G., Wilson, C.G., 2001. *Physiological pharmaceuticals: barriers to drug absorption*. Taylor & Francis, New York.
- Wen, M.M., 2011. Olfactory targeting through intranasal delivery of biopharmaceutical drugs to the brain — current development. *Discovery Medicine* 11, 497–503.

- Wolff, R.K., 1986. Effects of airborne pollutants on mucociliary clearance. *Environ Health Perspect* 66, 223–237.
- Wu, Z.H., Ping, Q.N., Wei, Y., Lai, J.M., 2004. Hypoglycemic efficacy of chitosan-coated insulin liposomes after oral administration in mice. *Acta pharmacologica Sinica* 25, 966–972.
- Yadav, V., Gupta, A.B., Kumar, R., Yadav, J., Kumar, B., 2010. Mucoadhesive polymers: Means of Improving the Mucoadhesive Properties of Drug Delivery System. *J. Chem. Pharm. Res.* 2, 418–432.
- Yang, C., Gao, H., Mitra, A.K., 2001. Chemical stability, enzymatic hydrolysis, and nasal uptake of amino acid ester prodrugs of acyclovir. *J Pharm Sci* 90, 617–624.
- Zhang, Y., Zhang, Q., Sun, Y., Sun, J., Wang, X., Chen, M., 2005. Nasal recombinant hirudin-2 delivery: absorption and its mechanism in vivo and in vitro studies. *Biol. Pharm. Bull.* 28, 2263–2267.
- Zhuang, J., Ping, Q., Song, Y., Qi, J., Cui, Z., 2010. Effects of chitosan coating on physical properties and pharmacokinetic behavior of mitoxantrone liposomes. *International journal of nanomedicine* 5, 407.

List of website references:

- www.snuffhouse.org
- www.lasinus.com
- www.trimelpharmaceuticals.com
- www.mybuchi.com
- www.adelphi-hp.com
- www.webpackaging.com
- www.aptar.com
- www.adelphi-hp.com
- www.webpackaging.com
- www.az.com
- www.penncentury.com
- www.optinose.com
- www.anton-paar.com
- www.malvern.com
- www.ami.ac.uk
- www.ami.ac.uk/courses/topics/0140_pl/

Conference Papers & Poster Presentations

1. Nozad Hussein, Joanne Hardman, Abdelbary Elhissi, Mohamed Alhnan, David Phoenix, Waqar Ahmed. Development and Characterization of Anti-Parkinson Mucoadhesive Spray-Dried Ropinirole Microparticle for Brain Targeting Via the Nasal Route. Presented at United Kingdom and Ireland Controlled Release Society (UKICRS) Symposium, (1-2) May 2012, Aston University, Birmingham, UK.
2. Nozad R. Hussein, Ava T. Ismael, Basel T. Arafat, Mohamed A. Alhnan, Abdelbary M. Elhissi, and Waqar Ahmed. Development and Characterization of Anti-Parkinson Mucoadhesive Microspheres for Brain Targeting Via the Nasal Route. Presented at Respiratory Drug Delivery Europe (RDD), (21-24) May 2013, Berlin, Germany.
3. Nozad Hussein, Basel T. Arafat, Mohamed Albed Alhnan, Abdelbary Elhissi, Waqar Ahmed. Development and Characterization of Anti-Parkinson Liposomes for Intranasal Drug Delivery. Presented at American Association of Pharmaceutical Scientists Annual Meeting and Exposition (AAPS), (10-14) November 2013, San Antonio, USA.
4. Nozad R. Hussein, Basel T. Arafat, Mohamed A. Alhnan, Abdelbary M. Elhissi, Waqar Ahmed. Delivery of Ropinirole Hydrochloride Loaded Chitosan Microspheres Using Miat[®] Nasal Insufflator. Present at Respiratory Drug Delivery (RDD), (04-08) May 2014, Fajardo, Puerto Rico, USA.